The Development and Implementation of a TMT-SRM Assay for the Validation of Candidate Biomarkers of Alzheimer's Disease

O'Brien, Darragh

Awarding institution:
King's College London

Title: The Development and Implementation of a TMT-SRM Assay for the Validation of Candidate Biomarkers of Alzheimer's Disease

Author: Darragh O'Brien

The Development and Implementation of a TMT-SRM Assay for the Validation of Candidate Biomarkers of Alzheimer's Disease

Darragh Patrick O'Brien

Department of Psychological Medicine
Institute of Psychiatry
King's College London
United Kingdom

2011

A thesis submitted in partial fulfillment of the requirements for the degree of Doctor of Philosophy from King's College London

Acknowledgements

Firstly, I would like to thank my supervisors Professor Simon Lovestone and Dr. Helen Byers for their excellent guidance and support throughout the course of my studies. Simon has always provided extremely useful and interesting discussions in the area of dementia research and it was great to get the opportunity to work with such a renowned leader in the field. Helen's experience in the practicalities of mass spectrometry has been invaluable and she has been a great role model for me for the past six years and has taught me lots. Further, she has been an excellent editor of this document. Many thanks go to Karsten Kuhn for sharing his considerable expertise in tandem mass tagging. I would also like to extend my gratitude to James Campbell and Loïc Dayon for their very helpful conversations and reading of this document.

I am indebted to my colleagues at Proteome Sciences plc and the King's College Proteomics Facility, past and present, for their technical expertise and for making me feel such and integral part of the team. Thanks to all of the Lovestones, particularly the Alzheimer's disease biomarker team of Abdul, Andreas, Madhav, Rufina and Jo. Further thanks go to Steve, Helen, Annette, David, Selina, Claire and Amy, all who have kept me sane throughout this project and made the lab such an enjoyable place to work!

On a personal level, I would like to thank my parents Michael and Angela, brothers John, Michael and Ciarán and sisters Siobhán, Edel and Christina, for their loving support and for always believing in me. Finally, to Flo, for giving me constant encouragment and understanding over the past few years and for this, I am forever grateful.

Contents

Index of Figures

Index of Tables

List of Abbreviations

$(Tyr)_{1-6}$	polytyrosine-1, 3, 6 standard
^{18}FDG	^{18}fluorodeoxyglucose
2DE	2-dimensional gel electrophoresis
A2M	Alpha-2-macroglobulin
AAA	Amino acid analysis
ACN	Acetonitrile
AD	Alzheimer's disease
ADAS-cog	Alzheimer's Disease Assessment Scale-Cognitive Subscale
AMD	Age-related macular degeneration
AMT	Accurate mass tag
amu	Atomic mass unit
ANOVA	Analysis of variance
ApoE	Apolipoprotein E
APP	Amyloid precursor protein
AQUA	Absolute quantitation
ART	Alzheimer's Research Trust
Aβ	Amyloid-beta peptide
$Aβ_{1-38}$	Amyloid-beta peptide (38 amino acids in length)
$Aβ_{1-40}$	Amyloid-beta peptide (40 amino acids in length)
$Aβ_{1-42}$	Amyloid-beta peptide (42 amino acids in length)
BACE-1	Beta-site amyloid precursor protein-cleaving enzyme 1
BBB	Blood-brain barrier
BPI	Base peak intensity
BRIMS	Biomarker Research Initiatives in Mass Spectrometry
BSA	Bovine serum albumin
CDK-5	Cyclin-dependent kinase-5
CE	Collision energy
CFH	Complement factor H
CI	Confidence interval
CID	Collision-induced dissociation
CO	Carbon monoxide
cps	Counts per second
CPHPC	(R-1-[6-[R-2-carboxy-pyrrolidin-1-yl]-6-oxohexanoyl] pyrrolidine-2-carboxylic acid)
CSF	Cerebrospinal fluid
CV	Coefficient of variation
CXP	Collision cell exit potential
DC	Direct current
DIGE	Differential gel electrophoresis
DLB	Dementia with lewy bodies
DP	Declustering potential
DSM-IV	Diagnostic and Statistical Manual of Mental Disorders, 4th edition
DDA	Data dependent acquisition
DYRK1A	Dual specificity tyrosine-phosphorylation-regulated kinase 1A
ECD	Electron-capture dissociation
EDTA	Ethylenediaminetetraacetic acid
ELISA	Enzyme-linked immunosorbent assay
emPAI	Exponentially modified protein abundance index
EPI	Enhanced product ion
ER	Enhanced resolution
ESI	Electrospray ionisation
ETD	Electron-transfer dissociation
FA	Formic acid

FASP	Filter-aided sample preparation
FDA	Food and Drug Administration
FGG	Fibrinogen gamma-chain
fMRI	Functional magnetic resonance imaging
FTDP-17	Frontotemporal dementia and parkinsonism linked to chromosome 17
FT-ICR	Fourier transform-ion cyclotron resonance
FWHM	Full width half maximum
GluFib	[Glu1]-Fibrinopeptide
gpmdb	Global proteome machine database
GS1	QTRAP ion gas 1
GSK-3	Glycogen synthase kinase 3
GWAS	Genome-wide association study
H_2O	18 MΩ water
HPLC	High performance liquid chromatography
IAA	Iodoacetamide
ICAT	Isotope-coded affinity tag
ICPL	Isoptope coded protein label
ID	Identification
IDA	Information dependent acquisition
IDE	Insulin-degrading enzyme
iSRM	Intelligent selected reaction monitoring
iTRAQ	Isobaric tags for relative and absolute quantitation
LC	Liquid chromatography
LINAC	Linearly accelerating
LOD	Limit of detection
LOQ	Limit of quantitation
LRP-1	Lipoprotein receptor-related protein 1
m/z	Mass-to-charge ratio
MALDI	Matrix assisted laser desorption/ ionisation
MCI	Mild cognitive impairment
MIDAS	Multiple reaction monitoring initiated detection and sequencing
MMSE	Mini mental state examination
Mr	Molecular mass
MRI	Magnetic resonance imaging
MS	Mass spectrometry
MS/MS	Tandem mass spectrometry
NDC	Non-demented control
NFT	Neurofibrillary tangle
NINCDS-ADRDA	National Institute of Neurological and Communicative Disorders and the Alzheimer's Disease and related Disorders Association
NSD	No significant difference
o/c	On column
OD	Optical density
PAGE	Polyacrylmide gel electrophoresis
PAI	Protein abundance index
PBS	Phosphate buffered saline
PBS-T	Phosphate buffered saline-Tween
PD	Parkinson's disease
PET	Positron emmision tomography
pI	Isoelectric point
PIB	Pittsburg compund B
PPG	Polypropylene glycol
ppm	Parts per million
PSAQ	Protein standard absolute quantitation
p-tau	Phospho-tau
PTM	Post-translational modification

PHF	Paired helical filaments
Q0	Quadrupole 0
Q1	Quadrupole 1
Q2	Quadrupole 2
Q3	Quadrupole 3
QC	Quality control
RAGE	Receptor for advanced glycation end-products
RCD	Rapid cognitive decline
RF	Radiofrequency
RP	Reversed-phase
RT	Room temperature
S/N	Signal-to-noise ratio
SAP	Serum amyloid P-component
SCD	Slow cognitive decline
SCX	Strong cation exchange
SD	Standard deviation
SDS	Sodium dodecyl sulphate
SELDI	Surface enhanced laser desorption/ionisation
SISCAPA	Stable isotope standards and capture by anti-peptide antibody
SNP	Single-nucleotide polymorphisms
SP	Senile plaque
SRM	Selected reaction monitoring
SRP	Single-reference point
ST	Stubby lens
TCEP	Tris(2-carboxyethyl) phosphine
TEAB	Triethylammonium bicarbonate
TFA	Trifuoroacetic acid
TMT	Tandem mass tag
Tof	Time of flight
t_R	Retention time
t-tau	Total-tau
WB	Western blotting
XIC	Extracted ion chromatogram

Abstract

Biomarker discovery studies in plasma have revealed several proteins which may have clinical utility in the diagnosis and prognosis of Alzheimer's disease. The qualification of these proteins as true biomarkers, sensitive and specific to the disease, requires rapid, high quality, quantitative assays. Selected reaction monitoring (SRM) has emerged as an accurate and precise method for targeted protein selection through signature peptide measurement in highly complex mixtures such as plasma. Quantitative SRM-based assays are an attractive alternative to immuno-based approaches where costs can be high and requisite antibodies unavailable. Furthermore, the highly multiplexed nature of SRM allows the quantitation of multiple peptides/proteins in one rapid analysis step. Herein, we combine SRM with isotopic versions of tandem mass tags (TMT) to provide an internal reference for quantitation, an approach termed TMT-SRM, for the validation of prognostic candidate biomarkers of Alzheimer's disease.

The panel of proteins included clusterin, complement C3, alpha-2-macroglobulin, gelsolin, fibrinogen gamma-chain, serum amyloid p-component and complement factor H. These proteins were previously found to be differentially expressed between plasma of Alzheimer's disease subjects and non-demented controls. Additionally, apolipoprotein E4 was included in the panel as possession of the apolipoprotein e4 allele is the only unequivocal genetic risk factor for late-onset Alzheimer's disease and the protein expression of this genetic association may translate as an Alzheimer's disease biomarker.

For technology validation, TMT-SRM was shown to strongly correlate with western blot measurements for one of the proteins, gelsolin, in a sample cohort. Furthermore, the performance characteristics were determined for each target analyte in the assay. For biomarker validation, a cohort of 90 subjects was selected as having Alzheimer's disease (n = 60) or as non-demented controls (n = 30). To monitor disease progression, the Alzheimer's disease group was sub-divided into two groups (n = 30

per group), rapid cognitive decliners and slow cognitive decliners, based on decline in Mini Mental State Examiniation score per year.

Plasma alpha-2-macroglobulin expression was found to significantly increase in Alzheimer's disease and the difference correlated with disease progression. No significant differences were observed for the remaining proteins in the panel. Western blot analysis was performed on the same cohort for alpha-2-macroglobulin and gelsolin. In accordance with the mass spectrometry results, gelsolin showed no significant differences between disease and controls groups, providing confidence that the mass spectrometry-based assay was reflecting the real expression of the protein in the cohort. However, in contrast to the mass spectrometry results, alpha-2-macroglobulin did not show a significant difference between disease and control groups, illustrating the fact that the TMT-SRM approach was able to detect more subtle changes in peptide/protein expression than western blot. Results were replicated on an analogous mass spectrometer with strong correlation, demonstrating the robustness and ease-of-transfer of the TMT-SRM assay. Here, we have demonstrated TMT-SRM to be a rapid, precise and selective strategy for the quantitation of candidate biomarkers of Alzheimer's disease in plasma.

Chapter 1

Introduction

1.0 Alzheimer's disease

1.0.1 Dementia

Dementia (from Latin *de-* "apart, away" + *mens* "mind") is the progressive deterioration in cognitive function as a result of damage or disease to the brain. To date, many different types of dementia have been described including dementia with Lewy bodies (DLB), vascular dementia, frontotemporal dementia and parkinsonism linked to chromosome 17 (FTDP-17) and Alzheimer's disease (AD; Fratiglioni *et al.,* 2000). The primary risk factor for most dementia is age. The prevalence of the condition rises exponentially from approximately 1% at the age of 60 up to 35% at the age of 85 years, making it one of the most widespread medical conditions affecting the elderly (Ferri *et al.,* 2005). Current estimates suggest that in 2010, 35.6 million people globally are living with dementia and the number of new cases will rise to approximately 67.5 million in 2030 and approximately 115.4 million by the year 2050 (www.alz.co.uk/research/files/WorldAlzheimerReport2010.pdf). In the UK, the number of people living with dementia today is estimated to be 700,000, at a cost to the economy of £17 billion per year (www.alzheimer's.org.uk).

AD is the most severe and debilitating type of dementia, accounting for about 60% of all cases (Van Marum, 2008). In addition, AD in combination with intracerebral vascular disease accounts for a further 13 – 17% of cases (Querfurth and LaFerla, 2010). The disease is a fatal neurodegenerative disorder characterised by the progressive loss of cognitive function. A number of changes occur in the AD brain leading to clinical manifestations such as memory impairment, disorientation, attention deficits, deterioration in language and drawing function, agitation, aggression, and impaired gait and movement (Kirk and Kertesz, 1991; Price *et al.,* 1993; Greene *et al.,* 1996; Karlawish and Clark, 2003; Salzman *et al.,* 2008).

Many molecular species have been implicated in AD, but the overriding hypothesis is that the aging brain accumulates misfolded proteins resulting in oxidative and inflammatory damage, which in turn leads to energy depletion, white matter and neuronal loss (Querfurth and LaFerla, 2010). Alois Alzheimer, a Bavarian psychiatrist

first described the clinicopathological symptoms of the disease in 1906. His original report based on a patient named Auguste D. characterised several features of the disorder which are still recognised as the major hallmarks of AD today, *i.e.,* progressive memory loss, hallucinations and delusions (Alzheimer *et al.,* 1995; English translation from original paper). Upon autopsy, Alzheimer noted the presence of sticky proteinaceous plaques and abnormal tangled filaments in the limbic and associated cortices. These structures are what we now refer to as amyloid or senile plaques (SP) and neurofibrillary tangles (NFT).

1.0.2 The classic neuropathological hallmarks of Alzheimer's disease

1.0.2.1 Amyloid plaques

Amyloid plaques are composed of insoluble 5 – 10 nm thick amyloid fibrils, surrounded by a halo of reactive astrocytes, dystrophic neuritis and activated microglia (Selkoe, 2001). The principle protein component of these cerebral plaques is the amyloid-beta (Aβ) peptide (Masters *et al.,* 1985). Aβ is derived from the cleavage of amyloid precursor protein (APP), a single transmembrane spanning glycoprotein of unknown function (Kang *et al.,* 1987). In the amyloidogenic pathway, APP is initially cleaved by beta-site APP-cleaving enzyme 1 (BACE-1), a β-secretase, releasing the majority of the protein into the extracellular matrix (Figure 1.1; Haass *et al.,* 1992; Seubert *et al.,* 1992). The remaining 99 amino acid membrane bound stub (C99) is cleaved by γ-secretase generating Aβ which can be 38, 40 or 42 amino acids long ($Aβ_{1-38}$, $Aβ_{1-40}$, $Aβ_{1-42}$; Walsh and Selkoe, 2007). Excess accumulation of Aβ is speculated to be one of the initiating factors in AD. Conversely, a non-amyloidogenic pathway occurs with APP cleavage by γ-secretase and α-secretase (Goedert and Spillantini, 2006). APP processing has been linked to an association with lipid rafts. APP molecules within rafts are cleaved by β-secretase whereas those outside the raft are cleaved by the non-amyloidogenic α-secretase (Figure 1.1; Ehehalt *et al.,* 2003). A further study has associated γ-secretase within the lipid rafts of Golgi and endosome structures (Vetrivel *et al.,* 2004).

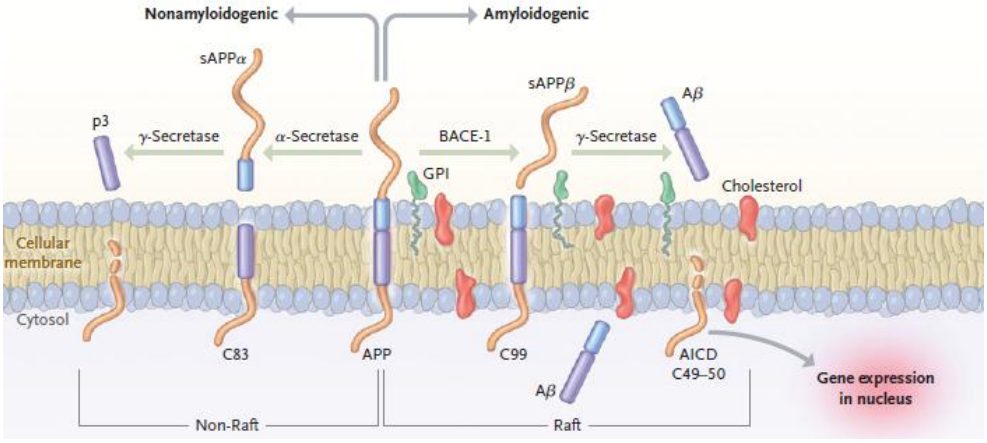

Figure 1.1 Production of Aβ from APP. The membrane spanning APP can be differentially cleaved to produce two distinct pathways. In the amyloidogenic (pathological) pathway, APP is cleaved by BACE-1 and γ-secretase to produce Aβ monomers. Conversely, cleavage of APP by α-sectretase and γ-sectretase produces the non-amyloidogenic p3 peptide. APP cleavage is facilitated by an association with lipid rafts. If Aβ cleavage occurs within the cell, *e.g*., within lysome or endosome structures, then that Aβ would be intracellular; if cleavage occurs in the secretory pathway or at the plasma membrane, then it would be released into the extracellular fluid (LaFerla *et al*., 2007; Figure extracted from Querfurth and LaFerla, 2010).

Considerable genetic and biochemical evidence gives rise to the 'amyloid hypothesis', suggesting that an increased production or defective clearance of Aβ results in excessive accumulation and aggregation of the protein which may instigate the disease course (Citron *et al.,* 1992; Carson and Turner, 2002; Nalivaeva *et al.,* 2008). Monomeric forms of $A\beta_{1\text{-}42}$ can spontaneously self-aggregate into multiple forms, *i.e.,* soluble oligomeric species which define intermediate diffuse plaques or the compacted, insoluble fibrillised structures of advanced SP (McDonald *et al.,* 2010). Several studies have implicated soluble oligomeric forms as the most potent species of Aβ, preceding insoluble amyloid deposits and synaptic dysfunction (Enya *et al.,* 1999; Walsh and Selkoe, 2007). Interestingly, the severity of neuronal deficits in AD correlates with the levels of oligomeric Aβ in the brain but not overall Aβ load (Lue *et al.,* 1999). The proteases plasmin, neprylisin and insulin-degrading enzyme (IDE) can regulate the steady-state levels of Aβ by degradation of Aβ monomers and oligomers (Ledesma *et al.,* 2000; Wang *et al.,* 2010). Reduction in either one of these enzymes can result in defective clearance and Aβ accumulation (Iwata *et al.,* 2001; Farris *et al.,*

2003). Conversely, neprylisin and IDE overexpression can prevent amyloid plaque formation (Leissring *et al.,* 2003).

The APP gene occurs on chromosome 21 and over 20 missense mutations within the gene have been associated with familial cases of AD (Citron *et al.,* 1992). It is well recognised that people with Down's syndrome or Trisomy 21 (due to an extra copy of chromosome 21) display amyloid deposits in brain and cerebral vasculature well before mid-life. However, mutations in presenelin-1 and presenelin-2 genes are the most common cause of familial AD (Goedert and Spillantini, 2006). The protein products of these genes are essential components of the γ-secretase catalytic complex, acting as diaspartyl proteases, which enable the γ-secretase cleavage of APP (Brouwers *et al*., 2008). This results in an increase in the ratio of the highly amyloidogenic $A\beta_{1-42}$, as compared to $A\beta_{1-40}$ (Citron *et al.,* 1996; De Strooper *et al.,* 1998).

1.0.2.2 Neurofibrillary tangles

Many areas of the AD brain such as the entorhinal cortex, hippocampus, amygdala and cerebral cortices contain intracellular neuronal deposits of a normally soluble protein called tau (Kosik *et al.,* 1986). Electron microscopy studies reveal that in AD, the tau protein is self-aggregated into a helical arrangement termed 'paired helical filaments' (PHF), the predecessor of NFT formation (Kidd, 1963; Wiśniewski *et al.,* 1976). In addition to AD, filamentous tau deposits have been implicated in several other types of dementia termed the 'tauopathies'. These include progressive supranuclear palsy and FTDP-17 (Hutton *et al.,* 1998; Lee *et al.,* 2001).

Six different isoforms of tau exist in the human central nervous system, each identified by the regulated inclusion of inserts near the N-terminus and the number of imperfect repeat tubulin binding domains near the C-terminus (Figure 1.2; Mulot *et al.,* 1994). Three isoforms have three highly conserved binding domains (3R) and the remaining three have four binding domains (4R; Goedert *et al.,* 1989). Each isoform is a result of alternative splicing in exons 2, 3 and 10 of the tau gene, which is located on

chromosome 17 (Goedert, 2004; Hanger *et al.,* 2009). In the normal brain, the 4R:3R ratio is equally expressed, however in most of the neurodegenerative tauopathies, this ratio is increased (Hanger *et al.,* 2009).

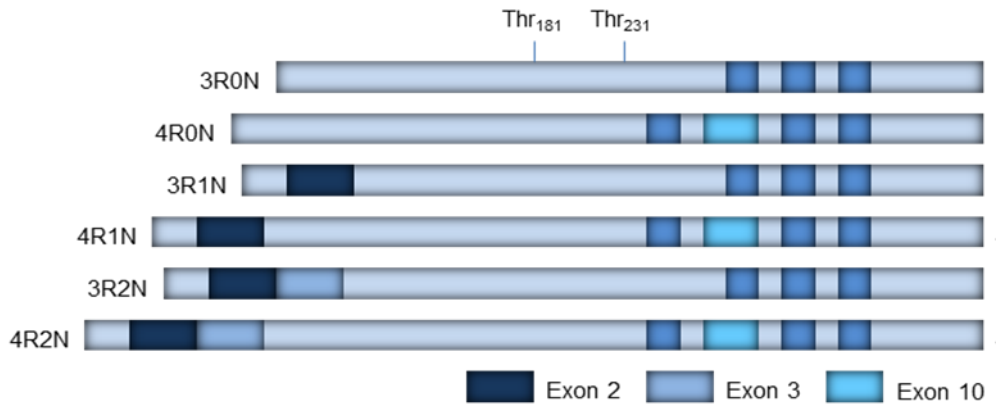

Figure 1.2 Alternative splicing results in different isoforms of tau. The tau gene undergoes alternative post-transcriptional splicing of exons 2, 3 and 10, producing tubulin binding domains. Tau isoforms have three (3R) or four (4R) binding domains. Tau can undergo phosphorylation/ dephosphorylation for microtubule organisation and stability, key sites are Thr_{181} and Thr_{231} (Figure adapted from Brunden *et al.,* 2009).

The primary function of tau is to interact with tubulin for microtubule assembly and stabilisation and phosphorylation is thought to be one of the key regulators of this (Weingarten *et al.,* 1975; Hanger *et al.,* 2009). In AD, tau becomes hyper-phosphorylated, resulting in reduced amounts of microtubule binding and increased PHF and NFT formation. More than 39 phosphorylation sites have been identified in PHF-tau in AD brain and their respective candidate protein kinases and phosphatases have been well researched, including glycogen synthase kinase 3 (GSK-3), cyclin-dependent kinase 5 (CDK-5), casein kinase 1 and protein phosphatase 1 (Anderton *et al.,* 2001; Johnson and Stoothoff, 2004; Liu *et al.,* 2005; Hanger *et al.,* 2007). The pathway linking Aβ and tau are not clearly understood and there is ongoing debate on which molecule, if either, is the causative agent of AD. Recent efforts on tau biology have provided new insights into the association of Aβ accumulation and exacerbation of NFT formation and neurodegeneration. Overall, the work suggests that abnormalities in tau and its aggregation are central to the clinical progression of AD. Studies have shown that intermediate aggregated forms of hyperphosphorylated tau can exert

pathological effects and induce neurotoxicity (Maeda *et al.,* 2007). Evidence indicates that Aβ accumulation precedes and initiates tau aggregation (Gotz *et al.,* 2001). From a genetic perspective, there are mutations in the tau-encoding *MAPT* gene (Kauwe *et al*., 2008), in addition to a major tau phosphatase, protein phosphatase B (Cruchaga *et al*., 2010) that do not add risk for AD, but affect its progression. Such effects are only observed in those people that already present brain Aβ accumulation. Furthermore, it has been observed that Aβ-induced neurodegeneration in culture neurons of mice requires the presence of tau (Rapoport *et al.,* 2002; Roberson *et al.,* 2007). DYRK1A (dual specificity tyrosine-phosphorylation-regulated kinase 1A) primes tau molecules for further phosphorylation by GSK-3 and might also be important in linking Aβ and tau, as the kinase is upregulated by Aβ (Liu *et al*., 2008). Thus, the neurodegeneration observed in AD may be a result of the pathological effects of Aβ and tau in concert.

1.0.2.3 Blood-brain barrier compromise in Alzheimer's disease

The blood-brain barrier (BBB) provides an interface between the brain and the peripheral blood system. The BBB is essentially a series of tight junctions in the capillary endothelial cells of the cerebral microvasculature, allowing the diffusion of small molecules such as O_2 or hormones, while restricting larger species such as bacteria (Donahue and Johanson, 2008). A combination of pericytes, astrocytes and neurons give rise to the 'microvasculature unit', the transport and enzymatic processes of which maintain BBB integrity and functioning (Hawkins and Davis, 2005). There is a growing body of evidence to suggest BBB compromise in AD, especially in those areas proximal to Aβ plaques (Blennow *et al.,* 1990; Hampel *et al.,* 1995; Bowman *et al.,* 2007; Algotsson and Winblad, 2007). Increased permeability of the BBB can result in increased deposition of Aβ in the AD brain and this has been confirmed in transgenic mouse models of the disease (Pluta *et al.,* 1996; Ujiie *et al.,* 2003). Indeed, the principal source of Aβ burden in AD is not clear, however circulating Aβ may contribute to Aβ deposition (Zlokovic, 2004). Transport of Aβ from the periphery into the brain *via* the BBB is facilitated by the low density lipoprotein receptor-related protein (LRP)-1

and P-glycoprotein receptors and the receptor for advanced glycation end-products (RAGE; Shibata *et al.,* 2000; Cirrito *et al.,* 2005; Deane *et al.,* 2008). Thus, in some instances, breakdown of BBB integrity and increased transport of Aβ across the structure may result in, or at least aggravate, the pathology of the disease.

1.0.2.4 Other neuropathological changes in the Alzheimer's disease brain

Findings suggest that there may be converging pathogenic mechanisms between amyloid plaque and cerebrovascular pathology (Farkas and Luiten, 2001; Mayeux, 2003). The neurovascular hypothesis proposes that dying blood vessels could add to cognitive dysfunction by preventing the delivery of nutrients to neurons and by reducing Aβ clearance from the brain (Iadecola, 2004). Other hypotheses proposed to explicate the pathogenesis of AD include abnormalities in inflammatory processes, failure of proteins regulating the cell cycle, reduction in cholinergic activity, oxidative stress and mitochondrial dysfunction with disruption in neuronal energy metabolism (Geula and Mesulam, 1995; Aisen, 2002; Webber *et al.,* 2005; Gibson and Huang, 2005; Reddy and Beal, 2005). While each could contribute to disease pathogenesis, to what extent they drive the neurodegenerative process remains uncertain.

1.0.3 Diagnosis and treatment of Alzheimer's disease

Currently there are several strategies available for the symptomatic treatment of AD including the acetylcholinesterase inhibitors donepezil, rivastigmine and galantamine (Steele and Glazier, 1999; Jann, 2000; Scott and Goa, 2000). Such species reduce the rate of acetylcholine catabolism, thus increasing the concentration of the neurotransmitter in the brain and replenishing the loss caused by the death of cholinergic neurons (Stahl, 2000). New drug candidates which may be able to reduce or slow the progression of the disease are also being produced, *e.g.,* secretase inhibitors, Aβ immunotherapy and tau aggregation inhibitors. These aim to prevent or reduce the neuropathology of the disease, *i.e.,* amyloid and tau deposition and the

inflammatory response. These molecules are now being tested in clinical trials. There are currently 50 compounds in Phase II trials for AD and a further ten in Phase III (Appendix Table 1.1; Pogacic and Herrling, 2009; Piau *et al*., 2011). Such therapeutic interventions would have the most beneficial effect at the very early stages of the disease, before neurodegeneration associated with SP and NFT deposition becomes too prevalent and severe. However, so far the clinical trials have produced somewhat negative results. In August of 2010, the γ-secretase inhibitor semagacestat was pulled from a Phase III trial of over 3000 subjects by Eli Lilly (Samson, 2010). Preliminary analysis showed that the drug not only failed to slow the progression of AD, but actually worsened cognition and functional ability. Further, the incidence of skin cancer was much higher in the treatment group than the placebo group.

The lack of availability of therapeutic interventions has highlighted the need for an early and precise diagnosis of AD. Diagnosis of AD is difficult and currently only possible in life using clinical symptoms to rate a tentative diagnosis, with a definitive diagnosis made possible only by *post mortem* analysis of the brain. AD is a progressive, neurodegenerative disease and one of the first clinical presentations of AD is a gradual and progressive memory loss (Carlesimo and Oscar-Berman, 1992). The subtlety of such memory deficits can result in a failure to diagnose the disease at the earliest stages, especially as linguistic, motor and sensory functions are relatively well preserved (McCarten, 1997). The correlation between clinical symptoms and specific stages in the pathological progression of AD was presented by Braak and Braak, where neurofibrillary changes in the AD brain were divided into six distinct phases of the disease (Braak and Braak, 1991). The first two stages (I-II) are defined by a mild or severe alteration in the transentorhinal region. Stages III and IV are marked by severe involvement of the entorhinal and transentorhinal (limbic) regions and stages V and VI are defined by severe isocortical destruction. Such progression in cortical pathology correlates with the gradual deterioration of clinical symptoms. Full-blown AD is clinically apparent at approximately stage IV.

In an aim to standardise the clinical diagnosis of AD, a working group was established in 1984, namely the National Institute of Neurological and Communicative Disorders and Stroke and the AD and Related Disorders Association (NINCDS-ADRDA; McKhann *et al.,* 1984). The NINCDS-ADRDA guidelines classify the diagnosis of AD into three distinct groups, which are, *possible* AD, *probable* AD and *definite* AD. Additional guidelines for the clinical diagnosis of AD include the Diagnostic and Statistical Manual of Mental Disorders, 4th edition (DSM-IV; American Psychiatric Association). Such guidelines were published up to 30 years ago and may not reflect the vast wealth of scientific understanding about AD gained over that time. Recently, both guidelines were revised to compensate for this and capture both the earliest stages and full spectrum of the illness (Dubois *et al.,* 2007). For a patient to be diagnosed as having AD they must have at least two of the following: the presence of an early and significant memory complaint, the presence of medial temporal lobe atrophy, an abnormal cerebrospinal fluid (CSF) biomarker pattern, a specific pattern on functional neuroimaging with positron emission tomography (PET) or an autosomal dominant mutation within the immediate family (Table 1.1).

Core diagnostic criteria	
A	Presence of an early and significant episodic memory impairment that includes the following features:
1	Gradual and progressive change in memory function reported by patients or informants for more than six months
2	Objective evidence of significantly impaired episodic memory on testing
3	The episodic memory impairment can be isolated or associated with other cognitive changes at onset of, or during AD
Supportive features	
B	Presence of medial temporal lobe atrophy Volume loss of hippocampi, entorhinal cortex, amygdala evidenced on MRI with qualitative ratings using visual scoring or quantitative volumetry of regions of interest
C	Abnormal cerebrospinal fluid biomarker Low $A\beta_{1-42}$ concentrations, increased t-tau concentrations, or increased p-tau concentrations, or combinations of the three
D	Specific pattern on functional neuroimaging with PET Reduced glucose metabolism in bilateral temporal parietal regions Other well validated ligands, including those that foreseeably will emerge such as Pittsburg compound B
E	Proven AD autosomal dominant mutation within the immediate family

Table 1.1 Core diagnostic criteria of Alzheimer's disease and supportive features as described by Dubois.

Several neuropsychological tests are available which aid in the assessment of the patient's cognitive ability as well as emotional, motor and sensory functions. These include the AD Assessment Scale - Cognitive Subscale (ADAS-Cog), the Mini Mental State Examination (MMSE) and the Clock Draw Test (Rosen *et al.,* 1984; Cockrell and Folstein, 1988; Lee *et al.,* 1996).

While many papers report a moderately accurate rate of clinical diagnosis (80 - 90%), it must be considered that such values are a result of expert research institutions and based on subjects in the final stages of AD, before confirmation at autopsy (Galasko *et al.,* 1994; Blennow and Vanmechelen, 2003). Diagnostic accuracy may be significantly lower in hospitals or care centres and at the very early stages of AD, when symptoms are less apparent. Patients need to be identified during the predementia phase (prodromal AD) before symptoms become obvious (preclinical AD). Preclinical AD is defined by AD pathology which is not prevalent enough to adversely affect episodic memory (Blennow *et al.,* 2010). Recently, interest has focused on the transitional period between normal aging and mild AD. Mild cognitive impairment (MCI) describes the clinical feature of memory impairment in individuals who have otherwise normal functioning and do not meet the clinical criteria for dementia (Petersen *et al.,* 1999). There is much debate as to whether MCI is a distinct cognitive aetiology or represents incipent AD (Arnaiz and Almkvist, 2003). Studies have shown that MCI subjects have a 50% higher risk of developing AD than cognitively normal individuals and MCI subjects' progress to AD at a rate of 10 - 15% per year (Petersen *et al.,* 1999; Grundman *et al.,* 2004). MCI patients may display diffuse amyloid pathology and frequent NFTs (Petersen *et al.,* 2006). Further, magnetic resonance imaging (MRI) scanning has demonstrated a progressive loss of grey matter of the brain from MCI to full-blown AD (Whitwell *et al.,* 2007).

Consequently, the availability of a diagnostic test or molecular marker which could support clinical measures would be highly desirable. Such tests may enable an earlier diagnosis, evaluate disease risk or prognosis and give a better understanding of treatment response. A biomarker can be any characteristic that is objectively measured

and evaluated as an indicator of normal biologic processes, pathogenic processes, or pharmacologic responses to a therapeutic intervention (Biomarkers Definitions Working Group, 2001). According to the 1998 Consensus Report of the Working Group on Molecular and Biochemical Markers of AD, the ideal biomarker for AD should be able to detect the underlying AD neuropathology with validation in an autopsy confirmed examination, precise (with the ability to distinguish AD from other dementias), non-invasive, inexpensive, reliable and simple to perform (The Ronald And Nancy Reagen Research Institute Of The Alzheimer's Association And The National Institute On Aging Working Group, 1998). Further, a biomarker that accurately echoes the progression of AD could be used as a surrogate endpoint to complement clinical measures in clinical trials.

1.0.4 Neuroimaging markers of Alzheimer's disease

Neuroimaging incorporates an array of techniques used for the structural and functional imaging of the brain including MRI, functional MRI (fMRI) and PET. Structural scanning produces highly detailed images of the brain whereas functional scanning enables the analysis of brain activity. Imaging techniques are useful for monitoring cognitive and pathological changes at the very earliest stages of AD, in addition to monitoring response to clinical interventions (Burggren and Brookheimer, 2002). Hippocampal volumetry using MRI is currently the most established structural biomarker of AD and can predict conversion to the disease with about 80% accuracy (Jack *et al.,* 1999; Wang *et al.,* 2006). Several studies have been published comparing the temporal rate of change of hippocampal atrophy in AD, where atrophy rates of 3 - 6% per year have been demonstrated compared to 0.3 - 2.2% in NDCs (Jack *et al.,* 2003; Kaye *et al.,* 2005; Barnes *et al.,* 2007; Henneman *et al.,* 2009). The diagnostic and prognostic value of MRI in AD has resulted in the inclusion of MRI in several clinical trials of candidate disease modifiers (Dubois *et al*., 2007; Jack *et al.,* 2003; Gauthier *et al.,* 2009; Frisoni and Delacourte, 2009). fMRI measures the change in blood flow associated with neural activity, generating images which reflect which areas

of the brain are activated during performance tasks. Studies have been published measuring such changes in MCI *versus* AD subjects, with the aim of finding a biomarker for early AD diagnosis (Rombouts *et al.,* 2005; Celone *et al.,* 2006). fMRI studies suggest that changes occur in the functional connectivity of visual processing areas in MCI subjects and these precede changes in brain activation between MCI and NDCs (Horwitz *et al.,* 2005; Bokde *et al.,* 2006). PET in combination with ^{18}fluorodeoxyglucose (^{18}FDG) can be used to measure cerebral glucose metabolism (Bodke *et al.,* 2005). In mild to moderate stages of AD, a reduction in cortical metabolism is observed in the temporal and parietal association cortices and these predict conversion to AD from MCI with over 80% accuracy (Modrego, 2006). ^{18}FDG-PET is regarded as the gold standard for the diagnosis of early AD *in vivo.* Recently, novel radiotracer compounds such as Pittsburg Compound B (PIB) have been used in combination with PET (Klunk *et al.,* 2004). The molecule binds to Aβ, enabling the imaging of amyloid plaques. Studies demonstrate enhanced uptake of PIB in the AD brain (Klunk *et al.,* 2004; Drzezga *et al.,* 2008; Grimmer *et al.,* 2009) and the technique has been shown to discriminate AD from other types of dementia (Rabinovici *et al.,* 2007). Although neuroimaging markers have shown great promise, their full potential as biomarkers of AD has yet to be fully described. Currently, they do not fulfill the requirements of an ideal biomarker of AD as set out by the Working Group on Molecular and Biochemical Markers of AD, *i.e*., the primary limitations associated with such techniques are the cost of implementation and the lack of widespread availability. Thus, human biological fluids may provide an alternative source of AD biomarkers due to their accessibility, reduced handling costs and indeed, vast protein signature.

1.1 Candidate protein biomarkers for the diagnosis and prognosis of Alzheimer's disease

1.1.1 Cerebrospinal fluid biomarkers of Alzheimer's disease

Numerous types of body tissue and fluids have been screened for AD biomarkers, including urine, erythrocytes, lymphocytes and skin (Inestrosa *et al.,* 1994; Bermajo *et al.,* 2008). The vast majority of AD biomarker studies to-date have focused on CSF, the extracellular fluid found circulating within the ventricles and subarachnoidal space of the brain. Here it performs several important functions, such as maintaining a constant molecular environment for neurons and allowing the transport of metabolites between brain regions and the circulatory system. The BBB is a single layer endothelium separating both the brain and CSF compartments, and thus, it has been hypothesised that a CSF biomarker of AD should echo the pathological process in the brain (Thorsell *et al.,* 2010). Protein biomarkers of AD can be separated into basic and core biomarkers. Basic biomarkers identify conditions that mirror or co-exist with AD and include measurement of BBB status and inflammation of the central nervous system (Blennow *et al.,* 2010). Core biomarkers measure the pathological hallmarks of the disease. For AD, these include markers that reflect neuronal degeneration, amyloid deposition in SP's and the hyperphosphorylation of tau that is associated with NFT pathology. The candidate CSF core biomarkers of $A\beta_{1-42}$, total tau (t-tau) and phosphorylated tau (p-tau) have been extensively assessed in numerous biomarker programmes.

1.1.1.1 Cerebrospinal fluid $A\beta_{1-42}$ as a biomarker of Alzheimer's disease

As previously described, $A\beta_{1-42}$ appears to be essential to the amyloid cascade hypothesis of AD, by initiating Aβ aggregation and deposition (Hardy and Selkoe, 2002). Several antibody-based assays such as the ''Innogenetics'' and ''Athena'' ELISA have been developed for the measurement of $A\beta_{1-42}$ in CSF. These assays have been shown to be highly specific for $A\beta_{1-42}$, with minimal cross-reactivity with other Aβ

species (Ida *et al.,* 1996; Tamaoka *et al.,* 1997; Jensen *et al.,* 2000; Mehta *et al.,* 2000). In many independent research studies, mean CSF $A\beta_{1-42}$ levels have consistently been shown to be markedly reduced in AD, that is, 30 - 50% less than that of control levels (Motter *et al.,* 1995; Galasko *et al.,* 1998; Kanai *et al.,* 1998; Andreasen *et al.,* 1999; Andreasen *et al.,* 2001; Sunderland *et al.,* 2003, Craig-Shapiro *et al.,* 2009; Tapiola *et al.,* 2009). Conversely, one study found an increase in CSF $A\beta_{1-42}$ in AD (Jensen *et al.,* 1999). This was likely due to differences in assay specificity, methodology or patient sampling. The sensitivity and specificity of CSF $A\beta_{1-42}$ for discriminating between AD and NDCs in the above studies was approximately 85%. Interestingly, a recent study has shown a correlation between CSF $A\beta_{1-42}$ and amyloid plaque load post-mortem while a separate study correlated antemortem CSF $A\beta_{1-42}$ with plaque load at autopsy (Strozyk *et al.,* 2003; Tapiola *et al.,* 2009). Further, $A\beta_{1-42}$ levels have been shown to decrease in individuals with MCI or very mild AD (Mattsson *et al.,* 2009). In 2004, Klunk and colleagues demonstrated a very strong inverse relationship between CSF $A\beta_{1-42}$ and *in vivo* cortical amyloid load measured by PET-^{11}C-PIB (Klunk *et al.,* 2004). This has since been replicated using the same techniques in other studies (Fagan *et al.,* 2006; Fagan *et al.,* 2007). It has been hypothesised that the reduced levels of CSF $A\beta_{1-42}$ observed in AD are due to the increased aggregation of $A\beta_{1-42}$ in SP's, resulting in lower levels diffusing into the CSF (Blennow and Nellgård, 2004). However, decreased levels of CSF $A\beta_{1-42}$ are also observed in the amyloid plaque-negative disorder of Creutzfeldt-Jakob disease (Otto *et al.,* 2000).

1.1.1.2 Cerebrospinal fluid t-tau as a biomarker of Alzheimer's disease

The total CSF tau level, independent of phosphorylation, can additionally be measured using the Innogenetics and Athena ELISA, which detect all isoforms of the protein. A consistent observation of increased CSF t-tau (over 300% compared to NDCs) has been found by numerous groups (Mecocci *et al.,* 1998; Andreasen *et al.,* 1999; Molina *et al.,* 1999; Andreasen *et al.,* 2000; Vanmechelen *et al.,* 2000; Sunderland *et al.,* 2003; Mattsson *et al.,* 2009; Visser *et al.,* 2009). Both ELISA's show

variation in performance, with a higher sensitivity observed for the Innogentics test and a higher specificity observed for the Athena test. Elevated levels of CSF t-tau have been associated with a more rapid progression from MCI to AD and a faster rate of cognitive decline in AD (Blom *et al.,* 2009; Wallin *et al.,* 2009). Elevated levels of CSF t-tau are not specific to AD however, with similar increases found in vascular dementia and frontotemporal dementia (Andreasen *et al.,* 1999; Molina *et al.,* 1999). Further, elevated levels of CSF t-tau are occasionally observed in other types of dementia such as progressive supranuclear palsy and Parkinson's disease (PD; Molina *et al.,* 1999; Urakami *et al.,* 1999). The observation that increased CSF t-tau, which is primarily derived from neurons and axons, is correlated to the level of neuronal degeneration leads to the theory that CSF t-tau levels are a marker for axonal damage in the brain (Bitsch *et al*., 2002; Blennow and Vanmechelen, 2003). A significant increase is observed in Creutzfeldt-Jakob disease where there is rapid and widespread degeneration, a moderate increase is observed in AD where there is moderate degeneration and no increase is observed in depression, where degeneration is absent (Blennow *et al.,* 1995; Otto *et al.,* 1997; Andreasen *et al.,* 1999).

1.1.1.3 Cerebrospinal fluid p-tau as a biomarker of Alzheimer's disease

Hyperphosphorylation of tau is the preceding event to tau aggregation and deposition in the AD brain. Such an event is specific to AD and CSF p-tau levels may therefore be used to distinguish AD from other types of dementia (Hampel *et al.,* 2004; Koopman *et al.,* 2009). Several ELISA's have been developed for different phosphorylation epitopes on tau, including serine 199 (Ishiguro *et al.,* 1999), threonine 181 and 231 (p-tau$_{181}$ and p-tau$_{231}$; Blennow *et al.,* 1995), threonine 231 and serine 235 (Ishiguro *et al.,* 1999) and threonine 231 (Kohnken *et al.,* 2000; Buerger *et al.,* 2002; Buerger *et al.,* 2002). In all studies to-date, an increased level of CSF p-tau was observed with a mean sensitivity of 70% and specificity of 94% for discriminating between AD and NDCs (Blennow and Vanmechelen, 2003). Correlations have been observed between CSF p-tau$_{181}$ and p-tau$_{231}$ measurements performed during life and

NFT pathology and rate of hippocampal atrophy at autopsy (Buerger *et al.,* 2006; Tapiola *et al.,* 2009). Elevated CSF p-tau has been linked with a more rapid progression from MCI to AD and a faster rate of cognitive decline in AD (Blom *et al.,* 2009; Samgard *et al.,* 2010).

1.1.1.4 Combined analysis of cerebrospinal fluid biomarkers

Many studies have shown that CSF $A\beta_{1-40}$ levels are unchanged in AD (Fukuyama *et al.,* 2000; Mehta *et al.,* 2000; Fagan *et al.,* 2007). However the ratio of $A\beta_{1-42}$: $A\beta_{1-40}$ has been shown to be a better distinguisher of AD, MCI and NDCs, than either marker alone (Lewczuk *et al.,* 2004; Hansson *et al.,* 2007). Furthermore, the combination of all three measures, *i.e.,* $A\beta_{1-42,}$ t-tau and p-tau in various ratios has been observed to perform better than either alone (Lewczuk *et al.,* 2008; Welge *et al.,* 2009). Although promising, the results of CSF biomarker studies in AD are not conclusive. The diagnostic performance of CSF biomarkers in distinguishing AD from other types of dementia is less than ideal. Consequently, alternative biofluids are currently being investigated.

1.1.2 Plasma biomarkers of Alzheimer's disease

Recent focus has moved to the analysis of the blood plasma proteome for biomarkers of AD diagnosis and prognosis. The extraction of CSF, that is, a lumbar puncture or 'spinal tap', is the standard method of obtaining CSF for biochemical analysis (Peskind, 2005). The procedure is relatively straightforward and recently the use of small caliber and blunt-ended needles has reduced discomfort and incidence of post-lumbar puncture headache to 1 - 3% (Blennow *et al.,* 1993; Zetterberg *et al.,* 2010). Nevertheless, obtaining the large volumes of CSF required for biomarker analysis on a repeated basis is challenging. The extraction of blood however is relatively non-invasive, simple and quick. Approximately 500 mL of CSF is produced per day. As the brain can only hold 135 - 150 mL at any one time, the fluid is drained

and ‘turned over’ in the peripheral circulatory system at a rate of about 3.7 times daily. Consequently, blood proteins may directly reflect pathologic changes in the AD brain. Further still, the disruption of the BBB in AD may increase the exchange of proteins between the CSF and blood and *vice versa* (Zipser *et al.,* 2007).

The human blood plasma proteome is a highly complex mixture, which encompasses many classes of proteins including immunoglobulins, secreted proteins, hormones, tissue leakage products and foreign proteins, introduced upon bacterial or parasitic infection. Current estimates suggest in excess of 1,000 unique plasma proteins exist, spanning over ten orders of magnitude from albumin at ~45 mg/mL down to cytokines and interleukins at 1 - 10 pg/mL or lower (Figure 1.3; Anderson and Anderson, 2002). Due to this large population of proteins, it has been hypothesised that human plasma may provide a rich source of novel biomarkers for human disease.

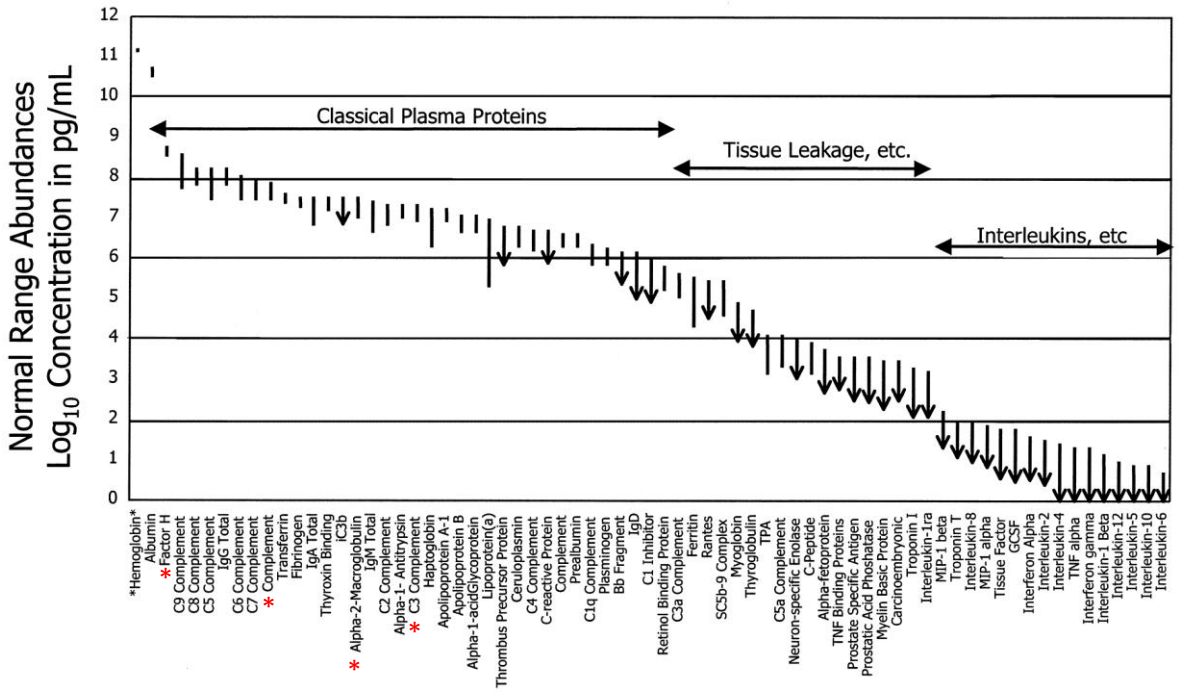

Figure 1.3 Abundance intervals for 70 proteins in plasma. The abundance of plasma proteins ranges over 12 orders of magnitude, from high mg/mL to low pg/mL. The upper and lower limits of abundance are defined by a blunt end interval line; an arrowhead represents an unknown value (taken from Anderson and Anderson, 2002).
* indicates candidate AD biomarker proteins addressed in this thesis

Much time and expense has been invested into biomarker discovery and validation programmes in plasma but to-date, there are no established protein markers, at least in brain diseases, in routine use in the clinic. The inherent properties of plasma itself present immense technical and practical challenges. Many possible candidate biomarkers occur at very low concentrations in plasma and are 'masked' by several highly abundant species, namely albumin, transferrin, haptoglobin, IgA, IgG and alpha-1 antitrypsin (Anderson and Anderson, 2002). These proteins constitute up to 90% of the total plasma proteome with a further 12 proteins accounting for 9%. Thus the majority of plasma proteins are found in only 1% of the total plasma proteome. Such problems may be overcome by extensive fractionation of the sample to remove the principal protein components, but this can prove to be costly, time-consuming and introduce a level of technical variability. Further, these species may have several proteins complexed to them and their removal may result in loss of valuable proteomic information.

1.1.2.1 Plasma biomarkers of Alzheimer's disease related to Aβ and tau

The pool of Aβ found in the circulatory system is comprised of Aβ produced by peripheral tissues and organs as well as that produced by the brain and transported across the BBB (Chen *et al.,* 1995; Zlokovic, 2004). Several factors alter circulating Aβ levels including age, AD-related pathology, cerebrovascular disease and liver metabolism (Lopez *et al.,* 2008). Soluble plasma Aβ is typically measured by sandwich ELISA but with more difficulty than CSF due to lipoprotein binding and (~10 fold) lower concentrations (Kawarabayashi and Shoji, 2008). The majority of groups investigating plasma $A\beta_{1-40}$, $A\beta_{1-42}$ and $A\beta_{1-42}$: $A\beta_{1-40}$ levels report no statistically significant differences between AD, incident MCI and NDCs (Scheuner *et al.,* 1996; Tamaoka *et al.,* 1996; Vanderstichele *et al.,* 2000; Fukumoto *et al.,* 2003; Blasko *et al.,* 2008; Song *et al.,* 2009; Roher *et al.,* 2009; Hansson *et al.,* 2010).

Several studies have reported that high baseline $A\beta_{1-42}$ levels in non-demented elderly were a risk factor for AD (Mayeux *et al.,* 2003; Pomara *et al.,* 2005; Lopez *et al.,*

2008, Schupf *et al.,* 2008). Conversely, lower plasma $A\beta_{1-42}$ and $A\beta_{1-42}$: $A\beta_{1-40}$ levels in AD and MCI compared to NDC have been reported (van Oijen *et al.,* 2006; Lewczuk *et al.,* 2008). This is in agreement with CSF $A\beta_{1-42}$ and $A\beta_{1-42}$: $A\beta_{1-40}$ studies and validates the findings by Graff-Radford and colleagues who showed that a low plasma $A\beta_{1-42}$: $A\beta_{1-40}$ ratio was associated with conversion to MCI or AD (Graff-Radford *et al.,* 2007). In a recent longitudinal study, low plasma levels of $A\beta_{1-40}$, $A\beta_{1-42}$ and C-reactive protein were associated with rapid cognitive decline (Locascio *et al.,* 2008). In another study, subjects who were followed for 2.5 years showed that high $A\beta_{1-42}$ levels were able to predict the conversion of NDC to MCI, but not MCI to AD (Blasko *et al.,* 2008). However, several further studies suggest that plasma $A\beta_{1-40}$ or $A\beta_{1-42}$ does not correlate with the progression of AD (Sundelof *et al.,* 2008; Roher *et al.,* 2009). When taken together, there is no definitive conclusion whether plasma Aβ levels directly reflect the disease. Conflicting results may be due to several reasons including assay methodology, differential antibody affinities and sensitivities for Aβ detection, binding of Aβ to several plasma proteins including albumin (Kuo *et al.,* 1999) as well as sample collection and handling. However, results of longditudinal studies are promising and assays of $A\beta_{1-40}$, $A\beta_{1-42}$ or $A\beta_{1-42}$: $A\beta_{1-40}$ ratio may have future use in stratifying patients at risk of MCI or AD (Thambisetty and Lovestone, 2010).

The measurement of peripheral tau has been somewhat challenging with little or no results on t-tau or p-tau plasma levels in AD. However, recently several novel sandwich ELISAs have been developed which allow for tau measurements in serum and plasma (*e.g.,* Applied Neurosolutions, Vernon Hills, IL, USA; Schneider *et al.,* 2009). The AD biomarker community eagerly awaits the initial findings from these technologies. In summary, the utility of plasma levels of Aβ and tau is not clear and attention has moved to the measurement of alternative proteins in plasma, with the hope of providing more sensitive and specific biomarkers of the disease.

1.1.2.2 Proteomic discovery of a panel of biomarkers of Alzheimer's disease in blood plasma

Numerous proteins have emerged as candidate biomarkers of AD from discovery studies in plasma by several independent groups. Table 1.2 outlines the principal plasma proteins proposed by these studies. Such candidates cover a broad range of functionalities, including transport proteins and proteins involved in immune regulation, inflammation, coagulation, proteolysis and apoptosis. It is not yet clear whether individual proteins may provide an ideal biomarker for the disease, although a combination of multiple biomarkers may increase the sensitivity and specificity of AD diagnosis and predictive power of prognosis, than single proteins alone (Mor *et al.,* 2005). In 2007, an elegant study was released in Nature Medicine, where 18 signalling proteins in blood plasma were used to classify blinded samples from AD and NDC subjects with up to 90% accuracy (Ray *et al.,* 2007). Further, the same multiplexed panel of proteins was able to identify MCI patients who progressed to AD 2 - 6 years later. However, only 5 out of the 18 proteins have been since validated and additional experiments are required to determine the full potential of these candidates (Marksteiner *et al.,* 2009). Further, the study used sandwich ELISA's to determine relative expression differences between AD and NDC groups and this approach has several disadvantages, *i.e.,* is largely dependent on high quality antibodies which may be subject to non-specific responses and thus, inaccuracies in quantitation.

From proteomic discovery studies in plasma in our laboratory and others, several proteins have been identified which have been shown to be differentially regulated in AD and which may serve as an ideal panel of biomarkers of AD diagnosis and prognosis. From these, a panel of nine proteins (as highlighted in bold in Table 1.2) were selected for development of a quantitative assay for validation as they were considered the most promising, in terms of quantitative differences from discovery and relation to AD biology, in providing robust biomarkers of the disease. Complement factor H (CFH), fibrinogen gamma-chain (FGG), complement C3, complement C3a, serum amyloid P component (SAP), gelsolin and alpha-2-macroglobulin (A2M) were

Function	Swissprot Accession No.	Protein	Sample	Expression in AD	Technique	Reference
Lipid transport	P10909	**Clusterin** [a]	Plasma	↓[b]	A[c]	(Corder *et al.,*1994; Thambisetty *et al.,* 2010)
	P04114	Apolipoprotein B100	Serum	↑	E	(German *et al.,* 2007)
	P02647	Apolipoprotein A–I	Plasma	↓	G	(Ganguli *et al.,* 2004)
	P02656	Apolipoprotein C-III	Plasma	↑	A	(Thambisetty *et al.,* 2010)
	P02649	**Apolipoprotein E** [a]	Serum	↑	H	(German *et al.,* 2007)
Actin assembly/ disassembly	P06396	**Gelsolin** [a]	Plasma	↓	K	(Güntert *et al.,* 2010)
Copper transport	P00450	Ceruloplasmin	Plasma	↓	A	(Chen *et al.,* 1995)
Thyroxine transport	P02766	Transthyretin	Serum	↑	D	(German *et al.,* 2007)
Oxygen transport	P69905	Hemoglobin alpha chain	Serum	↑	E	(German *et al.,* 2007)
Heme transport/ oxidative stress	P02790	Hemopexin	Plasma	↑	B	(Ferri *et al.,* 2005)
Iron carrier protein/ energy	P02787	Transferrin	Plasma	↑	B	(Ferri *et al.,* 2005)
Immune regulation	Q14624	Inter-alpha-trypsin inhibitor heavy chain H4	Plasma	↓	A	(Chen *et al.,* 1995)
	O43866	CD5 antigen-like	Plasma	↓	A	(Chen *et al.,* 1995)
	P02787	**SAP** [a]	Plasma	↑	A	(Chen *et al.,* 1995)
	P13501	C-C motif chemokine 5	Plasma	NA	L	(Ray *et al.*, 2007)
	P80098	C-C motif chemokine 7	Plasma	NA	L	(Ray *et al.*, 2007)
	Q16663	C-C motif chemokine 15	Plasma	NA	L	(Ray *et al.*, 2007)
	P55774	C-C motif chemokine 18	Plasma	NA	L	(Ray *et al.*, 2007)
	P10145	Interleukin-8	Plasma	↑	L	(Ray *et al.*, 2007)
	P01583	Interleukin-1α	Plasma	↓	L	(Ray *et al.*, 2007)
	P08700	Interleukin-3	Plasma	NA	L	(Ray *et al.*, 2007)
	P20809	Interleukin-11	Plasma	NA	L	(Ray *et al.*, 2007)
	P01375	TNF-α	Plasma	NA	L	(Ray *et al.*, 2007)
	Q9UBN6	TNF-related apoptosis-inducing ligand receptor-4	Plasma	NA	L	(Ray *et al.*, 2007)
Inflammation	P00738	Haptoglobin alpha 2 chain	Serum	↑	I	(German *et al.,* 2007)

Table 1.2 Putative plasma biomarkers of AD. The primary function of each candidate is displayed along with the sample and techniques used in the biomarker discovery studies (adapted from Song *et al.,* 2009).

[a] Candidate biomarkers included in the panel for development of a multiplexed mass spectrometry-based assay

[b] Found to be decreased in Corder *et al.,* 1994, but unchanged in Thambisetty *et al.,* 2010

[c] Proteomic approach listed overleaf

Function	Swissprot Accession No.	Protein	Sample	Expression in AD	Technique	Reference
	P02763	Alpha 1-acid glycoprotein	Serum	↓	J	(German *et al.,* 2007)
	Q14624	Inter-α-trypsin inhibitor family heavy chain-related protein	Plasma	↓	A	(Corder *et al.,*1994)
	P02774	Vitamin D-binding protein	Plasma	↑	A	(Corder *et al.,*1994)
	O15123	Angiopoietin-2	Plasma	NA	L	(Ray *et al.*, 2007)
Complement pathway	P0C0L4	Complement C4	Serum	↑	D	(German *et al.,* 2007)
	P01024	**Complement C3/ C3a** [a]	Serum	↑	D	(German *et al.,* 2007)
	P07360	Complement C8	Plasma	↑	A	(Thambisetty *et al.,* 2010)
	P08603	**CFH** [a]	Plasma	↑	A	(Chen *et al.,* 1995; Hye *et al.,* 2006)
Proteolysis	P01009	Alpha-1-antitrypsin	Plasma	↑	A, B, C	(Corder *et al.,*1994; Ferri *et al.,* 2005; Farlow *et al.,* 2004)
	P01023	**A2M** [a]	Plasma	↑	A, D	(German *et al.,* 2007; Chen *et al.,* 1995; Hye *et al.,* 2006)
	P05155	Serpin G1/C1 inhibitor	Plasma	↓	A	(Cutler *et al.,* 2008)
Blood coagulation	P04004	Vitronectin	Serum	↑	F	(German *et al.,* 2007)
	P17612	cAMP-dependent protein kinase catalytic subunit α	Plasma	↓	A	(Corder *et al.,*1994)
	P02671	Fibrinogen α-chain	Plasma	↑	A	(Hye *et al.,* 2006; Thambisetty *et al.,* 2010)
	P02675	Fibrinogen β-chain	Plasma	↑	A	(Hye *et al.,* 2006; Thambisetty *et al.,* 2010)
	P02679	**FGG** [a]	Plasma	↑	A	(Hye *et al.,* 2006; Thambisetty *et al.,* 2010)
	P00747	Plasminogen	Plasma	↓	A	(Thambisetty *et al.,* 2010)
Cell growth	P01133	Epidermal growth factor	Plasma	NA	L	(Ray *et al.*, 2007)
	P24592	Insulin-like growth factor–binding protein-6	Plasma	↑	L	(Ray *et al.*, 2007)
	P09603	Macrophage colony-stimulating factor	Plasma	↓	L	(Ray *et al.*, 2007)
	P01127	Platelet-derived growth factor BB	Plasma	↓	L	(Ray *et al.*, 2007)
	P39905	Glial-derived neurotrophic factor	Plasma	NA	L	(Ray *et al.*, 2007)
	Q99062	Granulocyte-colony stimulating factor	Plasma	NA	L	(Ray *et al.*, 2007)
Cell adhesion	P05362	Intercellular adhesion molecule-1	Plasma	↑	L	(Ray *et al.*, 2007)
Apoptosis	P47929	Galectin-7	Plasma	↑	A	(Chen *et al.,* 1995)
DNA/Gene regulation	P62807	Histone H2B type 1-C/E/F/G/I	Plasma	↓	A	(Chen *et al.,* 1995)
Unknown functions	P15924	Desmoplakin	Plasma	↑	A	(Chen *et al.,* 1995)
	P04196	Histidine-rich glycoprotein	Serum	↑	F	(German *et al.,* 2007)

Table 1.2 (continued)

A: 2DE LC/MS/MS B: Glycan affinity chromatography/ MALDI-TOF C: 2DE/ DNP-immunostaining/ MALDI-TOF D: DEAE/ 1DE/ MALDI E: 1DE/ MALDI F: Heparin/ 1DE/ MALDI G: 2DE/ MALDI-TOF H: DEAE/ LCQ I: DEAE or Ni 2DE/ MALDI J: ConA/ LCQ K: Isobaric mass tagging L Sandwich ELISA array

found to have potential in distinguishing AD patients from NDCs using two-dimensional gel electrophoresis (2DE; Chen *et al.,* 1995; Hye *et al.,* 2006; Thambisetty *et al.,* 2010).Further, 2DE and TMT-labeling technologies found clusterin and gelsolin may have utility in predicting the progression of the disease (Thambisetty *et al.,* 2010; Güntert *et al.,* 2010). Apolipoprotein E (ApoE) is of interest as the the E4 variant of ApoE is the largest genetic risk factor for AD (Corder *et al.,* 1993). The E4 variant may influence the ApoE protein level and thus, may serve as a good biomarker of the disease. The inclusion of the ApoE protein should thus be considered in any biomarker panel of AD. These candidate biomarker proteins now require validation, as their differential expression in AD may reflect the underlying pathology and course of the disease. Thus, the requirement to assess multiple candidate proteins in a single measurement results in the need to develop a multiplexed quantitative assay and determine whether the protein panel, or indeed a single protein, is a robust and valid diagnostic and/or prognostic biomarker of AD. A mass spectrometry (MS)-based approach was chosen for assay development as it offers an attractive alternative to ELISAs due to the sensitivity and selectivity of the technique, the capacity to multiplex and the ability to measure analytes for which no good quality antibodies are available, *e.g*., gelsolin (Section 1.4). The biochemistry and relation of each protein to AD in the assay under development will be discussed in detail in the following sections.

1.1.2.3 Clusterin

The glycoprotein clusterin, also known as apolipoprotein J, is a versatile molecular chaperone, so-called due to its ability to ‘cluster’ Sertoli cells involved in spermatogenesis (Fritz *et al.,* 1983; Blaschuk *et al.,* 1983; Hermo *et al.,* 1994). Clusterin is expressed in all mammalian tissues (Jones and Jomary, 2002) and has been implicated in cellular adhesion and aggregation (Silkensen *et al.,* 1995), development (French *et al.,* 1993), complement inhibition (Jenne and Tschopp, 1989) and transport of lipids (Jenne *et al.,* 1991). The precursor polypeptide chain is proteolytically cleaved, generating α and β chains. The protein structure comprises

several molecular domains including amphipathic and α-helical regions. The secondary structure of the protein contains three large disordered regions or 'molten globule domains' common to small heat shock proteins (Bailey *et al.,* 2001; Ganea, 2001). These flexible regions can bind to a wide range of molecular ligands involved in AD, including Aβ peptides and fibrils, lipids, and complement components (DeMattos *et al.,* 2001, Calero *et al.,* 2005; Trougakos and Gonas, 2002). Clusterin was first associated with AD by Caleb Finch's group where an increase in its expression was observed in the pyramidal neurons and non-pyrimidal cells of the hippocampus and entorhinal cortex of AD subjects, compared to NDCs (May *et al.,* 1990). This has been verified by several studies (Kida *et al.,* 1995; Calero *et al.,* 2000). Clusterin is highly abundant in the amyloid plaques of the AD brain and was first shown to bind to Aβ peptides by Ghiso and colleagues (Ghiso *et al.,* 1993). Several studies have demonstrated the ability of clusterin to increase Aβ solubility, stabilisation and prevent Aβ aggregation (Oda *et al.,* 1995, Matsubara *et al.,* 1996, Wilson *et al.,* 2008). The highly glycosylated and sialylated nature of the protein appears to act as a defence mechanism, masking fibrillised Aβ peptides and preventing an excessive inflammatory response (Kirszbaum *et al.,* 1992). The protein prevents the activation of the complement system and facilitates the clearance of amyloid deposits upon neuronal death (Bell *et al.,* 2007). Recently, an SNP within the clusterin gene (*CLU*) was shown to have genome-wide significant association with AD in a study of over 16,000 individuals (Harold *et al.,* 2009). The finding has since been confirmed independently (Lambert *et al.,* 2009, Seshadri *et al.,* 2010; Corneveaux *et al.,* 2010; Carrasquillo *et al.,* 2010).

1.1.2.4 Apolipoprotein E

Numerous studies have reported the apolipoprotein (APOE) genotype to be a major risk factor for early and late-onset AD (Corder *et al.,* 1993; Jones *et al.,* 2010). The human gene located on chromosome 19 contains several single-nucleotide polymorphisms (SNPs) which lead to the production of three common isoforms of ApoE, namely APOE ε2, APOE ε3 and APOE ε4 (Utermann, 1988). The substitution of

one or two amino acids results in a high degree of variability within structure and function of each isoform (Mahley *et al.,* 2006). The APOE ε4 allelle shows increased risk for AD, while the ε2 allelle is protective, by delaying onset and decreasing the risk of the disease (Corder *et al.,* 1993; Strittmatter *et al.,* 1993). Human ApoE, a 229 amino acid, 34 kDa apolipoprotein is expressed in many organs, with the highest concentrations observed in the liver, followed by the brain (Pitas *et al.,* 1987; Cedazo-Minguez and Cowburn, 2001; Grehan *et al.,* 2001). The primary source of ApoE in the latter is from non-neuronal cell types such as astrocytes and microglia. One of the main functions of ApoE in the body is the transport and metabolism of cholesterol and triglycerides (Cedazo-Minguez and Cowburn, 2001). Although the exact mechanism by which ApoE exhibits such effects in AD remains to be determined, evidence suggests this is done *via* interaction with amyloid. ApoE has been shown to bind to Aβ in SP, leading to the hypothesis that the protein plays an important role in Aβ transport, aggregation and metabolism in the brain (Wisniewski and Frangione, 1992; Naslund *et al.,* 1995). Some isoforms are more efficient than others, with studies suggesting that the ineffectiveness of the Apo ε4 variant results in increased susceptibility to AD (Jiang *et al.,* 2008). Given the importance of APOE alleles on AD risk, numerous studies have investigated the association of CSF and plasma ApoE protein levels in AD. The majority of results show no major difference in expression of ApoE in AD as compared to NDCs (LeFranc *et al.,* 1996, Mulder *et al.,* 1998). Similarly, no significant difference was observed in CSF ApoE levels among subjects with different isoforms of the gene (Wahrle *et al.,* 2007). Consistent with clusterin, ApoE has been shown to have an anti-inflammatory role in the AD brain, preventing the induction of cytokines and proinflammatory responses (LaDu *et al.,* 2001; Kim *et al.,* 2009). Clusterin and ApoE are expressed at similar levels and are the primary chaperones of Aβ in the brain (Harr *et al.,* 1996). Using transgenic mouse models, DeMattos and colleagues have shown that the two proteins work together at Aβ clearance and deposition in the brain (DeMattos *et al.,* 2004). Removal of either protein results in an increase in amyloid deposits in both plaques and CSF.

1.1.2.5 Alpha-2-macroglobulin

A2M is a member of a major group of plasma proteins which include complement components C3, C4 and C5 (Sottrup-Jensen, 1989). The protein family comprises up to 9% of total plasma protein and act as acute-phase pan proteinase inhibitors (Kovacs, 2000). Human A2M is a 720 kDa soluble glycoprotein encoded by a single copy gene on chromosome 12. The protein is composed of four identical subunits, which form two disulphide-linked dimers (Borth, 1992; Andersen *et al.,* 1995). The main function of A2M is the entrapment of proteases for subsequent lysosomal degradation (Borth, 1992). Each A2M subunit consists of a bait region, a string of 25 amino acids which is cleaved by aspartic-, cysteine-, serine- and metallo-proteinases. This cleavage event results in conformational change in the A2M-proteinase complex, inactivation of the proteinase itself and clearance by macrophages (Borth, 1992). A2M is an inhibitor of coagulation and fibrinolysis by inhibition of thrombin and plasmin, respectively (Marlar and Kressin, 1987; De Boer *et al.,* 1993). A2M was first associated with AD by the work done by Bauer in 1991. Here, an increase in A2M immunoreactivity was observed in the amyloid plaques of the hippocampus in the AD brain (Bauer *et al.,* 1991; Strauss *et al.,* 1992). The Aβ binding site is located within the bait region of each A2M subunit, resulting in a very strong affinity for Aβ peptides (Du *et al.,* 1997). The principle receptor for A2M in the brain is LRP, which facilitates Aβ internalisation in the brain (Narita *et al.,* 1997). Interestingly, LRP itself has been associated with late onset familial AD (Hollenbach *et al.,* 1998). *In vitro* studies in cultured neurons have shown A2M to be both neuroprotective and neurotoxic. The neurotoxic effect of aggregated Aβ was prevented upon binding of A2M (Du *et al.,* 1997, Hughes *et al.,* 1998). Conversely, activated A2M increased $A\beta_{25-35}$ – mediated neurotoxicity in neuroblastoma cells (Fabrizi *et al.,* 1999). The absence of LRP in these cell types resulted in an interference of A2M with TGF-β neuroprotection.

Two common polymorphisms within the A2M gene lead to increased risk of AD (Matthijs and Marynen, 1991; Blacker *et al.,* 1998; Saunders *et al.,* 2003). Both polymorphisms are associated with an increase in Aβ deposition in the brain

(Myllykangas *et al.,* 1999). However, several other case-control and family-based studies indicate no significant association of the gene polymorphisms with AD (Rogaeva *et al.,* 1999; Gibson *et al.,* 2000, Poduslo *et al.,* 2002; Bertram *et al.,* 2004).

1.1.2.6 Gelsolin

Gelsolin is a primary actin-binding protein that is involved in the capping and severing of growing and apoptotic cells (Sun *et al.,* 1999). Two monomeric molecules of actin bind to a single molecule of gelsolin in a calcium, tyrosine phosphorylation and phosphoinositide-dependant fashion (Chauhan *et al.,* 1999; Silacci *et al.,* 2004). Gelsolin, a protein of 82 - 84 kDa with six homologous subdomains (S1 - S6) is found both intracellularly in the cytosol and mitochondria and as an extracellular isoform in plasma and CSF (Kwiatowski *et al.,* 1988; Koya *et al.,* 2000; Qiao *et al.,* 2005). Both isoforms are encoded by a single gene on chromosome 9 and are a result of alternative splicing events. The secreted protein differs from the cytoplasmic version by inclusion of a 25 amino acid signalling peptide and the presence of disulphide bonds between Cys 188 and 201 (Kwiatowski *et al.,* 1988; Wen *et al.,* 1996). The protein is expressed in a wide variety of cell types indicating several alternative roles besides actin polymerisation. Gelsolin has been observed to modulate calcium channel activity and N-methyl D-aspartate receptors (Furukawa *et al.,* 1997) and plays a role in apoptosis (Kothakota *et al.,* 1997), haemostasis and inflammation (Witke *et al.,* 1995) and tumour suppression (Kuzumaki *et al.,* 1997).

Accumulating evidence has suggested that gelsolin plays an important role in AD. The protein is expressed throughout the central nervous system providing neuroprotection (Tanaka and Sobue, 1994; Endres *et al.,* 1999). Both cytoplasmic and secretory gelsolin have been shown to bind to Aβ (Chauhan *et al.,* 1999). From WB analysis and Congo red staining, gelsolin was observed to inhibit Aβ fibrillisation *in vitro* by up to 90% (Chauhan *et al.,* 1999; Ray *et al.,* 2000). In the same study it was observed that gelsolin could defibrillise pre-formed Aβ fibrils in a time-dependent manner. The anti-amyloidogenic properties of gelsolin were subsequently confirmed by

two independent studies using APP transgenic mouse models of AD (Matsuoka *et al.,* 2003; Hirko *et al.,* 2007). Increased expression of gelsolin has also been observed during periods of oxidative stress (Ji *et al.,* 2010). Interestingly, a mutation in gelsolin at Asp187Asn or Asp187Tyr results in a rare hereditary form of amyloidosis. Such mutations result in cleavage of the plasma gelsolin molecule and production of an amyloidogenic fragment (Maury *et al.,* 1997).

1.1.2.7 Serum amyloid P-component

SAP is a highly conserved plasma protein which was first identified as a component of amyloid plaques in the laboratory of A. S. Cohen (Cathcart *et al.,* 1967). SAP is a 25 kDa plasma glycoprotein produced exclusively in the liver and shares 51% sequence homology with C-reactive protein, a classical acute phase response plasma protein (Kalaria and Grahovac, 1990; Srinivasan *et al.,* 1994). It consists of five identical subunits, each consisting of 204 amino acids. SAP has been shown to bind to chromatin, DNA and glycosaminoglycans in a calcium dependent manner (Snow and Wight, 1989; Stenstad *et al.,* 1993). SAP is a component of amyloid deposits *in vivo*, including plaques in AD and NFTs (Kalaria *et al.,* 1991; Akiyama *et al.,* 1991; Pepys *et al.,* 1996). SAP can reversibly bind to Aβ fibrils *in vitro* in a highly specific and sensitive manner and constitutes up to 15% of dry mass deposits of amyloid *in vivo* (Pepys *et al.,* 1979). Although the exact physiological role of SAP remains unclear, it has been hypothesised that SAP may prevent degradation of fibrillar Aβ species and thus contribute to their persistence *in vivo* (Tennent *et al.,* 1995). Furthermore, human SAP has been shown to interact with neurons and rat brain *in vivo*, causing apoptosis and enhanced production of pro-inflammatory cytokines and Aβ (Veerhuis *et al.,* 2003; Urbanyi *et al.,* 2007). In contrast, a study using a transgenic mouse model overexpressing APP found no endogenous SAP immunoreactivity in the mouse brain (Shi *et al.,* 1999). This was in agreement with a finding of no difference in Aβ deposition between wild-type and SAP deficient mice (Togashi *et al.,* 1997). Recently, the interaction of SAP and Aβ has been identified as a possible drug target for AD using the

compound CPHPC (R-1-[6-[R-2-carboxy-pyrrolidin-1-yl]-6-oxohexanoyl] pyrrolidine-2-carboxylic acid). CPHPC has been shown to deplete circulating SAP *in vivo* leading to the destabilisation of Aβ fibrils in the CSF and AD brain (Kolstoe *et al.,* 2009). Recently, CPHPC has been shown to produce sustained depletion of >95% circulating SAP levels in 31 patients presenting systemic amyloidosis, with no significant adverse effects of either SAP depletion or CPHPC itself (Gillmore *et al*., 2010). No accumulation of amyloid was evident using SAP scintigraphy in any patient on the drug.

1.1.2.8 Fibrinogen gamma chain

Human fibrinogen is a large blood glycoprotein which is principally synthesised by hepatocytes (Wiesel, 2005). Fibrinogen occurs as a dimer, where each monomer is composed of three non-identical chains, Aα, Bβ and γ (FGG). Each peptide is encoded on chromosome four and mutations in the gene lead to disorders such as thrombophilia, dysfibrinogenemia and hypofibrinogenemia. The main Aα chain is 70 kDa and the Bβ chain 56 kDa (Herrick *et al.,* 1999). Both the charge and size of FGG is heterogeneous but the most abundant species is 48 kDa. The whole fibrinogen molecule is held together by 29 disulphide bonds between 58 cysteine residues (Herrick *et al.,* 1999; Weisel, 2005).

Inactive fibrinogen is cleaved by thrombin to form active fibrin, the principle component of blood clotting (Doolittle, 1984). Fibrinogen additionally functions as a key component of cell proliferation, angiogenesis, immunosuppression and cell migration (Herrick *et al.,* 1999). FGG has specific roles in initiation of fibrinolysis, interaction with platelets and mediating the interaction of thrombin and fibrin (Mosesson *et al.,* 2003). As AD pathology has a strong vascular component, it has been suggested that cerebrovascular dysfunction may contribute to the disease. Several groups have shown that increased concentrations of fibrinogen may result in an increased risk of AD (Lee *et al.,* 2007; Cortes-Canteli and Strickland, 2009; Cortes-Canteli, 2010). Upon reduction of fibrinogen levels using either a transgenic model of fibrinogen deficient mice or a fibrinogen inhibitor, ancrod, a significant decrease in vascular damage, BBB

permeability and neuroinflammation was observed (Suh *et al.,* 1995; Paul *et al.,* 2007). Interestingly, the same study showed the opposite effect upon reduction of fibrinogen levels by plasmin in AD mice, *i.e.,* an increase in neurovascular damage, inflammation and BBB permeability was observed. These studies reveal fibrinogen Aα, Bβ and indeed, FGG, may play a significant role in the pathophysiology of AD.

1.1.2.9 Complement C3, C3a and Factor H

The human complement system is the first line of defence against microbial infection. The innate immune system comprises over 40 plasma and membrane-associated proteins which form three activation pathways: the classical, alternative and lectin pathways (Rodriguez de Cordoba *et al.,* 2004, Donoso *et al.,* 2010). Human complement C3, the principle opsonic protein in the complement system, facilitates the activation of all three pathways (Sahu and Lambris, 2001). The protein is 185 kDa in weight, formed by a single disulphide bond and non-covalent forces between two peptide chains (termed α and β; Sahu and Lambris, 2001). Upon exposure to molecules on the surface of pathogens, each pathway leads to the formation of unstable protease complexes, the C3-convertases. These species cleave the α-chain of complement C3 to form the anaphylotoxin C3a and the active C3b (Figure 1.4; Rodriguez de Cordoba *et al.,* 2004). The C3b molecule in turn is cleaved by Factor I to form C3c and C3d, the latter of which binds to the invading microorganism, resulting in recognition for phagocytosis by neutrophils, macrophages and dentritic cells (Rodriguez de Cordoba *et al.,* 2004). This series of reactions is maintained at a relatively low level in blood allowing for targeted activation of complement on the surface of pathogens.

CFH is a key regulator of the alternative pathway, restricting the complement cascade to activating surfaces and preventing damage to host tissues. CFH is a large soluble glycoprotein of 155 kDa weight which was first identified by Nilsson and Muller-Eberhard in 1960 (Muller-Eberhard and Nilsson, 1960). The protein is constitutively produced by the liver, but also by a wide variety of peripheral cell types including lymphocytes, fibroblasts, neurons and glial cells (Schwaeble *et al.,* 1987; Friese *et al.,*

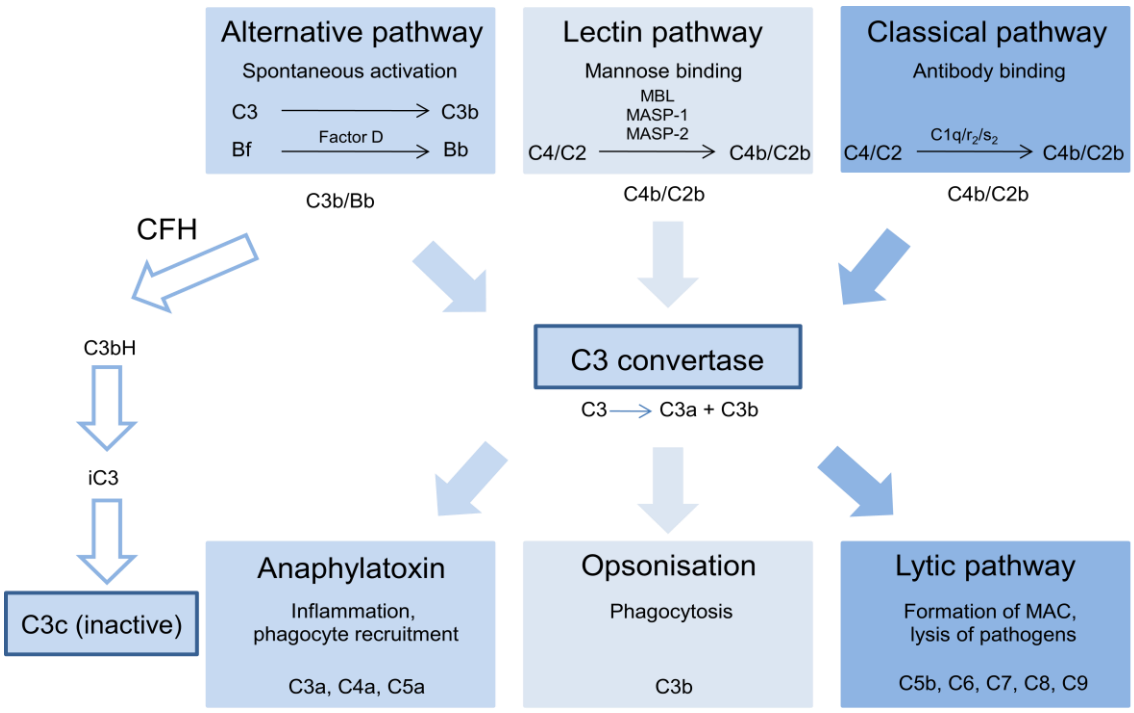

Figure 1.4 Inactivation of C3b by CFH. Upon microbial infection, complement C3 is cleaved by C3 convertase to form the anaphylotoxin C3a and C3b. C3b is further cleaved by Factor I for recognition of the pathogenic cell surface and activation of the complement cascade. The system is regulated by the inactivation of C3b by CFH, forming iC3b. The lectin pathway is activated by mannose or N-acetyl glucosamine surfaces leading to the formation of a membrane attack complex (MAC) on the cell surface leading to microbial destruction.

2000). It consists of a single polypeptide chain, composed of 20 highly conserved complement control protein modules of 60 amino acids (Ripoche *et al.,* 1988). CFH regulates complement activation by providing both cofactor activity for the factor I-mediated proteolytic inactivation of C3b and accelerating the decay of the alternative pathway C3-convertase, C3b/Bb (Weiler *et al.,* 1976; Pangburn *et al.,* 1977).

Given the importance that CFH plays in the regulation of complement, specific mutations or SNPs within the CFH gene, located on chromosome one, can impair the release of CFH into circulation. This results in uncontrolled complement activation described by several pathologies (Rodriguez de Cordoba *et al.,* 2004). Such instances include age-related macular degeneration (AMD), atypical haemolytic uraemic syndrome and glomerulonephritis (Hageman *et al*, 2005; Atkinson and Goodship, 2007; Hakobyan *et al.,* 2010; Donoso *et al.,* 2010). Indeed, AD and AMD share similar genetic

and biochemical features (Johnson *et al.,* 2002; Ding *et al.,* 2008) and an AMD-associated SNP within the CFH gene (the Y402H polymorphism) has been associated with increased risk for AD (Thakkinstian *et al.,* 2006; Zetterberg *et al.,* 2008). However, the result is not definitive, as prospective and cross-sectional studies from another study suggest that the CFH gene polymorphism is not a genetic determinant for AD (Le Fur *et al.,* 2010). However, it has been shown that Aβ is present in drusen, the hallmark extracellular deposit in AMD (Dentchev *et al.,* 2003). Recently, it has been shown the CFH is present in Aβ plaques in AD (Strohmeyer *et al.,* 2002). Here, the co-localisation of Aβ, heparin sulphate proteoglycan (agrin) and activated microglia (containing CFH receptors) was observed (Strohmeyer *et al.,* 2002). These findings may be of significant interest in understanding the roles of complement C3, C3a and CFH in AD.

1.1.3 Statistical tools for biomarker analysis

Biomarkers may serve several different purposes. These include the ability to provide a reliable disease diagnosis and assessment of disease severity. Additionally, biomarkers may be used for the prediction of drug treatment effects, monitoring of therapeutic interventions and for for risk stratification*, i.e*., the identification of those patients who may experience positive or negative effects upon exposure to a disease intervention. For each of these goals, it is imperative to understand the pathophysiological processes associated with the biomarker, including the synthesis and degradation of the biomarker, its kinetics and its physiologic effects (Ray *et al*., 2010).

The diagnostic performance of a given biomarker is typically estimated by its sensitivity and specificity. Sensitivity measures the proportion of actual positives which are correctly identified as such (*i.e.*, a true positive), whereas specificity measures the proportion of negatives which are correctly identified (*i.e.*, a true negative). The calculation of such indices requires prior knowledge of a subjects “true” disease state and a prediction based on the biomarker (*i.e.*, disease is predicted to be present or absent) to construct a 2 x 2 contingency table (Table 1.3; Ray *et al*., 2010).

Theoretically, optimal prediction aims to achieve 100% sensitivity and 100% specificity. The positive predictive value is the proportion of patientss who test positive for a given test who are correctly diagnosed (Altman and Bland, 1994). Its value depends on the prevalence of the outcome of interest, which can vary from one population to another. Similarly, the negative predictive value is the proportion of subjects who test negative for a given test who are correctly diagnosed. A further way of describing the prognostic or diagnostic value of a biomarker is by calculating the likelihood ratio. This corresponds to the ratio of the likelihood of the observed test result in the diseased *versus* non-diseased populations (Ray *et al*., 2010). Liklihood ratios are not dependant on the prevalence of the disease and are therefore considered as a robust global measure of the diagnostic properties of a test.

	Disease		
Biomarker	Present	Absent	Total
Positive	a (true positive)	b (false positive)	a+b
Negative	c (false negative)	d (true negative)	c+d
Total	a+c	b+d	a+b+c+d

Table 1.3 Primary diagnostic parameters used in biomarker analysis. Prevalence = (a + c)/(a+b+c+d); sensitivity = a/(a + c);specificity = d/(b + d); positive predictive value = a/(a + b);negative predictive value = d/(c + d); accuracy = (a + d)/(a+b+c+d); positive likelihood ratio (LHR+) = sensitivity/(1 -specificity); negative likelihood ratio (LHR-) = (1 - sensitivity)/specificity. Extracted from Ray *et al*., 2010.

To determine the accuracy of a given biomarker, a receiver operating characteristic (ROC), or ROC curve, is a simple graphical plot of the sensitivity, or true positive rate *versus* the false positive rate (1 − specificity; Figure 1.5) of diagnostic performance. The area under the receiver operating characteristic curve (AUC) is the most frequently used measure of the ability of a biomarker to distinguish between two populations, *e.g*., case and controls. This is equivalent to the probability that the biomarker is higher for a diseased patient than a control and, thus, is a measure of discrimination (Ray *et al*., 2010). Sensitivity cannot be interpreted without specificity and thus, when reading from the curve, if sensitivity = 0.50, then specificity = 0.50. Similarly, if sensitivity = 0.80, then specificity = 0.20 and *vice versa*. Generally, biomarkers are

considered as having good discriminatory properties when the AUC is > 0.75 and as excellent when the AUC is > 0.90.

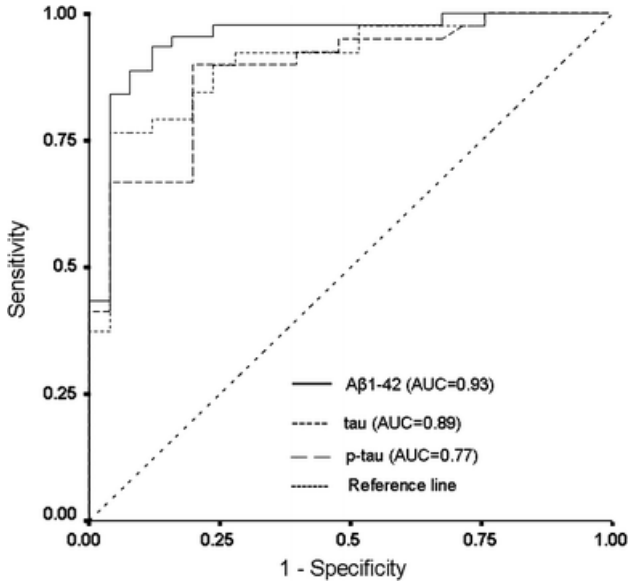

Figure 1.5 ROC analysis used to characterise the performance of a biomarker. For each candidate AD biomarker, $A\beta_{1-42}$, tau and p-tau, the sensistivity, specificity and AUC is extracted from the plot (Welge *et al*., 2009).

The ROC curve is used to determine a clinical cut-off point to make a clinical discrimination (Fan *et al*., 2006). The calculation of an appropriate cut-off value is usually a trade-off between specificity and sensitivity. As both change with each cut-off value, it becomes difficult to determine which cut-off point is ideal. Preferably, the the most appropriate cut-off value provides the highest sensitivity and the highest specificity. Nonetheless, it is infrequent that this ideal is achieved. Thus, one may opt to choose a higher sensitivity at the cost of lower specificity. In an effort to avoid providing a single cut-off that dichotomises the population, it has been proposed to provide two cut-off points surrounding a “grey zone” (Ray *et al*., 2010). The first cut-off point is chosen to exclude the diagnosis with near-certainty, while the second is chosen to include the diagnosis with near-certainty. If a value falls into the grey zone between the two cutoffs, uncertainty exists, and a diagnosis should be persued by other means. Such an approach is more beneficial from a clinical perspective and is therefore more widely used in clinical research.

Finally, before undertaking any large scale biomarker study, *e.g*., such as in clinical trials, it is imperative to perform an *a priori* calculation to determine the minimum sample size required so that one can be reasonably likely to detect an effect of a given cohort. Factors influencing such power calculations include the statistical significance measure used in the test, the sample size used to detect an effect and the magnitude of the effect of interest in the population (Muncer *et al*., 2002).

1.2 Mass spectrometry for biomarker discovery and validation in blood

1.2.1 Proteomic analysis by mass spectrometry

Proteomic techniques, incorporating the separation, identification, and quantitation of peptides and proteins, are becoming increasingly popular for biomarker discovery and validation. It has become apparent that human disorders such as AD are largely characterised by their protein complement. This was first noted upon completion of a full sequence for the human genome in 2004, where approximately 20,000 - 25,000 protein-coding genes were identified (International Human Genome Sequencing Consortium, 2004). This compares to the estimated 100,000 protein forms in man. Alternative-splicing, protein degradation and post-translational modification (PTM) events have been proposed to explain such a discrepancy. The term 'proteome' was first coined by Marc Wilkins in 1994 when describing the protein map of *Escherichia coli* and has since gained widespread popularity for the description of protein populations across dynamic biological matrices, none more so than in human blood plasma (Wasinger *et al.,* 1995; Wilkins *et al.,* 1996).

MS is being ever more applied to the proteomic profiling of plasma. Here, it is used for the determination of molecular mass and elemental composition of proteins. Further, MS-based proteomics allow for the quantitative comparison of proteins expression levels in healthy controls and disease-affected individuals. Mass spectrometers measure ions according to their mass-to-charge (*m/z*) ratio. Peptide analysis using modern day instruments is typically divided into four distinct phases; 1) molecular ionisation 2) mass analysis 3) peptide fragmentation and 4) ion detection.

1) Molecular ionisation: The principle of ionisation is the generation of gas-phase ions which can then be separated according to *m/z* in the mass analyser. Several types of ionisation techniques exist of which matrix-assisted laser desorption ionisation (MALDI; Karas and Hillenkamp, 1988) and electrospray ionisation (ESI; Fenn *et al.,* 1989) are the most common for the ionisation of proteins. ESI was used for the

proteomic analysis in this thesis, and thus, will be described in detail. ESI was first described for the ionisation of small molecules by Malcolm Dole in 1968 and was first used for ionisation of biological macromolecules in the kDa range by John Fenn in 1988 (Dole *et al.,* 1968; Fenn *et al.,* 1989). ESI is referred to as a 'soft' ionisation as very little energy is retained by the molecule after ionisation. The process involves the production of ions in the liquid phase at atmospheric pressure (Figure 1.6). Peptides and proteins are initially dissolved in water and volatile organic solvents such as methanol or acetonitrile (ACN) containing small volumes of acid (*e.g.,* formic acid; FA) for increased conductivity.

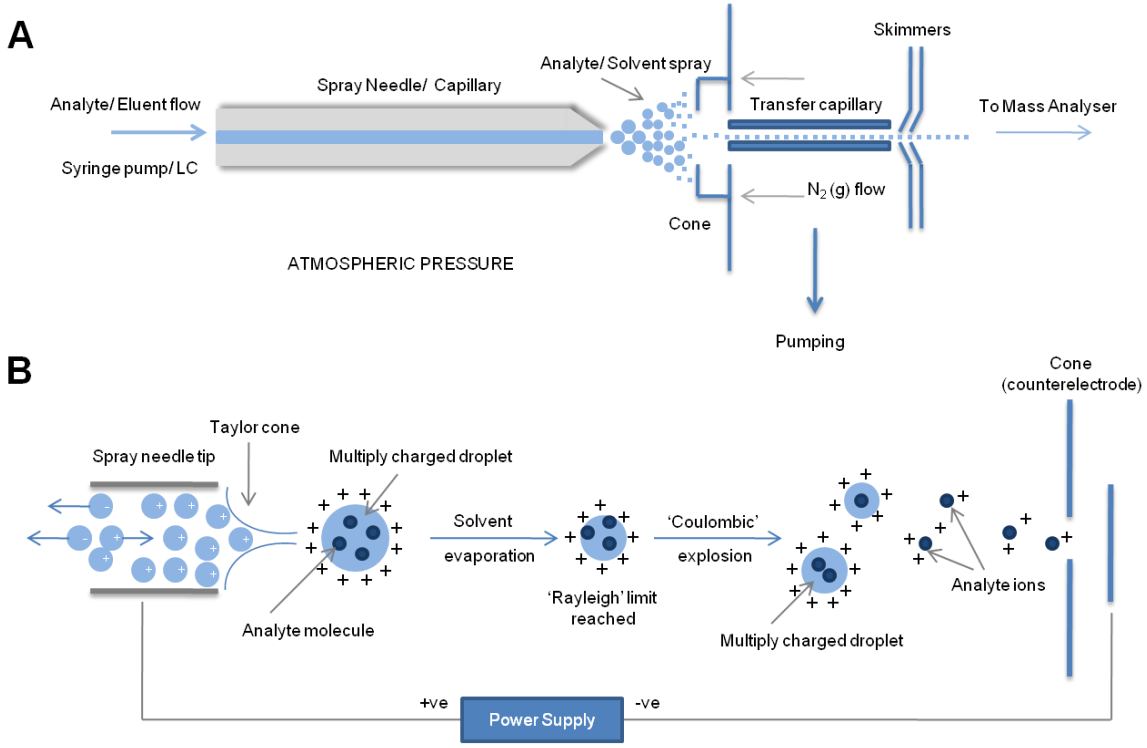

Figure 1.6 Formation of ESI. **A** Sample is introduced into the source from a syringe pump or HPLC system. As the sample flows through the electrospray needle, a high potential difference is applied, producing a spray of charged droplets, which can be either positively (as above) or negatively charged, depending on the nature of the analysis. The droplets are driven from the needle towards the source cone, aided by a nebuliser gas such as nitrogen. As the droplets travel between the needle tip and the cone, solvent evaporation occurs. If the applied field is sufficiently high, the solvent becomes unstable producing a fine jet of ions known as the 'Taylor cone' (Taylor, 1964). **B** Continual solvent evaporation forces droplet shrinkage until a point is reached where the surface tension can no longer sustain the charge (the Rayleigh limit). A 'Coulombic explosion' occurs and the droplet falls apart. The process produces smaller charged droplets and charged analyte molecules for entry and separation in a mass analyser (Figure adapted from www.chm.bris.ac.uk/ms/theory/esi-ionisation.html).

Prior to ESI or MALDI, analysis of large macromolecules such as peptides and proteins was problematic, as molecules with masses beyond 1000 Da could not be easily transferred into the gas phase and ionised with high efficiency. The advent of ESI, however, enabled a series of small multiply charged peptide ions to be produced, opening up entirely new areas of research in biochemistry. A further advancement of the technique was described by Wilm and Mann in 1996, namely, nanospray ionisation. This permits analytes to be introduced into the source at nanolitre flow rates (20 - 40 nL/min, compared to µL/min flow rates for ESI), which then become ionised within a miniaturised electrospray source (Wilm and Mann, 1996). The ionisation process produces droplets less than 200 nm, which are between 100 - 1000 times smaller than with conventional electrospray sources. The low flow rates associated with nanospray ionisation allow for extended sample analysis, enabling the characterisation of proteins down to attomole levels (Onisko *et al.,* 2007).

2) Mass analysers: The function of a mass analyser is to separate ions according to *m/z*. Several types of mass analyser exist that are suited to biological MS, including time-of-flight (Tof), quadrupole, ion trap, Fourier transform ion cyclotron resonance (FT-ICR) and Orbitrap (Comisarow and Marshall, 1974; Wollnik, 1993; Makarov, 2000; Hu *et al.,* 2005). Mass analysers are defined by their 'upper mass limit', *i.e.,* the highest *m/z* that they can measure, their mass accuracy and sensitivity, and their ability to resolve two distinct ions with a small mass difference (de Hoffmann and Stroobant, 2002). As both Tof and quadrupole mass analysers were used for MS analysis in this thesis, both shall be described in detail in subsequent sections.

3) Peptide fragmentation: Collision-induced dissociation (CID) is the most widely used technique for molecular ion fragmentation in MS (Wells and McLuckey, 2005). Here, gas phase peptide/protein cations in positive ionisation mode are accelerated by electrical energy to a higher kinetic energy and collide with neutral gas atoms (usually helium or argon). A proportion of this energy is converted into internal energy which causes fragmentation of the peptide into smaller ions. Fragmentation occurs along the peptide backbone at the C-N bond releasing a b-ion series from the

N-terminus and a y-ion series extending from the C-terminus (Figure 1.7). The signature ladder of b- and y-ions is diagnostic of the peptide amino acid sequence (Roepstorff and Fohlman, 1984).

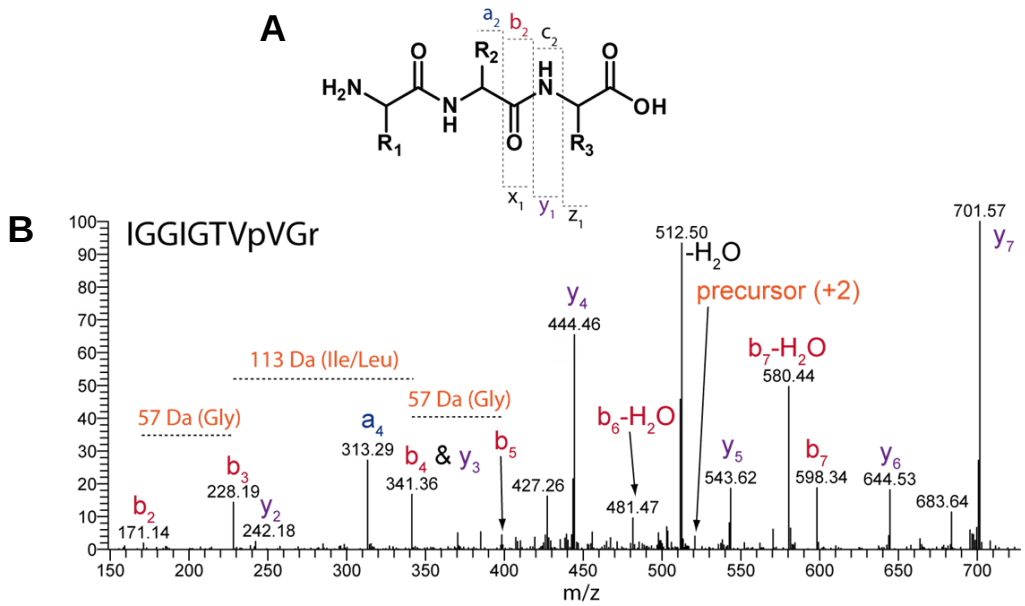

Figure 1.7 Fragmentation of peptides **A** Peptide fragment nomenclature is dependent on the backbone bond which is cleaved, whether the fragment contains the N- or C-terminus and the position along the peptide chain. For example, the b- and y-designations correspond to cleavage at the amide bond. Thus, a-, b- and c-ion types contain the N-terminus, whereas the x-, y- and z-ion types contain the C-terminus. The subscript number is the residue number relative to the terminus that the fragment contains. The remaining letters correspond to cleavage at additional bonds. **B** An MS/MS spectrum of doubly protonated IGGIGTVpVGr peptide, where p and r are "heavy" proline and arginine residues, respectively. The spectrum is dominated by the b- and y-ion series, providing good coverage of the peptide sequence. (http://www.lamondlab.com/MSResource/LCMS/MassSpectrometry/peptideFragmentation.php).

4) Ion detection: Following separation of ions according to their *m/z*, a detector is necessary to convert the ion signal into visual representation or mass spectrum. Typically, detectors record the charge induced or current produced when an ion hits a surface (Figure 1.8). To amplify the signal produced by experimental ions in a Tof instrument, a microchannel plate is generally used. For quadrupole instruments, this is performed by a conversion dynode and electron multiplier. The amplification of current provided by an electron multiplier is typically of the order of 10^5 to 10^6 for a singly charged ion hitting the entrance of the electrode.

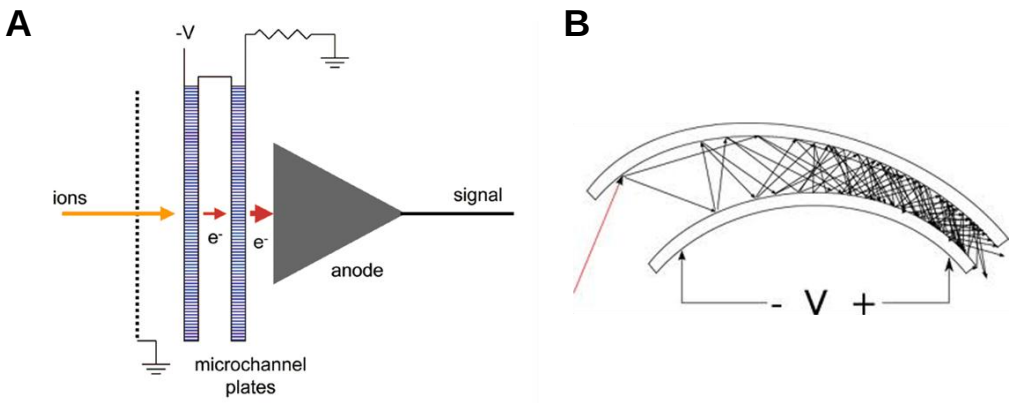

Figure 1.8 Ion detectors **A** Microchannel plate detectors are typically used in Tof instruments. Each plate is a continuous-dynode electron multiplier, in which the multiplication of electrons (e^-) takes place in the presence of a strong electric field (http://en.wikipedia.org/wiki/File:Mcp_schematic.gif). **B** Electron multipliers are found in quadrupole instruments. The multiplier is a vacuum-tube structure that multiplies incident charges. (http://en.wikipedia.org/wiki/File:Electron_multiplier.svg).

1.2.1.1 Time of flight and quadrupole mass analysers

The ToF mass analyser was first conceptualised by W.E. Stephens in 1946, and the design for the first commercial instrument was proposed by Wiley and McLaren in 1955 (Stephens, 1946; Wiley and McClaren, 1955). Advantages of Tof MS are its high sensitivity (all ions are transmitted and detected with high efficiency) and speed of analysis (full spectra can be obtained in msec and virtually unlimited mass range). Ions are accelerated into the Tof tube from the ion source (or other mass analyser) as a pulse (Figure 1.9). All ions of the same charge receive the same kinetic energy and so their velocity is inversely proportional to their mass. Ions are separated according to *m/z* in a field free drift zone (Figure 1.9). The time taken for each ion to travel along this drift zone to a detector of known distance is recorded. Lighter molecules travel faster than heavier ones and arrive at the mass detector first. Ions of the same *m/z* will reach the detector at the same time. Inclusion of a reflectron system corrects for differential energy distribution between ions of the same *m/z*. More energetic ions penetrate further into the reflectron system than less energetic ones, resulting in all ions of the same *m/z* reaching the detector at the same time. This greatly improves resolution and

in parallel, increases the length of time taken to reach the detector, allowing for improved separation of ions.

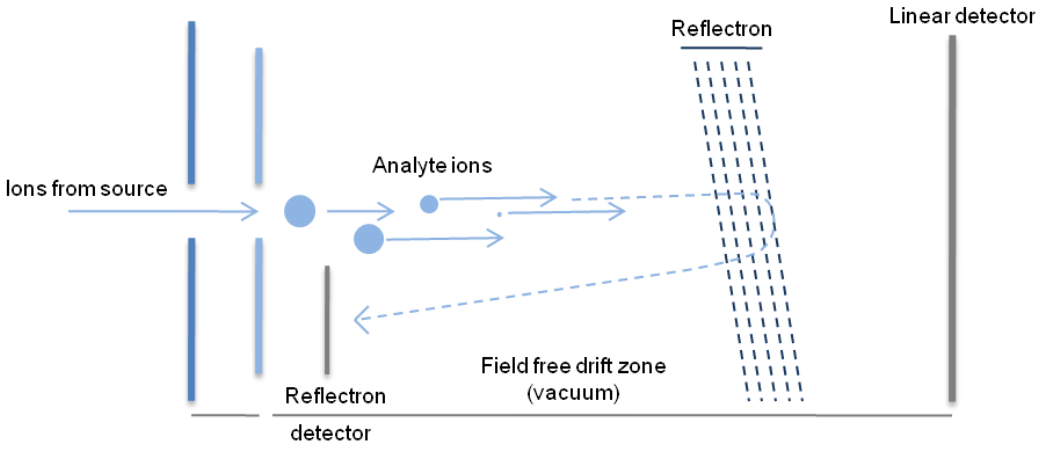

Figure 1.9 Principle of ToF mass analysers. Ions are separated according to *m/z* and acceleration in the flight tube (Figure adapted from www.chm.bris.ac.uk/ms/theory/esi-ionisation.html).

Quadrupole mass analysers consist of four metal rods which are parallel to each other. The rods may be cylindrical, or ideally, hyperbolic. The invention of the quadrupole is attributed to Wolfgang Paul who shared the Nobel Prize in Physics in 1989 for this work (Paul and Steinwedel, 1953). The separation of ions in a quadrupole is based on their trajectory stability in oscillating electric fields (de Hoffmann and Stroobant, 2002). Opposite rods are electrically paired with a fixed direct current (DC) and alternating radiofrequency (RF) applied between them. Ions from the source enter the quadrupole and are separated according to *m/z* based on the ratio of a particular set of voltages applied (Figure 1.10). Ions which do not complement a pre-defined RF/DC ratio will become unstable and collide with the rods. This enables the selection of ions of a particular *m/z* or a full scan of a specified *m/z* range by varying the voltages applied. The advantages of quadrupole mass analysers are their high sensitivity and high scan speeds. However, disadvantages include lower mass resolution, *i.e.*, 4,000 FWHM compared to 10,000 FWHM on Tof instruments and similarly, a lower *m/z* range *i.e.*, 4,000 compared to 10,000 on Tof instruments.

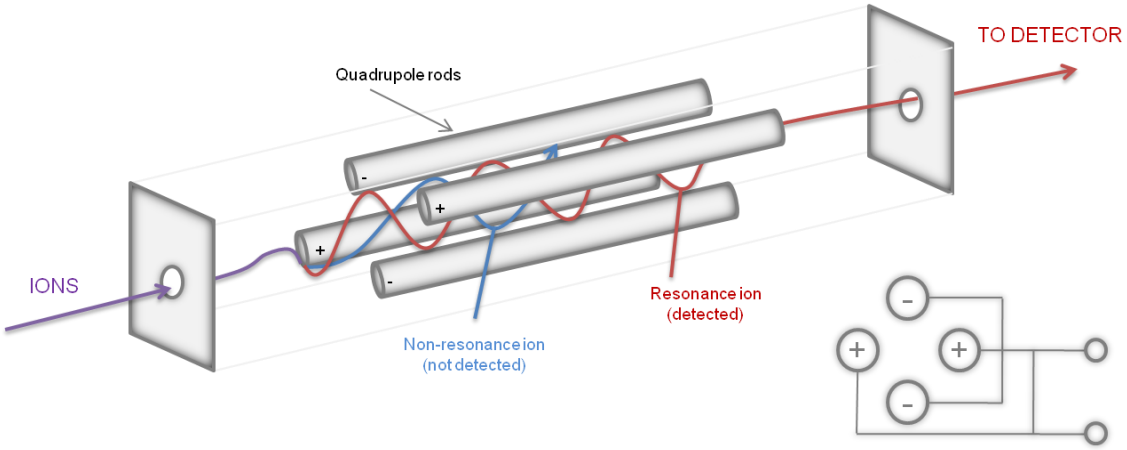

Figure 1.10 Layout of a quadrupole mass analyser. The system consists of four parallel rods which separate ions according to *m/z* based on the ratio of a particular set of voltages (DC/RF) applied (Figure adapted from www.chm.bris.ac.uk/ms/theory/esi-ionisation.html).

Several mass analysers can be arranged in tandem, depending on the type of analysis required. Two different MS formats were used in this thesis, a QTof and a triple quadrupole. QTof consists of a ToF and quadrupole mass analyser (Figure 1.11 A). Triple quadrupole mass spectrometers consist of a series of three quadrupoles (Figure 1.11 B and C). The first (Q1) and third (Q3) quadrupole can operate as mass filters, encompassing a central quadrupole ion guide (Q2) which has separate functionality such as a collision cell. The Q3 quadrupole can additionally be used for ion trapping and MS/MS (McLuckey *et al.,* 1994). Ions enter Q1 from the source where they can be separated by RF and DC according to *m/z*. Ions of a particular precursor *m/z* can then be selectively filtered to undergo fragmentation by low-energy CID in the RF-only Q2. MS/MS fragment ions are then ejected from Q2 for full scanning or fragment ion selection by alternate RF and DC voltages in Q3.

Triple quadrupole mass spectrometers enable a variety of different scan functions (Figure 1.12). 'Product ion scanning' selects ions of a particular *m/z* in Q1 to undergo fragmentation in Q2. The full range of precursor fragment ions is then scanned in Q3. This experiment is useful for providing peptide sequence information. 'Precursor ion scanning' scans the full *m/z* range of precursor ions in Q1 and a particular fragment ion can be selectively measured in Q3.

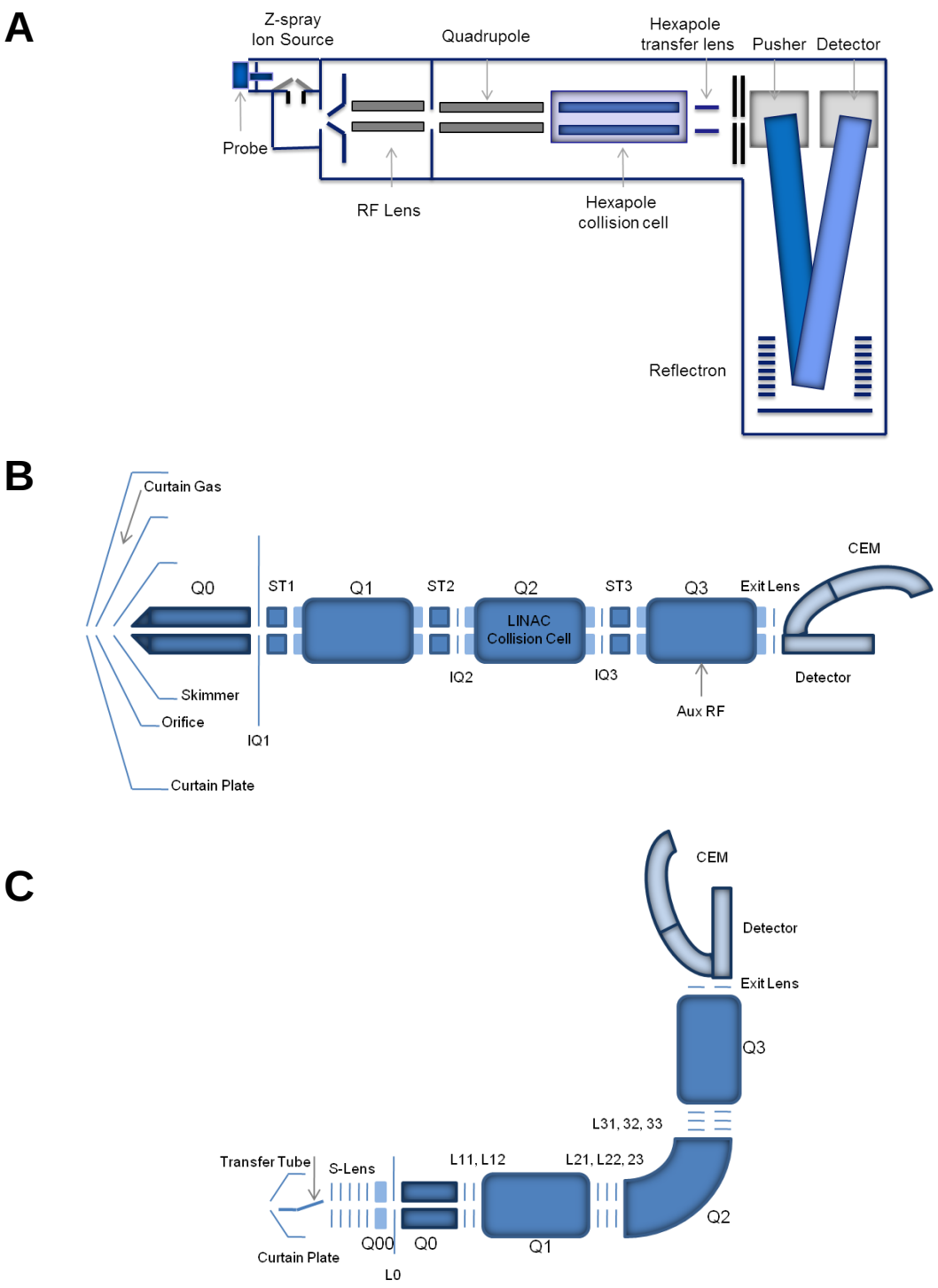

Figure 1.11 Layout of utilised mass spectrometers. **A** Layout of a QTof micro instrument consisting of a quadrupole and Tof tube with a reflectron system for improved separation of ions **B** Layout of a 4000 QTRAP® instrument consisting of a linear arrangement of three quadrupoles in tandem (Q1, Q2 and Q3). Ions enter Q0 from the source and are focused between quadrupoles by a series of stubby lenses (ST) for detection at the channel electron multiplier (CEM). **C** Layout of a TSQ Vantage instrument. Three quadrupoles are arranged in tandem, enabling a wide variety of scan functions. Ions are focused into the instrument *via* the S-Lens and through quadupoles *via* a series of lenses (*e.g.,* L11, L12). In both 4000 QTRAP® and TSQ Vantage instruments, peptide fragmentation occurs by CID in Q2.

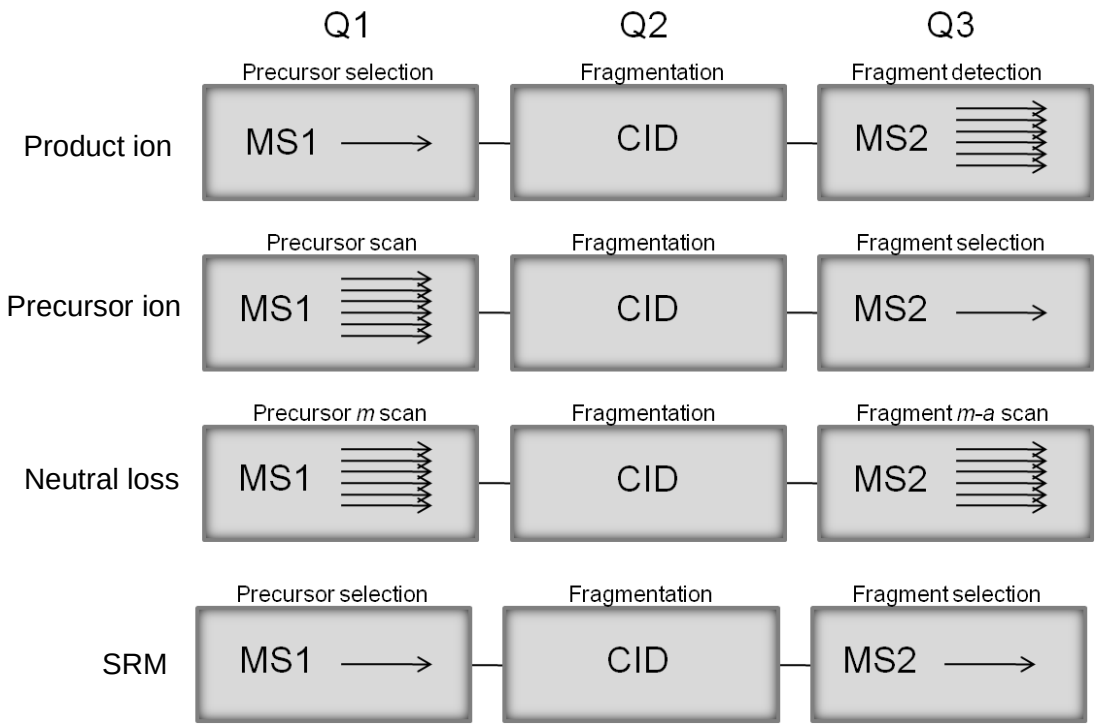

Figure 1.12 Primary scan functions of mass analysers. Scan functions are shown for triple quadrupole mass analysers, however, each can additionally be performed on QTof instruments (adapted from Hüttenhain *et al.,* 2009).

In a third scan mode, scanning occurs in the Q1 and Q3 mass analysers, but with a constant mass offset between both. Here, the exclusive loss of a molecule of sought mass, *e.g.,* 18 mass units for H_2O, upon fragmentation of a precursor ion is specifically measured in Q3. This type of 'neutral loss scanning' has particular utility in the measurement of peptide PTMs such as phosphorylation or glycosylation (Hager, 2003). Another scan mode which is commonly used on a triple quadrupole mass spectrometer is selected reaction monitoring (SRM). Here, Q1 of a triple quadrupole instrument is set to allow only specific precursor ions of a set *m/z* through. Selectivity for this particular ion is further achieved by setting Q3 to measure specific MS/MS fragment ions arising from the precursor being measured in Q1 (Figure 1.12). SRM is sensitive, selective, fast and quantitative. An added advantage of SRM is that analyses can be multiplexed, allowing the measurement of many peptides at any one time.

1.2.1.2 Reversed phase-high performance liquid chromatography

The complex and dynamic nature of the human plasma proteome presents an enormous technical challenge. The search for potential biomarkers needs a separation technique that would enable the analysis of a large number of samples in a relatively short time. High-performance liquid chromatography (HPLC) is a technique which allows for the separation and purification of complex mixtures of proteins or peptides prior to MS analysis, in a feasible time-scale for biomarker studies (Bączek *et al*., 2005). Prior to the 1970's, limited reliable chromatographic techniques were available to the laboratory scientist and methods which did exist, *e.g.,* open-column and thin layer chromatography, were inadequate for robust quantitation of compounds and resolution between similar species. The advent of HPLC revolutionised the analysis of peptides by MS, enabling faster and more reproducible separation of complex biological matrices such as plasma (Gygi *et al*., 2002). The improvement of LC column packing materials and the additional convenience of on-line detectors further revolutionised the approach. Peptide analysis by MS typically uses up-front reversed-phase (RP) chromatography (Washburn *et al*., 2001; Davis *et al*., 2001; Horvatovic *et al.,* 2010). RP-HPLC separates peptides according to their hydrophobicity over a gradient of increasing solvent, *e.g.,* ACN or methanol. Analytes with greater hydrophobic surface area (due to C-H or C-C) have longer retention as the molecule's non-polar surface area is non-interacting with water. Polar groups (-OH, $-NH_2$, COO^- or $-NH_3^+$) reduce retention as they are readily integrated into water. Resolved peptides are eluted from the RP column for entry into the mass spectrometer. RP-HPLC is compatible with MS as the chromatographic solvent typically contains acid, which aids molecular ionisation. Separations can be performed at nanoflow LC rates (*i.e.,* nL/min) for nanospray ionisation sources or microflow LC rates (*i.e.,* µL/min) for ESI.

HPLC retention time (t_R), is a chemical structure dependent parameter, which is maintained for a given analyte in particular separation conditions including temperature, pH, mobile phase and stationary phase composition (Bączek and Kaliszan, 2009). Consequently, prediction of the t_R for a given peptide structure could

be helpful to improve the confidence of peptide identifications and to increase the number of correct peptide identifications. Such knowledge is particularly useful when designing SRM experiments, in order to classify which peptides would provide the most robust quantitative information: hydrophilic peptides are poorly retained on the stationary phase, while very hydrophobic peptides may have tailing effects, will elute late, or may even stick on the LC column. Poor chromatographic performance may also add to an increased chemical background (Gallien *et al*., 2011). Several software packages have recently become available to aid in t_R prediction for LC-MS/MS experiments (Petritis *et al*., 2003; Bączek *et al*., 2005; Krohin *et al*., 2006; Gorshkov *et al*., 2006). In one such example, sequence-specific retention calculator (SSRCalc) was developed for t_R prediction of tryptic peptide digests during RP-HPLC (Krohkin *et al*., 2006). The algorithm was applied using a test library of 2,000 peptides and an array of biological samples. Good correlation between predicted and experimental t_R were found. Furthermore, the software helped in significantly reducing the instrument time required for a complete analysis of a digest separated by RP-HPLC.

1.2.2 Global mass spectrometry quantitation strategies

Global quantitation of peptides and proteins is the preferred strategy for the initial screening of patient populations in biomarker discovery. Such techniques generate extensive lists of candidate proteins for further evaluation by more targeted quantitative methods to determine a candidate biomarker's full diagnostic and prognostic utility. Biomarker quantitation strategies can incorporate both relative and absolute quantitative techniques. In relative quantitation, a comparison is made between changes in protein/peptide abundance in a given sample relative to another reference sample, *e.g*., an untreated control sample. Such methods require the least amount of optimisation. For absolute quantitation, quantitation of unknowns is based on a known quantity. Initially, a standard curve is created, from which, the quantity of unknown analyte is extrapolated. For such methods, it is essential to determine the

accurate value of the standard for which the unknown is being compared, and usually requires extensive method optimisation and validation.

Traditionally, global strategies have incorporated 2DE technology for the relative comparison of protein abundance across case and control groups. However, 2DE is limited due to its low dynamic range, high costs and low throughput. More recently, improvements in MS-based methods for the profiling and quantitation of complex biological mixtures have resulted in these approaches garnering more widespread popularity where biomarker discovery is being pursued. MS-based approaches for biomarker discovery encompass LC-MS and LC-MS/MS in conjuction with label-free or peptide/protein labeling approaches. Each technology will be discussed in the following sections.

1.2.2.1 Two dimensional gel electrophoresis

2DE allows for the separation of complex mixtures of proteins such as plasma based on differences in isoelectric point (pI), in the first dimension, and by molecular weight (*Mr*) in the second dimension. Separated proteins can then be visualised by binding to a Commassie or Silver stain (Sasse and Gallagher, 2004). Protein spot densities between two samples, *e.g.,* control and disease samples are compared to provide relative differences between the two populations. When combined with MS, peptide components of a gel spot can be identified. 2DE was first described in 1975 by independent studies on *E. coli* (O'Farrell, 1975) and mouse tissue (Klose and Spielmann, 1975). The method was rapidly applied to the separation of plasma, where approximately 300 proteins were successfully separated and visualised (Anderson and Anderson, 1977). Following this, the same group produced a more comprehensive database of plasma proteins, where 727 spots were fully resolved by 2DE, of which 376 were identified as 49 different proteins (Anderson and Anderson, 1991).

Since its inception, 2DE has proved popular in biomarker discovery studies in a range of biofluids and tissues with a plethora of publications released. 2DE studies in CSF and plasma have produced several interesting candidate biomarkers of AD,

cancer and Downs syndrome (Myrick *et al.,* 1990; Cochran *et al.,* 2003; Ahmed *et al.,* 2004; Davidsson and Sjögren, 2005; Hye *et al.,* 2006; Korolainen *et al.,* 2006; Maarouf *et al.,* 2009; Roher *et al.,* 2009). However, 2DE technology is limited to a low dynamic range of quantitation and the inability to separate and quantitate highly acidic, basic or hydrophobic proteins (Davidsson and Sjögren, 2005). Further, a large number of repeat analyses are required to minimise between-gel variances. This can be both costly and time-consuming. Differential gel electrophoresis (DIGE) is an extension of 2DE, which has addressed some of the problems associated with the technology. Here, the relative quantitation across protein populations is provided by differential fluorescence labeling (Unlü *et al.,* 1997; Gharbi *et al.,* 2002). DIGE has been used to detect protein expression changes in the CSF of neurological disorders such as dementia as well as cancer biomarker discovery studies (Maurya *et al.,* 2007; Kondo and Hirohashi, 2009; Tumani *et al.,* 2010).

1.2.2.2 LC-MS and LC-MS/MS-based biomarker profiling strategies

1.2.2.2.1 Label-free

Label-free quantitation methods are increasingly becoming more popular in biomarker discovery studies due to their clean, fast and less complex quantitation results (Old *et al.,* 2005; Patel *et al.,* 2009). Quantitation is generally performed by two different strategies: relative quantitation by alignment of RP-HPLC traces and comparison of peak intensities of MS ions or spectral counting of ions upon MS/MS analysis (Washburn *et al.,* 2001; Bondarenko *et al.,* 2002). The general hypothesis for peptide quantitation based on LC chromatograms and retention time is that during LC-MS/MS analysis, an ion of a particular *m/z* will be detected at a particular intensity and at a particular time. Label-free approaches have been used for biomarker discovery studies in sera and CSF of schizophrenia patients (Levin *et al.,* 2007; Huang *et al.,* 2007), Gaucher patients (Vissers *et al.,* 2007) and cancer (Xue *et al.,* 2010; Lengqvist *et al.,* 2009). Absolute quantitation between *E. coli* peptide populations has been demonstrated using solely accurate mass and retention time in combination with LC-

MS^E (Expression) mode (Silva *et al.,* 2005; Levin *et al.,* 2007). Here, the quadrupole mass analyser is set to transfer all ions as the collision cell switches from low to high collision energy intermittently during the course of the acquisition time. One of the main difficulties in label-free quantitation based on the alignment of LC chromatograms is the normalisation of the data to allow for the direct comparison of LC-MS/MS runs. There is a strict requirement for reproducible sample preparation and upfront fractionation as well as high resolution and highly reproducibility in online chromatography (Old *et al.,* 2005). Further, ion suppression may affect target analytes. This is a result of the presence of less volatile compounds that may change the efficiency of droplet formation or evaporation, which can alter the amount of charged ion in the gas phase that ultimately reaches the detector (Annesley, 2003). Such phenomena could perhaps have been compensated for by the inclusion of isotopically-labeled reference peptides.

There has been a large increase in the number of bioinformatics tools available to aid in the comparative analysis of label-free quantitation (Fischer *et al.,* 2006; Finney *et al.,* 2008; Haqqani *et al.,* 2008). Indeed, these also have utility in the analysis of stable isotope labeled experiments. Over 20 software packages are currently available which typically include processing parameters for data normalisation, LC-MS alignment for peak detection and matching and statistical packages for quantitation (America and Cordewener, 2008; Vandenbogaert *et al*., 2008). Perhaps the most popular of these include the accurate mass tag (AMT) approach and DeCyder^{TM} MS from GE Healthcare. AMT was developed in 2000 in response to metabolic labeling studies using FT-ICR MS (Conrads *et al.,* 2000). AMT later evolved to allow for label-free quantitation on the Micromass Q-Tof (Strittmatter *et al.,* 2003). DeCyder^{TM} MS transforms LC-MS/MS data into a virtual 2D gel format, where retention time is displayed on the *x*-axis, *m/z* on the *y*-axis and relative abundance on the *z*-axis. It consists of a PepDetect module for peptide detection and a PepMatch module for LC-MS matching (Johansson *et al.,* 2006). Quantitation is performed by comparing peak volumes of equivalent ‘spots’. Experimental ratios of peptides between samples can then be exported in database search engines for peptide and protein identification.

In the spectral counting approach, quantitation is based on the number of MS/MS scans per peptide (Washburn *et al.,* 2001). Proteins of higher abundance should produce a greater number of proteolytic peptides, which is reflected in an increase in protein sequence coverage, an increase in the number of unique MS/MS scan events and an increase in the total number of identified peptides. The concept has been extended to quantitation of absolute protein levels. The protein abundance index (PAI) was devised by Matthias Mann's group where the total number of all possible tryptic peptides of a protein is divided by the number of experimentally observed peptides within the *m/z* range of a given instrument (Rappsilber *et al.,* 2002). This was subsequently advanced into an exponentially modified form, emPAI (equal to 10^{PAI} minus one) for absolute quantitation, which is proportional to protein abundance in a mixture (Ishihama *et al.,* 2005). This successfully allowed for the absolute quantitation of 46 proteins in a mouse whole cell lysate.

1.2.2.2.2 Peptide labeling using differential isotopic coding

Peptide and protein quantitation by differential isotopic labeling is perhaps the most widespread and frequently used method in current biomarker discovery studies (Figure 1.13). Here, peptides are differentially coded by tagging with light or heavy versions of stable isotopic reagents, mixed and subsequently analysed together in the mass spectrometer. The relative comparison of the mass spectral signals of the isotopically-differentiated peptides determines up- or down-regulation of a species, when a known amount of internal standard is included. The concept of isotope dilution was first introduced in the 1970's to measure blood calcium and has since been applied to quantitate a large range of biological analytes including cholesterol and glucose (Moore *et al.,* 1972; Cohen *et al.,* 1980; White *et al.,* 1982). First, a known amount of an isotope, *e.g.*, ^{13}C or ^{15}N is added to the sample, altering its isotopic composition. Then, by measuring each isotope, the amount of ^{13}C or ^{15}N in the original sample can be calculated. In a typical gas chromatography analysis, isotopic dilution

can decrease the error of injection from 5% to 1%. In MS, the isotopic ratio can be calculated with precision typically better than 0.25%.

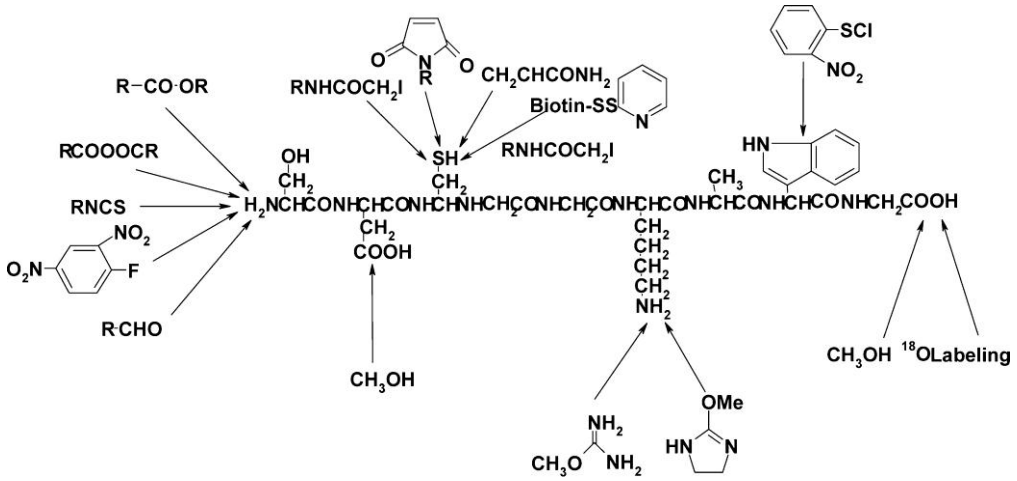

Figure 1.13 Overview of coding strategies currently employed to exploit various reactive centres in peptides. All reactions shown to occur on the amino terminus also apply to the ε-amino group of lysine residues.

Chemical labeling allows for the *in vitro* labeling of virtually any protein sample. The conditions of the labeling reaction and the amount of the label added to a protein sample can be strictly controlled. A novel tool for the identification and quantitation of cysteine-containing peptides in complex biological mixtures was introduced in 2004 by Wisniewski and colleagues (Olsen *et al*., 2004). The HysTag reagent is a decapeptide of the sequence H_6ARAC. Activation with 2,2-dipyridiyl disulphide enables the HysTag reagent to become reactive toward cysteine side chains. Each tag contains a trypsin cleavage site and isoforms of alanine (d_0 or d_4) for differential coding. The amino-terminal histidine residues allows for selective isolation of tagged peptides by metal-affinity or cation-exchange chromatography (Julka and Regnier, 2005). Differentially coded proteins are mixed and digested with Lys-C, preserving the tryptic cleavage site present in the HysTag reagent. Subsequent digestion of tagged peptides with trypsin releases the H_6AR portion of the tag from the peptide that is covalently bound *via* the disulphide bridge with the isotope-labeled dipeptide AC. Proof of principle experiments were used to identify and quantify plasma membrane proteins from a mouse brain extract (Olsen *et al*., 2004). A total of 355 proteins were identified, of which, 281 were

quantifiable. The light and heavy HysTag-labeled peptide pairs were shown to co-elute by HPLC. However, a large number of non-differentially coded histidine residues will also be captured by the system, leading to possible errors in interpreting differential regulation between two states. Similar cysteinyl selection strategies that have been released include the quanternary amine tag reagent, quantitative cysteinyl enrichment technology and fluorinated affinity tags (Ren *et al*., 2004; Liu *et al*., 2004 and Brittain *et al*., 2005).

Isotope Coded Affinity Tags (ICAT) were first introduced with the pioneering work of Gygi and Aebersold in 1999 (Gygi *et al.,* 1999). Here, reduced cysteine residues are specifically derivatised with a tag containing either zero or eight deuterium atoms, resulting in a mass difference of 8 Da between the two versions. ICAT labeling and mixing of samples is performed prior to digestion, minimising the variance which may be introduced due to differential digestion of individual samples. The inclusion of a biotin group in the tag facilitates the purification of cysteine-labeled tryptic peptides on avidin or streptavidin columns. Following elution from the column and LC-MS analysis, the relative abundance between light and heavy-labeled peptides can be compared. cICAT was produced subsequent to the first generation tag which incorporated nine ^{13}C atoms and a biotin moiety, cleavable upon acid treatment (Hansen *et al.,* 2003). Removal of the biotin group improved CID spectra, resulting in a larger number of protein identifications. Further, cICAT overcame the problems of oxidation and double labeling associated with the original tag (Zhang *et al.,* 2002). Further, the new generation tags avoided the problems associated with LC retention shifts between heavy and light deuterium-containing tags. ICAT technology has been widely used for biomarker discovery studies in liver and breast tumour cells in cancer and for candidate discovery in serum and plasma (Somiari *et al.,* 2005; Kang *et al.,* 2010; Kang *et al.,* 2010). Further, the approach has been applied to the analysis of quantitative differences between CSF proteins in AD and NDC where APP and cathepsin D were proposed as candidate biomarkers of the disease (Zhang *et al.,* 2005). Limitations of the technology include the specific requirement for the presence of cysteine residues,

making the quantitation of peptides without the amino acid, including many with PTMs, impossible (Vaughn *et al.,* 2006). Due to the availability of only light and heavy versions of ICAT, only two samples or conditions can be compared at any one time. Accurate quantitation requires LC-MS analysis for quantitation, with subsequent LC-MS/MS analysis for identification. Additionally, protein identifications are usually based on only one or two peptides, making quantitation less reliable.

Isotope-coded protein labels (ICPL) isotopically label the free amino groups of proteins (Schmidt *et al.,* 2005). The technique is derived from the work done by James and co-workers in 2000, where the N-terminus of a protein is labeled with either H4 of D4 versions of nicotinyl-N-hydroxysuccinimide (Munchbach *et al.,* 2000). ICPL regents introduce a mass difference of 6 Da between labeled and unlabeled peptides. A 4-plex version of the reagent, the Serva ICPL 4plex Kit, was introduced in 2008 (Elliott *et al.,* 2009). Recently, ICPL allowed for the quantitation of 211 serum proteins in combination with LC-MS/MS analysis (Turtoi *et al.,* 2010). Quantitative changes for eight of the proteins were validated by SRM. In an effort to increase the number of peptides quantitated using the technology, a modified strategy was recently described where ICPL reagents are added post-digestion (Fleron *et al.,* 2010; Leroy *et al.,* 2010).

1.2.2.2.3 Peptide labeling using isobaric chemical tags

Isobaric chemical tags are chemical molecules with identical structures which label the free amino group of lysine residues and N-termini of peptides and proteins (Thompson *et al.,* 2003; Ross *et al.,* 2004). Labeling is performed post-digestion, therefore, theoretically all the peptides in a given sample have the potential to be labeled. This results in multiple peptide measurements per protein, which increases the confidence of the protein identification and quantitative measurement as compared to isotopic labeling approaches. Another benefit of isobaric labeling is the ability to multiplex, allowing for several comparisons within a single experiment, *i.e*., up to eight for Isobaric tags for relative and absolute quantitation (iTRAQ) and up to six for tandem mass tags (TMT). Each isobaric tag consists of an N-hydroxysuccinimide moiety or

‘’peptide reactive group’’ for peptide and protein binding; a mass normalisation group and a reporter group (Figure 1.14). Introduction of different numbers of ‘’heavy’’ isotopes of ^{13}C or ^{15}N in the reporter and mass normalisation groups produced the different versions of the tags.

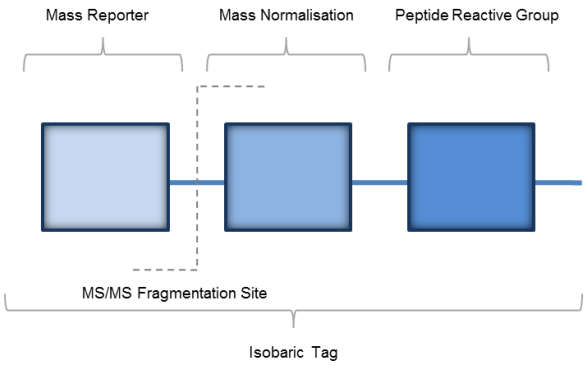

Figure 1.14 Structure of an isobaric chemical tag. Upon fragmentation in MS/MS mode, identification and quantitation is obtained from fragmentation of the peptide backbone, giving rise to mass reporter ions of *m/z* 113 - 121 for 8plex iTRAQ and *m/z* 126 - 131 for 6plex TMT (Thompson *et al.,* 2003; Pierce *et al.,* 2007; Ye *et al.,* 2010).

For TMT, there are currently three different types of products available, TMTzero, TMTduplex and TMTsixplex (Figure 1.15). TMTzero (TMT^0-126; 126 refers to the *m/z* of the mass reporter group) consists of the core TMT structure. Due to the lack of heavy isotopes, this tag enables peptide labeling during optimisation of sample preparation strategies, without the need for the more costly isotope labeled versions of the tag. TMTduplex (TMT^2-126 and TMT^2-127) allows for the relative comparison between two samples, which is beneficial in smaller scale experiments. TMTsixplex, as the name suggests, has the full set of six tags (TMT^6-126 - TMT^6-131).

For comparative analyses in biomarker discovery, peptide populations are differentially labeled and mixed. During MS analysis, samples are indistinguishable from each other due to the isobaric nature of the tag. Upon peptide fragmentation by CID both identification and relative quantitation of a peptide is achieved with release of the reporter group, giving rise to a unique singly-charged ion signature. Peptide quantitation is performed by comparing the reporter ion signal intensities between different tags and is made easier due to the perfect co-elution of differentially labeled

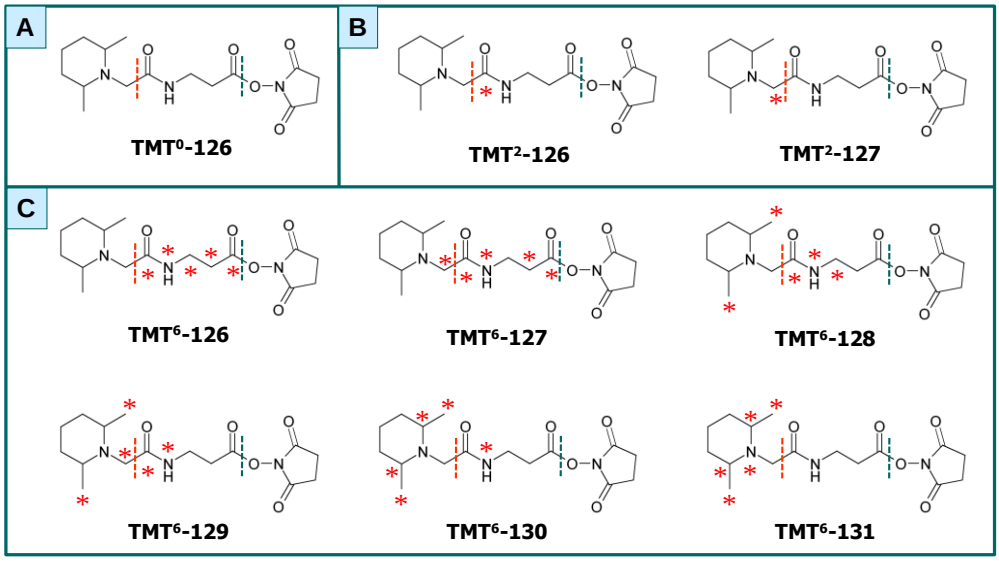

Figure 1.15 Structures of TMT labeling reagents. Three different types of TMT products are available, allowing for between two and six comparisons in a single experiment **A** TMTzero **B** TMTduplex **C** TMTsixplex.

peptides. A known amount of a synthetic peptide can be labeled and spiked into biological samples for internal standardisation and absolute quantitation. This holds particular promise for quantitative biomarker discovery studies. A large number (over 1,500, as of August 2011) of unique articles using the isobaric peptide tagging concept for biomarker discovery have appeared in the literature.

Isobaric labels have been used for a number of different applications in prokaryote and eukaryote samples including bacteria, yeast and human cells and biofluids such as serum, plasma, saliva and urine. iTRAQ has been applied to biomarker discovery explorations for several human conditions such as cancer, pre-eclampsia and Down's syndrome (DeSouza *et al.,* 2005; Chen *et al.,* 2010; Glen *et al.,* 2010; Auer *et al.,* 2010; Kolla *et al.,* 2010). Interestingly, iTRAQ has been utilised in the search for biomarkers of AD and neurodegeneration. In one study, the expression of 136, 72 and 101 proteins was found to be significantly changing in the CSF of AD, PD and DLB, respectively, compared to NDCs (Abdi *et al.,* 2006). Further, iTRAQ has revealed proteomic changes in the hippocampal, cortical and vesicular structures of triple transgenic AD mice (Martin *et al.,* 2008; Rhein *et al.,* 2009). iTRAQ has also been used to study CSF protein abundance changes upon neurodegeneration and

intravenous immunoglobulin treatment of AD (Abdi *et al.,* 2006; Ogata *et al.,* 2007; Choe *et al.,* 2007).

One of the first studies using TMT sixplex looked at the differential expression of CSF proteins using a model of brain injury from *post mortem* CSF compared to healthy *ante mortem* CSF (Dayon *et al.,* 2008). A total of 78 identified proteins were found to be significantly increased in the *post mortem* CSF using a differential TMT-labeling strategy. Confirmation of the quantitative TMT approach was confirmed for three of the proteins by ELISA. Very recently, TMTsixplex has been used in an AD biomarker discovery study (n = 45) in plasma (Güntert *et al.,* 2010). Here, plasma gelsolin was found to be decreased and correlated with the rate of cognitive decline in AD. Findings were confirmed by WB analysis. TMTsixplex has been also used in a biomarker discovery study for staging human African trypanosomiasis (Tiberti *et al.,* 2010). Here, 73 proteins were found to be overexpressed in the CSF of patients presenting the second stage of the disease. Beta-2-microglobulin and osteopontin were confirmed as candidate biomarkers for the disease upon validation by WB and ELISA. Van Ulsen and colleagues utilised TMTduplex tags to quantitate proteins in cell cultures of *Neisseria meningitidis* which were induced under iron-limiting conditions (van Ulsen *et al.,* 2009). TMT enabled the identification and quantitation of 35 proteins which were differentially expressed in response to iron limitation. These proteins represented both well-known and novel iron-regulated proteins.

In an effort to improve the quantitative coverage provided by iTRAQ and TMT, a novel quantitation concept based on isobaric peptide termini labeling (IPTL) was recently presented (Koehler *et al*., 2009). The approach is based on the crosswise chemical labeling of both peptide termini with complementary isotopically-labeled tags. This results in every N- and C-terminal fragment ion providing quantitative data for each peptide over the course of the MS/MS spectrum upon forming peak pairs during fragmentation. Thus, numerous quantitation points in each spectrum will likely increase the robustness and quality of the quantitative data. Additionally, the IPTL approach can be used in combination with any mass spectrometer as the quantitation points are

distributed throughout over the entire mass range (Koehler *et al*., 2011). Further, no chromatographic shift is observed between differentially-labeled peptides as both contain the same number of deuterium atoms. The IPTL strategy was used to compare the proteome of HeLa cells incubated with S-trityl-L-cysteine to induce mitotic arrest and apoptosis (Koehler *et al*., 2011). Over 50 proteins were found to have differential quantitation, with the majority previously reported in other proteome analyses of apoptotic cells.

1.2.3 Targeted MS quantitation strategies used in biomarker validation

To determine which candidates from the large numbers of proteins arising from discovery have the most potential as sensitive and specific biomarkers of a disease state, assays using targeted approaches to protein and peptide quantitation need to be employed. SRM in combination with stable isotope dilution is generally recognised by chemists as the 'gold standard' for the development of MS-based quantitative methods. SRM is not a new technique and has been used for over thirty years to characterise small molecules including drugs and pesticides in human biofluids such as plasma and urine (Baty and Robinson, 1977; Ohya and Sano, 1977; Ervik *et al*., 1981; Sutherland *et al.,* 2001; Koal *et al.,* 2005; Debayle *et al.,* 2008; Yao *et al.,* 2008; Estrela *et al.,* 2008; Kennedy *et al.,* 2010; Kay and Creaser, 2010). In terms of biomarker validation, the highly multiplexed nature of the technique allows for the simultaneous quantitation of many signature peptides of candidate biomarker proteins in the time-scale required for high throughput analyses.

In SRM mode on triple quadrupole mass spectrometers, a precursor ion of interest is selected in Q1, fragmented in Q2 and fragmentation products of the precursor selected in Q3 (Figure 1.16). Here, sensitivity is enhanced as the analysis time is dedicated only to the measurement of the ions of interest. The selection of suitable SRM precursor-to-product ion transitions is crucial for the approach, but predicting the best candidates can be challenging and slow. To alleviate this problem, software tools for the design and optimisation of SRM transitions have emerged,

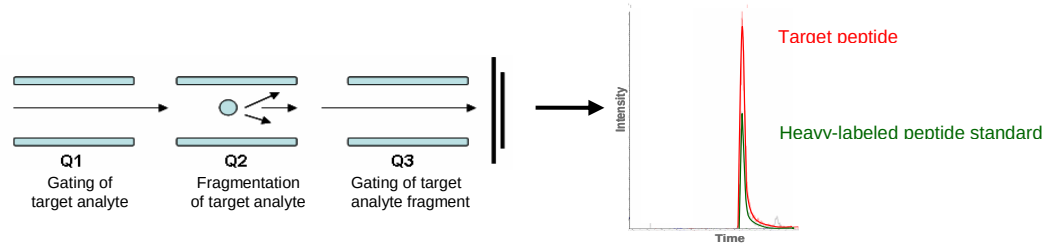

Figure 1.16 Overview of MS-based approaches utilising SRM for biomarker evaluation. Two phases of mass selection in SRM produces a selective response for target analytes. Advantages of SRM include its speed and high sensitivity. Incorporation of heavy-labeled peptides of known amount enables comparison to, and absolute quantitation of, experimental peptides.

largely driven by data from public proteomics libraries, including PeptideAtlas and the Global Proteome Machine database (gpmdb; Cham *et al*., 2010). Such tools include both public and proprietary software offerings. Commercial packages include Pinpoint, and P3 predictor (Thermo Scientific); MRMPilot software and multiple reaction monitoring initiated detection and sequencing (MIDAS) Workflow Designer (AB Sciex) and Verify^{E} (Waters). Feely available software packages include PeptideAtlas, MRMer, MRMaid MRM Worksheet, Skyline and MaRiMba (Deutsch *et al*., 2008; Martin *et al*., 2008; Mead *et al*., 2009; Walsh *et al*., 2009; Prakash *et al*., 2009; Sherwood *et al*., 2009).

The sensitivity and selectivity of the SRM approach has the capacity to detect and quantitate peptides in complex mixtures of wide dynamic range such as plasma without prior fractionation (Stahl-Zeng *et al.,* 2007). In SRM, signature peptides unique to the protein of interest are measured to provide quantitative information for that protein in the sample. Additionally, more accurate quantitation can be achieved, both relative quantitation and moving towards absolute quantitation, when isotopically-labeled versions of the peptide of interest are spiked into the sample at known concentrations. This can be achieved in several ways and will be reviewed in the next section.

1.2.3.1 AQUA peptides for absolute peptide quantitation

The concept of isotope dilution to provide a reference point for MS-based quantitation of proteins was introduced by Barr and colleagues in 1996. Here, a

deuterium-labeled hydrolysed peptide, unique to the protein apolipoprotein A-1, was used for internal standardisation and quantitation of the purified protein by LC-MS (Barr *et al.,* 1996). In 2003, Gerber and colleagues introduced the acronym AQUA (Absolute QUAntitation) for the determination of protein expression and PTM levels (Gerber *et al.,* 2003). The AQUA strategy uses synthetic internal standard peptides which can be introduced into experimental samples at known amounts during or after proteolysis, providing absolute quantitation of target analytes (Kirkpatrick *et al.,* 2005). Stable isotopically-labeled (*e.g.,* ^{2}H, ^{13}C, ^{15}N) amino acids are incorporated into the AQUA peptide for the mass discrimination (typically by SRM) of endogenous sample peptides and synthetic internal standards, which perfectly co-elute by LC-SRM (Figure 1.11). Since their inception, AQUA peptides have garnered widespread popularity due to their ease of use, rapid incorporation into experimental samples and their commercial availability. AQUA peptides can be engineered to suit experimental needs. However, problematic chemical synthesis (particularly for those containing PTMs) determine the availability of peptides; peptides should be less than 15 amino acids long and ideally be absent of any chemically modifiable residues such as cysteine or methionine (Brun *et al.,* 2009). Production of AQUA peptides is costly as each peptide undergoes individual synthesis, purification and usually, determination of accurate amount. Further, the heavy-labeled amino acid adds significant expense. As a result of such financial implications, several studies have been published where target proteins have been quantitated using just a single AQUA peptide (Cheng *et al.,* 2006; Bondar *et al.,* 2007). It is also worth noting that solubilisation and shelf-life properties of AQUA peptides are very much sequence-dependent and if not considered, can severely affect the quantitative measurement (Brun *et al.,* 2007; Mirzaei *et al.* 2008).

1.2.3.2 Peptide concatamers

In 2005, Beynon and Gaskell introduced the concept of QConCAT, that is, absolute quantitation based on an artificial concatamer of tryptic peptides, proteotypic to several test proteins (Pratt *et al.,* 2006). Here, target proteins are expressed in *E.*

coli and stable-isotope labeled upon growth in the presence of isotope-labeled precursors. QConCAT proteins are subsequently purified, quantitated by amino acid analysis (AAA) and spiked into complex mixtures such as plasma at known amounts (Pratt *et al.,* 2006). Thus, QConCAT is a biological means of producing AQUA standards. Once the QConCAT gene has been initially cloned, the protein product can be synthesised repeatedly, without limit. Commercially available QConCAT, or those synthesised in-house, are typically added before sample digestion and are released upon enzymatic cleavage to provide internal standards for quantitation. In parallel with AQUA peptides, it is necessary to assess the completeness of tryptic digestion for each target protein for accurate quantitation (Rivers *et al.,* 2007). Further, it is essential to determine the proof of equimolar release of the selected peptides (Arsene *et al*., 2008). QConCAT constructs are digested at high rates and this may be proteolytic efficiency may be highly variable compared to the native target peptides. In response to this, it has been proposed to surround QConCAT peptides with their respective native sequences (Kito *et al.,* 2007). The technique is somewhat cheaper than producing AQUA peptides synthetically as up to 50 peptides may be included in a single construct, providing multiplexed quantitative measurements (Rivers *et al.,* 2007). This strategy has been used to quantitate medium to high abundant plasma proteins over three orders of magnitude (Anderson and Hunter, 2006).

1.2.3.3 Synthetic protein standards for absolute quantitation

In an effort to minimise the variation in the quantitative measurement due to sample fractionation and digestion procedures, new strategies for peptide quantitation, namely Absolute Stabled Isoptope-Labeled Internal Stardards (SILAC; Hanke *et al.,* 2008) and Protein Standard Absolute Quantitation' (PSAQ; Brun *et al*., 2007), have been recently described. In such approaches, full length proteins are isotopically-labeled and introduced into the sample at the very start of the analytical procedure (Dupuis *et al.,* 2008). This has advantages, as both the target peptide and internal standard are generated to the same degree by proteolytic digestion. The PSAQ

strategy has been shown to be compatible with almost any method of sample prefractionation, including SDS-PAGE and immunoaffinity capture (Brun *et al.,* 2007; Dupuis *et al.,* 2008). For accurate peptide quantitation, highly purified proteins are required and AAA is essential. Other limitations include high costs and difficulty in production of the standards.

1.2.3.4 Isotopic peptide labels in combination with SRM

As described in Section 1.2.2.3.3, the application of isobaric labeling strategies such as iTRAQ and TMT have been successful where biomarker discovery in being pursued in complex mixtures such as CSF and plasma (DeSouza *et al.,* 2005; Dayon *et al.,* 2008; Güntert *et al.,* 2010; Chen *et al.,* 2010). Extending the tags utility for biomarker validation purposes, isotopic versions of iTRAQ labels, termed mTRAQ, have been introduced. Such tags enable the quantitation of signature peptides of candidate biomarker proteins based on iTRAQ in combination with SRM (DeSouza *et al.,* 2008; DeSouza *et al.,* 2009). Two versions of mTRAQ labels exist, *i.e.,* light and heavy tags which are chemically identical apart from the number of heavy isotopes (^{13}C or ^{15}N) in the heavy label (which is identical to the iTRAQ 117 label); the light mTRAQ label contains no heavy isotopes. A mass difference of 4 Da per tag is introduced between differentially labeled peptides, allowing for the discrimination between species in SRM mode. Absolute quantitation can be achieved by referencing a target tryptic peptide labeled with for example, the light label, against a known amount of synthetic peptide labeled with the heavy label.

The mTRAQ strategy was initially employed to measure the levels of a candidate endometrial cancer biomarker pyruvate kinase for iTRAQ-labeling discovery studies in tissue biopsied EmCa homogenates of 20 malignant tissues and non-malignant controls (DeSouza *et al.,* 2005; DeSouza *et al.,* 2007; DeSouza *et al.,* 2008). Here, differential labeling with mTRAQ in combination with SRM, allowed for the absolute quantitation and detection of a 4-fold increase in the protein (based on measurements for two peptides) in malignant tissues *versus* non-malignant controls

(DeSouza *et al.,* 2008). This was independently confirmed by ELISA. Further, the 4-fold increase was higher than the 2-fold increase for the discovery study, suggesting a compression of the dynamic range in the non-targeted iTRAQ labeling technique. Such compression effects have been demonstrated by others, who proposed that ratio compression arises from contamination during precursor ion selection, which occurs at a consistent proportion within an experiment and thus results in a linear relationship between expected and observed ratios (Karp *et al*., 2010; Ow *et al*., 2011).

Very recently, DeSouza and colleagues employed mTRAQ-SRM for the relative quantitation of pyruvate kinase and polymeric Ig receptor from endometrial epithelial cells in formalin-fixed paraffin-embedded tissues of cases and controls (DeSouza *et al.,* 2010). In a further advancement of the approach, mTRAQ labels have been used in parallel with ICAT for the relative quantitation of colon cancer tissues and plasma samples (Kang *et al.,* 2010).

Similarly, ICPL reagents have been used in combination with SRM (Lange *et al.,* 2008). Here, the reliable quantitation of low abundance virulence factors from cultures of the human pathogen *Streptococcus pyogenes* exposed to increasing amounts of plasma was performed. Experiemntal samples were labeled with ICPL 'light', and to provide an internal standard, a pool of all samples was labeled with ICPL 'heavy'. This enabled the successful identification and quantitation of a subset of virulence proteins that is regulated upon exposure to plasma.

In a similar fashion to mTRAQ, the combination of TMT and SRM may have applicability in the quantitation of candidate protein biomarkers of disease states. By employing an isotopic labeling scheme, *i.e.,* TMTzero and TMTsixplex versions of TMT, a mass difference can be introduced between two species. As the labels differ only by their isotopic constitution, differentially TMT-labeled peptides should co-elute during LC separation and can be discriminated in SRM mode. This novel approach, termed TMT-SRM, has potential for the targeted quantitation and validation of signature peptides of candidate biomarkers of AD (and other disorders) in complex biological matrices such as CSF and plasma.

1.3 Biomarker assay development and implementation

Biomarkers have enormous potential in clinical practice. Biologically-based diagnostic and prognostic tests may enable an earlier disease diagnosis, resulting in earlier treatments and the possibility to perhaps cure rather than to merely delay further injury or death (Carr and Anderson, 2008). Additionally, biomarkers could possibly be used for more accurate staging of a disease, identifying those individuals who are likely to respond to therapeutic interventions and assisting in the selection of appropriate treatments. Biomarkers may also be used for patient stratification and to serve as surrogate endpoints in early-phase drug trials, resulting in more targeted drug development and generation of more effective treatments.

A typical biomarker development pipeline as outlined in Figure 1.17 incorporates several distinct phases; 1) biomarker discovery in low (in the tens) sample numbers uses untargeted, semi-quantitative protein profiling approaches such as 2DE and isobaric mass tagging to establish protein signatures which are differentially expressed between case and control subjects; 2) assay development requires the generation and validation of assays for biomarker measurement using more targeted means of quantitation such as ELISA or SRM in combination with stable isotope dilution; 3) The developed and validated assay is performed for the verification of the differential abundance of candidate biomarkers in larger numbers (in the hundreds) of samples than that used in discovery. Here, the large panels of candidate biomarkers from discovery are refined to include only those candidates which have the most potential as providing sensitive and specific biomarkers of a disease state; 4) full biomarker validation and qualification, necessitating the evidentiary process of linking a biomarker with a clinical endpoint, requiring clinical trials and large population screening in thousands of samples (Thambisetty and Lovestone, 2010). The complete process can take many years without any guarantee of success. Consequently, there remains no qualified biomarker of AD meeting the United States Food and Drug Administration (FDA) approval and this may be due in part to poor selection of assay and lack of method validation (Pepe *et al.,* 2001; Katz, 2004; Carden *et al.,* 2010).

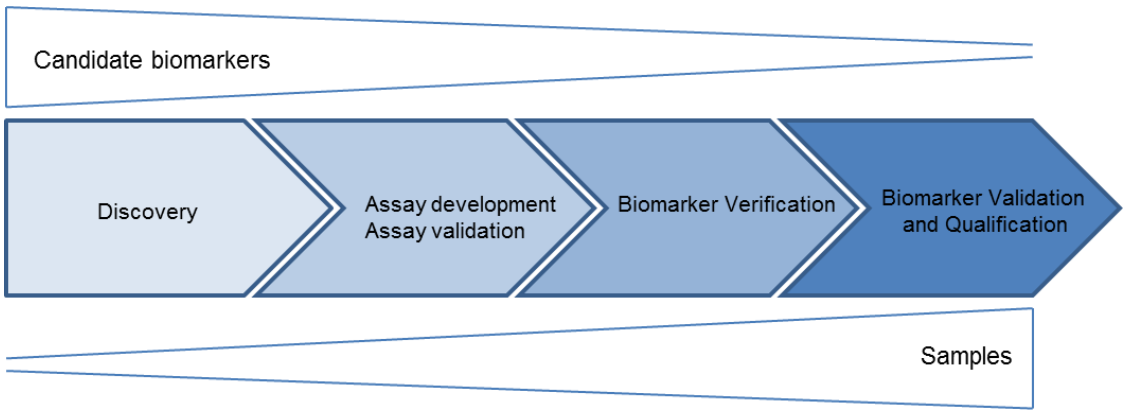

Figure 1.17 Overview of the biomarker development pipeline. The workflow consists of initial discovery of a panel of candidate biomarkers in low sample numbers followed by their verification and qualification in much larger sample cohorts for determination of the most sensitive and specific biomarkers of a respective disease state.

In October 2003, a Biomarker Method Validation Workshop was held in an effort to standardise the process of 'fit-for-purpose' biomarker assay development and validation (Lee *et al.,* 2006). A well validated quantitative assay includes full characterisation of the reagents and reference materials (plasma and internal standards in this case) in terms of matrix effects and the establishment of assay sensitivity, *i.e.,* the limit of detection (LOD) for each target analyte, the determination of the linear and dynamic range of quantitation, *i.e.,* definition of lower and upper limits of quantitation (LOQ), and the accuracy (trueness and precision) of the quantitative measurement. Table 1.4 provides a list of definitions commonly used in biomarker assay studies. Many different types of quantitative assays exist for biomarkers but to-date; the majority is based on antibody-based means of detection and quantitation.

1.3.1 Antibody-based assays

A clinical assay must be sensitive enough to measure target analytes of interest and all candidates must be quantitated with high reproducibility, accuracy and in a high throughput manner over a large number of patient samples. Despite the ever increasing surge in MS-based quantitation of peptides and proteins, antibody-based methods remain the 'gold standard' for the quantitation of proteins in tissues and biofluids and are readily available in clinical research laboratories. Ever since the first

Term	Definition
Accuracy	Closeness of agreement between a quantity value obtained by measurement and the true value of the measurand. Accuracy incorporates both trueness and precision.
Background interference	(1) Analytical interference: presence of entities in samples that causes a difference in the measured concentration from the true value. (2) Physicochemical interference (matrix interference): a change in measured physical chemical property of the specimen that causes a difference between the population mean and an accepted reference value.
Clinical endpoint	A characteristic or variable that reflects how a patient feels, functions, or survives.
Dynamic range	The range of the assay that is demonstrated from the pre-study validation experiments to be reliable for quantifying the analyte levels with acceptable levels of bias, precision, and total error. This can also be referred to as the linear range.
Limit of detection (LOD)	A concentration resulting in a signal that is significantly different (higher or lower) from that of background. LOD is commonly calculated from mean signal at background + 3 SD. This is often described as the analytical sensitivity of the assay in a diagnostic kit.
Limit of quantitation (LOQ)	The lowest concentration of analyte that have been demonstrated to be measurable with acceptable levels of bias, precision, and total error. LOQ is commonly calculated from mean signal at background + 10 SD.
Qualification	This refers to whether the candidate biomarker qualifies for use in a given context. Does it meet the standards required to be used in clinical trials as an indicator of drug response? Does it have sufficient positive and negative predictive power to act as a diagnostic tool? Might it qualify as a surrogate marker?
Precision	The closeness of agreement between independent test results obtained under stipulated conditions
Selectivity	The ability of a method to determine the analyte unequivocally in the presence of components that may be expected to be present in the sample.
Specificity	The ability of an assay to distinguish between the target analyte, to which the assay is intended to detect, and other components.
Surrogate endpoint	A biomarker that is intended to substitute for a clinical endpoint. A surrogate endpoint is expected to predict clinical benefit or harm (or lack of benefit or harm) based on epidemiologic, therapeutic, pathophysiologic, or other scientific evidence.
Trueness	The closeness of agreement between the average value obtained from a large series of test results and an accepted reference values
Verification	Verification of candidate biomarkers relies upon specific, quantitative assays optimised for selective detection of target proteins. The process involves the refinement of the long list of candidates from discovery, leaving only the most promising candidates for full validation. Thus, it is a critical step in the discovery pipeline that bridges unbiased biomarker discovery to preclinical validation.
Assay Validation	It is the confirmation *via* extensive laboratory investigations that the performance characteristics of an assay are suitable and reliable for its intended analytical use. It describes in mathematical and quantifiable terms the performance characteristics of an assay.

Table 1.4 List of definitions for commonly used terms in biomarker assay development and method validation (Lee *et al.,* 2006; Menditto *et al.,* 2007; Thambisetty and Lovestone, 2010).

immunoassay was described in the late 1950's, immuno-based measurement of protein concentrations in clinical samples has revolutionised the face of medicine (Yalow and Berson, 1960). The biochemical nature on the test relies on the high specificity between an antibody and antigen. A wide range of antibody-based assays are currently available for the examination of the human proteome including WB, ELISA, radioimmunoassay, Luminex, reverse phase protein arrays and tissue micro-

arrays combined with immunohistochemistry (Kartalov *et al.,* 2008; Brennan *et al.,* 2010).

ELISA assays are currently the most prominent technology for the validation of differential protein expression changes in biofluids, particularly blood plasma. The method was initially described by two groups in Sweden and The Netherlands in 1971 (Engvall and Perlmann, 1971; Van Weemen and Schuurs, 1971). In ELISA, a sample containing an unknown amount of antigen of interest is immobilised on a surface, usually a well of a microtitre plate, *via* adsorption to the surface or by capture by a primary antibody specific to the antigen (in the case of sandwich ELISA). A detection antibody is subsequently added which may be covalently linked to an enzyme (*e.g.,* horseradish peroxidise) to produce a detectable signal, *e.g.,* fluorescence. The magnitude of signal produced is relative to the amount of antigen in the sample (Figure 1.18). ELISA assays have been described for the quantitation of proteins in a wide variety of diseases such as Aβ and tau in CSF and plasma of AD subjects (as described in Sections 1.2.1 and 1.2.2), HIV testing (Hermez *et al.,* 2010), rabies (Moore and Hanlon, 2010), tuberculosis (Lalvani, 2007; Lalvani and Pareek, 2010) and cancer (Brennan *et al.,* 2010). The technique offers higher sensitivity than MS-based approaches for target analyte detection as demonstrated by the accurate quantitation of a very low abundant protein in plasma, interleukin-6, by ELISA down to concentrations as low as 15 pg/mL (Rifai *et al.,* 2006). Multiplexed assays based on traditional methods of ELISA have recently been described for the high throughput measurement of several target antigens in parallel, over a wide dynamic range (Morgan *et al.,* 2004; Leng *et al.,* 2008). Luminex xMAP technology from Innogenetics has been recently described for the multiplexed, immuno-based quantitation of proteins (Earley *et al.,* 2002). Luminex uses tiny, colour-coded beads which can be coated with a reagent specific to a particular assay, allowing the capture and detection of target analytes from a biological sample. Very recently, the technology has been applied to the measurement of $A\beta_{1\text{-}42}$, t-tau and p-tau in CSF (Shaw *et al.,* 2011). In theory, the

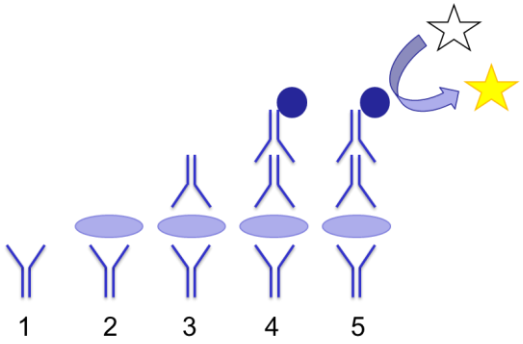

Figure 1.18 Overview of sandwich-ELISAs. (1) The ELISA plate is coated with a capture antibody. (2) The sample is added and any antigen present binds to the capture antibody. (3) The detection antibody is added and binds to the antigen. (4) The enzyme-linked secondary antibody is added and binds to the detecting antibody. (5) The substrate is added and is converted by enzyme to a detectable form. Figure extracted from http://en.wikipedia.org/wiki/File:ELISA-sandwich.svg.

approach enables the multiplexed measurement of up to 100 proteins, although in practice, a decline in assay performance as a result of an increase in overall protein concentration means that Luminex xMAP assays rarely complex more than 30 proteins at any one time (Lovestone and Thambiestty, 2010). Such techniques are very much in their infancy and their success and full potential for protein biomarker quantitation in other complex matrices such as human serum and plasma are yet to be determined. Thus, immuno-based assays in plasma currently remain limited as only one antigen can be accurately detected at any one time. It has been demonstrated that there may be genetic variability in epitope structure across populations, resulting in variability in assay specificity from person to person (Silva *et al.,* 2001). It is extremely challenging to develop antibodies which are specific to particular protein isoforms or PTMs. In addition, quantitation can be subject to interference from other species within the matrix, reducing assay specificity. The cost associated with immuno-assay development is generally very high, with usually a very long lead time. Further, and the most important drawback of all, is that their success is exclusively dependant on the availability of high quality antibodies for antigen detection. Failure to produce suitable antibodies is more frequent than desired.

1.3.2 Mass spectrometry-based assays

In response to the limitations associated with immuno-based assays for biomarker verification and validation, the scientific community has recently shifted attention to the development of MS-based assays such as those using SRM, as they may provide cheaper, quicker and more robust alternatives. Besides therapeutic monitoring of drug immunosuppressants or neonatal screening for inherited metabolic disorders, one of the most established SRM-based assays is that for the quantitation of 25-hydroxyvitamin D3 in serum (Vogeser, 2010). The molecule is accepted as the most useful biological marker for assessment of vitamin D status. Due to the unreliability of protein binding assays, several methods have been developed for the quantitation of the analyte and have since gained widespread and routine implementation in clinical and commercial laboratories (Higashi *et al.,* 2001; Vogeser *et al.,* 2004; Tsugawa *et al.,* 2005; Singh *et al.,* 2006). Differential mass tagging in LC-MS/MS measurement of the target analyte and its different forms allows for robust multiplexed quantitation, with sufficient throughput for biomarker verification and validation.

Desiderio and colleagues were the first group to apply similar techniques for the quantitation of peptides in complex biological matrices such as CSF and brain extracts (Desiderio and Kai, 1983; Desiderio, 1983; Desiderio *et al.,* 1984). More recently, the technique has been further advanced to the quantitation of plasma peptides with high analytical sensitivity, specificity and accuracy (Anderson and Hunter, 2006; Keshisihian *et al.,* 2007; Hüttenhain *et al.,* 2009; Yocum *et al.,* 2010). To-date, numerous studies have been published using MS-based assays to quantitate both individual, and panels of plasma proteins (Barnidge *et al.,* 2004; Kuhn *et al.,* 2004; Nicol *et al.,* 2008; Kuzyk *et al.,* 2009; Whiteaker *et al.,* 2010).

Proof-of-principal experiments of the application of the SRM approach to the targeted quantitation of plasma peptides were published by Anderson and Hunter (2006), where SRM experiments were performed on 53 medium to high abundant proteins in plasma. Of these, 47 produced acceptable quantitative data, demonstrating within-run coefficients of variation (CVs; n = 10) of 2 - 22%, with 78% of assays having

CVs <10%. Depletion of six high abundance proteins by immuno-subtraction significantly improved CVs compared with whole plasma, but analytes could be detected and quantitated in both sample types. The analysis of direct plasma digests is of a significant advantage as it enables for measurement of a higher throughput of samples, while reducing the potential for sample loss that may be introduced during sample pre-processing. In this context, an SRM assay in combination with stable isotope standards permitted the absolute quantitation of 45 endogenous proteins (31 of which are putative candidate biomarkers of cardiovascular disease) in human plasma trypsin digests without prior depletion or affinity enrichment (Kuzyk *et al.,* 2009). Due to likelihood of plasma background interference and matrix effects however, the LOD, LOQ and specificity of an SRM assay may be severely compromised by the complexity and large dynamic range of direct plasma digests. Thus several strategies have been proposed to reduce overall sample complexity and decrease the aforementioned assay parameters including depletion of high abundance plasma proteins, enrichment of target analytes or sample prefractionation. The upfront enrichment of target proteins before SRM has been demonstrated for the quantitation of plasma peptides in the low µg/mL range (Nicol *et al.,* 2008; Berna and Ackerman, 2009). Immuno-extraction of proteins by antibodies immobilised on a hydrazide resin, followed by SRM with stable isotope-labeled dilution has been used for the quantitation of candidate biomarkers of lung cancer in diseased and normal serum (Nicol *et al.,* 2008). Enrichment strategies have been proposed to isolate and enhance the detection of sub-proteomes in plasma including the selective isolation of *N*-glycosite peptides and quantitation *via* SRM (Stahl-Zeng *et al.,* 2007). Precise quantitation (CVs ~15%) was accomplished using stable isotope dilution by AQUA peptides. Multiplexed SRM assays have been developed to quantitate plasma proteins down to the 1 - 10 ng/mL range with CVs of 3 - 15% without immunoaffinity enrichment of either proteins or peptides, although pre-fractionation was performed in this case (Keshishian *et al.,* 2007).

Stable Isotope Standards and Capture by Anti-Peptide Antibody (SISCAPA) was introduced by Anderson and co-workers in 2004, where target experimental and

AQUA peptides are immuno-enriched prior to LC-MS/MS analysis (Anderson *et al.,* 2004). This has utility for the quantitation of low abundance proteins in plasma and may enable for evaluation of an extended population of candidate biomarkers of disease. Although the technique is dependent on high antibody affinity, selectivity requirments can be relaxed as the mass spectrometer platform is capable of specifically detecting and quantitating the signature peptides, even in the presence of a highly complex background (Carr and Anderson, 2008). In the initial experiments, rabbit polyclonal antibodies were raised against tryptic peptides of hemopexin, α1 antichymotrypsin, interleukin-6 and tumour necrosis factor-α. Antibodies were immobilised on POROS supports which were fully recyclable. Using SRM MS, a 120-fold enrichment of the target peptides was observed. As the internal standard was added prior to immunoaffinity step, quantitative variability due to this step was reduced and a relatively low CV was observed, *i.e.,* approximately 5% (Anderson *et al.,* 2004). Antibodies are very specific, and due to the enrichment process, SISCAPA is well suited to the quantitation of low abundant species in complex proteomes like plasma, without the need for other sample fractionation. This was demonstrated by Steve Carr's group, where SISCAPA in combination with SRM was used for the enrichment and quantitation of the cardiovascular biomarkers troponin I and interleukin-33, typically present in plasma in the low ng/mL range (Kuhn *et al.,* 2009). Quantitation was linear in the range of 1.2 ng/mL to 5 µg/mL, with CVs <15%. SISCAPA assays have been used for the quantitation of a range of target analytes, where up to three peptides per protein have been enriched in parallel (Berna *et al.,* 2006; Whiteaker *et al.,* 2007; Hoofnagle *et al.,* 2008). Indeed, SISCAPA coupled to SRM has also been demonstrated for the enrichment and subsequent quantitation of specific peptide glycoform in human serum (Ahn *et al.,* 2009).

In 2009, Anderson and co-workers further improved the method by introducing a simple magnetic bead protocol which formed part of a nanoflow LC-MS/MS system (Anderson *et al.,* 2009). The work used antibodies which were conjugated to small Protein-G coated beads which facilitating automated washing and elution of captured

peptides inside the nanoflow capillary and reducing peptide losses. Peptides of α1-antitrypsin and lipopolysaccharide-binding protein were enriched up to 18,000 fold in the new system (Anderson *et al.,* 2009). This was replicated by Amanda Paulovich's group for the high throughput quantitation of 15 peptides from a murine biomarker discovery study (Whiteaker *et al.,* 2007; Whiteaker *et al.,* 2010). The multiplexed platform was shown to be precise, with LODs down to ng/mL (using 10 µL of plasma). This was extended down to pg/mL using 1 mL of plasma, allowing for the quantitation of a broad range of peptide abundances (Whiteaker *et al.,* 2010). However, as with any method based on immuno-capture, the success of the technique is only as good as the antibody utilised. Monoclonal species have been recently suggested as a better source of antibodies compared to their polyclonal counterparts (Schoenherr *et al.,* 2010). In an effort to reduce the cost associated with SISCAPA-SRM, a workflow was recently described where the multiplexed immunisation of up to five proteotypic peptides from a single protein target in individual rabbits was incorporated (Whiteaker *et al.,* 2011). A total of 403 proteotypic tryptic peptides representing 89 target proteins were used as immunogens, with over half of the developed assays capable of detecting the target peptide at concentrations of < 0.5 fmol/µL in human plasma, equivalent to protein concentrations of < 100 ng/mL. Thus, it has been proposed that a single laboratory is capable of generating hundreds of assays per year using a cost-effective SISCAPA approach.

In conclusion, SRM-based assays have several attractive benefits suited to targeted biomarker verification and validation studies in plasma. The technology is sensitive, selective and multiplexable. In response to the limitations associated with ELISA's as described within, it is anticipated that MS-based quantitative technologies will be increasingly implemented in large scale biomarker studies, where hundreds to thousands of patient samples require analysis, within the confines of time and cost. The particular niche of SRM-based assays is that they potentially permit the quantitation of proteins for which ELISAs of good quality are unavailable, or of those for which quantitation of specific isoforms or PTMs is required (Diamandis *et al.,* 2009).

1.4 Aims of this thesis

The current diagnosis of AD is primarily based on clinical means and, to date, there is no reliable diagnostic or prognostic test for the disease. While many studies have investigated biomarkers of AD in various fluids such as CSF, the extraction of this matrix in the volumes required for routine clinical testing is difficult. Thus, attention has shifted to analysis of peripheral markers of AD. There is an urgent need for targeted, selective, specific and multiplexed quantitative assays to determine those candidate biomarkers of AD from discovery which have the most potential as sensitive and specific markers of the disease and which warrant further investigation in large-scale biomarker qualification studies. MS-based assays in combination with stable isotope dilution strategies have been proposed as advantageous over traditional immuno-based methods in this regard. This thesis aims to develop a novel MS-based assay for the multiplexed measurement of candidate plasma biomarkers of AD and to critically assess its quantitative performance. Such an assay would potentially provide a panel of biomarkers that would have diagnostic and prognostic utility such as prediction of those MCI patients which are likely to progress to AD, for example.

The specific aims of the thesis are:

- To assess the quantitative performance of utilising isotopic versions of TMT tags as a means of introducing an internal standard into an SRM experiment.

- To develop a multiplexed TMT-SRM assay for the measurement of signature peptides of nine candidate plasma biomarkers of AD. Specifically, an assay will be designed for the measurement of the candidate AD biomarkers clusterin, complement C3, complement C3a, CFH, A2M, FGG, SAP, ApoE and gelsolin in undepleted plasma.

- To validate the TMT-SRM assay against established biomarker technologies and determine the performance characteristics for each target analyte in the assay in terms of the dynamic range, LOD, LOQ and the accuracy of quantitation.

- To evaluate the performance of each candidate biomarker in cohorts of AD and NDC samples to determine if individual, or indeed the full panel of candidate biomarkers, have utility as diagnostic or prognostic biomarkers of AD.

Chapter 2

TMT-SRM – proof of principle experiments

2.0 Introduction

Biomarker discovery experiments in plasma have revealed several proteins which may be valuable in AD diagnosis and prognosis (Hye *et al.,* 2006; Thambisetty *et al.,* 2010; Güntert *et al.,* 2010). These proteins are of medium to high abundance in plasma and represent tractable analytes for targeted quantitation strategies. Robust, high performance quantitative assays are required to verify these candidate biomarkers in clinical sample cohorts. Recently, SRM mass spectrometry, utilising signature peptides of proteins, has been given considerable attention for the targeted quantitation of plasma proteins (Anderson and Hunter, 2006; Keshishian *et al.,* 2007; Pan *et al.,* 2009). SRM is an attractive alternative to immuno-based approaches due to its intrinsic capacity to multiplex, rapid development times and its ability to target specific protein isoforms and PTMs (Kirkpatrick *et al.,* 2005; Anderson and Hunter, 2006; Stahl-Zeng *et al.,* 2007).

SRM has routinely utilised AQUA peptides (heavy isotope-labeled versions of the target peptide) as internal standards for improved accuracy of quantitation (Gerber *et al.,* 2003; Brun *et al.,* 2009). Alternatively and more recently, internal standardisation may be achieved by comparison of target peptides to reference peptides, differentially labeled with isotopic versions of chemical tags such as mTRAQ or ICPL reagents (DeSouza *et al.,* 2008; Lange *et al.,* 2008; Kang *et al.,* 2010). This referencing approach is advantageous over AQUA peptides as the need for the synthesis of expensive heavy isotope-doped standards is avoided in the early stages of protein verification and both synthetic and biological reference standards can be utilised. In the case of the biological reference approach, an internal reference peptide standard can be generated for all endogenous proteins in the sample upon enzymatic digestion. Similarly to mTRAQ, isotopic versions of TMT (Figure 1.10; light TMT: TMTzero and heavy TMT: TMTsixplex) could be utilised for the internal referencing of target analytes for quantitation by SRM (TMT-SRM).

Here the performance of TMT-SRM was investigated for its potential to provide high quality quantitative measurements which could be later applied to the development of robust ‘‘fit for purpose’’ assays for the validation of candidate plasma biomarkers of AD. In the first instance, proof of principle experiments were designed for the targeted quantitation of high abundant tryptic plasma peptides by TMT-SRM. In this experiment, reference peptides were derived from a plasma sample (biological reference). These initial investigations were also designed to gain a first impression of the accuracy of TMT-SRM quantitation.

The complexity of the plasma matrix may detrimentally affect the quantitative measurement, due to the increased likelihood of contaminating background ions contributing to signals measured for target and reference analytes. Additionally, ion suppression effects from the plasma may result in reduced detection of target analytes. In a further proof of principal experiment, the effect of this interference was assessed on the accuracy of TMT-SRM quantitation. In the initial experiment, the plasma matrix effect could not be directly assessed as target analytes were endogenous to the plasma. A model experiment was therefore designed utilising peptides exogenous to plasma. Here, bovine serum albumin (BSA) peptides were spiked into a human plasma digest over a range of concentrations and the plasma matrix effects on the trueness and precision of TMT-SRM quantitation determined.

2.1 Materials and Methods

2.1.1 Initial assessment of the performance of TMT-SRM as a strategy for targeted MS assays in plasma

2.1.1.1 Estimation of plasma protein concentration by Bradford assay

The total protein content of a reference plasma sample, prepared from a healthy control subject (Dade Behring, Milton Keynes, UK) was determined by the Bradford colorimetric assay (Bradford, 1976). Lyophilised plasma was prepared by resuspension in 1 mL 18 MΩ water (H_2O; NB this water quality was used for all experimental procedures here-on-in) followed by gentle shaking for 1 min. Plasma was left to stand for 20 min at room temperature (RT) to ensure all proteins were fully solubilised whilst minimising proteolytic degradation. The sample was aliquoted into 25 µL volumes and stored at -80 ˚C until further use. For the determination of protein concentration, an aliquot was defrosted and diluted 1:300 (3 µL in 897 µL H_2O) in accordance with standard operating procedures and stored on ice. Plasma was compared to BSA standards (stock solution 2.96 µg/mL; Sigma-Aldrich Company Ltd, Dorset, UK) prepared over a concentration range 0 - 0.5 µg/µL in H_2O. Protein standards (10 µL) or diluted plasma (10 µL) were combined with 200 µL of Bradford dye reagent (Sigma-Aldrich) in a Nunc 96-well microplate (Thermo Scientific, Hemel Hempstead, UK), mixed, incubated at RT for 5 min and read at 595 nm using a Victor 3 1420 Multi-label Counter (Perkin Elmer, Cambridge, UK). BSA and experimental measurements were performed in triplicate. BSA absorbance at 595 nm (A_{595}) was plotted against concentration (µg/µL). The protein concentration of the plasma sample was estimated to be 47 µg/µL (Appendix Figure 2.1).

2.1.1.2 Solubilisation, reduction, alkylation and digestion of human plasma

Plasma was digested and labeled with TMT according to the manufacturer's instruction (Proteome Sciences R&D GmbH & Co., Frankfurt, Germany). Plasma (500

µg, 10.6 µL) was diluted to 1µg/µL with 100 mM borate buffer, pH 7.5 (Sigma-Aldrich) and 0.1% sodium dodecyl sulphate (SDS; Genomic Solutions, Huntingdon, UK). Borate buffer was used to provide an alkaline pH which was necessary for tryptic digestion and the TMT-labeling reaction. SDS was used to solubilise the plasma proteins, resulting in the loss of all secondary, tertiary and quaternary protein structures. To disrupt disulphide bonds between cysteines of the plasma proteins, the sample was reduced with 1 mM Tris(2-carboxyethyl) phosphine (TCEP; Sigma-Aldrich, stock solution 20 mM TCEP in H_2O) for 30 min at RT. Free cysteines were blocked by alkylation with 7.5 mM iodoacetamide (IAA; Sigma-Aldrich, stock solution 150 mM IAA in ACN; Fisher Scientific UK Ltd., Loughborough, UK), for 1 hr at RT in the dark. The digestion efficiencies of bovine and porcine trypsin were compared for the generation of plasma peptides. This comparison came about as bovine trypsin was routinely used in the London laboratory and porcine trypsin was utilised in the TMT protocol. Bovine trypsin (Roche, Welwyn Garden City, UK) and porcine trypsin (Promega, Southampton, UK) were solubilised to 400 ng/µL in 100 mM borate buffer pH 7.5 and added to the plasma sample (divided into 2 x 200 µg aliquots) to give a trypsin: protein ratio of 1:25. Samples were incubated on a Thermomixer (Eppendorf, Cambridge, UK) at 37 ^{o}C for 18 hr.

2.1.1.3 TMT-labeling of digested plasma peptides

Following digestion, the bovine- and porcine-digested plasma samples were divided into two 100 µg aliquots for TMT labeling. One aliquot of each digest was labeled with 15 mM light TMT (TMT zero tag) and the other with 15 mM heavy TMT (TMT sixplex-127 tag) at RT for 1 hr. The stock solution in both cases was 60 mM TMT reagent solubilised in ACN. All TMT labels were manufactured in-house at Proteome Sciences R&D GmbH & Co., Frankfurt, Germany. To remove non-specific TMT labeling of amino acids other than lysine and the N-terminus, each solution was brought to 0.25% hydroxylamine (25% stock solution in H_2O; Sigma-Aldrich) and incubated for 30 min at RT.

2.1.1.4 Purification of TMT-labeled peptides by reversed-phase and strong cation exchange chromatography

To remove excess TMT reagents, salts and SDS, TMT-labeled peptides were purified using RP and strong cation exchange (SCX) cartridges. The ACN concentration of the peptide samples was reduced from 24% to ~5% with 0.1% trifluoroacetic acid (TFA; Merck Services Ltd., Hull, UK). Samples were desalted by RP using HLB Oasis cartridges (30 mg bed volume, Waters, Hertfordshire, UK). Cartridges were prepared by conditioning with 1 ml 95% ACN, 0.1% TFA, followed by equilibration with 2 mL 5% ACN, 0.1% TFA. The diluted peptide sample was loaded onto the prepared cartridge and bound peptides were washed with 4 mL 5% ACN, 0.1% TFA, followed by elution with 3 mL 50% ACN, 0.1% TFA. Peptides from the RP step were eluted directly onto self-packed SCX cartridges. Cartridges were prepared using Chromabond 15 mL columns (Thames Restek Ltd., High Wycombe, UK) filled with 650 µL fast flow sepharose slurry (Sigma-Aldrich) and a frit placed on top of the resin bed. Prior to peptide loading, cartridges were washed with 2 mL 25% ACN, 0.1% TFA. The RP eluant was loaded onto the column and washed with 4 mL of 25% ACN, 0.1% TFA. Peptides were eluted from the cartridge with 2 mL of 25% ACN, 400 mM ammonium acetate (Fisher Scientific). Both purification procedures were performed with the aid of a vacuum manifold (Thames Restek). During loading and elution of the peptides, the flow rate of the system was maintained at approximately 1 drop/sec. The samples were lyophilised to dryness in a vacuum centrifuge (Savant Speedvac®, Thermo Scientific). To ensure the removal of the volatile salt used for SCX, the samples were resuspended in 25% ACN, 0.1% TFA and re-lyophilised to dryness. Samples were stored at -80 °C until further analysis.

2.1.1.5 LC-MS/MS analysis of plasma labeled with light TMT and heavy TMT on a Q-Tof to compare the digestion of plasma by different trypsin species

To assess the enzymatic efficiencies of both trypsin species for the generation of plasma peptides, LC-MS/MS analysis of each sample was performed on an Ultimate

LC system (Dionex Ltd., Camberley, UK) coupled to a Q-Tof micro (Waters). Specifically, a comparison of the MS survey scan and the peptides identified *via* MS/MS for each sample was made. Further, MS/MS data was used to assess the TMT labeling efficiency.

TMT-labeled plasma samples, digested with bovine or porcine trypsin, were resuspended to a final concentration of 1 µg/µL (*i.e.,* 100 µL in each of the four samples) in 5% ACN, 0.05% FA (BDH Chemicals, VWR, Leighton Buzzard, UK). Aliquots (10 µL) were stored at -80 ^{o}C for subsequent MS analysis. Aliquots of light and heavy TMT labeled plasma samples from each of the digests were combined in a 1:1 ratio, vortexed and diluted 20 fold to a final concentration of 0.05 µg/µL in 0.05% FA. Sample [20 uL full loop injection with 21 uL sample pick-up, *i.e.,* 1µg total protein load on column (o/c), 500 ng of each labeled sample] was loaded *via* a Famos™ autosampler (Dionex) onto a C18 pre-column (PepMap cartridge, 300 µm x 5 mm; Dionex) for concentration and further desalting. Washing was performed in loading buffer (0.1% FA) for 4 min at 30 µL/min. During washing the pre-column was out of line with the analytical column by means of a Switchos™ II microcolumn switching unit (Dionex), allowing all eluant to flow to waste. The pre-column was then switched in-line with the analytical column (C18 PepMap column, 75 µm x 15 cm; Dionex) and peptides were resolved over a gradient of 0 - 32% ACN, delivered by a combination of Buffer A (0.05% FA) and Buffer B (80% ACN, 0.05% FA) for 120 min and at a flow rate of 200 nL/min. Following delivery of the gradient, both columns were washed for 10 min with 60% Buffer B followed by 20 min with 95% Buffer B. The pre-column and analytical column were then equilibrated for 20 min in loading buffer and 95% Buffer A, respectively.

Peptides were ionised by ESI using a Z-spray ion source fitted to a Q-Tof micro. For MS/MS analysis of the plasma digest, the instrument was set to run in automated switching mode (data dependent acquisition, DDA), selecting precursor ions based on their intensity and charge state for sequencing by CID with argon gas. Singly charged ions were not selected for fragmentation as they commonly represent contaminating

ions. Furthermore, TMT-labeled peptides are typically multiply charged. A collision energy (CE) profile was applied for the fragmentation of peptides, optimised to the precursor ions *m/z* and charge state. For further optimisation, each setting in the CE profile was increased by 5 V for the fragmentation of TMT-labeled peptides. The source cone voltage was set to 30 V and the capillary voltage to 3500 V.

Mass calibration of the MS was performed on MS/MS fragment ions of synthetic human [Glu1]-fibrinopeptide (GluFib; Sigma-Aldrich) directly infused into the instrument at a concentration of 63 fmol/µL in 50% ACN, 0.5% FA and a flow rate of 0.2 µL/min using a syringe pump (Harvard Apparatus Ltd, Kent, UK). The accuracy of the calibration was ±0.05 amu (50 ppm or ±0.005% at *m/z* 785.85). Instrument performance was benchmarked prior to the analysis of samples using a tryptic digest of BSA. LC-MS/MS analysis was performed on 200 fmol BSA digest over a gradient of 0 - 32% ACN for 60 min. MS and MS/MS sensitivity, resolution, mass accuracy and peptide LC retention were assessed. Typically, 200 fmol BSA gave between 600 and 1000 base peak intensity (BPI) in the MS channel, 100 - 150 in first MS/MS and 50 - 100 in second MS/MS channel.

2.1.1.6 Database searching for peptide/ protein identification and for the determination of TMT-labeling efficiency

Mass spectral data was processed into peak lists (.pkl files) for database searching using ProteinLynx Global Server 2 (v2; Waters). Peak lists contained the precursor *m/z*, intensity and charge state along with MS/MS fragment ion *m/z* and intensity. All .pkl files were searched against the UniProtKB/Swiss-Prot database (release 54.0, 24th July 2007) using Mascot (v2.2; Matrix Science, London, UK). Parameters were set to identify tryptic peptides with up to three missed cleavages. To account for chemical modifications during sample processing, carbamidomethylation of cysteines and oxidation of methionines were set as variable modifications within search parameters. Similarly, light and heavy TMT-labeling of lysine residues and peptide N-termini were set as variable modifications. These TMT modifications were configured

manually into the in-house version of the software. Peptide identifications were ranked according to a scoring system based on the Mowse algorithm (Pappin *et. al.,* 1993). Ion score values below 10 were excluded from analysis. For confirmation of single peptide identifications of proteins the ion score of the peptide needed to be greater than the identity score.

2.1.1.7 LC-MS/MS analysis on a 4000 QTRAP mass spectrometer for peptide and transition selection to build the SRM method

The TMT-SRM method was developed using an UltiMate 3000 nano-LC (Dionex) coupled to a 4000 QTRAP triple quadrupole mass spectrometer (QTRAP; AB Sciex, Warrington, UK). Initially, information dependent acquisition (IDA, equivalent to DDA) was performed to select peptides and transitions representing high abundant species in human plasma. Two porcine trypsin digested plasma aliquots (one labeled with light TMT and one with heavy TMT) were combined in a 1:1 ratio and diluted as described in Section 2.1.1.5. Peptides were resolved by RP chromatography as described in Section 2.1.1.5. Peptides were introduced into the mass spectrometer using a Nanospray II source at a flow rate of 300 nL/min. Peptides were ionised by ESI using source-dependant voltages and gas pressures which had been optimised for maximal ion sensitivities using GluFib (*m/z* 785.85^{2+}, infused as described in Section 2.1.1.5). Specifically, the curtain gas was set to 10 p.s.i., the ion gas 1 (GS1) was 15 p.s.i. and the ion spray voltage was 3500 V. Peptides were fragmented by CID using nitrogen gas.

The linear ion trap was calibrated on the MS/MS fragment ions of GluFib using the conditions as described in Section 2.1.1.5. Instrument quality control checks were performed to monitor system performance. Here, LC-MS/MS analysis of a standard tryptic digest of BSA (as described in Section 2.1.1.5) was performed between the analysis of TMT-labeled samples to check MS sensitivity and to allow for LC column recovery. MS/MS data was analysed as described in Section 2.1.1.5, following

generation of raw data .wiff files. Such files are the MS data file format on AB Sciex instruments. Following IDA analysis peptides were selected for TMT-SRM quantitation.

2.1.1.8 Development of a TMT-SRM method to assess the co-elution and selectivity between light TMT and heavy TMT-labeled peptides

The performance of Q1 and Q3 of the QTRAP was assessed and corrected for mass accuracy, sensitivity, resolution and stability using polypropylene glycol (PPG; Agilent Technologies, West Lothian UK). The stock solution was diluted 1:50 with H_2O (< 0.01 wt %) and directly infused into the instrument at 10 µL/min.

An SRM method was initially established by inputting all Q1 and Q3 ion *m/z* for the selected peptides. Based on the number of transitions and SRM peak width, additional parameters were optimised for maximal SRM sensitivities and sampling over the peak. The optimal LC gradient time for separation of the plasma peptides was determined. LC-SRM analysis was performed over 30 min, 60 min and 120 min LC gradients. The most desirable LC gradient was that which gave smooth SRM peak shapes without compromise to SRM sensitivity or selectivity. Furthermore, the optimal mass resolution, dwell time and cycle time were determined. Several methods were then prepared to determine the approximate CE that gave optimal SRM sensitivities, *i.e.,* CE applied for MS/MS fragmentation +/- 5 V.

TMT-SRM analysis was performed over a 0 - 32% ACN gradient for 30 min. The detection of all transitions in the method was analysed using a light TMT and heavy TMT-labeled plasma sample combined in a 1:1 ratio. In the first instance, an SRM-triggered enhanced product ion (EPI) method was used to confirm the identity of each analyte in the method. From this, an accurate retention time (t_R) for each peptide and interference from the background matrix was extracted. To observe potential cross-talk between transitions, light TMT-labeled plasma was analysed over all light TMT and heavy TMT transitions (full method). Using accurate t_R, the SRM signal in the heavy TMT channel was directly aligned to the light TMT channel and quantitated. A

similar analysis was performed on heavy TMT-labeled plasma to observe SRM interference in the light TMT channel.

2.1.1.9 TMT-SRM analysis of light TMT and heavy TMT-labeled plasma mixed in different ratios to assess the accuracy of quantitation of target peptides

To gain a first impression of the trueness and precision of TMT-SRM quantitation, light TMT and heavy TMT-labeled plasma was combined in ratios of 1:1, 3:1, 9:1 and 27:1 (light TMT: heavy TMT, L/H), such that the total plasma load o/c remained at 1 µg. Each combined sample was analysed in triplicate (analytical repeats) using the method developed in Section 2.1.1.8. To minimise carryover from the higher amounts of light TMT-labeled peptides used, triplicate samples of each ratio were analysed in order of increasing light TMT-labeled peptides, *i.e.,* 1:1, 3:1, 9:1 and finally, 27:1. A blank sample (5% ACN, 0.05% FA) was analysed before each triplicate ratio and at the end of the sample set.

SRM transitions were visualised through Analyst® SRM quantitation software (v1.5; AB Sciex). The quantitation processing parameters were determined using SRM data acquired from a representative sample, *i.e.,* the light TMT and heavy TMT-labeled peptides combined in a 1:1 ratio. The minimum peak height for detection was set to 50 cps with minimum peak width of 30 sec. An SRM smoothing width of 3 points was applied to all transitions. All peak matching was visually verified and transitions were excluded if there was poor peak definition from the background signal. Peak areas were exported into Microsoft Excel 2003. The peak area for each light TMT-labeled transition was measured relative to the peak area of the corresponding heavy TMT-labeled transition, *i.e.,* representing the internal standard. The L/H ratio for corresponding transition pairs were taken forward for quantitative analysis. The mean L/H ratio for all transitions of each peptide was calculated across all repeats and used to determine the trueness and precision of TMT-SRM quantitation. Expected L/H ratios were plotted against observed L/H ratios to assess the linearity of TMT-SRM quantitation.

2.1.2 Assessment of the plasma matrix effects on the accuracy of TMT-SRM quantitation

To further investigate the TMT-SRM approach, plasma matrix effects on quantitation were explored. To address this, exogenous peptides to human plasma (BSA peptides) were spiked into the plasma and the effect of plasma background on these peptides was determined. Human plasma was labeled with light TMT and BSA peptides were labeled with light TMT and spiked into the light TMT-labeled plasma over a range of concentrations. Light TMT-BSA peptides were compared to a constant amount of heavy TMT-labeled BSA peptides also spiked into plasma, providing an internal standard for quantitation. As a control, the spiked BSA peptides were quantitated by the same TMT-SRM method in a buffer-only system.

2.1.2.1 LC-MS/MS analysis of TMT-labeled BSA for peptide and transition selection

BSA (200 µg) was reduced, alkylated, digested with porcine trypsin, divided into 2 x 100 µg aliquots and labeled with either light TMT or heavy TMT as described in Section 2.1.1.3. TMT-labeled peptides underwent RP and SCX purification as described in Section 2.1.1.4. BSA was processed in triplicate to provide three technical repeats. For peptide selection and method development, light TMT-labeled BSA peptides were analysed by LC-MS/MS on the QTRAP as described in Section 2.1.1.7. Light TMT-labeled BSA was loaded at 1 µg o/c and IDA analysis was performed over a 90 min LC gradient (0 - 32% ACN). MS/MS experimental data was searched against the sequence for BSA using Mascot with parameters set as described in Section 2.1.1.6 and peptides selected for TMT-SRM quantitation.

2.1.2.2 Optimisation of MS instrument parameters

QTRAP compound-dependent parameters were tuned with direct infusion of light TMT-labeled BSA peptides (0.9 µg/µL in 45% ACN, 0.25% FA) to achieve optimal fragmentation and maximal sensitivity of each peptide. Such parameters focus and

enhance the ion path of each analyte in the mass spectrometer and are specific for each analyte in the method. The compound-dependent parameters optimised in this experiment as defined by AB Sciex were:

- Declustering Potential (DP) controls the potential difference between Q0 and the orifice plate. It is used to minimise solvent cluster ions which may attach to the sample. The higher the voltage, the higher the fragmentation or 'declustering'.
- Collision Energy (CE) is the potential difference between Q0 and Q2 for MS/MS-type scans. It is the amount of energy that the precursor ions receive as they are accelerated into the Q2 collision cell, where they collide with gas molecules and fragment.
- Collision Cell Exit Potential (CXP) is used to focus and accelerate ions out of the collision cell (Q2). It is important for sensitivity in Q3.

Parameters were optimised by linearly ramping the voltages for each parameter (50 – 200 V for DP, 10 – 70 V for CE, 0 - 50 V for CXP) in the order of DP, CE and CXP, *i.e.,* the order of voltages applied along the ion path. For each parameter the voltage resulting in the maximal ion count over the range was selected as the optimal setting. The optimised compound-dependent parameters were added to the method along with dwell and cycle times.

2.1.2.3 Detection of BSA peptides in human plasma and determination of the effect of plasma background interference on the accuracy of TMT-SRM

A representative sample of light TMT and heavy TMT-labeled BSA combined in a 1:1 ratio and spiked into light TMT-labeled plasma (10 ng BSA peptides to 1 µg plasma o/c) was prepared. This was used to determine the optimal LC gradient time for quantitation of the spiked BSA peptides. LC-SRM analysis was performed over 30 min, 60 min and 90 min LC gradients.

Once the TMT-SRM method was established, crosstalk between transitions was assessed with analysis of light TMT-labeled BSA peptides only over all light TMT and heavy TMT transitions. Similarly, heavy TMT-labeled BSA peptides only were analysed over all transitions. To determine if there was any signal contribution from the plasma matrix which could effect quantitation of the target analytes, light TMT-labeled plasma (1 µg o/c) was combined with light TMT BSA (10 ng o/c) and analysed over all light TMT and heavy TMT transitions. An similar analysis was performed using heavy TMT-labeled BSA peptides. Plasma background interference on BSA peptides could be directly aligned in the heavy TMT channel using exact t_R from the light TMT-labeled BSA peptides and *vice versa*.

Light and heavy TMT-labeled BSA peptides were combined in 0.33:1, 1:1, 3:1, 9:1 and 27:1 ratios (L/H) and spiked into the light TMT-labeled plasma. One unit represented 10 ng BSA. This spiked concentration is equivalent to 800 µg/mL levels in plasma. For control purposes, an identical analysis was performed without plasma matrix. Three analytical and three technical replicates of BSA digest were analysed in the order of 0.33:1 1:1, 3:1, 9:1 and finally 27:1 over a 0 - 32% ACN gradient for 30 min. A blank sample (5% ACN, 0.05% FA) was analysed before replicate runs of each ratio and after the complete sample set.

2.1.2.4 Data processing and analysis

SRMs were processed using Analyst SRM quantitation software as described in Section 2.1.9. All peak matching was visually verified and peak areas were exported into Microsoft Excel 2003. The peak area for each light TMT-labeled BSA transition was measured relative to the peak area of the corresponding heavy TMT-labeled BSA transition. The L/H ratio for each transition was taken forward for quantitative analysis. The mean L/H ratios for all transitions of each peptide across all repeats were used to determine the trueness and precision of TMT-SRM quantitation. Expected L/H ratios were plotted against observed L/H ratios to assess the linearity of quantitation.

2.2 Results

2.2.1 Initial assessment of the performance of TMT-SRM as a strategy for targeted MS assays in plasma

2.2.1.1 TMT-labeling of plasma

A protocol for the digestion and TMT-labeling of plasma first needed to be established. To determine the optimal source of trypsin for digestion of plasma, equivalent amounts of plasma were digested with bovine and porcine trypsin and analysed by LC-MS/MS on the Q-Tof micro. In the first instance, LC-MS/MS experiments were performed on the Q-Tof micro due to its higher resolution (as compared to the QTRAP), improved mass accuracy and charge state recognition and higher quality MS/MS data. Overall, a higher BPI was observed in the MS survey scan of the porcine trypsin digested plasma sample than in the bovine trypsin digested plasma, with more ions detected in the earlier half of the gradient (Figure 2.1). These ions represented the more hydrophilic peptide ions which were potentially more amenable for SRM analysis.

The total number of peptides and proteins identified was compared between samples (Table 2.1). A greater number of peptides (218) and proteins (28) were identified in plasma digested by porcine trypsin as compared to the bovine trypsin digest (101 peptides and 20 proteins). The number of missed cleavages is an indication of the incompleteness of proteolytic cleavage by trypsin. An equivalent percentage of missed cleavages were observed in both experiments, with 82 - 87% of all identified peptides being fully cleaved by both trypsin species (Table 2.1). As plasma digested using porcine trypsin gave a much richer BPI and a greater number of peptide and protein identifications by LC-MS/MS as compared to bovine trypsin, porcine trypsin was used for all subsequent digestions. Of all identified peptides, 99% were fully labeled by TMT, demonstrating the high efficiency of the labeling reaction. The standard protocol for TMT labeling applied to plasma generated fully labeled plasma

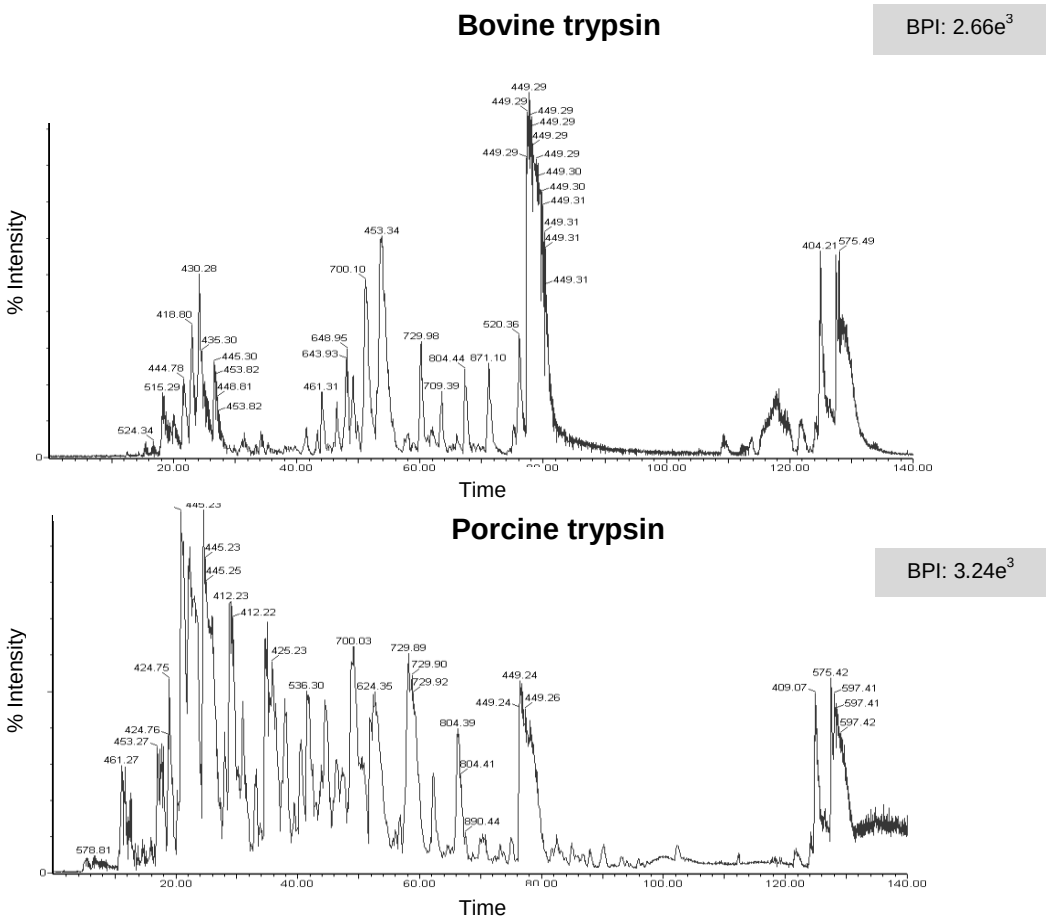

Figure 2.1 BPI chromatograms of plasma digested with bovine and porcine trypsin. A contaminant is observed at *m/z* 449 (suspected to be dicyclohexyl urea; http://www.waters.com/webassets/cms/support/docs/bkgrnd_ion_mstr_list.pdf) and can be excluded from the comparison. The number and intensity of ions in the early half of LC gradient is greater for plasma digested by porcine plasma as compared to plasma digested with bovine trypsin.

Instrument	Trypsin species	Peptide IDs	Protein IDs	Missed cleavages (% of total)			
				0	1	2	3
QTof	Bovine	101	20	88 (87.0)	10 (10.0)	3 (3.0)	0 (0.0)
	Porcine	218	28	176 (81.6)	36 (16.0)	4 (1.8)	2 (0.6)
QTRAP	Bovine	105	22	90 (85.7)	12 (11.4)	3 (2.9)	0 (0)
	Porcine	220	29	177 (80.5)	37 (16.8)	4 (1.8)	2 (0.0)

Table 2.1 The total number of peptides and proteins identified by LC-MS/MS on the Q-Tof micro and QTRAP for plasma digested by bovine or porcine trypsin. The number and proportion of missed cleavages for all identified peptides is also displayed. Results were comparable across platforms.

peptides and was therefore reasoned to be suitable for the preparation of TMT-labeled peptides in plasma for subsequent quantitation studies.

Equivalent to the QTof MS/MS analysis, MS/MS analysis of the same physical digests was performed on a QTRAP (DDA). Results were comparable across mass spectrometer platforms (Q-Tof micro and linear ion trap) with equivalent numbers of peptide and protein identifications and similar peptide fragmentation patterns observed (Table 2.1). This was encouraging as not only were the mass analysers different but different gases were used for CID on the two instruments, *i.e.,* argon on the Q-Tof micro and nitrogen on the QTRAP. This demonstrated the potential of MS/MS data from discovery experiments to be transferred into SRM methods for validation using experimental rather than theoretical data. As Q-Tof micro and QTRAP MS platforms were comparable, all future work-up and SRM assessment experiments were performed on the QTRAP only.

Q-Tof mass spectra of two representative plasma peptides are displayed in Figure 2.2 to demonstrate the mass difference between light TMT and heavy TMT-labeled versions of the same peptide. The expected mass differences between the differentially TMT-labeled versions of 2+ and 3+ peptide ions were observed. This is important for the derivation of SRM transitions. This demonstrates that, by applying an isotopic TMT-labeling strategy, a mass difference can be introduced between experimental sample peptides and internal standards, allowing for the differential detection of both by SRM; the selectivity of which still needed to be assessed by SRM.

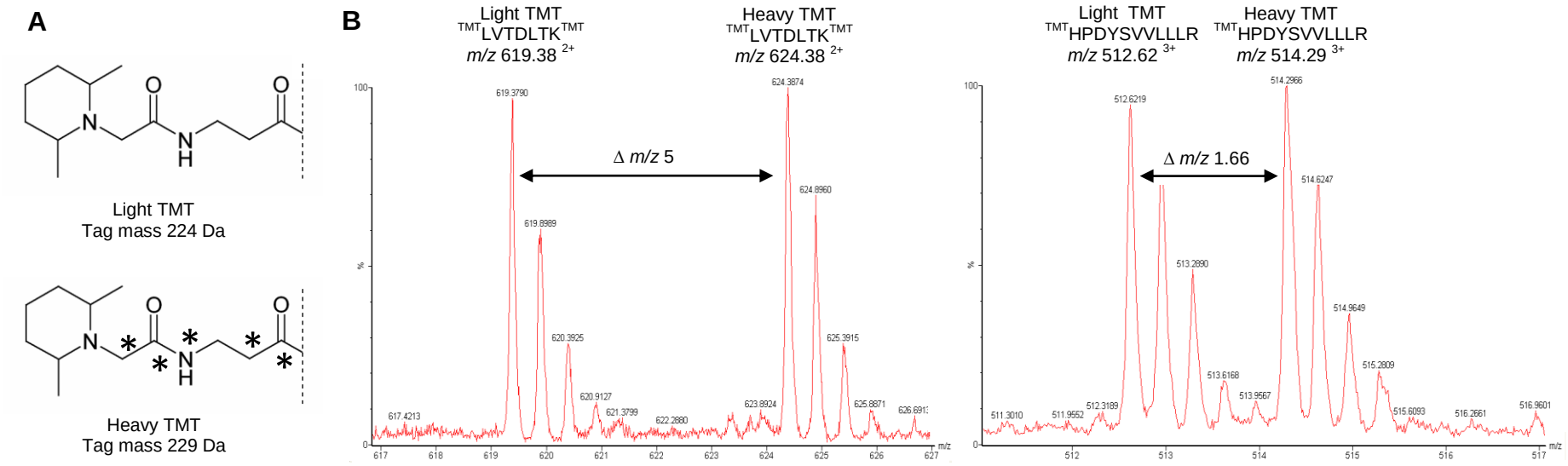

Figure 2.2 The mass difference observed between differentially labeled peptides by TMT at different charge states. **A** Structures of light TMT and heavy TMT (TMTsixplex – 127 tag). Heavy TMT has five isotopic labels (^{13}C and ^{15}N; denoted *). **B** Mass spectra of two peptides labeled with light TMT and heavy TMT. The peptide LVTDLTK is labeled at the N-terminus and lysine giving a difference of 10 Da between the labeled peptides. The doubly charged precursor ions have a *m/z* difference of 5. The peptide HPDYSVVLLLR is labeled at the N-terminus only, resulting in a mass difference of 5 Da between the differentially labeled peptides. The triply charged precursor ions have a difference of 1.66.

2.2.1.2 Peptide and transition selection

Table 2.2 displays a set of peptides representing high abundant plasma proteins which were selected for initial TMT-SRM quantitation. Following QTRAP IDA analysis of the light and heavy TMT-labeled plasma sample, peptides were taken forward as suitable candidates if they were fully hydrolysed with trypsin and had strong, high *m/z* MS/MS fragment ions. Additionally, peptides were selected that had both arginine and lysine at the C terminus (*i.e.,* either one or two TMT tags), were doubly or triply charged and had varying LC t_R. Theoretical *m/z* values were extracted from Mascot or calculated *in silico* for each light TMT and heavy TMT-labeled peptide. As an example, peptide G was doubly charged and had one N-terminal tag attached (Table 2.2). The Q1 *m/z* of the light TMT-labeled peptide was 592.90, therefore the *m/z* of the corresponding heavy labeled peptide was 595.40 (Δ *m/z* 2.5). The b5 ion (measured in Q3) had one tag attached and thus the singly charged fragment ions between the labeled versions had an *m/z* difference of 5 Th (*i.e., m/z* 798.50 and 803.50). As a second Q3 transition the pseudo y-ion was selected. Pseudo-y ions are TMT fragment ions common to all TMT-labeled peptides. The *m/z* of these ions is always the intact mass of the labeled peptide minus the reporter ion and carbon monoxide (CO; Figure 2.3). Pseudo y-ions may serve as Q3 transitions without prior insight into fragmentation patterns for peptide detection.

2.2.1.3 LC-TMT-SRM method development for target plasma peptides

A TMT-SRM method was compiled by first adding the *m/z* for each Q1 and Q3 ion representing the thirteen target analytes, resulting in a total of 26 transitions (13 light and heavy TMT pairs). The shortest LC-SRM gradient (30 min) was determined to be optimal for the separation of the peptides in that all target analytes were observed without compromise to the sensitivity or selectivity of each transition. Shorter gradients were favourable as analysis of the samples could proceed in a timelier manner. The dwell time, cycle time, mass resolution and CE were then optimised. The dwell time is the time required to scan each individual transition and the cycle time is the total time

Peptide ID	Protein	Peptide Sequence	Charge State (+)	t_R (min)	CE (V)	Light TMT			Heavy TMT		
						Mr (Da)	Q1 (*m/z*)	Q3 (*m/z*)	*Mr* (Da)	Q1 (*m/z*)	Q3 (*m/z*)
A	Alpha-2-macroglobulin	^{TMT}LVHVEEPHTETVR	3	9.3	38	1768.98	590.66	839.44 (y7)	1773.99	592.33	839.44 (y7)
B	Albumin	^{TMT}LTVDK^{TMT}	2	12.6	29	1022.58	512.29	653.39 (b4)	1032.58	517.29	658.39 (b4)
Ci	IgG	^{TMT}DTLMISR	2	13.5	40	1058.60	530.30	906.60 (p*)	1063.60	532.80	909.60 (p*)
Cii	IgG	^{TMT}DTLMISR	2	13.5	40	1058.60	530.30	685.40 (b4)	1063.60	532.80	690.40 (b4)
D	Haptoglobin	^{TMT}ILGGHLDAK^{TMT}	3	14.0	32	1370.82	457.94	670.42 (y4)	1380.81	461.27	675.42 (y4)
E	IgG	^{TMT}ALPAPIEK^{TMT}	2	16.2	35	1285.80	643.90	878.55 (y6)	1295.80	648.90	883.55 (y6)
F	Albumin	^{TMT}LVTDLTK^{TMT}	2	18.5	34	1236.76	619.38	585.40 (y3)	1246.76	624.38	590.40 (y3)
Gi	Albumin	^{TMT}FQNALLR	2	18.9	43	1183.80	592.90	1031.76 (p*)	1188.80	595.40	1034.76 (p*)
Gii	Albumin	^{TMT}FQNALLR	2	18.9	43	1183.80	592.90	798.50 (b5)	1188.80	595.40	803.50 (b5)
H	Serotransferrin	^{TMT}SASDLWDNLK^{TMT}	2	21.0	46	1696.94	849.47	598.40 (y3)	1706.94	854.47	603.40 (y3)
Ii	Albumin	^{TMT}LVNEVTEFAK^{TMT}	2	22.4	43	1596.96	799.48	819.46 (y5)	1606.96	804.48	824.46 (y5)
Iii	Albumin	^{TMT}LVNEVTEFAK^{TMT}	2	22.4	43	1596.96	799.48	589.38 (y3)	1606.96	804.48	594.38 (y3)
J	Complement C3	^{TMT}SSLSVPYVIVPLK^{TMT}	2	26.2	60	1849.10	925.55	581.41 (y3)	1859.10	930.55	586.41 (y3)

Table 2.2 Light and heavy TMT-labeled plasma peptides selected for SRM quantitation. For each peptide (A - J) the position of the TMT label is indicated along with the peptide's precursor ion charge state, molecular mass (*Mr*) and LC t_R. The CE is given for peptide fragmentation. The Q1 and Q3 transitions for the detection of both the light and heavy TMT-labeled versions of the peptides are also listed. One Q3 transition was selected per peptide with the exception of peptides C, G and I which were measured using two transitions. The Q3 transitions denoted (p*) represent the pseudo y-ion fragmentation.

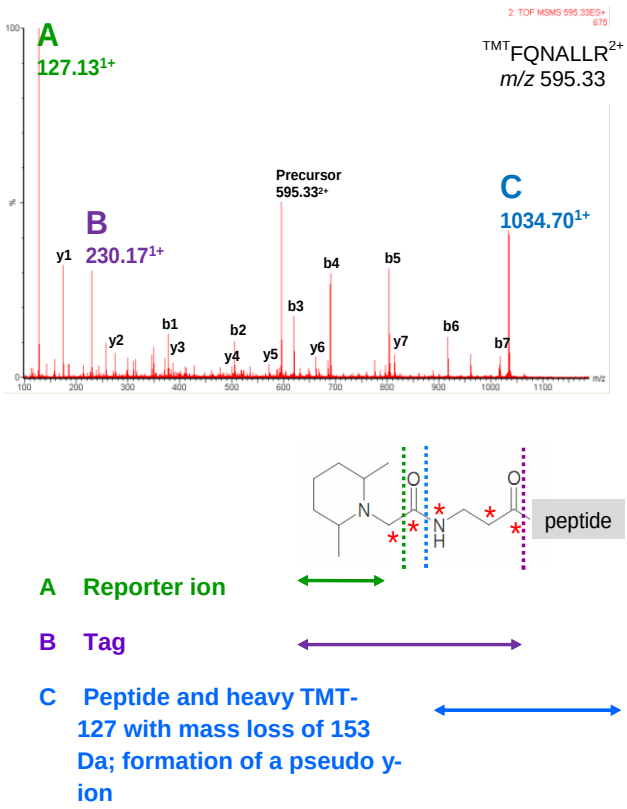

Figure 2.3 TMT fragment ions formed by CID highlighting the formation of the pseudo-y ion. **A** Upon fragmentation of the labeled peptide (with TMTsixplex-127), the TMT reporter ion is observed at *m/z* 127.13. **B** The tag is observed at *m/z* 230.17 Th. **C** The pseudo-y ion is observed at *m/z* 1034.53. This relates to the mass of the TMT-labeled peptide minus the reporter ion and a CO group. The *m/z* of the pseudo y-ion will change depending on the tag used within each isobaric set as the distribution of the heavy isotopes across the reporter ion and CO moieties differ.

to scan all transitions. At a fixed cycle time, dwell time is dependent on the total number of transitions in the method. For optimal sampling of the peak, a minimum of 10 data points at full width half maximum (FWHM) was required. SRM quantitation was performed with a dwell time of 100 msec per transition resulting in a total cycle time of 2.6 sec.

The peak width was 30 sec at FWHM, resulting in approximately 11 data points per SRM. The mass resolution is the mass window around the precursor ion mass in Q1 or fragment ion mass in Q3 and the number of ions which are scanned around each mass is relative to the size of the window. Although higher sensitivities are achieved with a wider window, the selectivity becomes compromised. A balance between sensitivity and resolution was therefore needed.

Labeled plasma peptides were analysed using the TMT-SRM method with the resolution of Q1 and Q3 set to either low (1 Da ± 0.1 amu FWHM), unit (0.7 Da ± 0.1 amu FWHM) or high (0.5 Da ± 0.1 amu FWHM) and the data compared. Unit resolution gave the highest SRM sensitivity whilst still maintaining selectivity and was therefore used for subsequent measurements (data not shown). Finally, the CE was tuned. Here, three analyses of TMT-labeled plasma were performed using methods with the CE set to the default MS/MS CE voltage and +/-5 V. The higher CE settings (+5 V) resulted in the loss of detection of transitions A, Ci, Cii, Gi and Gii. No significant differences in SRM sensitivities were observed for the remaining peptides in the method. The lower CE settings (-5 V) resulted in reduced (~20%) SRM sensitivities of all target analytes. The default CE (calculated depending on precursor ion m and z) was therefore taken as the most suitable for the detection of all transitions in the method.

Once the method was established it was important to define whether light and heavy TMT-labeled versions of the same peptide co-eluted following RP chromatography. Additionally, it was required that the approach was able to discern between light and heavy TMT-labeled transitions of the same peptide, *i.e.,* crosstalk. To assess co-elution, light and heavy labeled plasma peptides mixed in a 1:1 ratio were analysed using the TMT-SRM method. All peptides were observed by TMT-SRM. Figure 2.4 displays the SRM extracted ion chromatogram (XIC) for the target peptides. Light and heavy-labeled versions of the same peptide were shown to perfectly co-elute. This was crucial for the approach, as it allowed for the direct comparison and relative quantitation between different TMT-labeled versions of the same peptide, both here, and in subsequent TMT-SRM experiments.

To assess the selectivity between light TMT and heavy TMT transitions, light TMT-labeled plasma and heavy TMT labeled plasma were analysed individually. The method was shown to be highly selective and no significant crosstalk (< 1% of total SRM signal) was observed for the majority of transitions. However, at this stage it was not possible to discern between crosstalk and background interference due to the complexity of the sample. Even for precursors of 3^+ charge state with one tag attached,

selectivity was achieved (peptide A). Here, the approach discriminated between light TMT and heavy TMT transitions with an *m/z* difference of only 1.66 in Q1, whilst Q3 ion *m/z* were identical. Background interference (>1%) was observed for peptide Gi. Here, TMT-SRM quantitation was based on a pseudo y-ion in Q3. Pseudo y-ions would therefore be treated with caution in future TMT-SRM experiments, but at this stage warranted further consideration due to the benefit these ions provided in the absence of other fragmentation information.

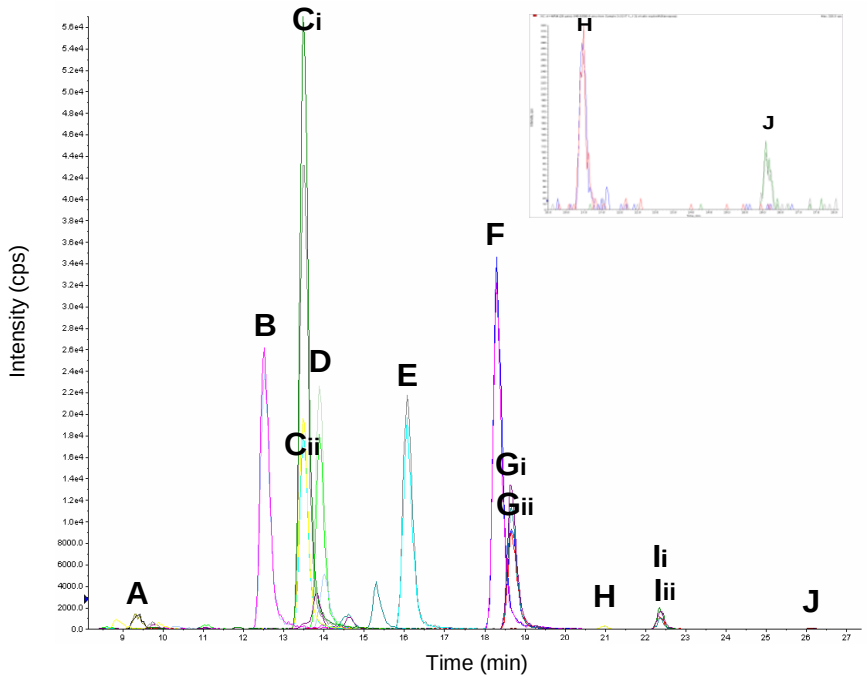

Figure 2.4 An SRM XIC for light TMT and heavy TMT-labeled peptides A - J spiked in a 1:1 ratio. All transitions listed in Table 2.2 are observed. The top right-hand panel displays the zoomed SRM XIC showing the lower intensity peptides H and J. For each peptide, it can be seen the light TMT and heavy TMT-labeled peptide pairs co-elute.

2.2.1.4 Accuracy of TMT-SRM quantitation of target plasma peptides

The trueness and precision of TMT-SRM quantitation was assessed by combining light TMT and heavy TMT-labeled standard plasma in 1:1, 3:1, 9:1 and 27:1 (L/H) ratios and comparing the observed experimental ratios to that of expected ratios. Three analytical repeats were acquired for each ratio. Figure 2.5 A displays the extracted transitions of peptide B across the different ratios for one analytical repeat.

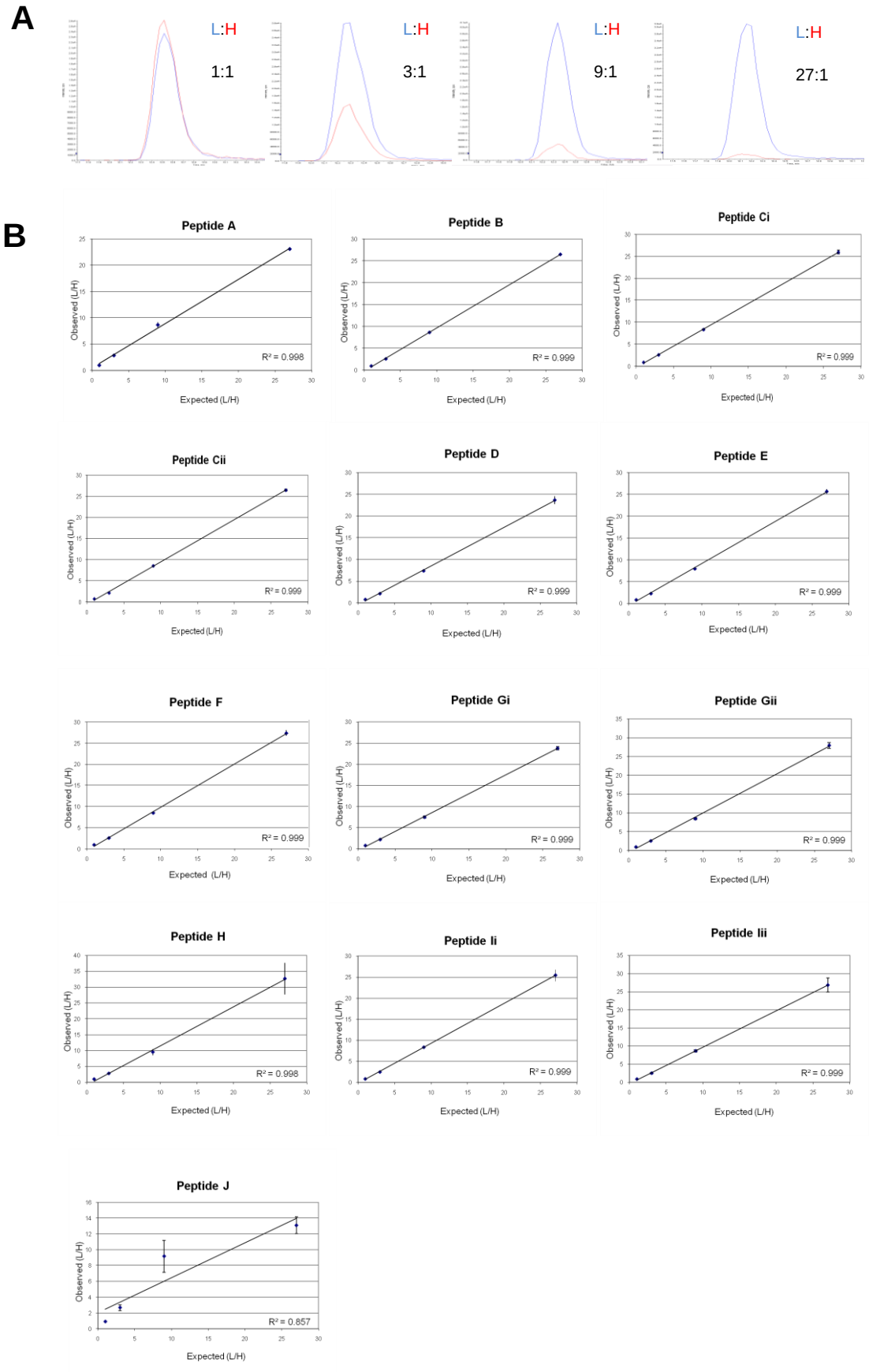

Figure 2.5 The accuracy of TMT-SRM quantitation. **A** SRM XIC for peptide B mixed in 1:1, 3:1, 9:1 and 27:1 (L/H) ratios. **B** Plots of observed *versus* expected L/H ratios for plasma peptides A – J. A linear response was observed for the majority of peptides with good precision from replicate runs. Less accurate TMT-SRM quantitation was observed for peptides H, Iii and J. Error bars indicate ± 1 SD.

Each ratio appeared to be as expected. Similar patterns were observed for all remaining peptides in the TMT-SRM method.

Good agreement was found between observed and expected ratios for peptides A - Iii (Table 2.3, Figure 2.5 B), indicating trueness in TMT-SRM quantitation. Using peptide B as the best example, observed mean ratios matched well with expected ratios and analytical repeats were precise, with CVs < 1% (Table 2.3). Peptides H – J had higher mean %CVs. This can be explained by the increased hydrophobicity of these peptides as they elute later in the LC gradient. These peptides typically have poorer elution properties exhibiting peak broadening and jagged peak shapes resulting in increased variability in peak area. Poor SRM peak shape may also explain the poorer trueness observed for the hydrophobic peptide J, where a mean ratio of 13:1 was observed for the expected ratio of 27:1. Furthermore, peptides eluting later in the LC gradient had the lowest SRM sensitivities and are thus more likely to be affected by background interference at the extreme ratios, *i.e.,* 27:1 L/H. Consequently, hydrophobic peptides of low SRM sensitivity may be less suitable for TMT-SRM quantitation. Considering all peptides however, the approach was shown to be precise, with 83% of all CVs < 5%. In summary, the results demonstrate the potential of TMT-SRM to be an accurate strategy for the quantitation of peptides in unfractionated plasma.

Peptide ID	Ratio (L/H)				Mean Precision (%CV)
	1:1	3:1	9:1	27:1	
A	0.91	2.87	8.67	23.08	2.60
B	0.90	2.53	8.60	26.46	0.59
Ci	0.91	2.61	8.36	25.96	1.18
Cii	0.78	2.20	7.24	21.91	0.99
D	0.76	2.11	7.36	23.67	2.23
E	0.84	2.28	7.96	25.68	2.23
F	0.96	2.58	8.50	27.39	1.78
Gi	0.82	2.24	7.54	23.80	2.01
Gii	0.94	2.55	8.44	27.93	1.72
H	0.98	2.77	9.50	32.64	8.70
Ii	0.87	2.51	8.38	25.45	5.43
Iii	0.87	2.51	8.67	26.84	5.87
J	0.91	2.68	9.18	13.09	11.39

Table 2.3 Observed ratios of L/H for plasma peptides A – J. Good agreement between observed and expected L/H ratios was shown for the majority of peptides in the TMT-SRM method. Peptides later in the LC gradient (peptides H - J) showed less precision.

2.2.2 Assessment of plasma matrix effects on the accuracy of quantitation by TMT-SRM

The previous experiment demonstrated the value of TMT-SRM as an approach for peptide quantitation with good accuracy observed. However, as referencing was performed between differentially labeled plasma samples, the background signal contribution from the plasma in each light TMT and heavy TMT channel could not be directly determined. Furthermore, only high abundant plasma peptides were targeted where the background matrix was found to have negligible effect on the quantitative measurement. To further appreciate the effect of the plasma matrix on the quantitation of less abundant molecules, an additional experiment was designed. Here, a protein exogenous to plasma (BSA) was spiked into plasma over a range of concentrations (µg/mL) representing the same magnitude as the endogenous levels of the candidate AD biomarker proteins in the assay required for development.

2.2.2.1 BSA peptide and transition selection

Following IDA analysis of light TMT-labeled BSA, peptides were selected for TMT-SRM quantitation that were proteotypic to BSA, *i.e.,* each peptide uniquely identified BSA and did not share any sequence homology with human serum albumin peptides (Table 2.4). This was a further advancement in the TMT-SRM workflow as peptide proteotypicity was not considered in the initial experiment. Each peptide had no known *in vivo* or *in vitro* modifications, was fully hydrolysed by trypsin, covered a good range of *m/z* in Q1 to assess selectivity and background interference at low and high *m/z* and had suitable MS/MS fragment ions for Q3 selection. Three transitions per peptide were selected (including pseudo y-ion fragments) to provide multiple measurements for the quantitation of each peptide. This was to increase the confidence in the quantitative measurement and would allow for the determination of aberrant transitions. The corresponding Q1 and Q3 masses of heavy TMT-labeled peptides were calculated *in silico* based on the number and position of TMT tags

Peptide ID	Peptide sequence	Charge State (+)	t_R (min)	Light TMT		Heavy TMT		DP (V)	CE (V)	CXP (V)
				Q1 (*m/z*)	Q3 (*m/z*)	Q1 (*m/z*)	Q3 (*m/z*)			
1[a]	^{TMT}LVNELTEFAK^{TMT}	2	31	806.52	819.47 (y5)	811.52	824.47 (y5)	120	44	13
					932.56 (y6)		937.56 (y6)			
					1175.64 (y8)		1180.64 (y8)			
2	^{TMT}AEFVENTK^{TMT}	2	22	685.92	1217.84 (p)*[b]	690.92	1226.84 (p)	75	48	9
					799.50 (b5)		804.50 (b5)			
					700.43 (y4)		705.43 (y4)			
3[a]	^{TMT}QTALVELLK^{TMT}	2	30	731.98	938.64 (y6)	736.98	943.64 (y6)	120	40	10
					830.55 (y5)		830.55 (y5)			
					984.59 (b7)		984.59 (b7)			
4	^{TMT}HLDVDEPQNLIK^{TMT}	3	21	585.39	711.48 (y4)	588.67	716.48 (y4)	75	28	9
					818.45 (b5)		823.45 (b5)			
					635.85 (b9++)[b]		638.35 (b9++)			
5[a]	^{TMT}HPYFYAPELLYANK^{TMT}	3	31	779.76	719.42 (y4)	783.09	724.42 (y4)	120	36	20
					882.48 (y5)		887.48 (y5)			
					1003.51 (b6)		1008.51 (b6)			
6	^{TMT}AWSVAR	2	17	457.27	739.42 (b5)	459.77	744.42 (b5)	75	36	9
					668.38 (b4)		673.38 (b4)			
					760.74 (p)[b]		764.54 (p)			
7[a]	^{TMT}LGEYGFQNALIVR	2	529	852.50	1180.65 (y10)	855.00	1180.65 (y10)	120	50	17
					1017.58 (y9)		1017.58 (y9)			
					1366.71 (y12)		1366.71 (y12)			
8	^{TMT}AFDEK^{TMT}	2	16	529.31	500.32 (y2)[b]	534.31	505.32 (y2)	75	40	9
					558.30 (b3)[b]		563.30 (b3)			
					904.62 (p)[b]		913.62 (p)			
9	^{TMT}DLGEEHFK^{TMT}	3	18	474.89	639.35 (b4)	478.23	644.35 (b4)	75	23	9
					518.34 (y2)		523.34 (y2)			
					728.39 (b5)[b]		733.39 (b5)			

Table 2.4 BSA peptides selected for TMT-SRM quantitation. The position of the TMT label is indicated for each peptide along with the peptide's precursor ion charge state and t_R. The Q1 and Q3 transitions for the detection of the light TMT and heavy TMT-labeled versions of each peptide are also listed. *the Q3 transitions denoted (p) represent the pseudo y-ion fragmentation. Compound-dependent parameter voltages are also given.

[a] Excluded due to poor endogenous detection in plasma. [b] Excluded from data analysis due to the presence of plasma background interference.

attached to the peptide and the charge state of the peptide (Table 2.4).

2.2.2.2 LC-TMT-SRM method development for target BSA peptides spiked into plasma digest

In contrast to the initial experiments, the availability of a BSA protein here-in enabled peptides to be generated for infusion into the mass spectrometer and optimisation of compound-dependent parameters for each peptide, *i.e.,* the DP, CE and CXP. The instrument was linearly ramped over a range of voltages in combination with SRM scanning of a representative transition for each BSA peptide in the TMT-SRM method. This was not performed for individual transitions of a peptide due to the limited sample amounts when using a purified protein as an internal standard. Therefore, it was decided to optimise the compound-dependent parameters on one transition for each peptide, *i.e.,* the transition which had the median *m/z* in Q3.

For each parameter, the voltage resulting in the maximal ion count over the range was selected as the optimal setting (Figure 2.6). The optimal DP voltage trace was found to plateau over a broad range, whereas for CE and CXP a much more defined voltage resulted in the optimal sensitivity for a given transition. The optimisation of the compound-dependent parameters resulted in a ~3-fold improvement in SRM sensitivities and was thus considered an important part of the SRM development process. The final TMT-SRM method was prepared by combining all transitions, dwell and cycle times and optimised compound-dependent parameters (Table 2.4). The method measured 54 transitions (27 light and heavy TMT pairs) with a dwell time of 50 msec per transition and a total cycle time of 2.7 sec. The peak width was 25 sec at FWHM, resulting in approximately 10 data points per SRM.

Crosstalk between transitions pairs of each peptide was further assessed with analysis of light TMT-labeled BSA peptides only (*i.e.,* no plasma matrix) over all light TMT and heavy TMT transitions using a typical 90 min LC gradient. Similarly, heavy TMT-labeled BSA peptides only were analysed over all transitions. All transitions were shown to be selective with <1% of the total SRM signal resulting from crosstalk or back

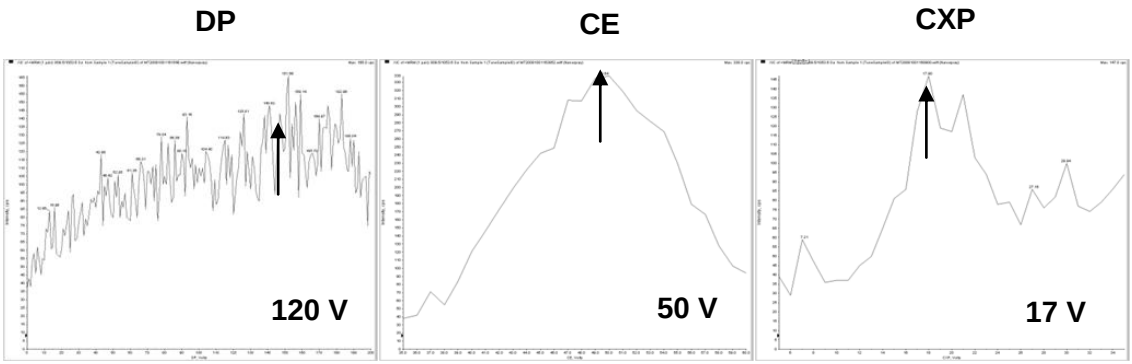

Figure 2.6 Voltage traces for DP, CE and CXP optimisation. The optimal DP, CE and CXP values of BSA peptide 7 are indicated by the arrow in the diagram.

-ground interference, *i.e.,* only pure peptides can truly measure crosstalk. This level of crosstalk or background interference was considered negligible to the overall quantitative measurement.

Following determination of crosstalk between light TMT and heavy TMT transitions, BSA peptides were spiked into plasma matrix and analysed by TMT-SRM over the same 90 min LC gradient. Spiking the BSA peptides into the light TMT-labeled plasma matrix had a detrimental effect on the detection of several peptides. The more hydrophobic peptides 1, 3, 5, and 7 were not quantifiable at the 1:1 ratio due to very low signal intensity and poor SRM peak shape. This is likely due to the fact that at this spike level in plasma these peptides are poorly detected in the complex background and also, the matrix may be causing signal suppression (Keshishian *et al.,* 2007). This highlighted the necessity of choosing several peptides per protein for TMT-SRM quantitation to compensate for the poor performance of certain peptides. Such peptides were excluded from further analysis resulting in peptides 2, 4, 6, 8 and 9 remaining for quantitation. LC gradient length (30, 60 and 90 min) was then assessed to determine the shortest gradient time which provided the best SRM peak profiles without compromise to selectivity and data points. Separation of peptides over the 30 min LC gradient achieved the highest SRM sensitivity and smoothest SRM peak shape for all transitions, whilst accuracy in quantitation was maintained (the 1:1 ratio for the combined peptides was observed). Shorter LC gradient lengths were highly desirable as the total analysis time was reduced, allowing for a higher throughput of samples.

Background interference from the plasma was observed in the light TMT and heavy TMT channels for seven BSA transitions when analysing either light TMT and heavy TMT-labeled BSA peptides spiked into light TMT-labeled plasma. This was found to be dependent on the *m/z* of the Q3 ion. A greater contribution of background SRM signal was observed for transitions which had low *m/z* Q3 fragment ions. For example, high plasma background interference was observed for the transitions which measured the low mass structural ions of peptide 8 (y2 and b3) and peptide 4 ($b9^{++}$; Table 2.4). This highlights the importance of selecting Q3 ions greater than the *m/z* of the precursor ion where possible as they provide greater selectivity between light TMT and heavy TMT transitions. All transitions which measured the pseudo y-ion in Q3 (peptides 2, 6 and 8) were significantly affected by background interference. This is demonstrated for peptides 2 and 6 in Figure 2.7, where all Q3 transitions based on high mass structural ions fall in the expected 1:1 ratio but transitions based on pseudo y-ions deviate from that expected. As pseudo y-ions are generated from all TMT-labeled peptides, this would result in the likelihood of less specific SRM transitions and less robust TMT-SRM quantitation. Consequently, pseudo y-ions will not be considered for future TMT-SRM quantitative measurements. Finally, the b5 transition of peptide 9 was adversely affected by high plasma background. As this transition represented a Q3 ion with an *m/z* above the Q1 precursor *m/z*, it is therefore important to select at least three transitions per peptide so as such aberrant transitions can be excluded. Further, it increases the chance of having transitions which can provide a robust quantitative measurement. In the subsequent analysis of the data, all transitions which were shown to be affected by the plasma background were removed to avoid inaccuracies in TMT-SRM quantitation (Table 2.4). All three transitions of peptide 8 were affected by background interference and therefore the peptide was excluded from the data analysis. Plasma background interference had a greater effect on certain SRM transitions in this experiment than was observed in the initial experiments (Section 2.2.1). This was speculated to be due to the analysis here of peptides at lower

concentrations to that described previously, where any background interference would have a greater contribution to overall SRM signal.

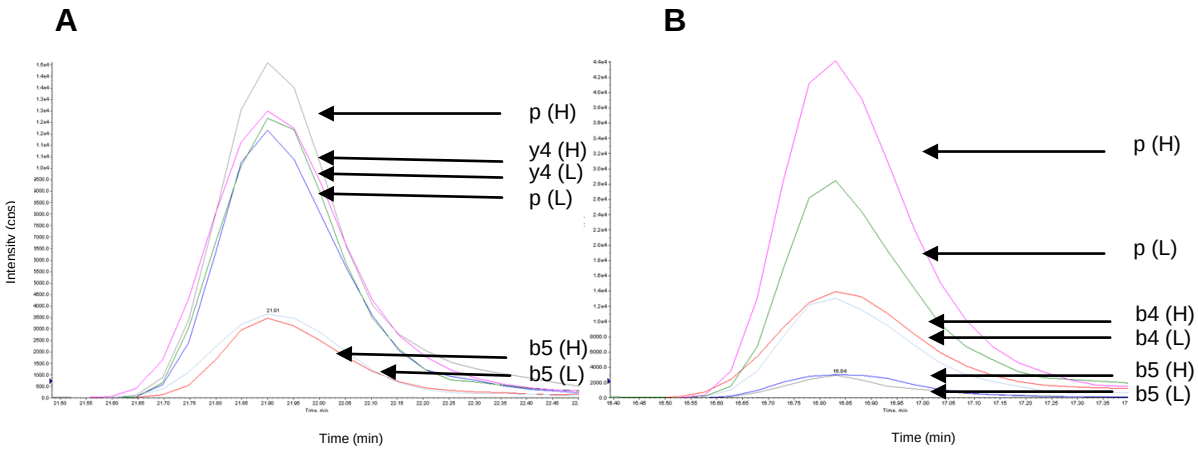

Figure 2.7 TMT-SRM XIC to highlight the varying selectivities of different transitions of BSA peptides. High plasma background interference is observed for the transition utilising the pseudo-y ion (p) for peptide 2 (A) and peptide 6 (B). For the remaining transitions of both peptides, the expected ratio of 1:1 L/H was observed.

2.2.2.3 Effects of plasma matrix on the accuracy of TMT-SRM quantitation

For the determination of accuracy of TMT-SRM quantitation, light TMT-labeled BSA was spiked into plasma over a range of concentrations. Heavy TMT-labeled BSA was spiked in at a constant amount of 10 ng to act as a reference. The ratios analysed were as follows: 0.33:1, 1:1, 3:1, 9:1 and 27:1 (L/H), representing levels in plasma from 266 µg/mL to 21.6 mg/ml with the reference spiked in at 800 µg/mL levels (12.6 µM). An identical analysis was performed without the presence of matrix. Three analytical and three technical replicates of each sample ratio were analysed. It was important to perform several analytical and technical repeats to characterise the precision of sample preparation procedures and QTRAP instrument performance. A linear relationship was found between observed and expected ratios for BSA peptides 2, 4, 6 and 9 in the presence of plasma matrix (Figure 2.8 A). Accurate TMT-SRM quantitation was observed across analytical and technical repeats with, as expected, better statistics for analytical over technical repeats (Table 2.5). Analytical repeats had CVs ranging from 1.3 – 11.4% (50% of CVs ≤ 5%) while technical repeats had CVs ranging from 0.82 -

A

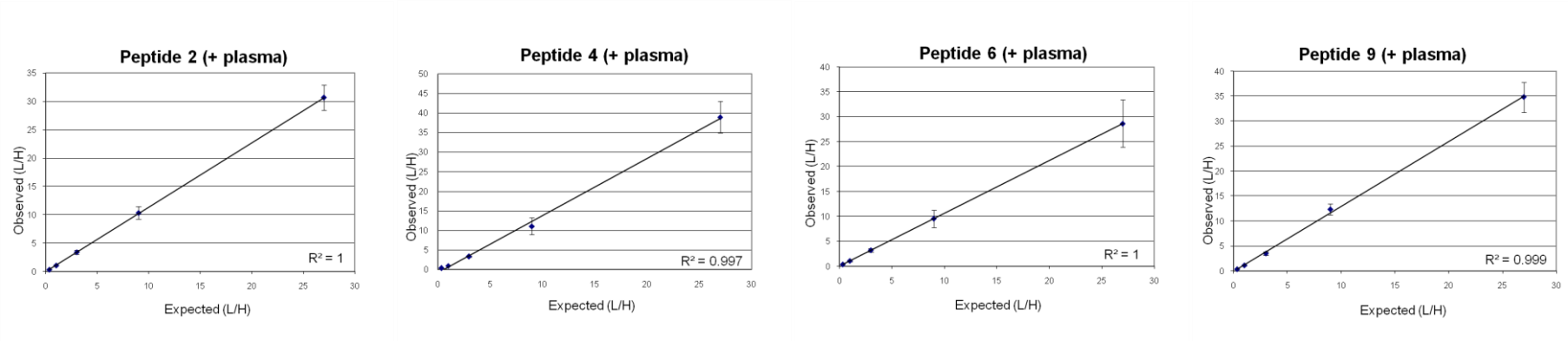

B

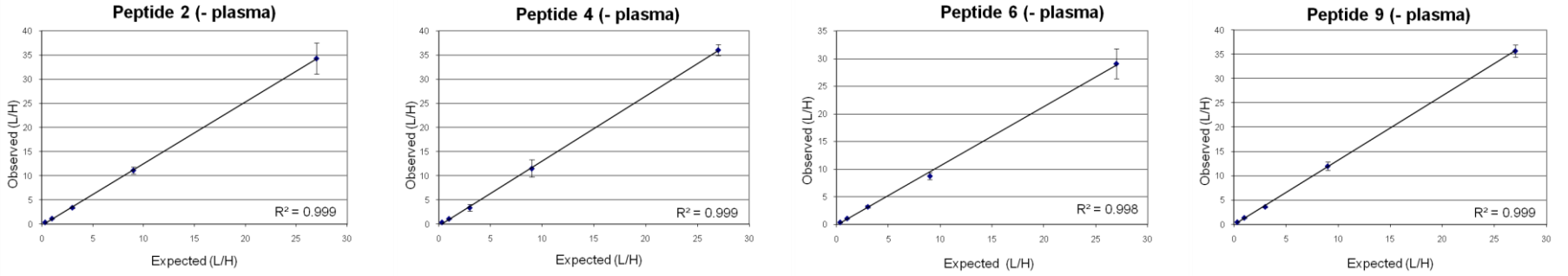

Figure 2.8 Observed *versus* expected L/H ratio for BSA peptides 2, 4, 6 and 9. **A** in plasma matrix and **B** buffer-only. The mean of three analytical measurements is plotted for each of the three technical repeats. Error bars indicate ± 1 SD.

Peptide 2	T1					T 1, 2, 3	T 1, 2, 3
L/H	A1	A2	A3	Mean L/H	%CV	Mean L/H	%CV
0.33:1	0.29	0.35	0.33	0.32	10.20	0.34	7.80
1:1	0.93	1.14	1.06	1.04	10.10	1.08	7.33
3:1	2.93	3.07	3.30	3.01	5.94	3.41	9.15
9:1	9.16	9.05	9.24	9.15	1.30	10.30	10.95
27:1	29.40	28.90	29.80	29.30	1.51	30.60	7.32

Peptide 4	T1					T 1, 2, 3	T 1, 2, 3
L/H	A1	A2	A3	Mean L/H	%CV	Mean L/H	%CV
0.33:1	0.29	0.29	0.32	0.30	6.85	0.30	0.82
1:1	0.87	0.99	0.86	0.91	8.15	0.95	10.33
3:1	2.64	2.91	2.92	2.82	5.61	3.25	11.79
9:1	8.94	9.67	9.11	9.24	4.16	11.10	15.93
27:1	37.40	36.20	39.30	37.60	4.18	38.90	11.62

Peptide 6	T1					T 1, 2, 3	T 1, 2, 3
L/H	A1	A2	A3	Mean L/H	%CV	Mean L/H	%CV
0.33:1	0.35	0.37	0.37	0.36	3.11	0.35	2.11
1:1	1.08	1.08	1.02	1.06	3.20	1.07	10.15
3:1	3.40	2.98	2.85	3.08	9.37	3.21	11.45
9:1	9.53	8.98	8.78	9.10	4.30	9.57	11.60
27:1	28.90	26.60	27.60	27.70	4.07	28.70	10.53

Peptide 9	T1					T 1, 2, 3	T 1, 2, 3
L/H	A1	A2	A3	Mean L/H	%CV	Mean L/H	%CV
0.33:1	0.32	0.35	0.37	0.35	6.85	0.35	0.61
1:1	1.05	1.14	1.06	1.08	4.67	1.11	4.43
3:1	3.43	3.42	3.38	3.40	7.41	3.48	3.04
9:1	9.63	9.37	10.50	9.83	6.01	12.30	17.86
27:1	31.20	32.60	32.00	31.90	2.08	34.80	12.10

Table 2.5 Accuracy of TMT-SRM for BSA peptides quantitated in the presence of human plasma matrix. As an example of the accuracy of analytical repeats, the individual and mean trueness (L/H ratio) for all analytical repeats (A1, A2 and A3) of technical replicate 1 (T1) is displayed. Furthermore, mean trueness and precision values across all technical replicates (T1, T2 and T3) are displayed.

17.9% (45% of CVs ≤ 10%, 85% of CVs ≤ 12%). This demonstrated highly precise QTRAP instrument performance and in the overall TMT-SRM sample preparation workflow. Buffer-only results were found to be comparable to those obtained in the presence of matrix, thus confirming that background interference due to the plasma matrix did not affect TMT-SRM quantitation of those peptides remaining in the method in this range of concentrations (Figure 2.8 B; Appendix Table 2.1). This was reflected in the strong correlation observed between corresponding ratios of BSA peptides quantitated in each (r = 0.97 for all measurements). Thus, upon removal of problematic transitions with high plasma background interference, robust TMT-SRM measurements were achieved for BSA peptides 2, 4, 6 and 9 across the spiked concentration range in the presence of plasma matrix.

2.3 Summary

- Proof-of-principle experiments have demonstrated TMT-SRM as an accurate quantitative strategy for the targeted measurement of multiple peptides in plasma at levels which represent medium to high abundant proteins.
- The TMT sample processing workflow has been optimised for plasma including the choice of digestion enzyme.
- By using isotopic versions of TMT's, biological samples and purified proteins, as well as synthetic peptides can be utilised as internal standards for quantitation.
- Important factors to achieve accurate quantitative measurements include:
  - Selection of multiple proteotypic peptides per protein. This allows for the removal of poor performing peptides and adds confidence to the protein measurement.
  - Selection of multiple high *m/z* structural ions in Q3 to build SRM transitions. This enables the determination of the most robust transitions for quantitation and adds confidence to the quantitative measurement.
  - Optimisation of compound-dependent parameters. This significantly improves SRM sensitivity by tuning voltages to the optimal detection of target peptides.
  - LC t_R of peptides. Later eluting peptides are less suited to the approach as they tend to have poorer SRM peak shape and detection.
  - Assessment of the contribution that the background matrix has on the quantitative measurement. Such transitions/peptides affected by background signal can be excluded from subsequent data analysis.
  - Consideration of analytical and technical repeats to add confidence to the measurement.
- Similar peptide fragmentation patterns were observed on Q-Tof micro and QTRAP MS platforms, demonstrating the ease at which MS/MS data from biomarker discovery analyses can be used for TMT-SRM methods in validation.

Chapter 3

Development of a multiplexed TMT-SRM assay for the quantitation of candidate Alzheimer's disease biomarkers in human plasma

3.0 Introduction

From biomarker discovery studies using 2DE and TMT labeling technologies, clusterin, complement C3, complement C3a, CFH, A2M, FGG, SAP, and gelsolin have emerged as candidate AD biomarkers (Hye *et al.,* 2006; Thambisetty *et al.,* 2010; Güntert *et al.,* 2010). Furthermore, possession of the ApoE ε4 allele is the only unequivocal genetic risk factor known to-date for late-onset AD and the protein expression of this genetic association may translate as an AD biomarker (Coon *et al.,* 2007). The expression levels of these proteins across large AD patient populations have yet to be determined.

Using the TMT-SRM strategy outlined in Chapter 2, this chapter focuses on the development of a multiplexed TMT-SRM assay for the quantitation of the AD candidate biomarkers in human plasma. This required that target analytes could be quantitated accurately, in parallel, and in a time scale which was viable for the analysis of a large number of samples. As the candidate proteins represent medium to high abundant species in plasma, it was hypothesised that the target analytes could be detected and quantitated in unfractionated plasma. This has obvious benefits as minimal sample manipulation will limit sample to sample variability, thereby improving accuracy in the quantitative measurement. Furthermore, limited sample processing allows for a potentialy higher throughput of samples, essential for any clinical assay. This MS assay approach relies on the quantitation of proteolytic peptides, which in turn act as a surrogate measurement for the level of the target protein in the sample. Robust quantitation is therefore dependent on the careful selection of peptides which are unique to the protein of interest, unmodified, *i.e.,* free of PTMs and digested in a reproducible manner. Also, to ensure accuracy of quantitation, SRM transitions are required to be specific for each target analyte. Both peptide choice and transition specificity needed to be established during the method development phase for the detection and quantitation of the target proteins. Further, a stable and reproducible

analytical platform was required to deliver high quality MS assay results and this was also considered in the development of the assay.

In contrast to the proof of principle experiments described in Chapter 2 where internal standardisation was performed against both a human plasma reference and purified protein (BSA), the choice was taken to utilise synthetic peptides for the AD protein panel TMT-SRM assay. This reference approach (as opposed to a biological reference) was taken to limit the overall sample complexity, improving the chance of detection and quantitation of the target proteins which are present in plasma down to low µg/mL levels. An additional advantage of using synthetic peptides is the ability to fine-tune instrument compound-dependant parameters during the method development process, thus enhancing the final detection of the target analytes in plasma. Furthermore, the use of synthetic peptides would provide absolute quantitative measurements.

3.1 Materials and Methods

3.1.1. Selection of target peptides

Clusterin (SwissProt accession number P10909), complement C3 (P01024), complement C3a (P01024 [formed from cleavage of amino acids 672-748 from full length complement C3]), CFH (P08603), A2M (P01023), FGG (P02679), SAP (P02743), ApoE (P02649) and gelsolin (P06396) were selected as candidate proteins for which AD diagnosis and prognosis may be monitored. In the first instance, an *in silico*-based approach was undertaken to determine the most suitable peptides from each target protein for TMT-SRM quantitation. It was crucial that each peptide uniquely identified the mature form of the target protein, that is, was proteotypic, with a unique sequence in the human proteome (Craig *et al.,* 2005). This was determined using custom built in-house software (Proteotype), where the number of occurrences of each tryptic peptide of each candidate protein in the human proteome was determined. The software is based on a Perl computer programming script, where each peptide sequence from an *in silico* digest of a protein of interest is compared against all sequences in the human database. The frequency of occurence of each sequence is calculated, generating an output .pl file. To ensure sufficient SRM selectivity, peptides with a minimum of six amino acids were selected for TMT-SRM quantitation (Picotti *et al.,* 2010). Further, peptides with a maximum of 25 amino acids were selected due to the financial burden and effort required to synthesise longer peptides. Additionally, such species are generally more hydrophobic, making them less suited for robust TMT-SRM quantitation (as demonstrated in Chapter 2). Peptides were also chosen that had no known PTMs to ensure the quantitative measurement reflected as closely as possible to the level of the protein in the sample. To determine this, each peptide was manually checked for the presence of known PTMs, *e.g.,* phosphorylation or glycosylation, against the annotation information for each accession number in SwissProt (release 54.0, 24th July 2007). Despite trypsin being highly specific and efficient for protein digestion, peptides with missed cleavage sites are frequently

observed. As a consequence, peptides which were not fully hydrolysed with trypsin, *i.e.,* had one or more missed cleavages, were not considered. Peptides were also checked for the presence of tryptic cleavage sites immediately upstream or downstream from the peptide. Peptides containing residues which may be chemically modified during sample processing were also excluded. Specifically, methionine and tryptophan residues were avoided as their side chains may become oxidised and peptides containing cysteine residues were excluded as they may become alkylated (Stadtman and Levine, 2003). N-terminal glutamic acid and glutamine residues were avoided as they can spontaneously cyclise to become pyroglutamate. Internal lysine, arginine (*i.e.,* KP/RP-non tryptic cleavage sites) and histidine residues increase the charge state of a peptide and thus, were avoided where possible (Yocum *et al.,* 2009).

MS/MS data of TMT-labeled and unlabeled plasma datasets from discovery studies were mined to determine which proteotypic peptides from the *in silico* analysis were routinely identified in shotgun proteomic experiments. Ideally, peptides that had been observed in TMT-labeled studies were taken forward for further consideration. However, where this information was limited, unlabeled plasma datasets were also considered.

Based on the criteria described, panels of peptides per candidate protein were taken forward for further consideration. In response to the cost and effort required to prepare synthetic peptides, the strategy was limited in the number of peptides available for TMT-SRM quantitation. However, at least three peptides per protein were considered essential to afford a robust quantitative measurement. Therefore, to further refine the list to three peptides per protein, peptides were excluded if problems were envisaged during synthesis and purification, *i.e.,* the presence of hydrophobic amino acids such as leucine, valine, isoleucine, phenylalanine and tryptophan. These peptides would difficult to solubilise in aqueous solution or in some cases, may be completely insoluble. Further, peptides were excluded which had many neighbouring tryptophan, isoleucine, valine, tyrosine, leucine, glutamine, phenylalanine, and threonine residues. These amino acids are responsible for beta-sheet formation which

can result in deletions and even truncations, resulting in a poor synthetic yield of the required product.

3.1.2 Synthesis and TMT-labeling of peptides for internal standardisation

The 32 peptides selected for TMT-SRM analysis of the candidate AD biomarker proteins were synthesised in-house at Proteome Sciences, Frankfurt, Germany. For TMT-SRM analysis, synthetic peptides were resuspended in 50% ACN, 0.1% FA to a final concentration of 3 nmol/µL (Keshishian *et al.,* 2007). Peptides were aliquoted into 50 µL and 100 µL volumes in 250 µL glass vials (Chromacol Ltd, Welwyn Garden City, UK) and stored at -80 °C until further use. Peptides (500 µg of each) were individually processed using the standard protocol for TMT labeling and purification by RP and SCX as described in Sections 2.1.1.3 and 2.1.1.4. The following exceptions were made: SDS was omitted from the protocol, and as there were no cysteine-containing peptides, no reduction was required. To maintain the concentration of all constituents to that of the standard TMT-labeling protocol, the volumes added for solubilisation, reduction and alkylation were replaced with equivalent volumes of H_2O or ACN. As all the peptides were tryptic, no digestion was necessary and so the trypsin solution was replaced with 100 mM triethylammonium bicarbonate (TEAB; Sigma-Aldrich). For method development purposes, individual peptide solutions were labeled with 15 mM light TMT (as per the standard protocol). Purified peptides were lyophilised to dryness and stored at -80 °C.

3.1.3 Transition selection and optimisation of compound-dependent parameters

Light TMT-labeled peptides were directly infused into the QTRAP to assess the quality of each peptide and to define the SRM parameters. Specifically, a 2 pmol/µL solution of each peptide was prepared in 50% ACN, 0.05% FA and infused at 1 µL/min. To assess purity, a total ion MS profile of each peptide solution was acquired using a Q1 positive ionisation scan at unit mass resolution over the mass range *m/z* 400 – 1600. This also enabled the determination of the predominant charge state for each

peptide (precursor ion *m/z*). For the selection of optimal Q3 ions to build the SRM method, an Enhanced Resolution (ER) and EPI scan was initially used to confirm theoretical *m/z* values for each peptide precursor and fragment ion. Using observed *m/z* values from ER, each peptide underwent EPI scanning (*i.e.,* MS/MS analysis). To improve the specificity and sensitivity of each transition in Q3, the highest intensity fragment ions above the *m/z* of the precursor ion were selected where possible. Three transitions per peptide were selected for quantitation. The SRM method was initially established by inputting all theoretical precursor and fragment ion masses for each light TMT-labeled peptide.

To enhance the sensitivities of each peptide and give the best chance of detecting each target analyte in plasma, the DP, CE and CXP were optimised for each individual transition. Peptides were infused into the QTRAP as described above and the DP, CE and CXP were optimised using the strategy as described in Section 2.1.2.2. Optimal values for each transition were then added to the SRM method.

3.1.4 Definition of peptide retention times and assessment of the selectivity and specificity of transitions by LC-SRM analysis

In the first instance, the SRM method containing the light TMT-labeled transitions and optimised voltages was used to determine the LC-SRM detection of a mixture of the 32 light TMT-labeled peptides. A mixture was prepared with each peptide at 5 fmol/µL (*i.e.,* 100 fmol o/c). An LC gradient of 0 - 32% ACN over 85 min was delivered for the resolution of the peptides. The LC was operated as described in Section 2.1.1.7. Washing and equilibration of the column increased the total analysis time to 100 min. Analysis of the peptide mixture was performed in triplicate to obtain a mean t_R for each light TMT-labeled peptide. Due to the large number of transitions in the method (the final method would have 192 transitions; 96 heavy and light TMT pairs), SRM scheduling was required to enhance the detection of each transition. Here, SRM transitions are monitored only around their expected elution times, reducing the number of transitions being monitored at any one time (Stahl-Zeng *et al.,* 2007). This

results in increased dwell and reduced cycle times, with enhancement of SRM sensitivity. Mean t_R for all peptides were used to build the SRM scheduled method. Once all peptides were detected within the SRM scheduling window, the method was developed further by adding corresponding heavy TMT ion masses for Q1 and Q3 (calculated *in silico*). Using the full method containing all 192 transitions, optimal dwell and cycle times for each transition could then be determined. An analysis was also performed whereby the light TMT-labeled peptides were analysed over the SRM scheduled method containing all light and heavy TMT transitions. From this, crosstalk between the light and heavy TMT transitions was directly determined.

The endogenous detection of the peptides in plasma next needed to be established. This was assessed with the analysis of light TMT-labeled peptides spiked into heavy TMT-labeled plasma (as prepared in Sections 2.1.1.2 - 4). Analysis was performed in triplicate. The mean t_R for each peptide in the presence of matrix was updated in the method. To establish the plasma load for the optimal detection of the endogenous peptides, light TMT-labeled peptides and heavy TMT-labeled plasma was run over the TMT-SRM method at 1 µg and 2 µg total protein loads o/c. The level of carry-over from TMT-labeled plasma samples was determined by running a blank over all light TMT and heavy TMT transitions before and after the heavy TMT-labeled plasma sample.

The TMT-SRM quantitation of the candidate biomarker panel will ultimately be performed in a large cohort of plasma samples. The composition of plasma samples may be largely varied, with different levels of background interference associated with each. It was important to determine such background for each transition in the method across different plasmas, so that potentially problematical transitions could be highlighted. Specifically, Dade Behring plasma (Plasma A) and a pooled plasma sample from an AD cohort (Plasma B; see Section 4.1.1) were compared. Plasma B was selected to represent the constitution of the clinical samples to be used in the final assay. Plasma A and B were labeled with heavy TMT in parallel as described in

Sections 2.1.1.2 – 4. Both plasma samples (2 µg o/c) were analysed over all light TMT and heavy TMT transitions and the signal in the light TMT channel assessed.

3.1.5 Determination of the precision of TMT-SRM using a nanoflow analytical platform

To assess the precision of TMT-SRM quantitation for each peptide, replicate analyses of plasma A spiked with peptides was performed. Specifically, heavy TMT-labeled plasma was spiked with the light TMT-labeled reference peptides and divided into four aliquots, with each aliquot having enough sample for five replicate runs. Each set of five replicate samples where run consecutively in a given day and this was repeated for each aliquot over a period of four consecutive days. Plasma was loaded at 2 µg o/c. The L/H ratio was determined for each transition across all replicates as described in Section 2.1.1.9.

3.1.6 Validation of microflow LC rates and ESI for TMT-SRM and development of assay design

Higher LC flow rates (*i.e.,* 100 µL/min) and ESI were investigated with the objective of improving the robustness of the assay. In parallel, an assay design was also developed such that the accuracy, linearity, LOD and LOQ could be derived for the assay of each analyte in an efficient and workable manner. To investigate this, a simple target analyte not endogenous to plasma was utilised. A synthetic tryptic peptide was selected which was available in-house (peptide sequence VATVSLPR) and labeled with light and heavy TMT as described in Section 2.1.1.3. The TMT-SRM method was developed with the selection of optimal Q1 and Q3 ions and compound-dependent parameters as described in Section 2.1.2.2.

TMT-SRM analysis was performed on a QTRAP coupled to an Ultimate 3000 LC system (Dionex) as described in Section 2.1.1.7. The initial format of the microflow LC system was implemented in the laboratory following discussion with the Biomarker Research Initiatives in Mass Spectrometry Centre (BRIMS) in Cambridge,

Massachusetts, USA. The mass spectrometer was fitted with a micro-ion spray source with a 27-gauge needle insert for microlitre flow rates and operated in positive ionisation mode. Q1 and Q3 mass resolution was set to unit. To establish optimal ion source voltage and gas parameters at the higher flow rate, light and heavy TMT-labeled peptides were infused into the instrument at 100 µL/min. Optimal detection was obtained with an ion spray voltage of 5250 V, interface heater temperature of 475 °C, curtain gas of 20 p.s.i and nebuliser gas of 25 p.s.i. For the LC, an in-line filter (0.2 µm; Upchurch Scientific, Cambridgeshire, UK) was placed upstream of the analytical column (Hypersil gold, 1 mm i.d. x 50 mm; 1.9 µm, Thermo Fisher Scientific), providing protection of the column by removing particulates which may be present in LC buffers and/or analytical samples. The autosampler was configured to enable sample pick-up (20 uL full loop injection with 21 uL sample pick-up) from a microtitre plate format. Peptides were resolved by RP-LC, over a 9 min gradient of 5 - 30% ACN, delivered by a combination of Buffer A (0.2% FA) and Buffer B (80% ACN, 0.2% FA) at a flow rate of 100 µL/min. Washing and equilibration of the column increased the total run time to 15 min. To prevent contaminants entering the mass spectrometer, all eluant during the first minute and final three minutes of each run was diverted to waste. Using stock solutions of 5 pmol/µL, light and heavy TMT-labeled VATVSLPR peptides were combined in a 1:1 ratio and diluted to 5 fmol/µL in 3% ACN, 0.2% FA. LC-SRM analysis of this solution was performed in triplicate to determine the accurate t_R.

To minimise peptide losses due to non-specific binding to plastics, VATVSLPR peptides were redissolved in a scavenger protein, glucagon (200 µg/mL in 3% ACN, 0.2% FA, glucagon solution; Sigma-Aldrich) to provide new stock solutions of 5 pmol/µL. An 11-point calibration curve was produced by varying the concentration of light TMT-labeled peptide whilst keeping the heavy TMT-labeled peptide constant. Specifically, a working solution of 5 fmol/µL heavy TMT-labeled VATVSLPR (to provide 100 fmol o/c) in glucagon solution was prepared from the stock and used as the diluent for preparation of the concentration range of light TMT-labeled peptides (0.25, 0.5, 1, 2, 5, 10, 50, 100, 250, 500 and 1000 fmol o/c) to build the curve. A comparison was made

between curves prepared in the presence and absence of glucagon. Subsequently, calibration curves prepared using VATVSLPR peptides resuspended in glucagon solution were quantitated in buffer-only (in duplicate) or plasma (one replicate; prepared as described in Section 3.1.7, sample C). The process of assay development required the evaluation of the accuracy of quantitation. Accuracy incorporates both trueness and precision of a measurement. To determine this, triplicate measurements (here-in referred to as QCs) of the 5 and 50 fmol o/c dilutions prepared above were acquired for each calibration curve, which were performed over two days (buffer-only measurements) or within a single day (plasma measurements). From these, the intra-batch (within day) and inter-batch (across day; *i.e.,* measurement only available for buffer-only experiments) variation was determined. Following peak area extraction as described in Section 2.1.1.9, standard curves (L/H *versus* L concentration) were plotted in Microsoft Excel 2003. Plots were $\log_{10}$ transformed to better visualise the lower points of the curve. The curves were used to interpolate QC amounts for the determination of the trueness and precision of TMT-SRM quantitation. The LOD was defined as the lowest concentration where the SRM sensitivity for each target analyte was three times the S/N. The LOQ was defined as the lowest concentration where precision was < 20%.

3.1.7 Upscaling of plasma digestion, TMT-labeling and purification protocols

Due to the increased amount of protein required for microflow/ESI analysis (30 µg of plasma protein per analysis), TMT-labeling and sample purification procedures were upscaled. To ensure the sample quality was not compromised and the sensitivity of the workflow was maintained, several comparisons were performed as outlined in Table 3.1. The same digested plasma sample was used across all comparisons.

In addition to adapting the standard protocol (Section 2.1.1.3) to account for higher protein amounts, several formal changes had been made to the standard protocol by the developers and manufacturers of TMT. Specifically, borate buffer was replaced with TEAB as this is a volatile buffer and easier to prepare.

Sample	Amount	TMT	Standard RP	Standard SCX	Upscaled RP	Upscaled SCX	Microtitre plate (30 µg)
A	100 µg	✓	✓	✓			
B	100 µg	✓		✓	✓		
C	1.8 mg	✓			✓	✓	✓

Table 3.1 Comparisons made to assess the effect of upscaling the TMT-labeling protocol.

Additionally, the time and temperature required for sample reduction was increased to 1 hr and 55 °C, respectively. Plasma A (25 µL; 2 mg, Section 3.1.5) was diluted to 1 µg/µL in 0.1% SDS, H_2O and 100 mM TEAB (pH 8.5). The sample was reduced, alkylated, digested and labeled with light TMT using concentrations as per the standard protocol. Labeled plasma peptides were diluted with 0.1% TFA to reduce the ACN concentration to ~ 5%. From this, 100 µg (1 mL; Sample A) was removed and purified by RP and SCX as per the standard protocol (Section 2.1.1.4). The remainder (1.9 mg, 19 mL) underwent an up-scaled RP procedure using Hypersep C18 Cartridges with a 500 mg bed volume (Thermo Fisher Scientific). Column conditioning, equilibration, washing and peptide elution was performed using volumes upscaled accordingly to the standard protocol. To determine if upscaling of the RP protocol had any detrimental effects, 100 µg of protein was taken from the RP eluant and subjected to SCX purification *via* the standard protocol (Sample B). The remaining 1.8 mg underwent SCX purification using an upscaled version of the protocol (Sample C). Specifically, SCX cartridges were prepared in-house using 2.6 mL sepharose suspension (four times the standard protocol). Washing and equilibration volumes were upscaled accordingly. Peptides were eluted in 3 mL SCX elution buffer and a further 1 mL of SCX loading buffer was added to reduce the concentration of salt in the sample. An aliquot (100 µg) was removed and lyophilised in an eppendorf as normal. The remaining sample was aliquoted into a Thermo-Fast® 96 Robotic PCR Plate (Thermo Fisher Scientific) with 30 µg of peptides per well (resulting in approximately 60 wells for analysis). Following lyophilisation, each well containing peptides was resuspended in SCX loading buffer to 0.5 µg/µL and lyophilised for a second time. Samples A, B and C

were analysed in duplicate by LC-MS/MS (1 µg protein load o/c, 60 min 0 - 32% ACN) as described in Section 2.1.1.5.

3.1.8 Preparation, TMT-labeling and purification of equimolar mixtures of candidate AD peptides of the same protein

Clinical sample cohorts, comprising large numbers of samples, consume large amounts of TMT label. The more cost-effective approach from here-on-in was to label plasma with the less expensive light TMT label (due to the lack of heavy isotopes) and label the synthetic peptide internal standards with heavy TMT. As a first step to minimise the variation in TMT-SRM quantitation between peptides of the same protein, the accurate concentration of each peptide was determined. AAA was performed at the Protein and Nucleic Acid Chemistry Facility, Department of Biochemistry, Cambridge, UK (Norden *et al.*, 2004). Specifically, all aliquots prepared in Section 3.1.2 were re-combined and the AAA concentration of each peptide solution determined. A suitable volume of each peptide stock solution (1.5 nmole/uL) and of L-norleucine internal standard was pipetted into a microtube (4 cm × 3 mm), which was cleaned beforehand by heating to 500°C for 15 hours and lyophilised to dryness. Gas phase acid hydrolysis was performed at 115°C for 22 hours. The residue was then dissolved in sodium citrate loading buffer (pH 2.2) and filtered by centrifugation through a 0.2 µm filter. An aliquot of the filtrate was injected into a loading capsule and placed in a Biochrom 30 Analyser © amino acid analyser (Biochrom Ltd., Cambridge, UK). Chromatography performed on a sodium system ion exchange resin eluting with buffers over the pH range 3.2 - 6.45. Peak detection was achieved by mixing the eluate with ninhydrin at 135°C and measuring the absorbance at 570 and 440 nm.

To further reduce quantitative variability, peptides of the same protein were combined in equimolar mixtures and labeled with light TMT (15.5 nmol of each peptide per mixture) and heavy TMT (62 nmol of each peptide per mixture) as described in Section 2.1.1. Heavy TMT-labeled peptides were used for method development, the generation of calibration curves and to act as an internal standard for TMT-SRM

quantitation. Light-labeled peptides were required for method development and the generation of calibration curves.

As each synthetic peptide was already in high concentrations of ACN (50%), adjustments were made to the standard protocol to ensure the concentration of ACN was in the acceptable range for TMT-labeling. TEAB (400 mM) stock solution was added to reach a final concentration of 100 mM for TMT-labeling. Solutions of IAA and TCEP were replaced with H_2O. Trypsin was replaced with 100 mM TEAB. A more concentrated stock solution of TMT was prepared (90 mM in 100% ACN) and added to reach a final concentration of 15 mM. Post-TMT labeling, 10 µL was removed from each equimolar mixture for quality assessment. Both light and heavy TMT-labeled equimolar mixtures underwent subsequent purification by RP and SCX as per the standard protocol. Post-purification, a 10 µL aliquot was removed from each mixture for quality assessment. The remaining volume was lyophilised to dryness and stored at -80 ^{o}C. Labeled and unlabeled equimolar mixtures of each protein were infused into the QTRAP. Solutions were diluted in 50% ACN, 0.25% FA and infused at 500 fmol/µL for 2 min over *m/z* 400 – 1200 in Q1 positive ionisation mode. All major ions in each mixture were assessed.

3.1.9 Modification of the LC-SRM method for the analysis of the AD candidate biomarker panel at microflow LC rates

LC and SRM parameters for the AD candidate biomarker panel using microflow LC conditions were determined. Important considerations were the reduction in gradient length and decrease in SRM peak widths. To determine whether the SRM detection of the target analytes in plasma was altered using microflow as compared to nanoflow LC rates, a full method was prepared for the analysis of all 32 original target analytes on the new platform. Heavy TMT-labeled equimolar mixtures of each protein were combined and diluted in glucagon solution to provide a stock solution of all peptides at 5 pmol/µL. This was further diluted to a peptide working solution of 5 fmol/µL. Light TMT-labeled plasma (30 µg o/c) was resuspended in 25 µL of the

working solution, thus providing 100 fmol of each internal standard o/c. To ensure sufficient LC separation of all target AD candidate biomarker peptides, the LC gradient was increased by 5 min to that used for TMT-SRM analysis of VATVSLPR. Thus, peptides were resolved by RP-LC over a 14 min gradient of 5 - 30% ACN at a flow rate of 100 µL/min. Washing and equilibration of the column increased the total run time to 20 min. QTRAP source parameters were as described in Section 3.1.6, with exception of the curtain gas which was increased to 30 p.s.i and the nebuliser gas which was increased to 30 p.s.i. Instrument performance was benchmarked prior to analyses using the TMT-SRM method established for the analysis of VATVSLPR in Section 3.1.6. Light TMT and heavy TMT-labeled versions of the peptide in glucagon solution were combined in a 1:1 ratio (100 fmol of each o/c) and the SRM sensitivity and elution profile assessed. Specifically, an SRM sensitivity of > 1.5 e^4 and t_R of ~ 7.9 min was required. This light TMT/ heavy TMT mix was used as a standard for the future assessment of the performance of the platform.

3.2 Results

3.2.1 Selection of peptides

Strict criteria were applied to ensure only the most specific peptides were selected to build the TMT-SRM method. In the first instance, a list of the frequency of occurrence in the human SwissProt database of all tryptic peptides for each candidate protein was generated *in silico* and filtered according to size and presence of unfavourable amino acids (Appendix Tables 3.1 – 3.9). Peptides were considered unsuitable for the TMT-SRM method if they were not between 6 - 25 amino acids in length and if they contained cysteine, methionine, tryptophan, glutamic acid or glutamine residues. To avoid peptides of multiple charge states, internal lysine, arginine and histidine residues were avoided where possible. Peptides shortlisted for TMT-SRM quantitation were proteotypic except for peptides of clusterin, complement C3, complement C3a, SAP and gelsolin, which had sequence frequencies in the human proteome of two or three. Two isoforms of clusterin exist in blood (isoform 1 and 2) as a result of alternative splicing, with isoform 2 having an extra 52 amino acids at the N-terminus compared to isoform 1. None of the selected peptides were present in this sequence and thus, the peptides measured either isoform. Complement C3 peptides were also specific to the complement C3 β-chain. Both these proteins are observed in blood plasma. Shortlisted peptides of complement C3a were also specific to the full complement C3 protein and complement C3 β-chain. However, circulating C3a is distinguished from other complement species by the C-terminal proteotypic peptide ASHLGLA. Upon processing of C3a *in vivo*, the C-terminal R residue is cleaved from the protein. SAP is observed in plasma as two different isoforms which differ by a single amino acid at the C-terminus. Thus, peptides selected for SAP measured either isoform. Similarly, the gelsolin protein is found as two distinct isoforms with isoform 1 having an extra 51 amino acids at the N-terminus compared to isoform 2. Isoform 1 is found in plasma and isoform 2 is cytoplasmic and thus it was isoform 1 that would be measured in the method under development. Following these exclusion

criteria, the final panel of signature peptides for the TMT-SRM method was selected based on experimentally-derived data and whether the peptide could be easily synthesised, with a high yield (Table 3.2). Factors considered here included whether shortlisted peptides from the *in silico* analysis were previously observed in MS/MS datasets, with focus on LC t_R and peptide fragmentation patterns where available. Several peptides (Appendix Tables 3.1 - 3.9) were not shortlisted for quantitation in this instance, in favour of peptides previously observed. However, these may serve as possible target analytes in future studies. Using CFH as an example, all shortlisted peptides were observed in TMT-labeled or unlabeled plasma MS/MS datasets. Although possessing early to middle LC t_R and high MS/MS fragment ions, CFH peptides SSNLIILEEHLK and SSIDIENGFISESQYTYALK were estimated to have problematic synthesis and produce a low yield. This was due to the presence of hydrophobic partial structures and N-terminal serine residues which cause side reactions to occur during cleavage of the peptide from the synthesis solid support. Thus, three peptides of CFH remained which were considered suitable for synthesis and inclusion in the final TMT-SRM panel. However, despite not being observed in discovery datasets or having potential problems during synthesis, the Apo E peptides LQAEAFQAR, LGPLVEQGR and SELEEQLTPVAEETR were selected for TMT-SRM method development over a potentially more suitable peptide (LAVTQAGAR). The first peptide was proteotypic in both the mouse and rat plasma database (data not shown), thus allowing for potential future application of the assay in these species. The latter two peptides were previously synthesised (even though problems were envisaged in synthesis here) and thus, the peptides were selected for TMT-SRM analysis of the protein. In total, three peptides per protein candidate were selected for quantitation (32 in the full panel, Table 3.2). This was with exception as for clusterin, six peptides were selected for the protein with three each for α- and β-chains. For complement C3a, only a single peptide (ASHLGLA) was available to discriminate this target from the full complement C3 protein. Further, due to their availability in-house, one extra peptide of A2M and three extra peptides of gelsolin were included for TMT-SRM quantition.

Protein	SwissProt	Proteotypic Peptides (6 - 25 aas)	Discovery	*In silico* frequency	Observed experimentally		LC t_R*	Presence of high mass MS/MS ions*	Synthesis
				Human	TMT	Unlabeled			
Clusterin α-chain	P10909	TLLSNLEEAK	Y	2	Y	Y	early/middle	moderate	Y
		SGSGLVGR		2	Y	N	NA	NA	
		ASSIIDELFQDR	Y	2	N	Y	late	good	Y
		IDSLLENDR		2	N	N	NA	NA	Y
Clusterin β-chain	P10909	VTTVASHTSDSDVPSGVTEVVVK	Y	2	Y	Y	middle	good	Y
		ALQEYR		2	Y	N	NA	NA	Y
		YNELLK		2	N	N	NA	NA	Y
		LANLTQGEDQYYLR		2	N	N	NA	NA	
Complement C3	P01024	TIYTPGSTVLYR		2	Y	Y	middle	good	Y
		IPIEDGSGEVVLSR		2	Y	N	NA	NA	
		VVLVAVDK		2	Y	N	NA	NA	
		AEDLVGK		2	Y	N	NA	NA	
		LLPVGR		2	Y	N	NA	NA	
		LVAYYTLIGASGQR		2	Y	N	NA	NA	Y
		FYYIYNEK		2	Y	N	NA	NA	Y
		GVFVLNK		2	Y	N	NA	NA	
		VLLDGVQNPR		2	Y	N	NA	NA	
		ISLPESLK		2	Y	N	NA	NA	
Complement C3a	P01024	SVQLTEK		3	Y	N	NA	NA	
		ASHLGLA		1	N	N	NA	NA	Y
CFH	P08603	SPDVINGSPISQK		1	Y	Y	middle	good	Y
		SSNLIILEEHLK		1	Y	Y	middle	good	
		VGEVLK		1	Y	N	NA	NA	Y
		SSIDIENGFISESQYTYALK		1	N	Y	NA	NA	
		IDVHLVPDR		1	Y	N	NA	NA	Y
A2M	P01023	AIGYLNTGYQR		1	Y	Y	middle	good	Y
		TGTHGLLVK		1	Y	Y	early	poor	Y
		GEAFTLK		1	Y	N	NA	NA	Y
		LPPNVVEESAR		1	Y	N	NA	NA	
		VSVQLEASPAFLAVPVEK		1	Y	Y	middle	good	

Table 3.2 Overview of the selection of signature peptides for the TMT-SRM method. Peptides highlighted red were estimated to have problematic purification, those in orange were estimated to have problematic synthesis and those in yellow were estimated to have a low overall yield from synthesis. Also included is the proteotypicity, LC t_R, fragmentation properties and whether the peptide was selected for synthesis. * from discovery datasets
NA: this information was not available for the TMT-labeled dataset as the identification was in the Proteome Sciences Frankfurt research facility and the information was not easily retrievable.

Analyte Protein	SwissProt	Proteotypic Peptides (6 – 25 aas)	Discovery	*In silico* frequency	Observed experimentally		LC t_R	Presence of high mass MS/MS ions	Synthesis
				Human	TMT	Unlabeled			
A2M (continued)		AAQVTIQSSGTFSSK		1	Y	N	NA	NA	
		SLNEEAVK		1	Y	N	NA	NA	
		GPTQEFK		1	Y	N	NA	NA	
		LLIYAVLPTGDVIGDSAK	Y	1	Y	Y	late	good	Y
		SDIAPVAR		1	Y	N	NA	NA	
		FEVQVTVPK		1	Y	N	NA	moderate	
		ALLAYAFALAGNQDK		1	Y	Y	late	moderate	
FGG	P02679	YLQEIYNSNNQK	Y	1	Y	Y	early/middle	good	Y
		LDGSVDFK	Y	1	Y	Y	middle	good	Y
		YEASILTHDSSIR		1	N	Y	NA	NA	
		IHLISTQSAIPYALR		1	Y	N	NA	NA	
		VGPEADK	Y	1	N	N	NA	NA	Y
SAP	P02743	IVLGQEQDSYGGK	Y	2	Y	Y	middle	good	Y
		VGEYSLYIGR	Y	2	Y	Y	middle	good	Y
		AYSLFSYNTQGR	Y	2	Y	Y	middle	good	Y
		DNELLVYK		2	Y	N	NA	NA	
		AYSDLSR		2	N	Y	NA	NA	
		VFVFPR		2	Y	N	NA	NA	
ApoE	P02649	LGPLVEQGR		1	Y	Y	middle	good	Y
		LAVYQAGAR		1	Y	N	NA	NA	
		GLSAIR		1	N	N	NA	NA	
		LQAEAFQAR		1	N	N	NA	NA	Y
		AATVGSLAGQPLQER		1	N	N	NA	NA	
		VEQAVETEPEPELR		1	N	N	NA	NA	
		LEEQAQQIR		1	N	N	NA	NA	
		SELEEQLTPVAEETR		1	Y	Y	NA	NA	Y
		DADDLQK		1	N	N	NA	NA	
Gelsolin	P06396	QTQVSVLPEGGETPLFK	Y	2	Y	Y	late	moderate	Y
		AGALNSNDAFVLK	Y	2	Y	Y	late	moderate	Y
		TASDFITK	Y	2	Y	Y	middle	good	Y
		AVEVLPK	Y	2	Y	Y	middle	good	Y
		HVVPNEVVVQR	Y	2	Y	Y	early	good	Y
		EPGLQIWR	Y	2	Y	Y	late	moderate	Y

Table 3.2 (continued)

From the selected peptides, 16 were observed in biomarker discovery plasma datasets (Table 3.2). This was desirable as it enabled the direct transfer of information from TMT-labeled discovery. In summary, peptides were selected which fulfilled the characteristics required for robust TMT-SRM quantitation, *i.e.,* were between 6 - 25 amino acids in length, were fully hydrolysed by trypsin, contained no variable modifications, either *in vivo* or *in vitro* and typically, doubly charged. Further, each peptide could be easily synthesised with a high yield expected.

3.2.2 Selection of transitions

The TMT-SRM method was initially developed with direct infusion of the light TMT-labeled synthetic peptides for the assessment of purity and for the selection of suitable SRM transitions. An MS spectrum was acquired to assess the purity of the TMT-labeled peptide standards. All peptides were free from contaminating ions. MS/MS spectra were acquired following fragmentation of the predominant peptide ion and three fragment ions were selected as Q3 transitions for each precursor ion (Table 3.3). The selectivity of SRMs was aimed to be improved by choosing those fragment ions with an *m/z* greater than that of the precursor ion *m/z*. Further, ions of the highest intensity were selected, ensuring high SRM sensitivity. Figure 3.1 displays the MS/MS spectrum of peptide 31 to demonstrate fragment ion selection. The unfragmented precursor ion is observed along with the selected Q3 fragment ions. Optimal light TMT transitions for all 32 peptides were combined to initially build the TMT-SRM method (Table 3.3).

3.2.3 Optimisation of compound-dependant parameters and application of SRM scheduling

To give the best chance of detecting each target analyte in undepleted plasma, the sensitivity of each transition was optimised with fine-tuning of the DP, CE and CXP.

In Section 2.1.2.2, optimised values for one transition were taken as representative of all transitions within a peptide. This was due to the limitations in

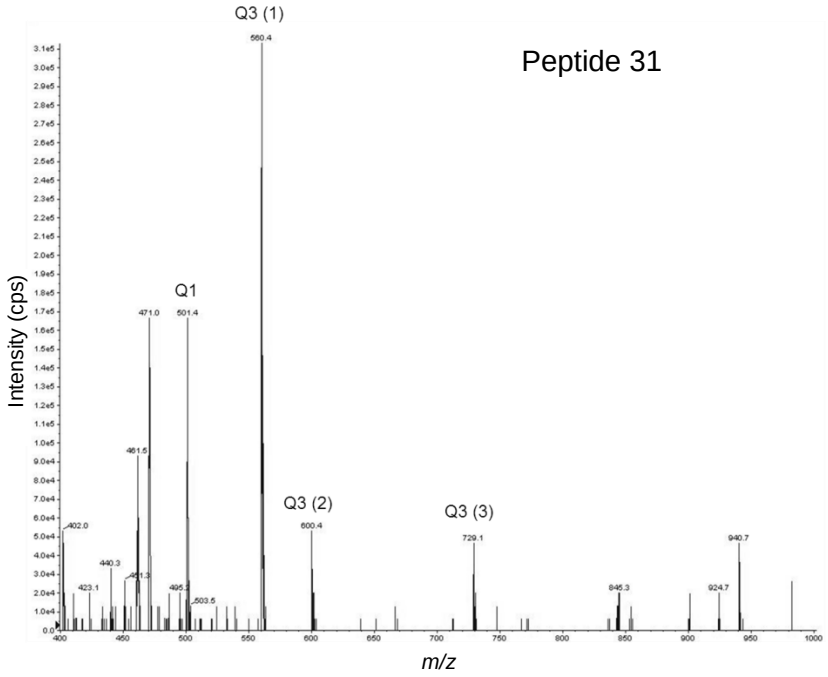

Figure 3.1 Selection of optimal MS/MS fragment ions for TMT-SRM quantitation. Upon CID of the precursor ion (Q1), fragment ions are measured in Q3 (1, 2 and 3) and used to build the TMT-SRM method.

analyte amount upon utilisation of a purified protein as an internal standard. In contrast here, the incorporation of synthetic peptides for internal standardisation provided increased amounts of each analyte. This enabled the optimisation of compound-dependent parameters for individual transitions in the TMT-SRM method. This further demonstrates the advantage of using synthetic peptides as an internal standard for TMT-SRM quantitation. Appendix Table 3.10 displays the optimised DP, CE and CXP voltages for all target analytes which were used to build the TMT-SRM method. For transitions of the same peptide, the DP value was identical. Optimal CE and CXP values were very defined and could vary greatly between different transitions of the same peptide, depending on the *m/z* of the ion selected in Q3. This underlined the necessity of optimising the CE and CXP for each individual transition in future TMT-SRM methods. Also displayed are the mean t_R for each peptide which was used to build the SRM scheduled method. A 360 sec SRM scheduling window was applied for the measurement of each peptide and all peptides were observed in the centre of each window (± 30 sec). Heavy TMT transitions were subsequently added to build the final method. The busiest point of the gradient (containing 13 overlapping peptide elution

Protein	Peptide ID	Candidate peptide	Charge State (+)	Light TMT					Heavy TMT				
				Mr (Da)	Q1 (*m/z*)	Q3 (1) (*m/z*)	Q3 (2) (*m/z*)	Q3 (3) (*m/z*)	*Mr* (Da)	Q1 (*m/z*)	Q3 (1) (*m/z*)	Q3 (2) (*m/z*)	Q3 (3) (*m/z*)
Clusterin α-chain	1	^{TMT}TLLSNLEEAK^{TMT}	2	1565.00	783.5	995.6	1014.6	1124.6	1575.00	788.5	1000.6	1019.6	1129.6
	2	^{TMT}ASSIIDELFQDR$^{a, b}$	2	1616.92	809.5	940.5	1053.6	1443.7	1621.92	812.0	945.5	1058.6	1448.7
	3	^{TMT}IDSLLENDR	2	1297.76	649.9	766.5	846.5	1124.6	1302.76	652.4	771.5	846.5	1129.6
Clusterin β-chain	4	^{TMT}VTTVASHTSDSDVPSGVTEVVVK$^{TMT\ a, b}$	3	2761.65	921.6	898.6	1238.7	1337.8	2771.64	924.9	903.6	1243.7	1342.8
	5	^{TMT}ALQEYR	2	1002.66	502.3	537.4	666.5	829.4	1007.66	504.8	542.4	671.5	834.4
	6	^{TMT}YNELLK^{TMT}	2	1226.80	614.4	744.4	840.5	857.4	1236.80	619.4	749.4	845.5	862.4
Complement C3	7	^{TMT}TIYTPGSTVLYR^{b}	3	1594.08	532.4	703.4	795.4	892.5	1599.09	534.0	708.4	795.4	892.5
	8	^{TMT}FYYIYNEK^{TMT}	2	1587.02	794.5	811.4	890.5	1217.6	1597.02	799.5	816.4	895.5	1222.6
	9	^{TMT}LVAYYTLIGASGQR	2	1735.08	868.5	1228.6	1299.7	1398.7	1740.08	871.0	1228.6	1299.7	1398.7
Complement C3a	10	^{TMT}ASHLGLA$^{a, c}$	2	892.40	447.2	492.2	520.2	633.5	897.40	449.7	497.2	520.2	633.5
CFH	11	^{TMT}SPDVINGSPISQK$^{TMT\ a}$	2	1789.14	895.6	1054.6	1167.7	1266.7	1799.14	900.6	1059.6	1172.7	1271.7
	12	^{TMT}IDVHLVPDR	3	1286.91	430.0	552.3	599.4	689.4	1291.92	431.6	557.3	599.4	694.4
	13	^{TMT}VGEVLK^{TMT}	2	1091.82	546.9	609.4	722.5	769.5	1101.82	551.9	614.4	727.5	774.5
A2M	14	^{TMT}AIGYLNTGYQR	2	1478.88	740.4	1014.5	1071.5	1184.6	1483.88	742.9	1014.5	1071.5	1184.6
	15	^{TMT}TGTHGLLVK^{TMT}	2	1372.84	687.4	753.5	904.5	1003.6	1382.84	692.4	758.5	909.5	1008.6
	16	^{TMT}LLIYAVLPTGDVIGDSAK$^{TMT\ a, b}$	3	2293.32	765.4	814.3	1010.8	1283.7	2303.31	768.8	819.3	1015.8	1288.7
	17	^{TMT}GEAFTLK$^{TMT\ c}$	2	1212.80	607.4	732.5	803.5	843.5	1222.80	612.4	737.5	808.5	848.5
FGG	18	^{TMT}YLQEIYNSNNQK$^{TMT\ a}$	2	1961.12	981.6	1091.6	1204.6	1333.7	1971.12	986.6	1096.6	1209.6	1338.7
	19	^{TMT}LDGSVDFK^{TMT}	2	1327.78	664.9	811.4	876.4	991.5	1337.78	669.9	816.4	881.4	996.5
	20	^{TMT}VGPEADK^{TMT}	2	1162.78	582.4	783.5	793.4	840.4	1172.78	587.4	788.5	798.4	845.4

Table 3.3 Tryptic plasma peptides from each candidate AD biomarker selected for TMT-SRM quantitation. For each protein the sequence of each peptide is indicated, along with the precursor ion charge state and peptide *Mr*. The *m/z* of Q1 and Q3 for the specific detection of the light and heavy TMT versions of the peptides are listed.

[a] indicates those peptides with poor endogenous detection in plasma by nanoflow LC/ nanospray MS.

[b] indicates those peptides which were adversely affected by sample preparation procedures (as described in Section 3.2.8).

[c] indicates those peptides with poor endogenous detection in plasma by microflow LC/ electrospray MS (as described in Section 3.2.9).

Protein	Peptide ID	Candidate peptide	Charge State (+)	Light TMT					Heavy TMT				
				Mr (Da)	Q1 (*m/z*)	Q3 (1) (*m/z*)	Q3 (2) (*m/z*)	Q3 (3) (*m/z*)	*Mr* (Da)	Q1 (*m/z*)	Q3 (1) (*m/z*)	Q3 (2) (*m/z*)	Q3 (3) (*m/z*)
SAP	21	^{TMT}IVLGQEQDSYGGK^{TMT} [c]	2	1841.08	921.5	1107.6	1292.6	1504.8	1851.08	926.5	1112.6	1297.6	1509.8
	22	^{TMT}VGEYSLYIGR	2	1379.78	690.9	871.5	1036.5	1057.5	1384.78	693.4	871.5	1041.5	1057.5
	23	^{TMT}AYSLFSYNTQGR	2	1629.90	816.0	972.5	1172.6	1335.8	1634.90	818.5	972.5	1172.6	1335.8
ApoE	24	^{TMT}LGPLVEQGR	2	1191.66	596.8	704.5	833.5	855.5	1196.66	599.3	709.5	838.5	855.5
	25	^{TMT}LQAEAFQAR	2	1256.74	629.4	737.4	884.5	1012.5	1261.74	631.9	742.4	889.5	1017.5
	26	^{TMT}SELEEQLTPVAEETR[a, b]	2	1954.06	978.0	1053.5	1154.6	1272.6	1959.06	980.5	1058.5	1159.6	1272.6
Gelsolin	27	^{TMT}QTQVSVLPEGGETPLFK^{TMT}	3	2277.60	760.2	867.5	980.6	1298.7	2287.59	763.5	872.5	985.6	1303.7
	28	^{TMT}AGALNSNDAFVLK^{TMT} [b]	2	1767.08	884.5	967.4	1038.5	1397.7	1777.08	889.5	972.4	1043.5	1402.7
	29	^{TMT}TASDFITK^{TMT}	2	1329.80	665.9	732.5	859.5	1005.5	1339.80	670.9	737.5	864.5	1010.5
	30	^{TMT}AVEVLPK^{TMT}	2	1202.78	602.4	736.5	809.5	908.6	1212.78	607.4	741.5	814.5	913.6
	31	^{TMT}HVVPNEVVVQR[a]	3	1498.92	500.6	560.4	600.4	729.4	1503.93	502.3	565.4	600.4	729.4
	32	^{TMT}EPGLQIWR[a, c]	2	1221.82	611.9	749.4	862.5	869.5	1226.82	614.4	754.4	867.5	874.5

Table 3.3 (continued)

windows) had a dwell time of 37.8 msec per transition, a cycle time of 2.5 sec with 21 data points at FWHM. Further, doubling the number of transitions in the method upon inclusion of the heavy TMT transitions reduced SRM sensitivities of those target analytes which elute during the busiest point in the LC gradient by approximately one third. All other target analytes had negligible reductions in SRM sensitivities.

The incorporation of pure synthetic peptides into the TMT-SRM workflow additionally allowed for the direct determination of crosstalk between light TMT and heavy TMT transitions, *i.e.,* the signal in the heavy TMT channel in the presence of light TMT-labeled peptides only. All transitions were found to be selective, *i.e.,* the signal in the heavy TMT channel was < 1%.

3.2.4 Detection of target analytes in human plasma and assessment of plasma background interference on SRM transitions

The endogenous detection of each peptide in plasma was next determined. Light TMT-labeled peptides were spiked into heavy TMT-labeled plasma. The presence of plasma matrix resulted in a shift in t_R for all target analytes and a new SRM scheduled method was established to account for this. The 2 µg plasma load was determined to be the optimal for the detection of target analytes (as compared to the 1 µg load) as the majority of peptides were observed with good SRM sensitivities. No major carry-over (<1%) was observed from the plasma load in the blank analyses between runs. Figure 3.2 displays the detection of light TMT-labeled internal standards spiked into heavy TMT-labeled plasma.

Peptides 2 (clusterin α-chain), 4 (clusterin β-chain), 10 (complement C3a), 11 (CFH), 18 (FGG), 26 (ApoE) and 32 (gelsolin) were not endogenously detected in plasma, indicating that detection was dependent on individual peptide properties rather than at the protein level (Table 3.2). The peptide which distinguished complement C3a from complement C3 (peptide 10) was not detected in the plasma sample and consequently, the protein was excluded at this stage. This was perhaps unsurprising as peptide 10 was a short, non-tryptic peptide and was not previously observed in MS/MS

datasets. However, it was important to at least initially consider complement C3a in the candidate AD biomarker panel. Peptides 2, 4, 10, 11, 18, 26 and 32 were excluded at this stage. Therefore, 25 peptides remained for quantitation (150 transitions; 75 light TMT and heavy TMT pairs), with at least two peptides per candidate protein. Ten peptides now eluted during the busiest point in the gradient. The dwell time was increased from 37.8 msec to 45 msec per transition with a cycle time of 2.5 sec and 22 data points at FWHM.

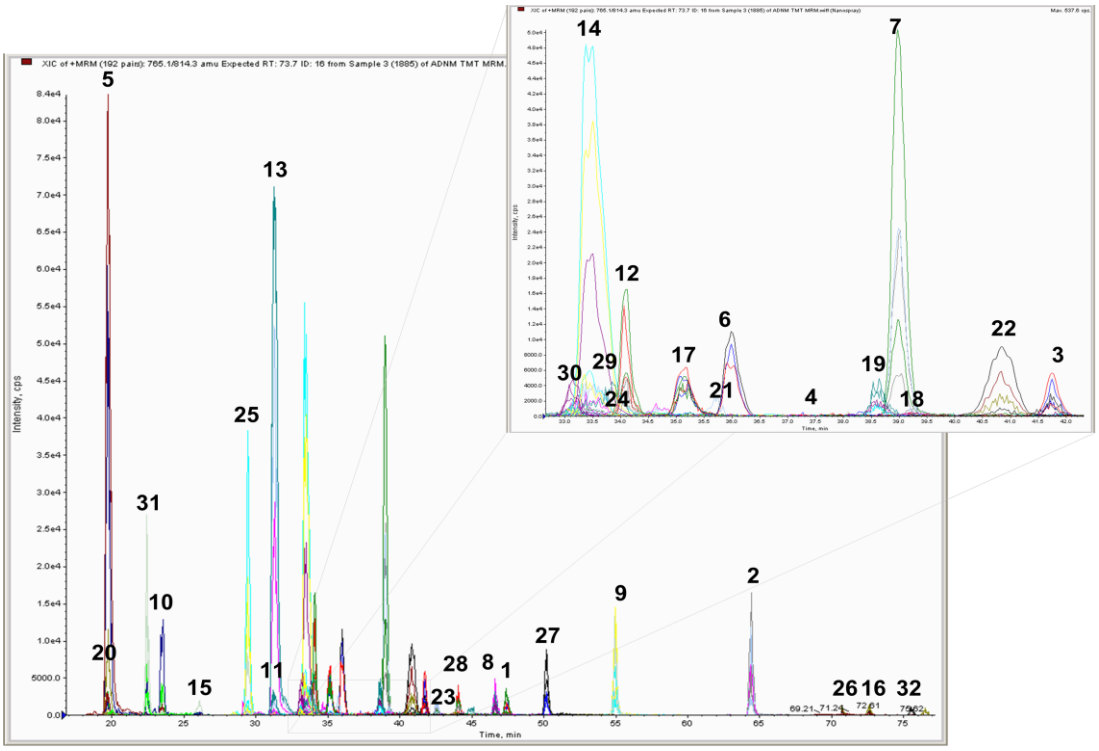

Figure 3.2 An SRM XIC for light TMT-labeled synthetic peptides 1 – 32 spiked into heavy TMT-labeled plasma. All light TMT transitions listed in Table 3.3, representing the internal standard, were observed in the method. The zoomed panel shows those peptides which elute during the busiest part of the LC gradient (*i.e.,* 32 – 42 min).

To assess the background interference associated with different sources of plasma, heavy TMT-labeled plasmas A and B were analysed over all light TMT and heavy TMT transitions. Target peptides were generally detected at similar SRM sensitivities in both plasmas (r = 0.95 for all measurements). Those transitions which had plasma background effects were generally common to both (Table 3.4). All transitions with high background interference were highlighted as potentially less

accurate, but remained in the method for further investigation in subsequent TMT-SRM quantitation studies.

Protein	Peptide ID	Candidate peptide	Light TMT		Heavy TMT	
			Q1 (*m/z*)	Q3 (*m/z*)	Q1 (*m/z*)	Q3 (*m/z*)
Clusterin α-chain	1	TLLSNLEEAK	783.5	995.6 (b7)	788.5	1000.6 (b7)
	3	IDSLLENDR	649.9	766.5 (b5)	652.4	771.5 (b5)
				1124.6 (b8)		1129.6 (b8)
Clusterin β-chain	5	ALQEYR	502.3	666.5 (b4)	502.3	671.5 (b4)
				829.4 (b5)		834.4 (b5)
	6	YNELLK	614.4	744.4 (b4)	619.4	749.4 (b4)
				840.5 (y5)		845.5 (y5)
				857.4 (b5)		862.4 (b5)
Complement C3	9	LVAYYTLIGASGQR	868.5	1228.6 (y11)	871.0	1228.6 (y11)
CFH	12	IDVHLVPDR	430.0	552.3 (b3)	431.6	557.3 (b3)
	13	VGEVLK	546.9	769.5 (y5)	551.9	774.5 (y5)
A2M	14	AIGYLNTGYQR	740.4	1014.5 (y8)	742.9	1014.5 (y8)
SAP	21	IVLGQEQDSYGGK	921.5	1107.6 (b8)	926.5	1112.6 (b8)
				1292.6 (y10)		1297.6 (y10)
				1504.8 (y12)		1509.8 (y12)
	22	VGEYSLYIGR	690.9	1036.5 (b7)	693.4	1041.5 (b7)
				1057.5 (y9)		1057.5 (y9)
Gelsolin	29	TASDFITK	665.9	1005.5 (y7)	670.9	1010.5 (y7)
	30	AVEVLPK	602.4	736.5 (b5)	607.4	741.5 (b5)

Table 3.4 SRM transitions with high plasma background interference in plasma A and B. Such transitions remained in the TMT-SRM method for further investigation.

3.2.5 Precision of TMT-SRM quantitation by nanoflow LC-SRM

Once the TMT-SRM method was refined and good endogenous detection of each of the 25 peptides was established, the precision of TMT-SRM quantitation was assessed. Light TMT-labeled synthetic peptides were spiked into heavy TMT-labeled Plasma A and replicate analyses (n = 5) performed over four days. One run each from batch 1 and 2 were excluded due to poor SRM signal intensity. Therefore, a total of 18 replicate runs were taken forward for data analysis. Figure 3.3 displays the L/H ratio for each transition of each peptide across all runs and batches. Each line represents a given transition of a peptide and each colour represents all transitions within a peptide. Peptides of the same protein are plotted on the same graph. High precision in TMT-SRM quantitation would be presented as a flat line plotted across replicate runs of each peptide, *i.e.,* the same L/H ratio.

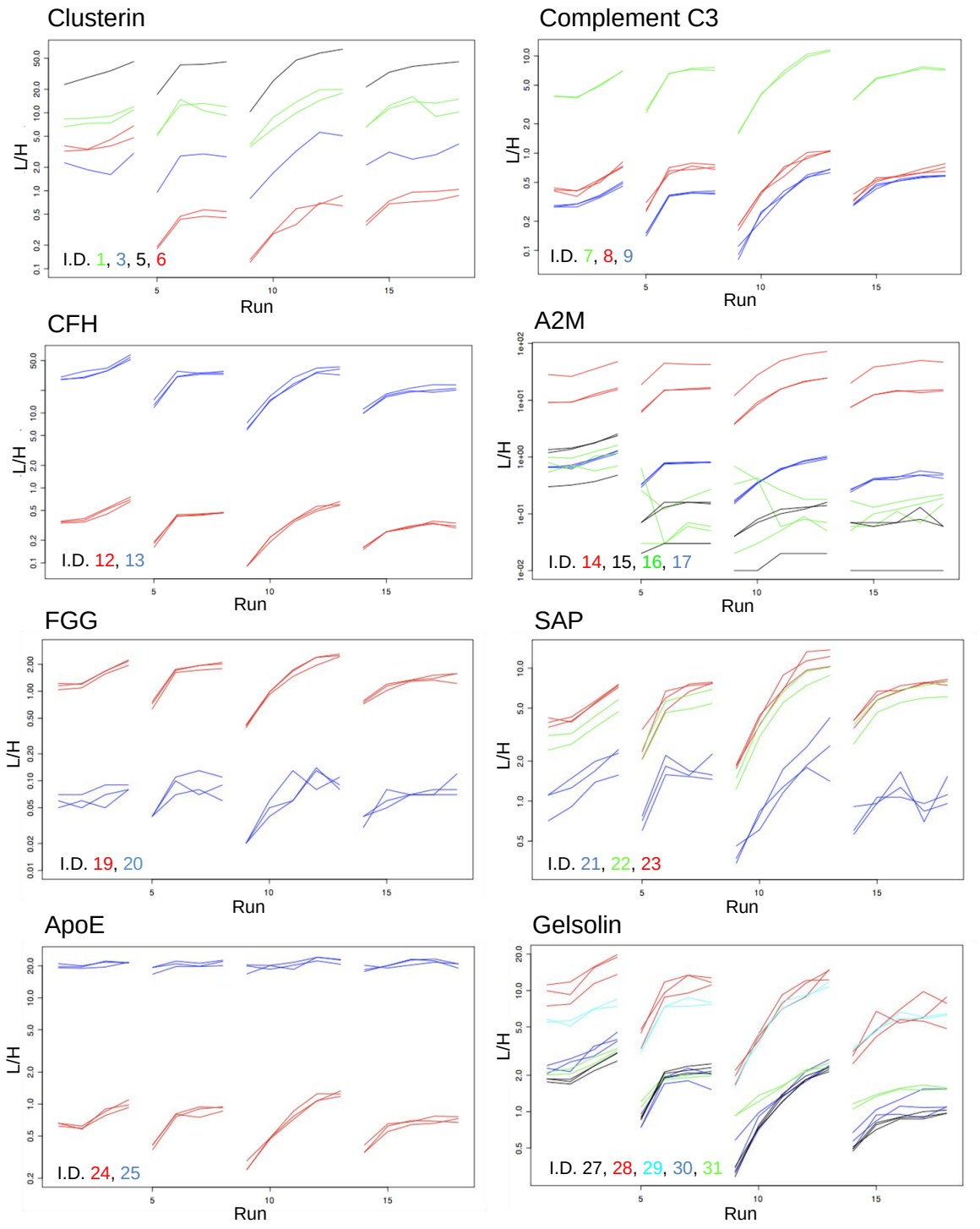

Figure 3.3 The accuracy of TMT-SRM quantitation of AD candidate peptides. Replicate runs of each peptide (I.D.) of each protein are displayed. Each colour represents a specific peptide, while individual lines represent a specific transition for that peptide.

Systematic fluctuations of L/H ratios within a batch were observed and consistent between different transitions, peptides and proteins. Different fluctuations were observed across batches. The large fluctuations observed indicated that large variation existed between measurements of the same analyte across runs and batches. Taking peptide 17 as representative of all peptides of A2M, a CV value of 31% was observed across batch one. Such high imprecision was in contrast to those results described in Section 2.2.1.4, where the majority of target analytes were shown to have precise TMT-SRM quantitation. A greater number of replicate runs (n = 18) was performed on the same sample in this set of experiments compared to previously (n = 9), providing a more extensive characterisation of TMT-SRM precision. Plasma carryover o/c was not the reason for the variability observed as the heavy TMT (plasma) peak areas across all transitions of all peptides was consistent, *i.e.*, did not increase over the course of a batch of samples (Appendix Figure 3.11).

In this instance, visualisation of the data by means of a line graph allowed for further characterisation of aberrant transitions and peptides as they displayed deviations from the trend which could be excluded from future analysis, *e.g.,* all transitions of A2M peptide 16 and SAP peptide 21. Due to the imprecision observed between analytical repeats, an alternative platform to the nanoflow LC needed to be considered.

A comparison was made between amounts expressed for peptides of the same protein (Figure 3.3). Variation in amounts recovered was observed for all peptides of clusterin, CFH, FGG and ApoE. The variations observed may be due to a number of reasons including differential peptide production during plasma digestion and differences in the recovery of each synthetic peptide following TMT-labeling and RP and SCX purification. Further, non-specific binding of peptides to plastics may have resulted in losses, the extent of which being dependant on the properties of individual peptides. The storage of the peptide solutions across multiple aliquots of low volume may have added to peptide instability. The latter two were likely to be major factors in the fluctuations observed and thus, the preparation of the internal standards needed to

be addressed. However, at least two peptides of complement C3 (peptides 8 and 9), SAP (peptides 22 and 23) and gelsolin (peptides 27, 30 and 31 and peptides 28 and 29) gave endogenous plasma amounts within the same range. This was very encouraging, as it provided the first indication that certain peptides of the same protein performed similarly by TMT-SRM.

3.2.6 Assay development for TMT-SRM using microflow LC rates and ESI

Based on the results in Section 3.2.5, the nanoflow LC system was not robust enough for a high quality assay. Imprecise TMT-SRM quantitation was observed for the majority of peptides in the AD candidate biomarker panel. For any assay to be successful, accurate quantitation is essential. An added disadvantage of nanoflow LC flow rates is the requirement of long LC gradients for peptide separation, resulting in a lower throughput of samples. To resolve this, the configuration of the LC was changed to enable microflow rates. A combination of higher flow rates and decreased elution peak widths would potentially allow for more robust TMT-SRM quantitation and sample analysis times could be reduced from 100 min to 15 min per sample. Furthermore, an ESI probe was used in combination with the microflow LC rates. The robustness of this source was a major benefit over the nanospray source, the fused silica of which was very fragile, resulting in frequent blockage or damage and thus required regular replacement and position optimisation.

The performance of the microflow LC system was assessed with the determination of the assay performance characteristics of a synthetic peptide, VATVSLPR. Table 3.5 displays the precursor and fragment ion *m/z* and compound-dependent parameters used to build the TMT-SRM method. The final TMT-SRM method monitored 10 transitions, had a dwell time of 50 msec per transition, a cycle time of 0.5 sec with 20 data points at FWHM. To minimise peptide losses due to non-specific binding to plastics which may have ultimately affected the peptide quantitative amounts described in Section 3.2.5, VATVSLPR was resuspended in the presence of a scavenger protein, glucagon. As can be seen in Figure 3.4, the incorporation of

Light TMT		Heavy TMT		DP (V)	CE (V)	CXP (V)
Q1 (*m/z*)	Q3 (*m/z*)	Q1 (*m/z*)	Q3 (*m/z*)			
	595.5		600.5	100	40.6	8.4
	664.5		669.5	100	39.1	9.6
534.0	682.5	546.4	687.5	100	39.2	9.6
	743.5*		743.5	100	36.8	11.3
	842.6*		842.6	100	35.0	13.6

Table 3.5 Selected transitions and optimised instrument voltages for the TMT-SRM quantitation of VATVSLPR peptide. The peptide was doubly charged and fully TMT-labeled. The DP was constant for all transitions while the CE and CXP were dependent on Q1 and Q3 *m/z*.

* removed from the data analysis due to crosstalk between light and heavy TMT transitions

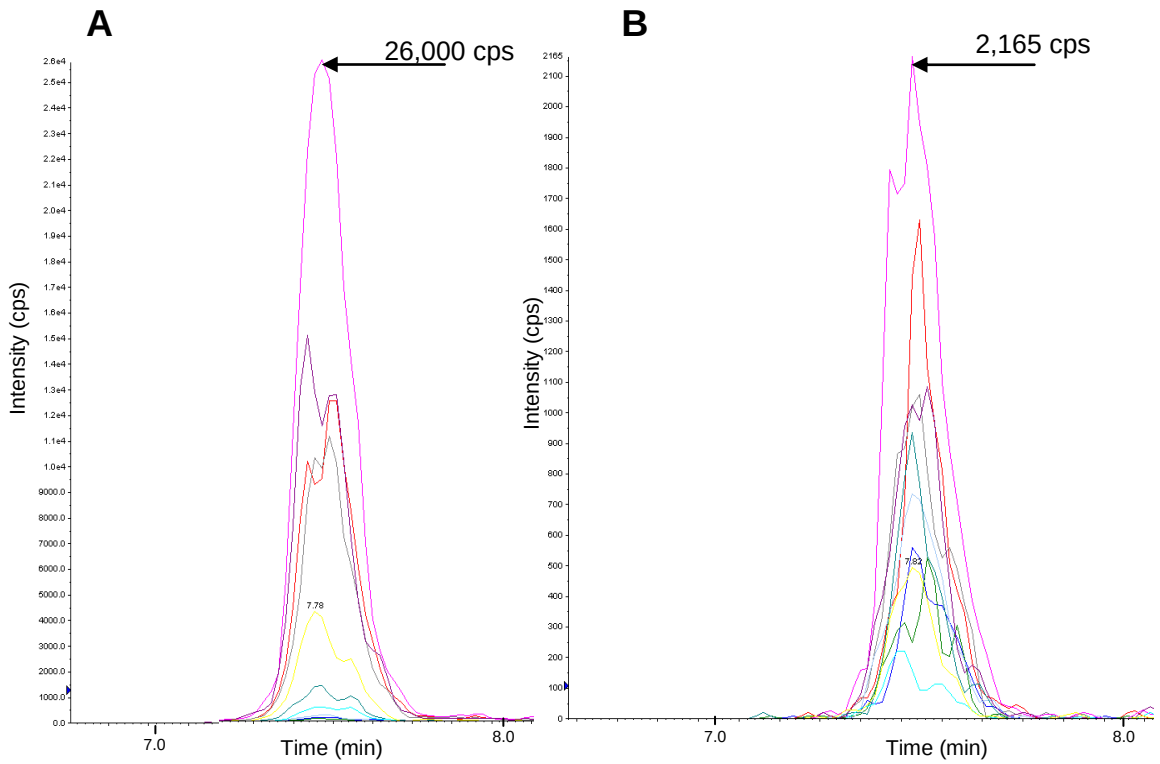

Figure 3.4 The effect of glucagon on SRM sensitivities of VATVSLPR peptide. VATVSLPR peptides (light and heavy TMT-labeled) were loaded at 50 and 100 fmol o/c, respectively and quantitated by TMT-SRM in **A** the presence of glucagon and **B** the absence of glucagon. Light TMT-SRM transitions are coloured in purple, magenta, red and grey and heavy TMT-SRM transitions are coloured in blue, cyan, green and yellow. The incorporation of glucagon as a scavenger peptide resulted in at least a 10 fold improvement in SRM sensitivities.

glucagon resulted in a 10 fold improvement in SRM sensitivities at 50 fmol light VATVSLPR peptides and 100 fmol heavy TMT-labeled VATVSLPR peptides o/c. Due to such significant benefits, all subsequent dilutions were performed in the presence of the scavenger peptide.

Calibration curves were prepared for VATVSLPR peptide in buffer-only (in duplicate over two days) and plasma (one replicate over one day) and the linearity, LOD and LOQ for the target analyte assessed (Section 3.1.6; Figure 3.5 and Table 3.6). Crosstalk was observed for two transitions (those that had the same Q3 ion *m/z;* Table 3.5) which was revealed by a tailing-off at the lower points of their respective calibration curves in buffer-only (data not shown). These transitions were less selective as they differed only by Q1 *m/z* and were removed from the data analysis. For the remaining three transitions in buffer-only, linearity in TMT-SRM quantitation was observed down to 0.25 fmol light TMT-labeled VATVSLPR peptide o/c. In the presence of plasma, linearity was observed down to 2 fmol o/c. This difference to the buffer-only results was speculated to be due to the increase in overall background signal and ion suppression from the complex matrix during ESI. The LODs and LOQs were < 0.25 fmol o/c in buffer-only. Once again, an expected increase was observed for equivalent values in the presence of plasma with an LOD of 1 fmol o/c and an LOQ of 2 fmol o/c.

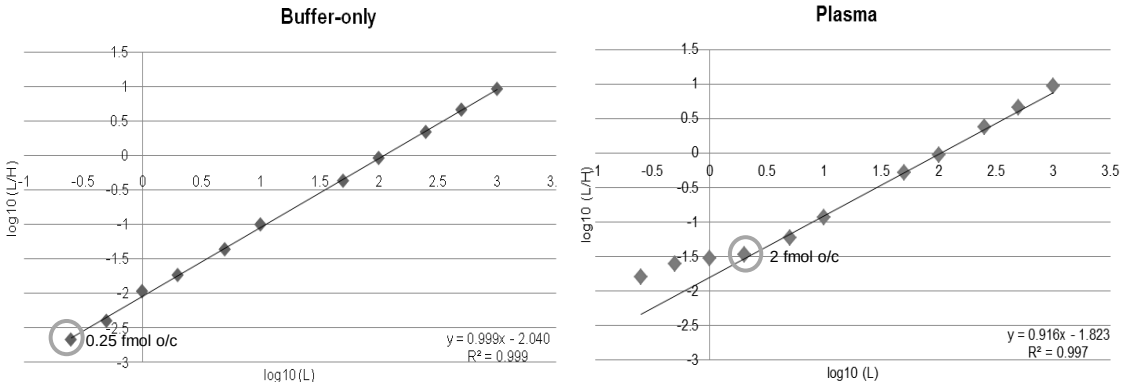

Figure 3.5 Calibration curves for VATVSLPR peptide quantitated by TMT-SRM in buffer-only and plasma. The curves (based on the mean of three transitions) were used to interpolate QC amounts for the determination of the trueness and precision of TMT-SRM quantitation. Linearity was observed down to 0.25 fmol o/c in buffer-only and 2 fmol o/c in plasma.

To determine the accuracy of TMT-SRM quantitation, triplicate QC measurements of 5 and 50 fmol o/c light TMT-labeled VATVSLPR peptide were analysed for each calibration curve. The trueness for VATVSLPR measurements in buffer-only (mean across three replicates) and plasma (mean across three replicates) is displayed in

	LOD (fmol o/c)	LOQ (fmol o/c)	QC (fmol o/c)	Trueness* (%CV)	Intra-batch precision (%CV)	Inter-batch precision (%CV)
Buffer-only	< 0.25	< 0.25	5	4.4	4.62 and 5.21	4.72
			50	4.02	2.69 and 4.03	3.61
Plasma	< 1	< 2	5	9	7.51	NA
			50	13.02	7.19	NA

Table 3.6 Performance of TMT-SRM for VATVSLPR peptide in buffer-only and plasma using microflow LC rates coupled to ESI. The LOD, LOQ, trueness and intra- and inter-batch variation of TMT-SRM quantitation in buffer-only and plasma is displayed. Accuracy values are based on triplicate QC measurements of 5 and 50 fmol o/c. NA = not applicable. * taken from one representative calibration curve.

Table 3.6. The trueness observed in buffer-only was better than that in plasma, indicated by lower %CVs. This was speculated to be due to the reduced complexity of the buffer-only samples in that the background interference from the plasma matrix contributes to the signal, resulting in an over-estimation of the actual amount compared to the matrix-free result. When evaluating the precision of the method, it was necessary to assess the performance of QC replicates within a day (intra-batch variation) and over several days (inter-batch variation; buffer-only QCs only). The intra- and inter-batch variation for buffer-only experiments was comparable, thus confirming the stability of the platform over a given time period. The intra-batch variation was slightly higher for experiments performed in plasma matrix and this was once again attributed to the added complexity of the plasma matrix. However, the overall precision and variation of TMT-SRM measurements of VATVSLPR peptides in the presence of plasma matrix was considered favourable. Thus, acceptable accuracy was observed for both QC amounts in buffer-only and plasma. The SRM peak areas of the internal standard (100 fmol o/c) remained constant at ~100,000 cps across samples. The microflow LC was very stable with highly reproducible t_R (7.43 - 7.47 min, CV of 0.11%), demonstrating the robustness of the new platform.

In summary, a TMT-SRM assay format was established using a microflow LC platform in combination with ESI, enabling the determination of the linearity, LOD, LOQ

and accuracy of TMT-SRM quantitation. As well as significantly reducing individual sample analysis times and an increasing sample throughput, the new system had a more robust LC. Accuracy in TMT-SRM quantitation was observed at the higher flow rates. Further, the introduction of glucagon as a peptide scavenger significantly improved SRM sensitivities, as less synthetic peptide was lost due to non-specific binding to plastics. The new system was a significant improvement in the overall TMT-SRM quantitation strategy. This strategy was therefore taken forward for the quantitation of candidate AD biomarker peptides in plasma.

3.2.7 Assessment of modified plasma digestion, TMT-labeling and purification strategies

To enable the preparation of the higher protein amounts consumed by microflow LC rates, several adjustments to the purification protocol of TMT-labeled peptides were performed as outlined in Table 3.1. A larger amount of plasma (2 mg) compared to the standard protocol (100 µg) was digested and light TMT-labeled. A comparison was made between the TMT-labeled plasma sample which was purified using either the standard protocol for RP and SCX, an upscaled RP in combination with the standard SCX protocol or both an upscaled RP and SCX protocol. All analyses were performed in duplicate. Additionally, the integration of a microtitre plate format for the preparation of plasma matrix was assessed using the sample that was purified using upscaled RP and SCX protocols. Samples were analysed by LC-MS/MS and compared using the number of identified peptides in each (Figure 3.6). Comparable MS ion distribution and ion intensities were observed using the standard protocol (A) and those purified using an upscaled protocol for RP (B) and upscaled RP and SCX (C). Equivalent numbers of peptides and proteins were identified across the three purification protocols. Samples lyophilised in a microtitre plate were comparable to those lyophilised in the standard way, *i.e.,* in an eppendorf. A significant advantage of the microtitre plate format was that it enabled increased sample throughput. Both upscaling and microtitre plate format were thus integrated into the TMT-SRM workflow.

A

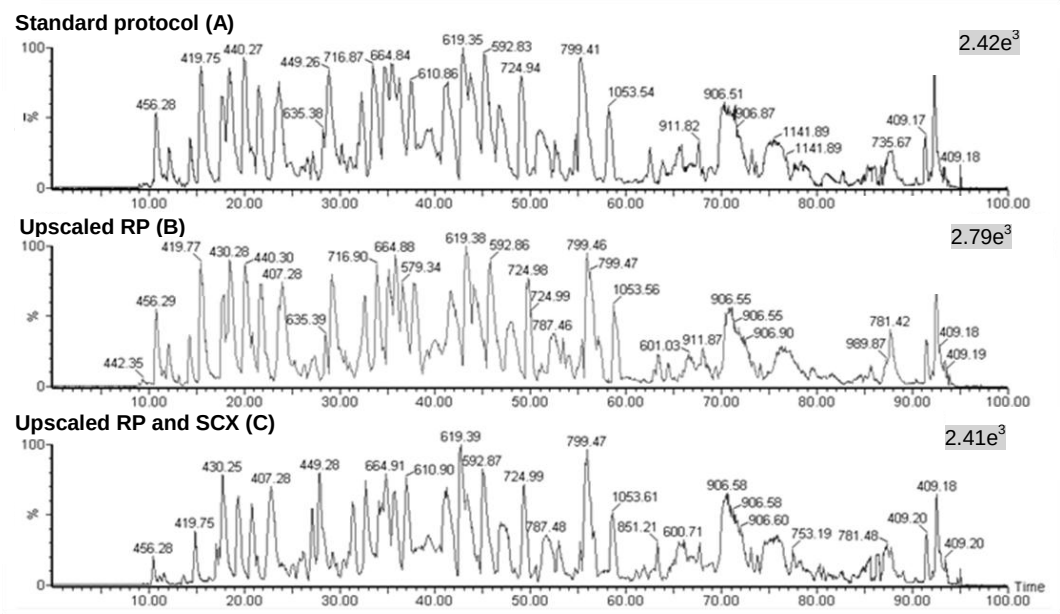

B

Sample	Replicate	Peptide IDs	Protein IDs
A	1	225	36
	2	269	25
B	1	206	20
	2	275	30
C	1	238	26
	2	246	25

Figure 3.6 Comparison of standard and upscaled sample preparation protocols. **A** BPI chromatograms for plasma digested, TMT-labeled and purified using the standard protocol, an upscaled protocol for RP and an upscaled protocol for RP and SCX. **B** The number of plasma peptide and protein IDs for each protocol.

3.2.8 Preparation of equimolar mixtures to minimise quantitative differences between peptides of the same protein

In an effort to minimise the difference observed in endogenous plasma amounts of peptides of the same protein (Section 3.2.5), peptides within a protein were combined in equimolar mixtures. The full panel of 32 synthetic peptides were included in the generation of the mixtures as it was hypothesised the new microflow LC configuration may improve the TMT-SRM detection of those peptides previously determined to be untraceable in undepleted plasma by nanoflow LC (Section 3.2.4). In the first instance, AAA was performed on all synthetic peptide solutions to determine the accurate concentration of each. For the majority of peptides, the actual

concentration of each peptide solution as determined by AAA was lower than the estimated concentration upon initial solubilisation (Table 3.7). Possible factors explicating the observed differences include the synthetic peptides were not fully solubilised during initial resuspension, peptide losses to the sides of the sample vials or losses due to long-term sample storage. AAA should therefore be an essential step in all TMT-SRM strategies where accurate and absolute quantitation is being pursued. Further, sample storage is an important consideration. Initially, peptide stock solutions were aliquoted into small volumes across many sample vials which could have compounded the peptide losses observed. In an effort to minimise this, aliquots of the same peptide were combined into one large volume and stored in a single sample vial. Using accurate concentrations from AAA, peptides of the same protein were subsequently combined in equimolar mixtures.

The quality of equimolar mixtures was assessed at each stage of the sample preparation workflow. Assessments were performed on the peptide solutions in an unlabeled state, post light TMT and heavy TMT-labeling and post RP and SCX purification. The majority of peptides across mixtures had strong signal intensities prior to TMT-labeling and RP and SCX purification. Taking clusterin peptides as an example, a large decrease in the signal intensity of peptide 4 was observed after TMT-labeling and a large decrease in the signal intensity of peptide 2 was observed after RP and SCX purification (Figure 3.7). Such losses were speculated to be a result of the different ionisation properties of unlabeled and TMT-labeled peptides and losses during RP and SCX purification. The poor performance of these peptides was in agreement with Section 3.2.4, where clusterin peptides 2 and 4 were not endogenously detected in plasma and removed from the initial TMT-SRM method. Such problems were further highlighted in Table 3.7 where the actual concentration of peptide 4 was significantly lower than the estimated concentration of the peptide as determined by AAA. Thus, it has been demonstrated here that certain peptides have reduced SRM sensitivies after TMT-labeling and purification and this could explain the endogenous detection, *i.e*., below LOD, of certain peptides in plasma. Nevertheless, the remaining clusterin pep-

Peptide	Estimated conc. (µg/µL)	Actual conc. (µg/µL)	Difference (%)	Peptide	Estimated conc. (µg/µL)	Actual conc. (µg/µL)	Difference (%)
1	3.35	2.93	-13	**17**	2.29	2.67	17
2	4.18	3.81	-9	**18**	4.54	3.12	-31
3	1.29	1.46	13	**19**	2.64	2.18	-17
4	6.95	2.8	-60	**20**	2.15	1.61	-25
5	2.34	1.71	-27	**21**	4.04	3.35	-17
6	2.34	1.72	-27	**22**	1.74	1.91	10
7	4.11	3.39	-18	**23**	2.53	1.66	-34
8	3.42	2.7	-21	**24**	2.91	1.38	-53
9	4.54	2.74	-40	**25**	3.1	2.62	-15
10	2.47	1.58	-36	**26**	5.19	3.89	-25
11	4.03	2.32	-42	**27**	6.86	5.51	-20
12	3.19	1.73	-46	**28**	5.33	4.56	-14
13	1.93	1.5	-22	**29**	3.99	3.81	-5
14	3.77	2.75	-27	**30**	3.64	3.93	8
15	2.78	2.07	-26	**31**	2.24	1.81	-19
16	0.92	0.40	-57	**32**	3.67	3.15	-14

Table 3.7 Concentration (µg/µL) of peptides 1 - 32 as determined by AAA. A large variation was observed for estimated and actual concentrations of each peptide.

-tides (1, 3, 5 and 6) were relatively constant at each stage, indicating robust sample preparation of these peptides. Due to significant losses in SRM sensitivities at different stages of sample preparation, peptides 2, 4, 7, 16, 26, and 28 were not considered for future TMT-SRM quantitation (Table 3.3). Such losses in sensitivity were in agreement with the fact they weren't detectable in plasma (peptides 2, 4 and 26) or had significantly lower concentrations determined by AAA than expected (peptides 4, 16, and 26).

3.2.9 SRM detection of target analytes in plasma using ESI

The evolution of the TMT-SRM method to incorporate microflow LC rates and ESI resulted in the necessity to re-examine the endogenous detection of the target peptides in plasma. Excluding those six peptides which were shown to be affected by sample preparation procedures in Section 3.2.8, the method now measured 26 peptides. Following analysis of plasma using the microflow LC-SRM platform, peptides 10 and 32 were poorly detected by TMT-SRM and were excluded from the method (Table 3.3).

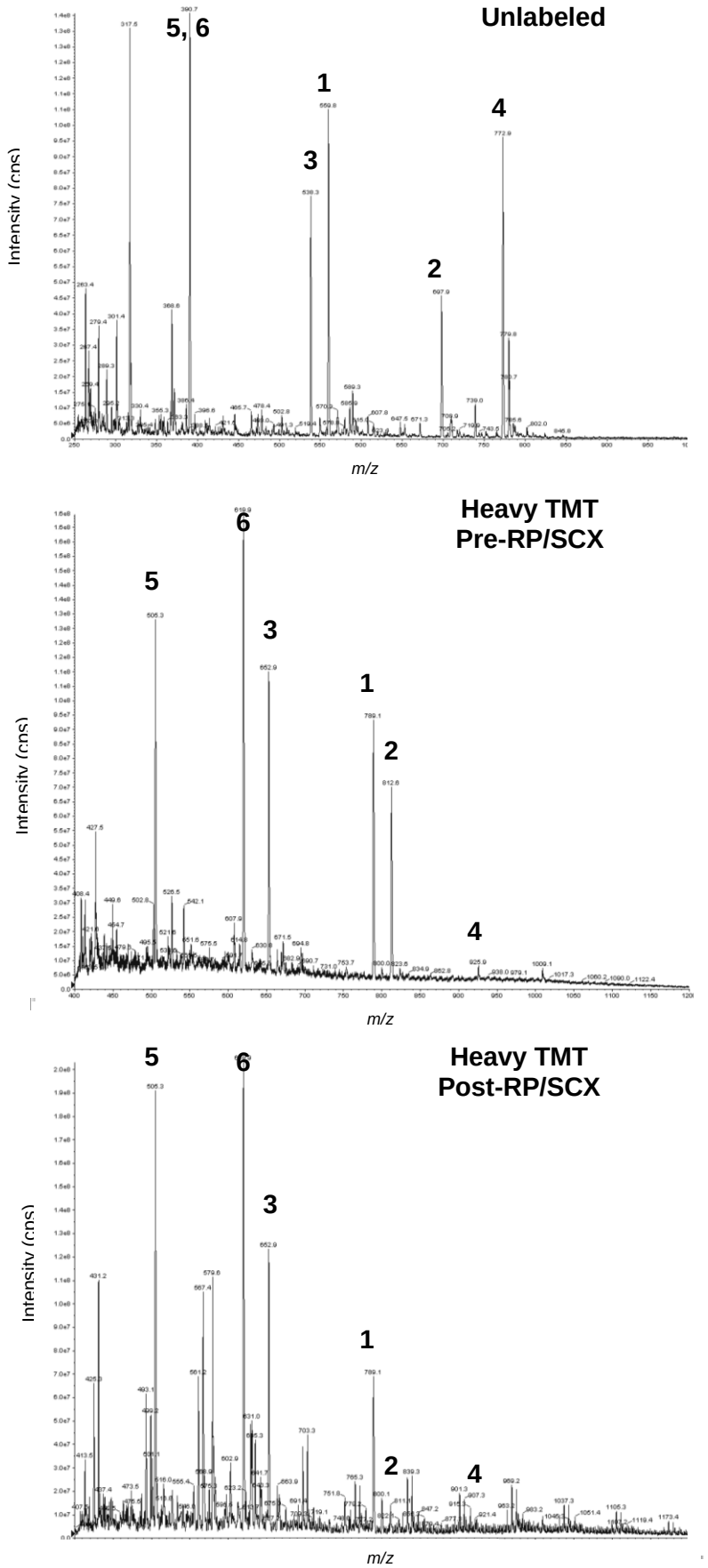

Figure 3.7 MS spectra for the equimolar mixture of clusterin peptides at different stages of sample preparation. TMT-labeling decreases the MS detection of peptide 4. Purification procedures decrease the MS detection of peptide 2. Peptides 1, 3, 5 and 6 remain relatively constant at each stage.

This was in agreement with the results using the nanoflow LC-SRM platform. Additionally, poor detection of peptides 17 and 21 resulted in their exclusion at this stage. This is in disagreement with the results using the nanoflow LC platform as described in Section 3.2.4, where the endogenous plasma detection of both peptides was not problematic. Conversely, peptides 11 and 18, which were initially excluded in Section 3.2.4, were detected using the new platform and thus, remained in the TMT-SRM method. Such discrepancies highlight the differential performance of the two platforms for TMT-SRM quantitation, attributed to the different LC column specifications or the varying levels of background interference and ion suppression associated with individual nanospray/ESI platforms. The results underline the importance of re-analysing the SRM detection of individual target analytes when moving between different LC-SRM platforms. As established for the nano-LC-SRM system in Sections 3.2.4 and 3.2.5, the presence of background interference on certain SRM transitions needed to be ascertained on the new system. This will be addressed in further development of the assay in Chapter 4.

In summary, six peptides had significant losses during preparation of the equimolar mixtures (peptides 2, 4, 7, 16, 26, and 28) and a further four peptides had poor endogenous detection in plasma by TMT-SRM using ESI (peptides 10, 17, 21 and 32). These peptides were removed from the method. Therefore, 22 peptides remained with importantly, at least two peptides per protein (Table 3.3), for TMT-SRM assay validation and the determination of TMT-SRM assay performance characteristics.

3.3 Summary

- A TMT-SRM method has been developed for the quantitation of eight medium to high abundant proteins in plasma which were proposed from AD biomarker discovery studies as providing protein expression signatures of AD diagnosis and prognosis. Complement C3a was initially considered in the method but was excluded as no endogenous proteotypic peptides could be detected for this protein.
- Synthetic peptides were used for internal standardisation over a biological reference or synthetic proteins as they reduced the overall complexity of the analysis and enabled tuning of compound-dependant parameters for enhanced detection of endogenous target analytes in plasma. Further, synthetic peptides allow for absolute quantitative amounts to be determined, provided the accurate amount of each peptide is known.
- Proteotypic peptides were selected which fulfilled criteria for robust TMT-SRM quantitation, *i.e.,* were completely hydrolysed by trypsin and fully TMT-labeled, contained no known *in vivo* or experimental modifications. Further, peptides between 6 - 25 amino acids were chosen to ensure sufficient SRM selectivity, whilst minimising the cost and effort required for their synthesis. Weight was gived to the selection of peptides which had been previously identified. Here, the MS detection of the peptide had already been ascertained and LC-MS and LC-MS/MS properties defined.
- In total, 32 peptides were selected for TMT-SRM quantitation, with at least three peptides per protein. Three SRM transitions were selected for each target peptide. Both factors improved the quantitative statistics and added confidence to the result.
- From the selected peptides, 16 were observed in biomarker discovery plasma datasets, enabling the rapid transfer of such data into methods for biomarker verification and validation.

- A stable and reproducible analytical platform was essential for delivering high quality MS assay results. The TMT-SRM assay was initially developed using nanoflow LC in combination with nanospray ionisation. However, this LC-SRM platform was shown to be imprecise and unstable for the quantitation of the target analytes. Accordingly, an alternative assay design was developed for the TMT-SRM method. This incorporated:
    - Microflow LC rates in combination with ESI. This resulted in a significant improvement in assay accuracy and stability. Analysis times were reduced from 2.5 h to 15 min, enabling high sample throughput which is essential for a robust clinical assay.
    - A scavenger peptide (glucagon) was used for the preparation of all peptide stock and working solutions. This resulted in a significant improvement in SRM signal intensities and stability.
    - An assay design was developed which enabled the determination of the LOQ, LOQ, linear range and a measurement of the accuracy of TMT-SRM quantitation for the target analytes of interest.
- Losses were observed for several peptides upon TMT-labeling. Further, the RP and SCX purification resulted in significant losses for several other peptides. Thus, AAA is essential at each stage of the TMT-SRM workflow, *i.e.,* pre- and post-TMT-labeling, to compensate for this and accurately measure the amount of internal standard peptides at each point in the process. Only then can absolute TMT-SRM quantitation truly be determined.
- The TMT-SRM method quantitated 22 peptides, with at least two peptides for each of the eight proteins remaining in the panel, and could now be applied for TMT-SRM assay validation and to determine the TMT-SRM assay performance characteristics for each target analyte in plasma.

Chapter 4

Performance and validation of a multiplexed TMT-SRM assay for the quantitation of Alzheimer's disease biomarkers in human plasma

4.0 Introduction

For the TMT-SRM approach to be used or shown to be useful as an alternative technology for peptide and protein quantitation, it was required that the assay was validated against more traditional methods. The current gold standard for the quantitation of protein biomarkers in plasma is by antibody-based assays such as ELISA (Engvall and Perlman, 1971). Further, WB is commonly used in candidate biomarker verification (Hye *et al.,* 2006; Rifai and Gerszten, 2006; Güntert *et al.,* 2010; Haverland *et al.,* 2010). Such techniques are problematic however, as their success is primarily dependent on the availability of high quality antibodies. Further, it is very difficult to accurately quantitate several target analytes in one fluid volume. It was hypothesised that the multiplexed TMT-SRM assay developed here may overcome such limitations. The primary goal of this chapter was to perform a direct comparison between quantitative values of a sample cohort, measured using an antibody-based approach and TMT-SRM. To achieve this, a subset of samples (n = 20) was selected from a discovery cohort of AD and NDC subjects (n = 90) where one of the candidate AD biomarkers, gelsolin, was found to be differentially expressed between groups by WB (Güntert *et al.,* 2010). Here, signature peptides of gelsolin (as refined in Chapter 3) were measured by TMT-SRM between disease and control groups. Agreement between WB and TMT-SRM measurements for gelsolin would confirm the validity of TMT-SRM assay for the quantitation of signature peptides of the candidate proteins in undepleted plasma. Further, the TMT-SRM quantitation of the remaining peptides in the panel provided an initial insight into their performance in terms of robustness in clinical sample cohorts and agreement between peptides within a protein.

Once the TMT-SRM assay was validated for suitability and refined to include only the most robust signature peptides of a protein, the assay performance characteristics were determined for each target analyte in undepleted plasma. Here, each candidate AD biomarker peptide was defined in terms of linearity, LOD, LOQ and the accuracy of TMT-SRM quantitation (Whiteaker *et al.,* 2010). To demonstrate the

robustness and portability of the TMT-SRM assay across MS platforms, the assay performance characteristics were additionally defined for the target analytes on a separate triple quadrupole instrument to the QTRAP, a TSQ Vantage.

4.1 Materials and Methods

4.1.1 Sample selection based on western blot measurements of gelsolin

Samples were collected from a largely community-based population of subjects with AD and aged people, funded by the Alzheimer's Research Trust (ART). All subjects were white UK citizens with grandparents born in the UK and were assessed annually by cognitive measures including the MMSE and the Clinical Dementia Rating. A demographic and medical assessment was also performed. Cases with probable AD (NINCDS-ADRDA criteria) were identified using methods shown to have a high diagnostic validity (Foy *et al.,* 2007). NDCs, defined as having no evidence of cognitive impairment, were collected from primary care patient lists. The study was approved by the relevant research ethics committees. Blood was extracted from each subject according to standardised operating guidelines and collected in 10 mL ethylenediaminetetraacetic acid (EDTA) coated glass tubes (Sigma-Aldrich). Upon arrival at the laboratory, each blood sample was centrifuged at 3000 rpm using a Clinispin Horizon 853VES centrifuge (Woodley Equipment Company Ltd., Bolton, UK) at 4 °C for 8 min to isolate the plasma fraction from white and red blood cells. Plasma was aliquoted into 0.5 mL volumes and stored at -80 °C. Gelsolin was quantitated by WB in 140 plasma samples representing AD and NDCs (Güntert *et al.,* 2010). A sub-set of these were selected for TMT-SRM quantitation which showed the greatest difference in gelsolin levels between AD and NDC samples (n = 10 per group, Table 4.1).

4.1.2 Light TMT labeling of AD and NDC plasma samples

An aliquot of each plasma sample was removed from the freezer and brought to RT on ice. An equal volume (25 µL) of each was diluted 10-fold with H_2O. From this, 12.5 µL was removed, providing approximately 100 µg of protein per digest (based on a theoretical plasma concentration of 80 mg/mL). This strategy, based on equal volumes as opposed to equal protein amounts, was equivalent to that used in the WB

studies. In parallel, a pool of all samples (100 µg per sample, 2 mg total protein) was prepared to provide the sample matrix for calibration curves and to assess instrument performance.

AD		NDC	
ART ID	**Gelsolin relative OD**	**ART ID**	**Gelsolin relative OD**
68	0.33	352	1.55
156	0.37	436	1.55
284	0.27	446	1.80
371	0.40	449	1.67
768	0.36	520	2.16
891	0.48	880	1.63
1212	0.34	886	1.53
1219	0.52	960	1.78
1239	0.43	1035	2.99
1312	0.52	1172	1.76
Mean	**0.40**	**Mean**	**1.84**

Table 4.1 Gelsolin measurements for AD and NDC groups by WB. The samples displayed are those which gave the greatest difference in mean relative optical density (OD) for gelsolin between groups (*n* = 10 per group) and thus, selected for validation of the TMT-SRM assay. ART ID indicated the identification code for each sample within the database.

Experimental samples were solubilised with SDS, reduced, alkylated and digested with trypsin as described in Section 2.1.1.2. Tryptic plasma peptides were labeled with light TMT and purified by RP and SCX as described in Sections 2.1.1.3 - 4. All experimental samples were processed in triplicate (technical repeats). Each plasma was aliquoted across three microtitre plates (60 µL per sample; 30 µg per well) to provide three analytical repeats. Each microtitre plate was lyophilised to dryness. To further remove the high ammonium acetate content introduced during SCX elution, samples were resuspended in 100 µL SCX loading buffer and lyophilised to dryness for a second time. The pooled plasma sample was prepared using the upscaled version of the TMT-labeling and purification protocols as described in Section 3.1.7, aliquoted into a single microtitre plate and lyophilised twice as above. All microtitre plates were stored at -80°C until further use.

4.1.3 TMT-SRM analysis of the sample cohort

TMT-SRM analysis of the cohort was performed on a QTRAP mass spectrometer as described in Section 3.1.9. For internal standardisation, all heavy TMT-labeled equimolar mixtures representing the eight candidate proteins as prepared in Section 3.1.8 were combined and diluted in glucagon solution to provide a stock solution of 5 pmol/µL of each peptide. This was further diluted in glucagon solution to provide a working solution of 5 fmol/µL. Immediately prior to analysis, plasma samples were resuspended in 25 µL of the internal standard working solution, resulting in 100 fmol of each peptide standard being injected o/c (20 µL injection). This concentration of sample ensured good detection of the peptide analytes with no carry-over taken into subsequent runs. The run order of each set of analytical repeats (60 samples, *i.e.,* 20 samples, 3 technical repeats) was randomised to exclude run time and run order bias. LC-SRM performance was benchmarked prior to analyses using light and heavy TMT-labeled VATVSLPR peptides as described in Section 3.1.9.

TMT-SRM quantitation was performed with the aid of calibration curves. In the 'normal' curve approach, curves are constructed using a constant amount of heavy peptide against a varying amount of light peptide, spiked into plasma matrix. This was demonstrated in Chapter 3 for the determination of the performance characteristics for VATVSLPR peptide. However, this approach is problematic for the assay described within, as the presence of endogenous analyte excludes the possibility of determining the linear range and the LOD and LOQ. To overcome this, a 'reverse' calibration curve approach was undertaken to determine the performance characteristics for the AD candidate peptides in plasma. Here, a constant amount of light TMT-labeled peptide and a varying amount of heavy TMT-labeled peptide are spiked onto light TMT-labeled plasma matrix. As there is no contribution to heavy signal from the endogenous analyte, it is possible to measure the equivalent of a blank sample and determine both LOD and LOQ (Figure 4.1).

A 12-point reverse calibration curve was produced by combining light and heavy TMT-labeled peptides (internal standard of light TMT-labeled peptides constant

at 100 fmol o/c and heavy TMT-labeled peptides, varied 1, 100, 200, 300, 400, 500, 600, 700, 800, 900, 1000 and 6,000 fmol o/c). For the purposes of the curve, additional to the heavy TMT-labeled peptide stock solution prepared as above, a stock solution of light TMT-labeled peptides (5 pmol/µL) was prepared as described above. In the first

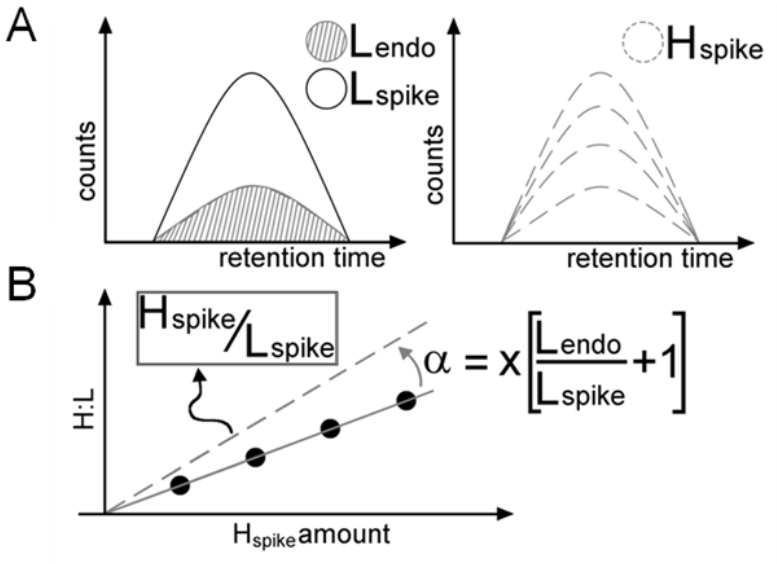

Figure 4.1 Overview of the 'reverse' calibration curve approach to provide TMT-SRM quantitation. **A** When constructing the reverse curve, the peak area corresponding to the light peptide internal standard (L) is contributed to by the endogenous amount of light peptide. The varying amounts of heavy peptide spikes (H) are free of endogenous analyte so the curve crosses the origin. **B** Correcting the reverse curve for the endogenous analyte contributing to the internal standard peak area requires a rotation of the curve about the intercept. This is the equivalent of increasing each curve point by an amount proportional to the ratio of the amounts of endogenous light peptide to the spiked light peptide (Campbell *et al.,* 2011).

instance, an analysis was performed to ensure that light and heavy TMT solutions were comparable in SRM sensitivity, *i.e.,* equivalent signal of light and heavy TMT peptides when combined in a 1:1 ratio and loaded at 100 fmol each o/c. Each point on the curve was generated by employing a similar dilution strategy as described in Section 3.1.7. The pooled plasma sample (30 µg per well) was resuspended in combined light TMT and heavy TMT-labeled peptides at each calibration concentration, gently vortexed and spun down in a Speedvac to collect the sample into one volume. A rubber seal (Thistle Scientific Ltd., Uddingston, UK) was placed on the plate to protect the contents of the wells from particulates such as dust and to avoid evaporation. Prior to, and upon completion of a set of 60 samples, samples were analysed for the preparation of a

calibration curve. Immediately before the analysis of the sample set, system checks were undertaken using VATVSLPR peptides to ensure the LC-SRM system was performing with optimal sensitivity, mass accuracy, calibration and ion stability. During the analysis of the sample set, light TMT-labeled pooled plasma spiked with internal standard was acquired after every 20 samples to ensure LC-SRM performance was maintained across the entire sample set (Section 3.1.9).

4.1.4 Data processing for TMT-SRM assay validation

LC-SRM data on the QTRAP was visualised through Analyst's quantitation wizard as described in Section 2.1.1.9. All peak matching was visually verified and peak areas were exported into Microsoft Excel 2003. Transitions were excluded if there was poor peak definition from the background signal. For generation of calibration curves, the peak area for each heavy TMT transition across the concentration range was measured relative to each light TMT transition, representing the endogenous target analyte in plasma and the internal standard spiked on top (100 fmol o/c). For TMT-SRM assay validation, the peak area of each light TMT transition, representing the endogenous target analyte in plasma, was measured relative to the peak area of the corresponding heavy TMT transition (constant synthetic peptide internal standard). The amount (fmol o/c) of individual transitions of each target peptide across analytical and technical repeats in AD and NDC samples were interpolated from the respective reverse calibration curves, *i.e.,* each transition had a calibration curve. The presence of the internal standard, as well as the endogenous signal in the light TMT channel, results in an overestimation of experimental values when reading from the curve (Figure 4.1). To account for this, the peak area of the internal standard (100 fmol o/c) is subtracted from the total peak area to leave the peak area representing the endogenous signal only. To achieve this, it is assumed that the light and heavy TMT signals give the same response. Thus, for further confidence in the accuracy of the measurement, light TMT and heavy TMT-labeled peptides were combined at 100 fmol each o/c to ensure they give a ratio of 1:1. Single-reference point (SRP) calibration was

performed upon the relative comparison of the L/H ratio for each transition, *i.e.,* measurement of the endogenous plasma amount (L) relative to the internal standard at 100 fmol o/c (H).

4.1.5 Statistical analysis for TMT-SRM assay validation

Using values calculated from the calibration curve and SRP, the absolute amount (µg/mL) of each transition was calculated using the *Mr* of the respective protein. A grand mean concentration was then calculated for each peptide in each sample using combined transitions of a peptide and compared between AD and NDC groups. Error bars were plotted using the 95% confidence interval (CI) associated with each mean value.

TMT-SRM quantitation of each peptide was compared between AD and NDC groups using SPSS (v12.0, SPSS Ltd., Surrey, UK). The experimental design resulted in pseudo-replication of the data, *i.e.,* three transitions per peptide, three analytical repeats, three technical repeats and case (Appendix Figure 4.1). Thus, hierarchical three-way analysis of variance (ANOVA) was used to maintain the appropriate degrees of freedom. Appendix Figure 4.2 displays the syntax script used to perform the statistical analysis in SPSS. The approach was used to separate and estimate the different sources of variation and these were then recombined to give an estimate of the variance of the mean. A method was chosen for analysis that would give a realistic estimate of the 95% CI, taking into account the variance attributable to all factors in the hierarchy. The variance of the mean was used to estimate the standard error and this, together with a value from the *t*-distribution, was used to estimate the 95% CI around the mean difference between the AD and NDC groups. Further, to estimate the contribution of variance associated with each level in the hierarchy (case, technical repeat, analytical repeat or transition), a variance components analysis was performed.

The mean concentration of each gelsolin peptide in AD and NDC samples was used to directly compare the difference in gelsolin levels between groups. A student's t-test was performed to determine if this difference was statistically significant.

Spearman correlation coefficients were calculated to determine the agreement between the TMT-SRM measurement of each gelsolin peptide across experimental samples and the corresponding WB measurement.

4.1.6 Determination of TMT-SRM assay performance characteristics on a QTRAP mass spectrometer

To determine the TMT-SRM assay performance characteristics, 16-point reverse calibration curves were produced. Here, the internal standard peptides (light TMT-labeled) constant at 100 fmol o/c were combined with heavy TMT-labeled peptides (varied from 0.5, 1, 2.5, 5, 10, 25, 50, 75, 100, 250, 500, 1000, 2500, 5000, 7500 and 10,000 fmol o/c). Each calibration mix was generated by employing a similar dilution strategy as described in Section 3.1.7. The pooled plasma sample (30 µg per well; prepared in Section 4.1.2) was resuspended in the light TMT and heavy TMT-labeled peptides across the concentration range, as described in Section 4.1.3. All curves were measured in triplicate over three independent days. LODs and LOQs were determined by measuring 12 replicates of a blank sample of light TMT-labeled peptide and light TMT-labeled plasma only, *i.e.,* less the heavy TMT-labeled peptide (Whiteaker *et al.,* 2010). To assess the trueness and precision of TMT-SRM quantitation, replicate samples were analysed between curves. Specifically, the pooled plasma sample (30 µg) was resuspended in combined light TMT-labeled internal standards at 100 fmol o/c and heavy TMT-labeled peptides (at 5 fmol or 50 fmol o/c; QCs). Replicate analyses (n = 5) were performed at each amount for each curve. All data was processed for construction of the curves as described in Section 4.1.4.

4.1.7 Statistical analysis for determination of TMT-SRM assay performance

Linear regression was performed using Prism software v5.0 (Graphpad Software Inc., CA, USA) using $1/SD^2$ weighting to construct calibration curves. Axes were $\log_{10}$ transformed to better visualise the lower points on the plot. Evidence for non-linearity was tested using second and third order polynomial best-fits. Absolute

values for each transition of each peptide in each QC sample were interpolated from the curves as described in Section 4.1.4. Trueness and precision values for each transition of each peptide were determined by calculating the %CV across all QC replicates. The LOD was calculated from the mean heavy TMT signal (noise) in the 12 blank replicates plus three times the SD of the noise in the blank (response at the time of peptide elution). Similarly, the LOQ was calculated from the mean heavy TMT signal in the 12 blank replicates plus ten times the SD of the noise in the blank.

4.1.8 TMT-SRM assay development on a TSQ Vantage mass spectrometer

To demonstrate the portability of the TMT-SRM assay across MS platforms, a method was developed for quantitation of the AD candidate biomarker panel on a TSQ Vantage triple quadrupole mass spectrometer (Thermo Fisher Scientific). For confirmation of QTRAP transition selection and optimisation of instrument voltages for each transition, equimolar mixtures as prepared in Section 3.1.8 were infused into the TSQ Vantage. Specifically, mixtures were prepared in 50% ACN, 0.2% FA and introduced into the instrument *via* a Nanospray-1 ion source (Thermo Fisher Scientific) at 500 nL/min. For each transition, the CE and S-Lens voltages were optimised to enhance the detection of target analytes in light TMT-labeled plasma. The S-Lens is specific to Thermo Fisher Scientific instruments, improving SRM sensitivities by focusing ionised peptides into a tight beam before introduction to the mass analyser. Instrument voltages were optimised by linearly ramping the voltage over an instrument-defined range. The maximal voltage over the ramping trace was selected as the optimal CE and S-Lens value.

On-line LC analysis was performed on a Finnigan Surveyor MS Pump Plus LC system (Thermo Fisher Scientific). Peptides were resolved using an identical LC column, ACN gradient and flow rate as for that on the QTRAP (as described in Section 3.1.9). However, the slower injection speed of the Finnigan Surveyor MS Pump Plus LC system increased the total analysis time to 22 min. Peptides were introduced into the instrument using a heated-electrospray ionisation (HESI)-II probe in positive

ionisation mode. Peptides were ionised by ESI and source-dependant voltages and gases were optimised for maximal ion sensitivities. Specifically, the entrance pressure of nitrogen (used for sheath and auxiliary gas) was ~6 bars, the ion spray voltage was 4000 V, the vaporising temperature was 200 °C, the sheath gas pressure was 60 bar, the auxiliary gas pressure was 15 bar and the capillary temperature was 230 °C. Peptides were fragmented by CID using argon gas at 1 mTorr. Mass calibration of the TSQ Vantage was performed on MS/MS fragment ions of polytyrosine - 1, 3, 6 standard [$(Tyr)_{1-6}$; Thermo Fisher Scientific]. Specifically, a solution of 4 – 24 ng/µL $(Tyr)_{1-6}$ was prepared in 0.1% FA, 50% methanol and infused into the instrument at 1.5 µL/min using a syringe pump as described in Section 2.1.1.5. LC-SRM performance was benchmarked prior to analyses using light and heavy TMT-labeled VATVSLPR peptides as described in Section 3.1.9. The determination of accurate t_R for application of SRM scheduling to the method was performed using a mixture of all heavy TMT-labeled peptides (100 fmol each o/c) spiked into 30 µg of the light TMT-labeled plasma pool sample. The mean t_R of three replicates was used to build the SRM scheduled method. For determination of TMT-SRM assay performance characteristics, calibration curves were constructed using an identical experimental design as described in Sections 4.1.7.

4.1.9 Data processing and determination of TMT-SRM assay performance characteristics on the TSQ Vantage

LC-SRM data on the TSQ Vantage was processed using Pinpoint Software (v1.0, Thermo Fisher Scientific). Processing parameters included an SRM smoothing of 7 points, an SRM peak width of 1 min and a minimum signal intensity of 20 cps. All peak matching was visually verified. Peak areas were exported into Microsoft Excel 2003. Transitions were excluded if there was poor peak definition from the background signal. Calibration curves were constructed as described in Section 4.1.6. To determine the assay performance characteristics, statistical analysis was performed as described in Section 4.1.7.

4.2 Results

4.2.1 Validation of the multiplexed TMT-SRM assay

4.2.1.1 Assessment of SRM transitions

The TMT-SRM assay was validated for suitability to measure the AD candidate protein biomarkers in plasma by comparison to measurements obtained using a widely established immuno-based platform. Here, the TMT-SRM method as optimised in Section 3.2.9 containing 22 peptides and all SRM transitions for these peptides was applied to a cohort of 10 AD and 10 NDC samples, previously shown to have a difference in plasma geslolin levels between groups. A reverse calibration curve strategy was incorporated here which was expanded over the range measured in Chapter 3, *i.e.,* 1 – 6000 fmol o/c to ensure TMT-SRM quantitation covered the range of endogenous levels of the target analytes in plasma, from low (21.4 – 44.2 µg/mL) SAP levels (Nybo *et al.,* 1998; Pepys *et al.,* 2002) to high (2,000 – 2,400 µg/mL) A2M levels (Barrett, 1981). Transitions were removed from the data analysis if they possessed high plasma background (Figure 4.2). Taking only those peptides which remained in the TMT-SRM method up to this stage, plasma background interference was observed for transitions of peptides 1, 5, 9, 12, 13, 14, 22 and 30 (Appendix Figure 4.3). This was in agreement with the results in Section 3.2.4, with all transitions highlighted in Table 3.4 having comparable plasma background interference in this sample set.

4.2.1.2 Measurement of gelsolin by TMT-SRM

Figure 4.3 A displays a representative calibration curve for gelsolin peptide 31. The normal human plasma concentration of the protein is 180 – 200 µg/mL (Osborn *et al.,* 2008). However, the actual amounts measured here for gelsolin were ~10 fold lower and these levels fell towards the lower limits of the calibration curve range

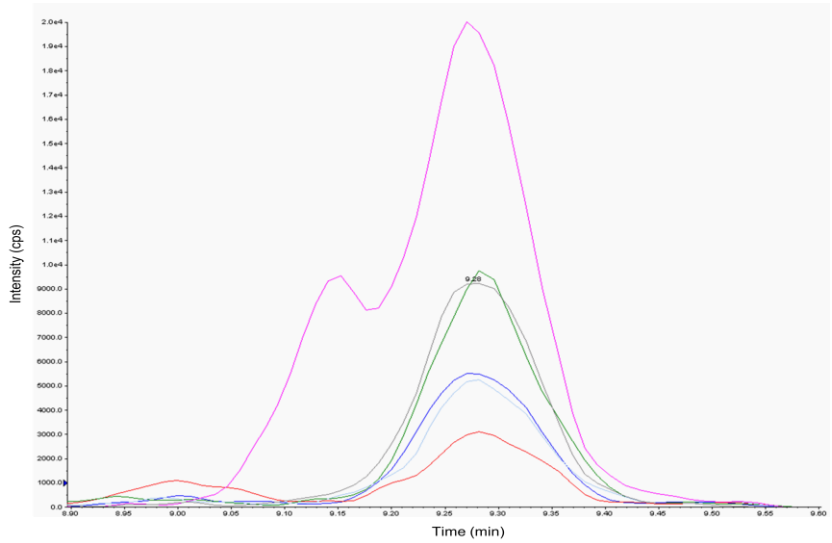

Figure 4.2 An XIC of the light TMT and heavy TMT for peptide 13. One transition has been affected by high plasma background (coloured in pink; heavy TMT-labeled) and subsequently, this transition and its corresponding light-TMT partner were removed from the analysis.

(although these levels fall within the linear range of quantitation). Therefore, a future advancement to the strategy was needed, *i.e.,* it was necessary to expand the linear range down to lower concentrations. This was essential to account for potential reductions in the endogenous amounts measured by the TMT-SRM assay, as compared to theoretical endogenous amounts.

Figure 4.3 B displays the bar chart of the endogenous plasma amounts of all peptides of gelsolin in AD and NDC samples as quantitated by TMT-SRM. Visualisation of the data in this manner was advantageous as the difference in the expression of each peptide between groups could be readily ascertained. Further, it enabled the characterisation of the most robust signature peptides of a protein across sample sets. Considering all gelsolin target analytes, peptide 27 had the lowest SRM sensitivity across samples and replicate measurements for this peptide were less robust than for peptides 29, 30 and 31, *i.e.,* peptide 27 had a CV of 27.14% across technical repeats compared to a CV of 7.57% for peptide 31. Peptide 27 was therefore excluded from the data analysis and no longer considered for TMT-SRM quantitation. Peptides 29, 30 and 31 performed similarly, with equivalent absolute amounts quantitated in the plasma, *e.g.,* the mean gelsolin level of each signature peptide in AD samples was 16.1 µg/mL for peptide 29, 11.0 µg/mL for peptide 30 and 16.9 µg/mL for peptide 31 (Table 4.2).

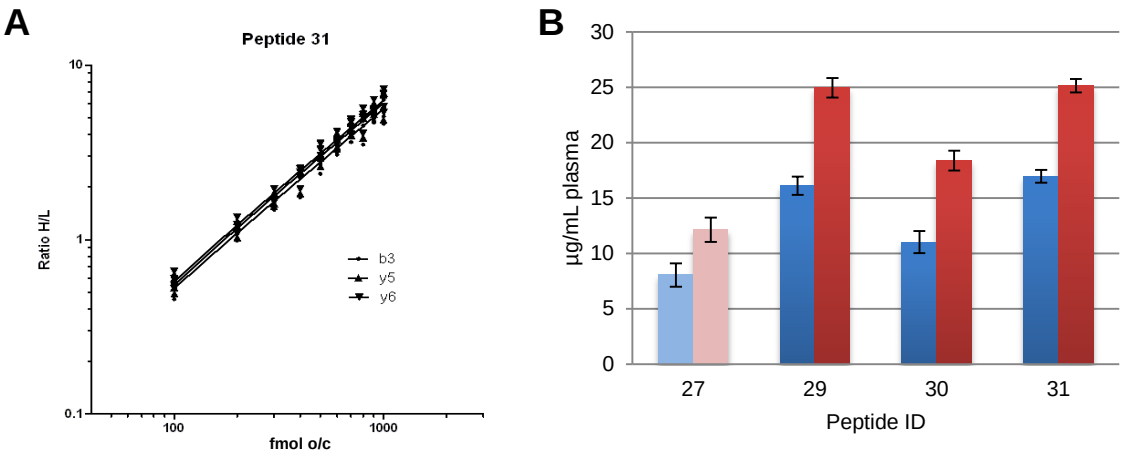

Figure 4.3 TMT-SRM quantitation of gelsolin in AD and NDC samples. **A** Reverse calibration curve for gelsolin peptide 31 (displaying 100 – 1000 fmol o/c). Each of the three TMT-SRM transitions for the peptide are plotted on the curve **B** Bar charts displaying the difference in the amounts of gelsolin peptides between AD (blue) and NDC (red) samples, as measured by TMT-SRM. Peptides with less robust TMT-SRM quantitation are faded. Error bars indicate the 95% CI.

Protein	Peptide ID	Calibration curve				TMT-SRM v WB
		Mean AD (µg/mL)	Mean NDC (µg/mL)	Fold Change	*p*-value	Spearman correlation coefficient
Gelsolin	29	16.1	24.9	0.65	0.0002	0.65
	30	11.0	18.4	0.60	0.0021	0.68
	31	16.9	25.1	0.67	0.0001	0.73

Table 4.2 Comparison of TMT-SRM and WB of gelsolin for TMT-SRM assay validation. Plasma amounts (µg/mL) of each gelsolin peptide in AD and NDC samples, as determined by the TMT-SRM assay are displayed. Equivalent amounts of each peptide and similar fold changes were observed across the three gelsolin peptides selected for data analysis. Strong correlation (*i.e.,* > 0.5) was observed between each gelsolin peptide and the corresponding WB measurement as determined by Spearman correlation coefficients (taking all samples into account).

Similarly, for NDC samples, endogenous plasma gelsolin levels were calculated to be 24.9 µg/mL for peptide 29, 18.4 µg/mL for peptide 30 and 25.1 µg/mL for peptide 31. Such agreement between signature peptides demonstrated the robustness of the TMT-SRM workflow and gave confidence to the quantitative result.

4.2.1.3 Correlation of TMT-SRM and WB measurements for gelsolin

Previous TMT discovery studies in our laboratory have shown plasma gelsolin levels to be decreased in AD subjects as compared to NDCs, with strong correlation to the rate of cognitive decline (gelsolin decreases as cognitive ability decreases). Findings were validated by WB (Güntert *et al.,* 2010). In-line with the WB results, a statistically significant ($p < 0.0021$) difference in plasma gelsolin levels was observed for all peptides between AD and NDC groups. Fold changes of 0.65, 0.60 and 0.67 were observed between AD and NDC groups for peptides 29, 30 and 31, respectively (Figure 4.3 B, Table 4.2). The calculation of Spearman correlation coefficients was selected as a suitable method to compare the TMT-SRM and WB platforms. A strong correlation (0.65, 0.68 and 0.73; Cohen, 1988) was observed for gelsolin peptides 29, 30 and 31 in each sample, as compared to the corresponding WB measurement (Table 4.2). Excellent agreement with the established immuno-based platform thus validated the TMT-SRM assay as fit-for-purpose for the targeted measurement of gelsolin in undepleted plasma.

4.2.1.4 Quantitation of the remaining peptides in the TMT-SRM assay

In addition to gelsolin, the endogenous levels of the signature peptides of the seven other proteins could be quantitated between AD and NDC samples in the multiplexed TMT-SRM assay, giving an initial insight into their performance in clinical samples (Figure 4.4). Due to the small subject numbers utilised however, it was unwise to draw definitive conclusions regarding the expression of each signature peptide between the different groups. Fold changes for these peptides as described in Table

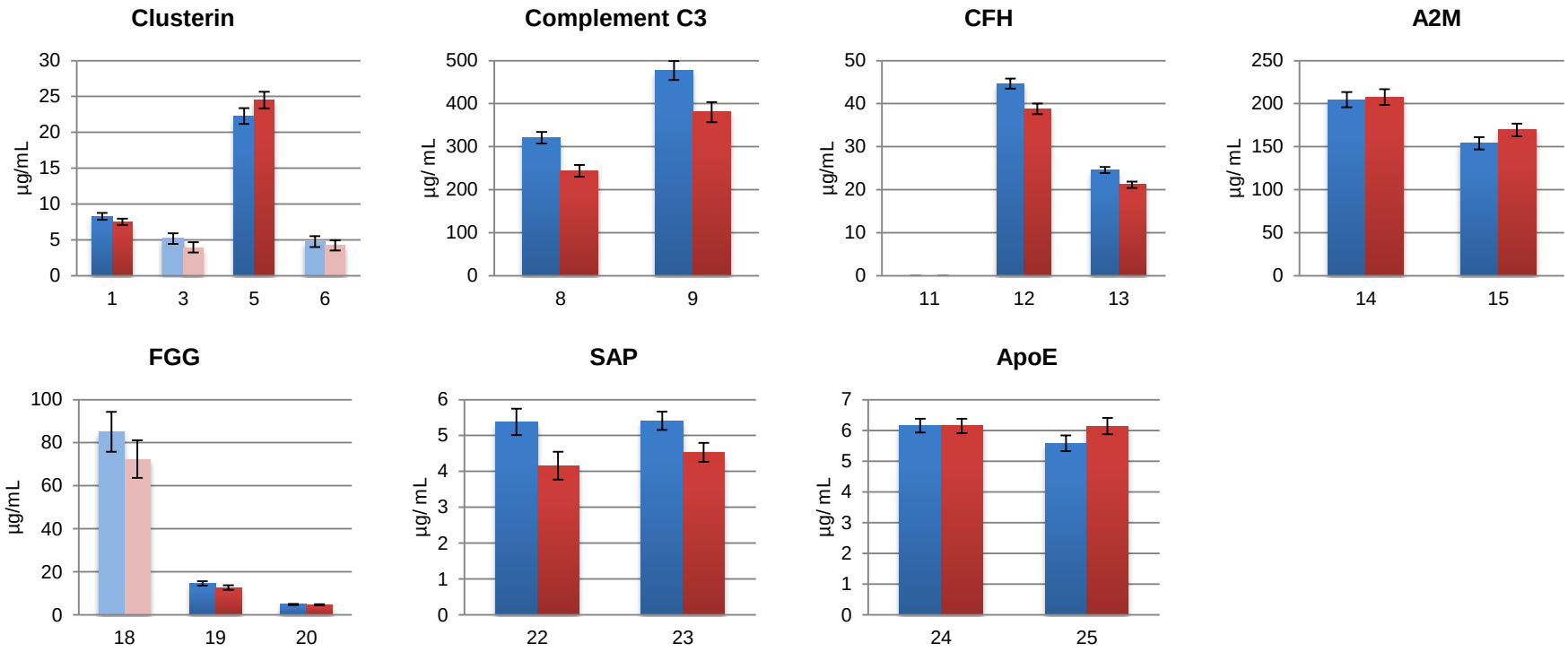

Figure 4.4 Assessment of the TMT-SRM performance of peptides of the same protein across AD and NDC groups. Peptides of the same protein (*x*-axis) are plotted on the same graph. Peptides with less robust TMT-SRM quantitation are faded. Error bars indicate the 95% CI.

Protein	Theoretical amounts in plasma (µg/mL)	Peptide ID	Calibration curve			SRP		
			Mean AD (µg/mL)	Mean NDC (µg/mL)	Fold Change	Mean AD (µg/mL)	Mean NDC (µg/mL)	Fold Change
Clusterin α chain	35 - 105	1	8.3	7.5	1.10	7.6	6.7	1.14
Clusterin β-chain		5	22.3	24.5	0.91	24.8	27.2	0.91
Complement C3	670 - 1290	8	321.1	243.8	1.32	316.8	241.6	1.31
		9	477.0	380.3	1.25	457.8	365.9	1.25
CFH	400 - 800	12	44.7	38.8	1.15	45.7	39.5	1.16
		13	24.6	21.2	1.16	24.3	20.8	1.17
A2M	2000 - 2400	14	204.6	207.5	0.99	199.7	202.4	0.99
		15	154.0	169.4	0.91	141.6	155.5	0.91
FGG	80 - 500	19	14.7	12.7	1.16	14.7	12.3	1.19
		20	4.9	4.7	1.04	3.6	3.4	1.06
SAP	21 – 44	22	5.4	4.2	1.29	5.4	4.6	1.29
		23	5.4	4.5	1.19	4.6	3.5	1.32
ApoE	34 - 74	24	6.2	6.1	1.00	6.0	6.0	1.00
		25	5.6	6.1	0.91	4.8	5.5	0.88
Gelsolin	179 - 200	29	16.1	24.9	0.65	16.3	25.5	0.64
		30	11.0	18.4	0.60	11.3	17.7	0.64
		31	16.9	25.1	0.67	16.8	25.7	0.65

Table 4.3 Plasma amounts (µg/mL) of target peptides in AD and NDC samples, as determined by the TMT-SRM assay using calibration curves and SRP quantitation. Only those peptides included in the final data analysis are displayed. Equivalent amounts of each peptide and similar fold changes were observed between both calibration approaches.

4.3 were therefore considered as purely representative of the level of agreement between peptides of the same protein.

In addition to gelsolin peptide 27, all transitions of four other peptides (3, 6, 11 and 18; Figure 4.4, greyed out) were removed from the analysis as the endogenous detection was poor in the majority of samples or a high variance was observed for all measurements across all samples. Clusterin peptides 3 and 6 were not consistently detected in all samples and thus, considered less robust for TMT-SRM quantitation and removed from the method. Importantly however, one peptide remained for each of the different clusterin chains to be measured. Peptide 11, measuring CFH, was of weak SRM sensitivity compared to the other peptides (peptides 12 and 13) within the protein and was not consistently detected across all samples. This was reflected in a CV across technical replicates of 24.35%, compared to 9.45% for peptide 12. A high variance was observed for FGG peptide 18 for all measurements across all samples. This peptide was deemed less robust compared to other peptides (peptides 19 and 20) within the FGG protein. Therefore, five peptides were removed from the TMT-SRM method at this assay validation stage (peptides 3, 6, 11, 18 and 27) with 17 peptides remaining for quantitation, and importantly, at least two peptides per protein.

It can be clearly seen from Figure 4.4 that the endogenous plasma amounts between peptides of the same protein were not in agreement in several cases, *i.e.,* peptides of clusterin, complement C3, CFH, A2M and FGG. Taking clusterin as an example, a large difference was observed, *i.e.,* peptides 1 and 5 had mean amounts of 8.3 and 22.3 µg/mL in AD and 7.5 and 24.5 µg/mL in NDC, respectively (Table 4.3). This was speculated to be due to several factors including the unique clusterin chains measured and the different susceptibilities of each peptide to trypsin cleavage. Further, peptide losses during TMT-labeling or purification stages may have compounded the observed difference. Such factors may additionally explicate the lower absolute amounts quantitated for the clusterin peptides as compared to theoretical amounts. A lower amount compared to theoretical amounts was a trend observed for all signature peptides in the TMT-SRM method. Conversely, peptides of the same protein were

equivalent in several cases (peptides of SAP and ApoE), *e.g.,* equivalent absolute amounts in plasma were observed for Apo E peptides 24 and 25, which had mean amounts of 6.2 and 5.6 µg/mL in AD and 6.1 and 6.1 µg/mL in NDC (Table 4.3).

Despite discrepancies in the peptide amounts for a number of the proteins, it was very encouraging to observe equivalent performance for peptides of the same protein, which added confidence to the quantitative result. The most important factor for any quantitative biomarker technology is the ability to determine relative differences between disease and control groups, rather than absolute amounts. Taking complement C3 peptides 8 and 9 for example, excellent agreement in TMT-SRM quantitation for the two peptides was indicated by similar fold changes between AD and NDC groups, *i.e.,* 1.32 for peptide 8 and 1.25 for peptide 9 (Table 4.3).

4.2.1.5 TMT-SRM quantitation by single reference point quantitation

To surpass the need for calibration curves, SRP calibration was assessed for the quantitation of peptide amounts in AD and NDC groups. Here, quantitation is based on relating the endogenous analyte to the known amount (100 fmol o/c) of spiked heavy TMT-labeled internal standard (Campbell *et al.,* 2011). This spiked amount fell well within the linear range of quantitation (as determined by the calibration curves) for all target analytes and could therefore be used for accurate quantitation. The benefits of SRP calibration compared to the calibration curve approach are its simplicity and the ability to achieve a higher throughput of samples. SRP quantitation was performed by calculating the endogenous plasma amount relative to the known amount of internal standard spiked in at 100 fmol o/c.

It can be seen from Table 4.3 that there was excellent agreement between the TMT-SRM quantitation determined by interpolation from the calibration curve and SRP calibration. Equivalent absolute plasma amounts were quantitated for each target analyte and similar fold changes between AD and NDC groups were observed for all peptides. When taking gelsolin peptides in the NDC grouping as an example, endogenous plasma amounts determined for peptides 29, 30 and 31 using the

calibration curve approach were 16.1, 11.0 and 16.9 µg/mL in AD and 24.9, 18.4 and 25.1 µg/mL in NDC. The amounts determined for the same peptides by the SRP approach were 16.3, 11.3 and 16.8 µg/mL in AD and 25.5, 17.7 and 25.7 µg/mL in NDC, respectively. The three gelsolin peptides had fold changes of 0.65, 0.60 and 0.67 between AD and NDC using the calibration curve approach and 0.64, 0.64 and 0.65 using SRP calibration. The goal of the calibration curve approach was for assay performance characteristic definition and to ensure that linearity was achieved across the range required for the measurement of endogenous analytes. Once these performance characteristics have been established, TMT-SRM quantitation could then proceed by SRP calibration.

4.2.1.6 Variance associated with technical and analytical repeats

To understand the contribution of variance introduced by technical and analytical procedures, the variance was assessed between technical repeats of each sample (in triplicate) and analytical repeats of each digest (also in triplicate). Table 4.4 displays the results for the variance components analysis for the TMT-SRM of the 17 peptides remaining in the TMT-SRM assay (upon exclusion of five peptides during TMT-SRM assay validation; Sections 4.2.1.3 and 4.2.1.4). For A2M peptide 15, some variance was explained by transition, *i.e.,* different transitions of this peptide had differences in TMT-SRM quantitation. However, when averaging all transitions of this peptide as in Section 4.2.1.4, equivalent fold changes were observed for this peptide compared to its sister peptide (14). Overall, up to 99.99% of the variance in the samples was explained by case (either AD or NDC grouping). As expected, more variance was attributed to technical rather than analytical repeats. Such variation may be explained by the variable enzymatic efficiency of trypsin, resulting in varying rates at which the tryptic peptide is generated across multiple digests. However, both technical and analytical repeats had minimal contribution to any variance observed and the majority was explained by the factor of case. Thus, for the TMT-SRM quantitation of future cohorts, only one technical and one analytical repeat was considered sufficient.

It was observed here that this won't impact the results and prevent the identification of differences between AD or NDC groups. Further, this has major benefits as doing multiple technical repeats severely impacts on sample throughput.

Peptide ID	% of variance			
	Case	Technical repeats	Analytical repeats	Transition
1	99.99	0.00	0.01	NA
5	99.99	0.00	0.01	NA
8	94.11	1.98	0.00	3.91
9	97.61	2.39	0.00	0.00
12	97.78	2.22	0.00	0.00
13	99.13	0.87	0.00	0.00
14	99.98	0.02	0.00	0.00
15	54.71	13.05	0.00	32.23
19	89.38	10.62	0.00	0.00
20	99.69	0.31	0.00	0.00
22	98.37	1.63	0.00	NA
23	99.57	0.43	0.00	0.00
24	94.03	5.97	0.00	0.00
25	99.77	0.23	0.00	0.00
29	99.89	0.11	0.00	0.00
30	99.57	0.43	0.00	0.00
31	99.88	0.12	0.00	0.00

Table 4.4 Variance components analysis for target analytes in the TMT-SRM assay validation experiments. For those peptides included in the data analysis, any variance observed by TMT-SRM was primarily explained by the factor of case. NA = not applicable.

4.2.2 Assessment of TMT-SRM assay performance on the QTRAP and TSQ Vantage platforms

4.2.2.1 Final TMT-SRM method on the QTRAP

From the 22 peptides which were brought forward from Chapter 3, five peptides were excluded after the TMT-SRM assay validation stage due to their poor quantitative performance across a sample set. Therefore, a total of 17 peptides remained in the final TMT-SRM assay, with a least two signature peptides for each protein. As different plasma samples in different cohorts may have varying levels of plasma background interference associated with them, all TMT-SRM transitions for the 17 peptides were included in the final method, including those which were shown to be problematic in Sections 3.2.4 and 4.2.1.1. However, such transitions may still be filtered out at the

data analysis stage. The TMT-SRM method on the QTRAP was updated accordingly. Figure 4.5 displays the SRM XIC of the final TMT-SRM assay. The method monitored 102 transitions (51 light TMT heavy TMT pairs) and had a scheduling window of 45 sec, 1 sec cycle time, 20.8 msec dwell time per transition with ~8 data points at FWHM.

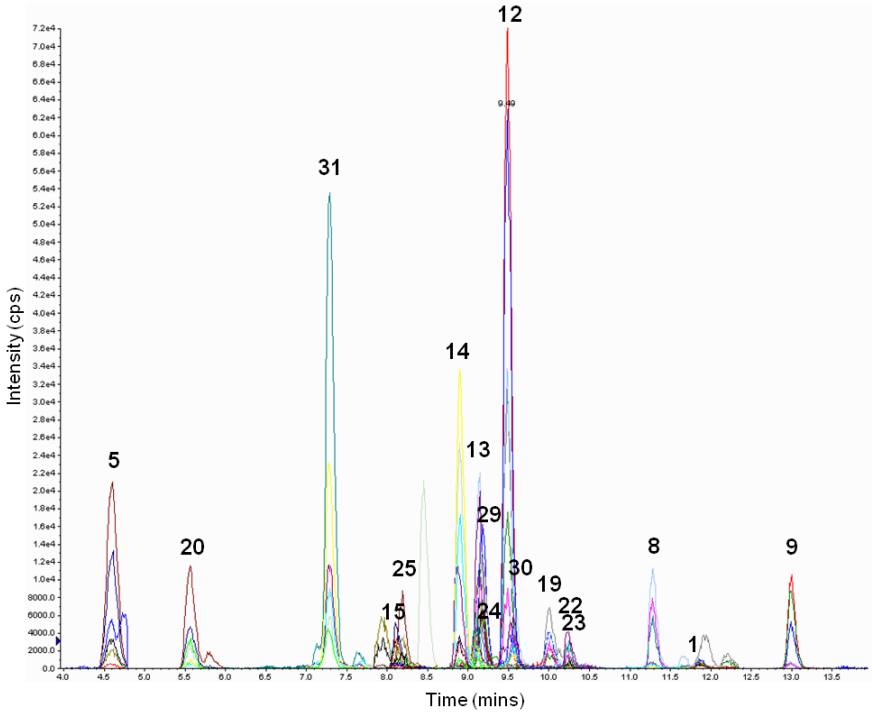

Figure 4.5 SRM XIC of the 17 target analytes remaining in the final TMT-SRM assay. Light TMT-labeled plasma was spiked with heavy TMT-labeled peptides and analysed by TMT-SRM.

4.2.2.2 Performance characteristics of the multiplexed TMT-SRM assay on the QTRAP

Once the most robust peptides for TMT-SRM were defined in terms of quantitation in clinical sample cohorts, *i.e.,* upon validation of the assay, it was necessary to determine the assay performance characteristics for each target analyte remaining in the refined method. This enabled the comparison of assay performance to more established methods of peptide/ protein quantitation such as ELISA. During TMT-SRM assay validation experiments as described in Section 4.1.3, 12-point calibration curves were utilised, measuring the range of 1 - 6,000 fmol heavy TMT-labeled peptides o/c. Such a range confirmed linearity in quantitation but was unable to define the lower and upper points of linearity. To determine this, 16-point reverse calibration

curves were constructed here to expand over the range which was achieved. Further, as opposed to the equal spacing of concentration points in the strategy previously utilised, more points were acquired at lower concentrations and less points acquired at higher concentrations. This was done to ensure full characterisation at the lower limits of the curve. TMT-labeled peptides were varied over 0.5 - 10,000 fmol o/c, whilst light TMT-labeled peptides (100 fmol o/c) were spiked on top of the light TMT-labeled endogenous analyte in plasma. A blank sample was integrated, enabling the determination of definitive LODs and LOQs for each target analyte in plasma. Definition of exact LODs and LOQs here was advancement to the strategy as described in Section 3.2.6, where LODs and LOQs were based on the lowest concentration points measured on the curve which were within acceptable precision levels, *i.e.,* where the %CV was < 20. A complete calibration curve was performed each day for three days to assess precision. Figure 4.6 displays examples of the calibration curves of peptides of CFH, A2M and ApoE. Transitions of the same peptide and peptides of the same protein plotted similar curves, adding confidence to the quantitative measurement. The linear range of quantitation was defined as the lowest and highest concentration of heavy TMT-labeled peptides at which linearity was still observed (Table 4.5). The determination of this parameter was essential to confirm that quantitation was being performed within the linear range of the endogenous levels of the target analytes in plasma. The dynamic range of response was over three orders of magnitude with excellent linearity (R^2 > 0.99). Taking complement C3 peptide 8 as an example, the dynamic range of the TMT-SRM assay was 5.78 - 2311.68 µg/mL in plasma, when taking the best transition as representative of the peptide. This range ensured that linear TMT-SRM quantitation was observed for this peptide within the levels expected for the protein in plasma (670 - 1290 µg/mL).

To assess the trueness and precision for each target analyte in plasma, replicate analyses were performed at 5 fmol o/c and 50 fmol o/c of heavy TMT-labeled peptides combined with 100 fmol o/c light TMT-labeled peptide internal standards and spiked on top of light TMT-labeled plasma (30 µg). Five replicates of each QC were

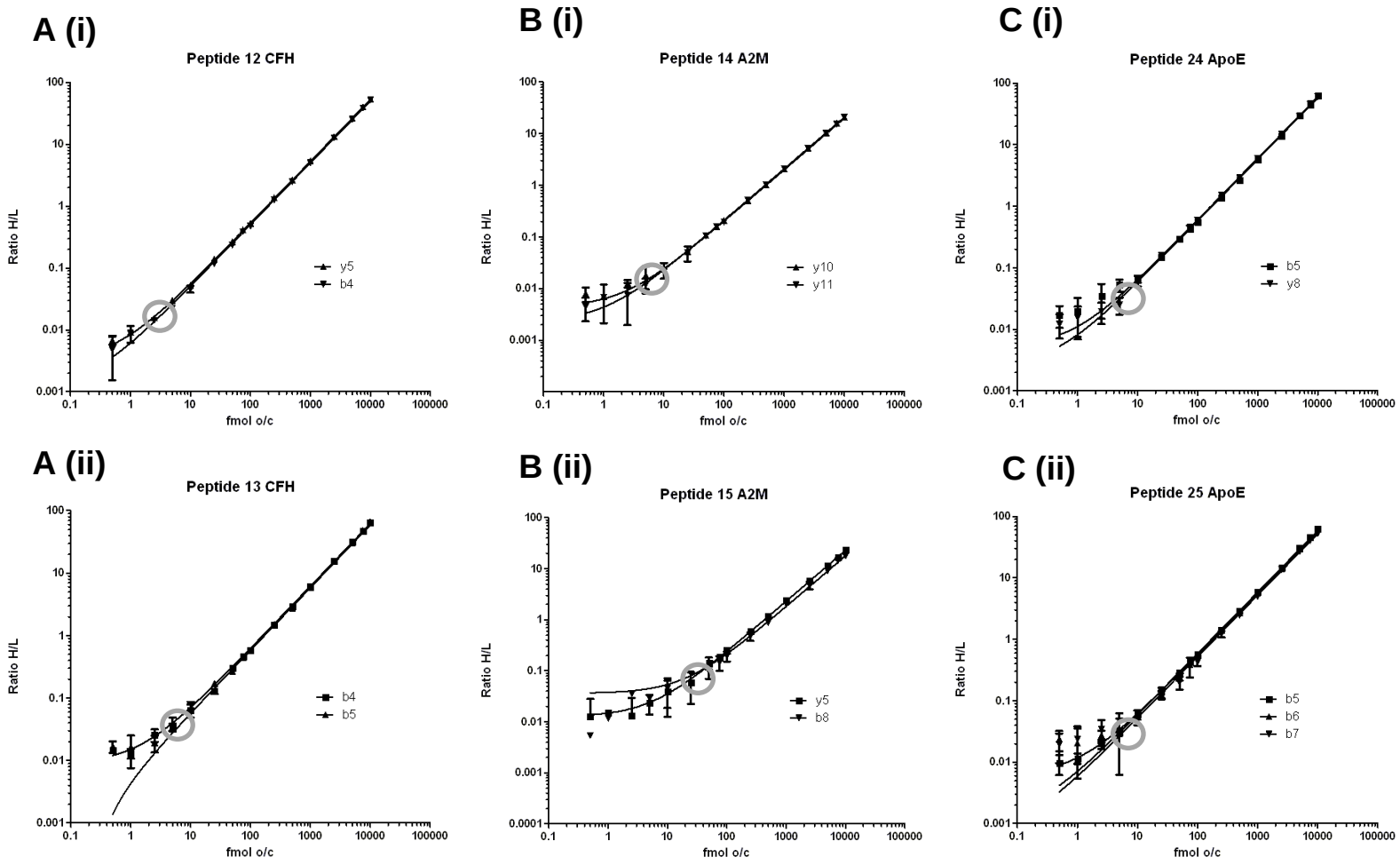

Figure 4.6 Calibration curves on the QTRAP mass spectrometer. **A** CFH, **B** A2M and **C** ApoE. Comparable performance was observed for transitions of the same peptide. The lowest point of linearity is circled on each calibration curve. All curves were acquired in the presence of plasma.

Protein	Peptide ID	Peptide *Mr* (Da)	Protein *Mr* (kDa)	LOD		LOQ		Lower point of linearity		Upper point of linearity		Trueness %CV	Precision %CV
				Peptide	Protein	Peptide	Protein	Peptide	Protein	Peptide	Protein		
				(µg/mL)	(µg/mL)	(µg/mL)	(µg/mL)	(µg/mL)	(µg/mL)	(µg/mL)	(µg/mL)		
Clusterin α-chain	1	1116.7	50	0.025	1.10	0.081	3.64	0.070	3.13	13.96	625.58	17.5	2
Clusterin β-chain	5	778.5	50	0.007	0.47	0.019	1.24	0.005	0.31	9.73	625.58	1.4	2.7
Complement C3	8	1138.7	185	0.018	2.94	0.045	7.32	0.036	5.78	14.23	2311.68	8.8	3
	9	1510.9	185	0.030	3.66	0.091	11.10	0.047	5.78	18.89	2311.68	1.6	5.1
CFH	12	1062.8	137	0.005	0.60	0.013	1.71	0.003	0.43	13.28	1712.94	0.3	2.8
	13	643.5	137	0.002	0.47	0.006	1.32	0.004	0.86	8.04	1712.94	1.8	4.9
A2M	14	1254.7	161	0.002	0.29	0.013	1.61	0.008	1.00	15.68	2009.74	2.7	3.2
	15	924.5	161	0.013	2.26	0.040	6.96	0.029	5.02	11.56	2009.74	1.3	2.7
FGG	19	879.5	48	0.001	0.05	0.006	0.33	0.006	0.30	10.99	605.83	13.7	5.1
	20	714.5	48	0.001	0.04	0.001	0.05	<0.001	0.03	8.93	605.83	1.3	1.2
SAP	22	1155.6	23	0.036	0.72	0.110	2.20	0.072	1.45	14.45	290.51	0.3	15.9
	23	1405.7	23	0.017	0.28	0.060	0.99	0.018	0.29	17.57	290.51	9.1	8.9
ApoE	24	967.5	34	0.003	0.11	0.010	0.34	0.006	0.21	12.09	427.74	2.8	1.8
	25	1032.6	34	0.007	0.22	0.015	0.51	0.013	0.43	12.91	427.74	0.8	2.6
Gelsolin	29	881.5	83	0.009	0.58	0.025	1.65	0.016	1.04	11.02	1036.79	5.9	6.1
	30	754.5	83	0.019	0.94	0.059	3.53	0.047	1.04	9.43	1036.79	7.6	5.4
	31	1274.8	83	0.005	0.33	0.015	0.99	0.001	0.05	15.93	1036.79	0.7	2.4

Table 4.5 Assay performance characteristics of the TMT-SRM method on the QTRAP. For each target analyte, the LOD, LOQ, linearity, trueness and precision is displayed. Protein concentrations (in µg/mL) represent the amount of protein corresponding to a given spike amount of the peptide, assuming 100% recovery.

performed on three days for each calibration curve. All target peptides could not be detected and accurately quantitated by TMT-SRM at the 5 fmol heavy TMT-labeled peptide QC, which reflected endogenous plasma levels below the LOQ for several target analytes, *e.g.,* peptide 9, and so trueness and precision values were calculated for the 50 fmol QC measurements only. The accuracy for the QTRAP is displayed in Table 4.5. Overall, the accuracy was favourable, with a mean CV of trueness across all target analytes of 4.6% and mean CV of precision of 4.5%.

LODs and LOQs were calculated from the mean response measured in the blank runs plus three times the SD (LOD) and 10 times the SD (LOQ). LODs and LOQs were determined at both the peptide and protein level, as ultimately, TMT-SRM quantitation was performed at the peptide level which was used as a surrogate to reflect the endogenous protein level. The calculated LODs and LOQs for the best transition of each target peptide are displayed in Table 4.5. Peptide quantitation was observed at low ng/mL levels, which was equivalent to low µg/mL protein levels, assuming complete digestion by trypsin (*e.g.,* peptide 20). LODs ranged from 0.001 - 0.036 µg /mL for peptides and 0.04 - 3.66 µg/mL for proteins (Table 4.5). LOQs ranged from 0.001 - 0.109 µg /mL for peptides and 0.05 - 11.10 µg/mL for proteins. All LOD and LOQ values were well within the physiologically relevant range in plasma.

4.2.3 Portability of the TMT-SRM assay across MS platforms

4.2.3.1 Method development

Once the TMT-SRM assay performance characteristics were determined for the QTRAP, experiments were replicated on an analogous triple quadrupole instrument, a TSQ Vantage. The assessment of assay portability was considered an essential process, giving an indication of the overall robustness of the TMT-SRM assay across MS platforms. A robust, fit-for-purpose assay is particularly crucial if it is to be implemented in independent laboratories. Heavy TMT-labeled equimolar mixtures of each protein were infused into the TSQ Vantage and MS/MS analysis performed to

confirm those transitions determined as optimal for the TMT-SRM assay on the QTRAP. Excellent accordance of fragmentation patterns and thus, transitions, was observed across platforms and all three transitions for each of the 17 peptides remaining in the method were included (Table 3.3). In addition, a fourth transition of peptides 14, 15, 22, 25 and 29 was selected for the TSQ Vantage. This instrument had faster scanning capabilities and thus, enabled the assessment of more transitions (Table 4.6). Figure 4.7 displays representative voltage traces for CE and S-Lens optimisation. S-lens values were optimised for the detection of each precursor ion. As with CE values on the QTRAP, the CE values on the TSQ Vantage were specific to individual transitions and thus needed to be optimised accordingly (Appendix Table 4.1). In general, less CE was needed for optimal detection of fragment ions on the TSQ Vantage as compared to the QTRAP, *e.g.,* transition 1 of peptide 1 had a CE of 48 V on the QTRAP and 34 V on the TSQ Vantage.

The TSQ Vantage facilitates the division of SRM scheduling windows into several segments in order to maximise the number of data points of each transition at FWHM. A segmented SRM scheduling scheme was implemented as outlined in Appendix Table 4.2 using the mean t_R of triplicate measurements of each peptide. All light TMT and heavy TMT transitions were combined to build the final method. Figure 4.8 displays the SRM XIC for heavy TMT-labeled internal standards (100 fmol o/c) spiked into light TMT-labeled plasma (30 µg o/c). Similar peptide t_R and relative intensities were observed for all target analytes on the TSQ Vantage as compared to the QTRAP. TMT-SRM quantitation was performed at unit resolution of 0.7 Da ± 0.1 amu FWHM for both Q1 and Q3, a scan time of 0.02 sec, a scan width of 0.02 Da, with a minimal SRM scheduling window of 1 min per peptide. This resulted in a maximal cycle time of 0.72 sec.

Protein	Peptide ID	Candidate peptide	Charge State (+)	Light TMT			Heavy TMT		
				Mr (Da)	Q1 (*m/z*)	Q3 (4) (*m/z*)	*Mr* (Da)	Q1 (*m/z*)	Q3 (4) (*m/z*)
A2M	14	AIGYLNTGYQR	2	1478.88	740.4	1014.6	1483.88	742.9	1019.6
	15	TGTHGLLVK	2	1372.84	687.4	791.5	1382.84	692.4	796.5
SAP	22	VGEYSLYIGR	2	1379.78	690.9	873.5	1384.78	693.4	878.5
ApoE	25	LQAEAFQAR	2	1256.74	629.4	920.5	1261.74	631.9	920.5
Gelsolin	29	TASDFITK	2	1329.8	665.9	746.4	1339.8	670.9	751.4
	30	AVEVLPK	2	1202.78	602.4	623.4	1212.78	607.4	628.4

Table 4.6 Additional transitions for the TMT-SRM quantitation of the AD candidate biomarker panel on the TSQ Vantage. In addition to the three transitions common to both instruments, an extra transition was utilised for peptides 14, 15, 22, 25, 29 and 30.

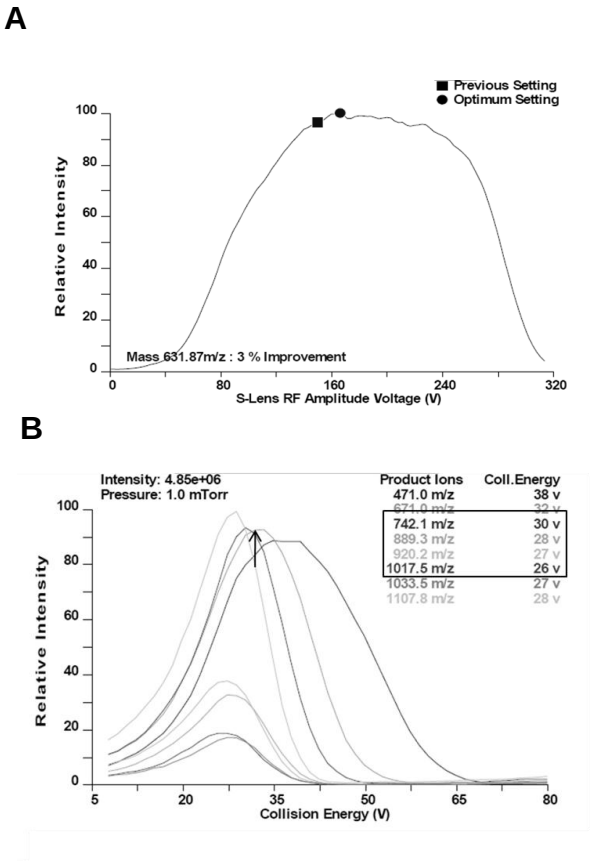

Figure 4.7 Optimisation of TSQ Vantage S-Lens and CE values. Optimal values for the S-Lens were those where the SRM voltage ramping trace was maximal (● in panel A). Similarly, optimal CE for a transition of peptide 25 is indicated by an arrow in panel B.

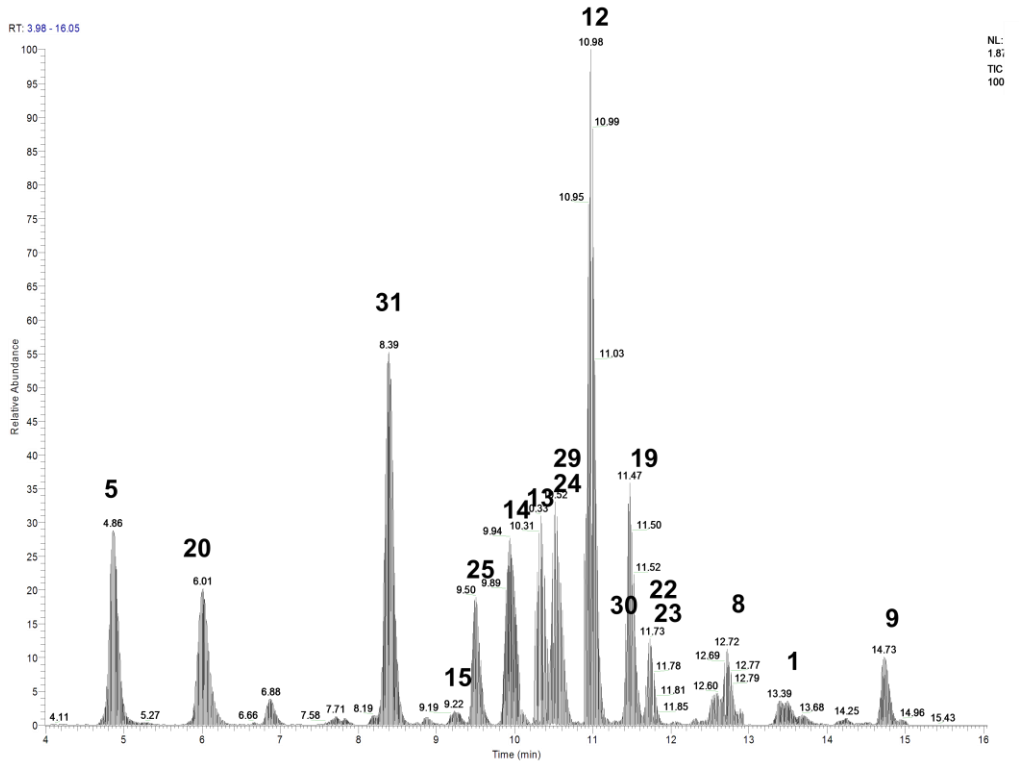

Figure 4.8 SRM XIC of the TMT-SRM method on the TSQ Vantage mass spectrometer. Light TMT-labeled plasma was spiked with heavy TMT-labeled peptides and analysed by TMT-SRM.

4.2.3.2 Performance characteristics of the multiplexed TMT-SRM assay on the TSQ Vantage

As with the QTRAP, 16-point reverse calibration curves were performed on the TSQ Vantage over three independent days. To demonstrate the agreement across mass spectrometer platforms, the calibration curves on the QTRAP and TSQ Vantage for three target analytes (peptides 1, 20 and 31) in the multiplexed TMT-SRM assay are displayed in Figure 4.9. All transitions of the same peptide plotted equivalent curves and corresponding curves on QTRAP and TSQ Vantage instruments were comparable. As with the QTRAP, the dynamic range of response was over three orders of magnitude with excellent linearity (R^2 > 0.99) on the TSQ Vantage. Using complement C3 peptide 8 as an example, an equivalent dynamic range was observed as on the QTRAP, where the dynamic range of the TMT-SRM assay was 2.31 – 2311.68 µg/mL, when taking the best transition as representative of this peptide (Table 4.7). This pattern was repeated for all peptides across the two LC-SRM platforms.

The calculated LODs and LOQs for target peptides on the TSQ Vantage are displayed in Table 4.7. In agreement with the QTRAP, peptide quantitation was observed at low ng/mL levels, *e.g.,* peptide 20. LODs on the TSQ Vantage ranged from 0.001 - 0.47 µg /mL for peptides and 0.07 - 57.70 µg/mL for proteins. LOQs ranged from 0.003 - 1.65 µg /mL for peptides and 0.11 - 202.02 µg/mL for proteins.

TMT-SRM assay performance characteristics varied greatly for several peptides between the QTRAP and TSQ Vantage instruments, *e.g.,* for peptide 9 and peptide 23 the truness (%CV) was much higher as measured on the TSQ compared to the QTRAP (39.4 and 41.4% on the TSQ and 1.6 and 9.1% on the QTRAP; Tables 4.5 and 4.7). Such species had robust TMT-SRM quantitation in the assay validation experiments, *i.e.,* followed the same trend as corresponding peptides within a protein, although these experiments were performed on the QTRAP only. Nevertheless, the peptides remained in the assay to allow for continued comparison of TMT-SRM quantitation between these peptides and those within the same protein.

Trueness and precision on the TSQ Vantage was determined as for the QTRAP using the 50 fmol QC measurements only (Section 4.2.2.2). Table 4.7 displays the accuracy for TSQ Vantage. Overall, the mean CV of trueness was 8.9% on the TSQ Vantage. The higher mean CV of trueness on the TSQ Vantage compared to the QTRAP was attributed to higher values for peptides 9 and 23. However, mean precision CV values on both instruments were considered favourable in the context of quantitative biomarker assays. When looking at precision, a mean CV of 6.1% was observed across all target analytes on the TSQ Vantage. In summary, the accuracy of the TMT-SRM assay on both LC-SRM platforms was comparable and the assay was considered fit-for-purpose assay.

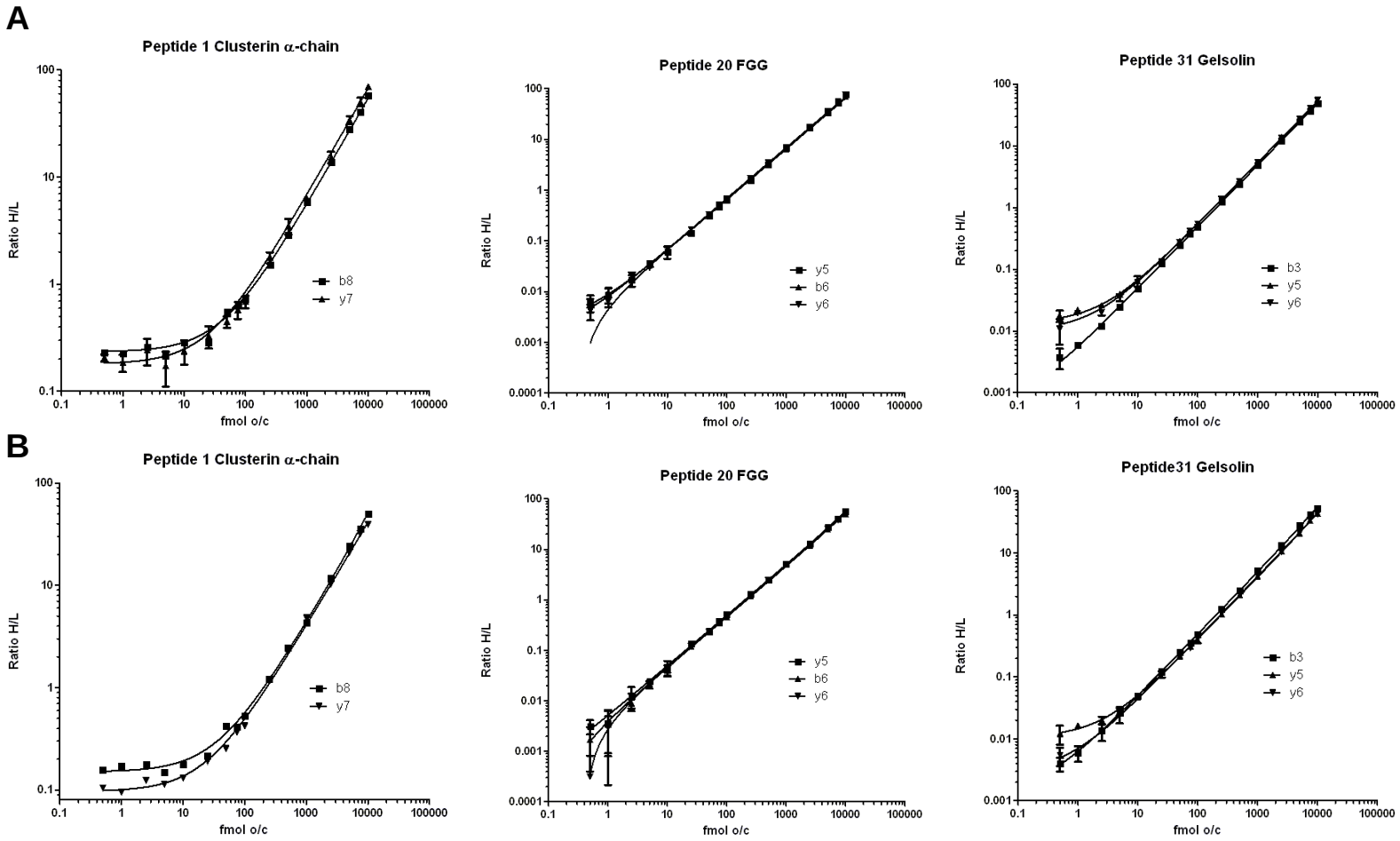

Figure 4.9 Calibration curves for peptides clusterin α-chain, FGG and gelsolin. **A** Calibration curves on the QTRAP. **B** Calibration curves on the TSQ Vantage. Curves were used to determine the TMT-SRM assay performance characterisitics for all target analytes in the method. Excellent agreement between calibration curves analysed on the two LC-SRM platforms was observed.

Protein	Peptide ID	Peptide *Mr* (Da)	Protein *Mr* (kDa)	LOD		LOQ		Lowest point of linearity		Upper point of linearity		Trueness %CV	Precision %CV
				Peptide	Protein	Peptide	Protein	Peptide	Protein	Peptide	Protein		
				(µg/mL)	(µg/mL)	(µg/mL)	(µg/mL)	(µg/mL)	(µg/mL)	(µg/mL)	(µg/mL)		
Clusterin α-chain	1	1116.7	50	0.045	2.04	0.163	7.30	0.070	3.13	13.96	625.58	7.9	2.1
Clusterin β-chain	5	778.5	50	0.003	0.22	0.011	0.68	0.002	0.13	9.73	625.58	2.2	4.2
Complement C3	8	1138.7	185	0.038	6.17	0.121	19.62	0.014	2.31	14.23	2311.68	2.6	16.5
	9	1510.9	185	0.471	57.70	1.650	202.02	0.472	57.79	18.89	2311.68	39.4	0.1
CFH	12	1062.8	137	0.007	0.84	0.021	2.72	0.001	0.17	13.28	1712.94	0.7	4.1
	13	643.5	137	0.005	1.14	0.016	3.42	0.004	0.86	8.04	1712.94	0.3	1.4
A2M	14	1254.7	161	0.003	0.34	0.008	1.09	0.008	1.00	15.68	2009.74	28.1	11.4
	15	924.5	161	0.016	2.77	0.046	7.98	0.012	2.01	11.56	2009.74	0.8	8.5
FGG	19	879.5	48	0.009	0.49	0.026	1.43	0.011	0.61	10.99	605.83	1.7	5.7
	20	714.5	48	0.001	0.07	0.003	0.18	0.002	0.15	8.93	605.83	2.5	2
SAP	22	1155.6	23	0.038	0.76	0.121	2.43	0.014	0.29	14.45	290.51	1.2	8.5
	23	1405.7	23	0.005	0.08	0.006	0.11	0.004	0.07	17.57	290.51	41.4	15.3
ApoE	24	967.5	34	0.003	0.09	0.008	0.29	0.006	0.21	12.09	427.74	6.8	2.3
	25	1032.6	34	0.003	0.11	0.010	0.34	0.006	0.21	12.91	427.74	1	1.1
Gelsolin	29	881.5	83	0.001	0.13	0.004	0.40	0.002	0.26	11.02	1036.79	7.7	16.4
	30	754.5	83	0.008	0.84	0.024	2.69	0.024	2.59	9.43	1036.79	2.8	1.3
	31	1274.8	83	0.002	0.12	0.006	0.40	0.001	0.05	15.93	1036.79	0.5	3

Table 4.7 Assay performance characteristics of the TMT-SRM method on the TSQ Vantage. For each target analyte, the LOD, LOQ, linearity and trueness and precision is displayed for comparison to the corresponding performance characteristics on the QTRAP (Table 4.5). Protein concentrations (in µg/mL) represent the amount of protein corresponding to a given spike amount of the peptide, assuming 100% recovery.

4.3 Summary

- The TMT-SRM assay was validated as fit-for-purpose for the measurement of signature peptides of candidate AD biomarkers in plasma. A strong correlation was observed between quantitation provided by TMT-SRM and an immuno-based approach for one of the candidate biomarkers, gelsolin, in AD and NDC samples (n = 10 per group).
- The TMT-SRM assay enabled quantitation of all target analytes in plasma, with all measurements within the linear range of quantitation for all peptides.
- Peptides of the same protein performed similarly by TMT-SRM in terms of expression. Equivalent fold changes were observed between AD and NDC groups for peptides of the same protein, demonstrating the robustness of the quantitative measurement.
- Target peptides for the measurement of SAP, ApoE and gelsolin gave equivalent absolute amounts by TMT-SRM. For all other proteins, differences were observed and attributed to differential tryptic digestion of each peptide and/or differential peptide losses during sample preparation.
- Equivalent TMT-SRM quantitation was provided by interpolation from reverse calibration curves and SRP calibration. Thus, in a further improvement to the assay, the more simplified SRP approach will be used in all future TMT-SRM analyses. This significantly reduces data analysis times, resulting in a higher throughput of samples.
- One technical digest is sufficient for each experimental sample in future TMT-SRM analyses. This results in a significant reduction in sample preparation times with the benefit of higher throughput.
- The determination of assay performance is essential to enable comparison to related biomarker quantitative technologies, *e.g.,* ELISA. A workflow was designed to determine the TMT-SRM assay performance for each target analyte in plasma in terms of linearity, accuracy and the LOD and LOQ.

- The TMT-SRM assay was portable across LC-SRM platforms. Here, the method was transferred to a TSQ Vantage triple quadrupole mass spectrometer. The fragmentation, t_R and relative intensities between target peptides were equivalent for all target analytes across MS platforms, demonstrating the robustness of the TMT-SRM assay. Further, equivalent assay performance characteristics were observed on both MS platforms with favorable statistics.

Chapter 5

Implementation of a multiplexed TMT-SRM assay for the validation of diagnostic and prognostic biomarkers of Alzheimer's disease

5.0 Introduction

Once the TMT-SRM assay was validated as fit-for-purpose using assay performance criteria for each target analyte in undepleted plasma, the assay was applied for the evaluation of the candidate AD biomarkers in a clinical cohort (*n* = 90). The primary goal of this chapter was to determine if the TMT-SRM assay could validate any of the candidate proteins as prognostic and/or diagnostic markers of AD. Several of the plasma proteins were shown in discovery studies to have utility in predicting the progression rate of AD. A prognostic biomarker of the disease would be extremely beneficial, potentially allowing for treatments at the earliest stages of the disease. Further, prognostic markers may facilitate the development of targeted drugs and enable the monitoring of their therapeutic actions. Specifically, plasma levels of gelsolin have been shown to be decreased in AD subjects as compared to NDC, with strong correlation to the rate of cognitive decline (Güntert *et al.,* 2010). Plasma clusterin was shown to be associated with the pathology, severity and progression rate of AD (Thambisetty *et al.,* 2010). However, the protein was not shown to have potential for AD diagnosis as no change in plasma clusterin levels was observed when directly comparing AD and NDC samples. Plasma concentrations of complement C3, CFH, A2M, FGG and SAP have all been shown to be elevated in AD (Tennent *et al.,* 1995; Hye *et al.,* 2006; Lee *et al.,* 2007; Maier *et al.,* 2008). Results for ApoE are conflicting; however the majority of studies find no changes in plasma concentrations of this protein in AD (Romas *et al.,* 1999; Scacchi *et al.,* 1999). It was hypothesised that these results may be validated using the novel, multiplexed TMT-SRM assay. TMT-SRM quantitation was performed on both QTRAP and TSQ Vantage instruments to confirm the findings between both. TMT-SRM quantitation was confirmed by WB for selected proteins.

5.1 Materials and Methods

5.1.1 Validation of Alzheimer's disease candidate biomarkers by TMT-SRM

5.1.1.1 Modification of the TMT-SRM purification protocol to increase sample throughput

To enable the analysis of a larger number of samples in an appropriate timescale required for biomarker validation and qualification studies, a modification to the TMT-SRM sample preparation workflow was assessed where the RP step of TMT-labeled peptide purification was removed. As the purification of TMT-labeled peptides has been thus far the most rate-limiting step in the overall workflow, such a simplification would be highly desirable. The purpose of RP in the standard protocol was to reduce the salt content of TMT-labeled peptide samples, thus maximising the efficiency of SCX purification for the removal of SDS and excess TMT-labeling reagents. It was hypothesised that removal of the RP step here may have negligible effects on TMT-SRM quantitation. A pooled plasma sample (600 µg) from the 20 AD and NDC subjects as described in Section 4.1.2, was reduced, alkylated, digested with trypsin and labeled with light TMT as described in Sections 2.1.1.2 to 2.1.1.3. The light TMT-labeled plasma digest was split into six aliquots of 100 µg. Three aliquots were purified using an SCX-only approach. Here, each aliquot was diluted with 3 mL RP elution buffer to maintain the conditions of the standard protocol prior to SCX purification. Peptides were then purified using the standard SCX protocol as described in Section 2.1.1.4. As a control experiment, the remaining three aliquots of light TMT-labeled plasma peptide digest underwent individual RP and SCX purification procedures using the standard protocol. All samples were aliquoted into a microtitre plate (60 µL per sample; 30 µg per well) and underwent two stages of lyophilisation as described in Section 4.1.1.2. TMT-SRM quantitation was performed for each of the 17 peptides in the TMT-SRM method on the TSQ Vantage, with each light TMT-labeled plasma sample referenced against heavy TMT-labeled synthetic peptides (100 fmol

o/c). In the first instance, the detection and relative levels of all target analytes by SRM upon purification by the SCX-only and standard RP + SCX purification strategies was assessed. Comparison between the two approaches was performed using the mean L/H ratios of a subset of peptides, selected to incorporate a range of t_R over the course of the LC gradient (peptides 1, 5, 12, 14, 15, 22, 23 and 25). Due to pseudo-replication (*i.e.,* multiple replicates of each purification protocol), the experimental design was hierarchical to maintain the appropriate degrees of freedom, with peptide nested within protocol. Two-way ANOVA was used to separate and estimate the different sources of variation, which were combined to give an estimate of the variance of the mean. All data analysis was performed in SPSS as described in Section 4.1.1.8.

5.1.1.2 Selection of a large cohort of subjects from multi-centre sites for validation of the candidate Alzheimer's disease biomarkers

Samples were collected from a European-wide population of subjects with AD and aged people (AddNeuroMed cohort; Lovestone *et al.,* 2009). Samples were selected from six centres across Europe located in London (UK), Toulouse (France), Kuopio (Finland), Perugia (Italy), Thessaloniki (Greece) and Lodz (Poland). Ethical approval was obtained in each of the participating countries. All subjects were assessed at baseline and every three months thereafter for one year (five visits in total) by cognitive measures including MMSE, ADAS-cog and the Clinical Dementia Rating scale. Blood from each subject at each time point was collected in EDTA coated tubes, processed for the extraction of plasma as described in Section 4.1.1.1, aliquoted and stored at -80 ^{o}C according to standardised protocols. To determine the minimum sample size required for the cohort selected here-in, an *a priori* power analysis (Shappiro-Wilks method) was performed in G*Power using the mean amounts of each target analyte between AD and NDC groups as described in Section 4.2.1 (Appendix Table 5.1; Faul *et al.,* 2007). A total of 90 subjects at baseline were selected for TMT-SRM analysis (60 AD and 30 NDC subjects). To determine if any of the candidate biomarkers could predict the progression rate of the disease, within the AD group,

samples were sub-divided into rapid cognitive decliner (RCD) and slow cognitive decliner (SCD) groups based on MMSE decline per year. RCD, SCD and NDC groups (*n* = 30 per group) were matched for age and sex.

5.1.1.3 Implementation of the TMT-SRM assay on the QTRAP for the validation of the Alzheimer's disease candidate biomarkers

An aliquot of each plasma sample was removed from the freezer and brought to RT. An equal volume (25 µL) from each aliquot was diluted 10-fold with H_2O. As described in Section 4.1.2, this strategy was in-line with the biomarker discovery studies where an equal volume of each sample as opposed to an equal protein amount was used for comparison (Hye *et al.,* 2006; Güntert *et al.,* 2010). From this, 12.5 µL was removed, providing approximately 100 µg of protein per digest. Plasma samples were reduced, alkylated, digested with trypsin and light TMT-labeled (Sections 2.1.1.2 and 2.1.1.3) and then SCX-purified as described in Section 5.1.1.1. Each experimental plasma sample was resuspended in 25% ACN, 0.1% FA and aliquoted in triplicate across three microtitre plates (30 µg per well) as described in Section 4.1.1.2. This gave a total of 90 samples per plate with one plate for TMT-SRM analysis on the QTRAP, one for the TSQ Vantage and a 'spare' microtitre plate if a repeat analysis of any sample was needed on either instrument. To allow for instrument performance checks, a pool of all samples (2 mg total protein) was digested, TMT-labeled and SCX purified using the up-scaled procedures as described in Section 3.1.7. Purified peptides of the pooled sample were aliquoted on a separate microtitre plate. All microtitre plates were lyophilised to dryness and stored at -80 °C. Immediately prior to analysis, samples were resuspended in 25 µL of a 5 fmol/µL solution of heavy TMT-labeled peptide internal standards, providing 100 fmol of each o/c. TMT-SRM analysis was performed on the QTRAP as described in Section 3.1.6. One analytical repeat of each sample was acquired with RCD, SCD and NDC groups randomised to exclude run-time and run order bias. The plasma pool was acquired every 15 samples to ensure LC-SRM performance was maintained over the course of the sample set. SRMs were

processed and peak areas extracted using Analyst's quantitation wizard as described in Section 2.1.1.9.

5.1.1.4 Implementation of the TMT-SRM assay on the TSQ Vantage

TMT-SRM analysis was performed on the TSQ Vantage as described in Section 4.1.7. Mirroring the TMT-SRM analysis on the QTRAP, one analytical repeat was acquired for each sample in a randomised run order (the same order as that on the QTRAP) and the plasma pool acquired every 15 samples to ensure consistent LC-SRM performance. To minimise the variation in TMT-SRM quantitation between the QTRAP and TSQ Vantage, the same heavy TMT-labeled peptide solution was used for internal standardisation on both instruments. SRMs were processed and peak areas extracted using Pinpoint software as described in Section 4.1.9.

5.1.1.5 Data Analysis for candidate biomarker validation

SRP calibration was performed by calculating the L/H ratio for individual transitions of each peptide in each sample. Two-way ANOVA was used to separate and estimate the different sources of variation and these were then recombined to give an estimate of the variance of the mean. Appendix Figure 5.1 displays the syntax script used to perform the statistical analysis in SPSS. The grand mean concentration calculated from all transitions of each sample was calculated for each peptide in RCD, SCD and NDC groups. Error bars were plotted using the 95% CI associated with each mean value. For biomarkers of AD prognosis, the mean concentration was used to directly compare the difference in plasma protein levels between RCD, SCD and NDC groups. For biomarkers of AD diagnosis, a direct comparison was performed between AD and NDC groups. All measurements from the RCD and SCD groups were combined into a single AD group and compared to NDC. A student's t-test was calculated to determine if the difference in the mean concentrations between RCD, SCD and NDC or AD and NDC groups was statistically significant.

5.1.2 Validation of TMT-SRM results

5.1.2.1 Western blotting of A2M and gelsolin

For confirmation of TMT-SRM results, WB analysis was performed for A2M and gelsolin on the same cohort of 90 AD and NDC subjects. Plasma samples (3 µL) were diluted in 97 µL phosphate buffered saline (PBS) containing protease inhibitor cocktail (Complete®, Roche) and 100 µL of 2x Laemmli buffer (Sigma-Aldrich), heated to 100 °C for 5 min and clarified at 15,500 *g*. Plasma proteins were separated for 45 min by one-dimensional SDS polyacrylmide gel electrophoresis on 26 well NuPAGE® Novex 4 - 12% Bis-Tris Midi Gels, (Invitrogen Ltd., Paisley, UK) using the NuPAGE® Electrophoresis System (Invitrogen). All samples were equally loaded (10 µL). To account for intra-gel variability, samples were run in duplicate across eight gels and standardised against a pool of all 90 samples (as prepared in Section 5.1.1.3) which was run in duplicate on each gel. Separated proteins were transferred to 0.2 µm nitrocellulose membranes (Schleicher & Schuell, NH, USA). Wet transfer was at 80 V for 1 hr at RT. The success of transfer was determined by visualising the membrane-bound proteins with Ponceau S solution for 1 min. Ponceau S was removed by two washes of H_2O for 5 min. A2M and gelsolin analyses were performed on the same blot. Blots were blocked for 2 h with 5% non-fat milk in 0.1% PBS-Tween (PBS-T) and probed with antibodies to A2M (diluted 1:5,000, goat monoclonal, M5649, Sigma-Aldrich) and gelsolin (diluted 1:500, mouse monoclonal, ab55070, Abcam plc, Cambridge, UK) for 16 h at 4 °C. Excess primary antibodies were removed with three washes of PBS-T for 5 min. A2M primary antibodies were incubated for 1 h with rabbit anti-goat secondary antibodies (diluted 1:5,000). Similarly, gelsolin primary antibodies were incubated for 1 h with donkey anti-mouse secondary antibodies (diluted 1:10,000). All dilutions of both primary and secondary antibodies were previously optimised by Andreas Güntert and Mirsada Causevic at the MRC Centre for Neurodegeneration Research, King's College London. Excess secondary antibodies were removed with three washes of PBS-T for 5 min. Secondary antibodies were

conjugated to fluorophors, emitting at wavelengths of either 680 or 800 nm, using a near infrared Odyssey imager (Licor, Lincoln, NE, USA). Densitometric analysis was performed using the Odyssey software v2.1.

5.1.2.2 Data analysis of WB

The ODs of each sample were standardised against the mean OD of the pooled plasma sample separated on the same gel. Duplicate measurements for each of the 90 samples were averaged and the mean value was used to directly compare the difference in plasma A2M and gelsolin levels between RCD, SCD and NDC groups. A student's t-test was calculated to determine if the difference in the mean ODs between groups was statistically significant as described in Section 5.1.1.5. In accordance with the TMT-SRM analysis of the cohort, a single AD group of combined RCD and SCD groups was also compared to NDCs. Furthermore, the precision of WB quantitation between replicate blots was assessed. Pearson correlation coefficients were calculated to determine the agreement between the TMT-SRM measurement of each A2M and gelsolin peptide across experimental samples and the corresponding WB measurement.

5.2 Results

5.2.1 Validation of AD candidate biomarkers by TMT-SRM

5.2.1.1 Modified purification strategy for higher throughput of TMT-labeled plasma samples

In each of the experiments described so far, the purification of TMT-labeled peptides for TMT-SRM quantitation incorporated both RP and SCX purification. Here, both were performed separately and on each sample. This resulted in sample preparation timescales which were unfavourable for the high throughput analyses required for biomarker validation across large numbers of samples. In response to this and to decrease peptide purification times by approximately half, an experiment was designed to assess the TMT-SRM quantitation of light TMT-labeled plasma peptides purified by SCX only. Using aliquots of the same plasma digest, light TMT-labeled peptides were purified by SCX-only and as a control, the standard protocol of RP and SCX. All peptides were detected by SRM at equivalent relative intensities in those samples purified by SCX-only and by RP followed by SCX. A comparison was made by analysing the variance in the TMT-SRM quantitation of a subset of peptides across all replicate measurements between each purification strategy. There was no significant difference in the L/H ratios when directly comparing the same peptide between the two strategies and a very strong correlation was observed when comparing all measurements (p = 0.9). Further, the effect of RP removal was similar for peptides of varying t_R. As there was no difference to the TMT-SRM quantitation of peptides purified by SCX-only, this strategy was used to purify the light TMT-labeled plasmas of the 90 AD and NDC subjects, resulting in significantly reduced sample preparation times.

5.2.1.2 Sample selection and classification into RCD, SCD and NDC groups

A total of 90 subjects were selected for validation of the AD candidate biomarkers. This comprised 60 AD subjects and 30 NDC subjects. Samples were selected at baseline to determine which proteins tracked with decline in cognitive

ability. Here, the AD group was further divided into RCD and SCD groups depending on MMSE decline per year (Table 5.1; Appendix Table 5.2). MMSE testing is used by clinicians to estimate the degree of cognitive impairment in an individual at a given point in time or to follow the decline in cognitive ability over time (Folstein *et al.,* 1975). The RCD group had an MMSE decline of > 2 points per year over the three to five years of follow-up data available (median of 3.8 points). The SCD group had an MMSE decline of 0 - 2 points per year (median of 0.8 points). There was no change in MMSE scores per year within the NDC group. RCD, SCD and NDC groups were age and sex-matched, with a higher representation of females to males. Furthermore, a higher proportion of APOE ε4 carriers were observed in RCD and SCD groups, as compared to NDC (Table 5.1).

	RCD	SCD	NDC
Number	30	30	30
Mean Age (yrs)	75.2	75.2	73.2
% Female	77	73	73
% APOE ε4/'	50	60	29
% APOE ε4/4	13	20	3
Mean MMSE decline per year (median)	3.8	0.8	0

Table 5.1 Subject characteristics of RCD, SCD and NDC groups. All subjects were age and sex-matched. Subjects were either heterozygous (ε4/') or homozygous (ε4/4) for the APOE e4 allelle. RCD, SCD and NDC groups were separated according to MMSE decline per year.

5.2.1.3 TMT-SRM analysis of RCD, SCD and NDC on the QTRAP

Using the higher throughput, multiplexed TMT-SRM assay, the quantitation of eight candidate biomarkers of AD in a clinical sample cohort of RCD, SCD and NDC subjects (n = 30 per group) was performed. For two of the peptides (5 and 20), variable t_R combined with a narrow SRM scheduling window resulted in a failure to capture a complete SRM peak in 25 of the samples. A repeat analysis was performed in such cases, ensuring a complete dataset. Absolute amounts of endogenous signature peptides were determined using the SRP approach. To visualise the data and allow for ease of comparison between groups, bar charts were plotted, comparing the mean absolute amount of each peptide across RCD, SCD and NDC groups (Figure 5.1).

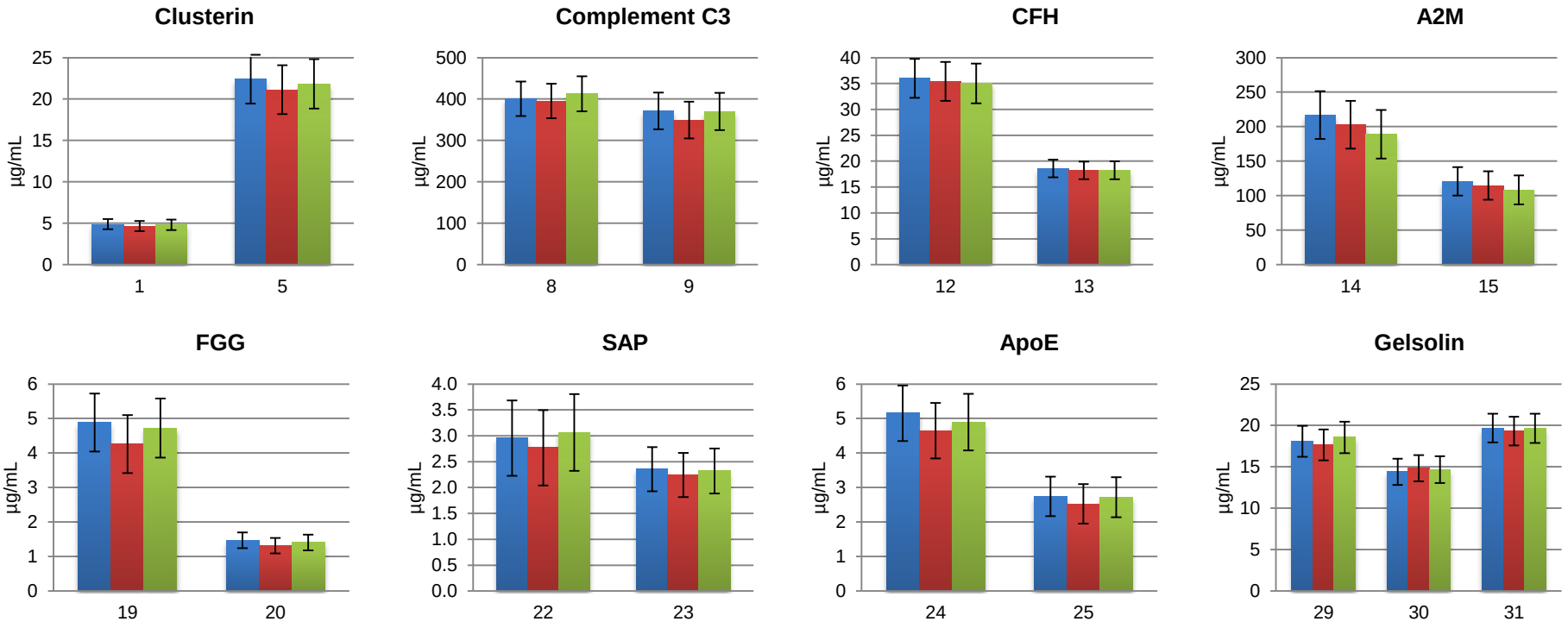

Figure 5.1 Bar charts displaying the difference between RCD, SCD and NDC for all peptides in the multiplexed TMT-SRM assay. Peptides of the same protein are plotted on the same graph. The RCD group is displayed in blue, SCD in red and NDC in green. Error bars indicate the 95% CI.

Generally, patterns of TMT-SRM quantitation and fold changes between RCD, SCD and NDC groups were similar for peptides of the same protein (Figure 5.1, Table 5.2). Further, the endogenous plasma concentrations of each targeted peptide were in the same range as those in the assay validation experiments described in Section 4.2.2. For example, peptide 5 had mean concentrations of 24.5 µg/mL and 21.8 µg/mL in the NDC grouping across the TMT-SRM assay validation and biomarker validation cohorts, respectively. This was very encouraging as it demonstrated the robustness of the TMT-SRM workflow across different sample sets. This was essential as ultimately if the assay is to have widespread implementation in independant laboratories, target analyte concentrations should be generally consistent across cohorts. The result confirmed the suitability of the TMT-SRM assay to quantitate the AD candidate biomarkers in independant studies.

5.2.1.4 A2M is increased predicts the rate of cognitive decline in Alzheimer's disease

Both A2M peptides quantitated by the TMT-SRM assay (peptides 14 and 15) performed congruently, showing a statistically significant difference (p = 0.0146 and 0.0293, respectively) between RCD, SCD and NDC subjects (Table 5.2). The observed difference tracked with AD progression, *i.e.,* A2M concentrations increased as the rate of cognitive decline increased. A small but statistically significant negative correlation was observed between A2M concentrations and MMSE decline per year, *i.e.,* an increase in A2M concentration correlated with a decline in MMSE score.

A statistically significant difference (p = 0.0173) was observed between RCD, SCD and NDC groups for FGG peptide 20. However, this result was not given much importance as it was primarily based on the difference between RCD and SCD groupings, which flanked the mean concentration of the NDC group, *i.e.,* a consistent increase or decrease for the peptide was not observed across the three groups (Table 5.2). Further, the statistical result was not in-line with the second FGG peptide in the assay, peptide 19 and thus, confirmation of its validity was not possible. All other

Protein	Theoretical amounts in plasma (µg/mL)	Mean RCD (µg/mL)	Mean SCD (µg/mL)	Mean NDC (µg/mL)	Fold change			*p*-value
					RCD v SCD	RCD v NDC	SCD v NDC	
Clusterin α-chain	35 - 105	4.9	4.7	4.8	1.04	1.02	0.98	0.8971
Clusterin β-chain		22.4	21.1	21.8	1.06	1.03	0.97	0.473
Complement C3	670 - 1290	400.4	395.3	412.6	1.01	0.97	0.96	0.9278
		371.2	349.3	369.9	1.06	1.00	0.94	0.5542
CFH	400 - 800	36.0	35.4	35.0	1.02	1.03	1.01	0.9428
		18.6	18.2	18.2	1.02	1.02	1.00	0.7481
A2M	2000 - 2400	216.7	203.0	189.1	1.07	1.15	1.07	0.0146
		120.8	114.8	108.4	1.05	1.11	1.06	0.0293
FGG	80 - 500	4.9	4.3	4.7	1.14	1.04	0.91	0.1643
		1.5	1.3	1.4	1.15	1.07	0.93	0.0173
SAP	21 – 44	3.0	2.8	3.1	1.07	0.97	0.9	0.145
		2.4	2.2	2.3	1.09	1.04	0.96	0.9567
ApoE	34 - 74	5.2	4.6	4.9	1.13	1.06	0.94	0.1488
		2.7	2.5	2.7	1.08	1.00	0.93	0.402
Gelsolin	179 - 200	18.1	17.6	18.6	1.03	0.97	0.95	0.7005
		14.4	14.8	14.7	0.97	0.98	1.01	0.8382
		19.7	19.3	19.6	1.02	1.01	0.98	0.9027

Table 5.2 Plasma amounts (µg/mL) of each peptide in RCD, SCD and NDC groups as determined by the multiplexed TMT-SRM assay on the QTRAP. For each peptide, the protein from which it is derived is indicated along with biomarker discovery results. It can be seen that peptides of A2M showed a statistically significant ($p < 0.05$) difference between RCD, SCD and NDC groups.

peptides included in the TMT-SRM assay showed no significant differences between RCD, SCD and NDC groups.

Baseline plasma samples were selected for analysis in this study to evaluate the potential of each candidate biomarker as a prognostic marker of AD. In addition to this, the diagnostic utility of each could be determined, even though this may be weak in the chosen cohort, *i.e*, samples were taken at baseline, rather than taken later in the pathology of the disease, where differences between groups are likely to be greater. Nevertheless, to determine if any of the target analytes had utility as a diagnositic biomarker of AD, both RCD and SCD groups were combined to create one AD group. This was used to directly compare disease and control groups (Figure 5.2). Both A2M peptides showed a statistically significant increase in AD (Table 5.3), validating the original discovery study where an increased plasma A2M levels were observed in AD subjects as compared to NDC (Hye *et al.,* 2006). All other peptides showed no statistically significant difference between AD and NDC groups. For clusterin and ApoE, this was in-line with discovery, where no differential expression was observed for these proteins between AD and NDC groups (Scacchi *et al.,* 1999; Thambisetty *et al.,* 2010).

5.2.1.5 TMT-SRM analysis on the TSQ Vantage

TMT-SRM quantitation of the experimental sample cohort was replicated on the TSQ Vantage to validate the results on the QTRAP and to confirm the portability of the assay across different MS platforms. In accordance with the QTRAP results, peptides of the same protein had equivalent patterns of expression between RCD, SCD and NDC groups (Table 5.4). The endogenous plasma amounts of each peptide were highly comparable to TMT-SRM on the QTRAP in the majority of cases. However, deviations did occur with, peptides 9, 24 and 25 being ~ 40% lower on the TSQ Vantage. Indeed, as determined in Chapter 4, peptide 9 had poorer trueness on the TSQ Vantage compared to the QTRAP (39.4% compared to 1.6%, Tables 4.5 and 4.7)

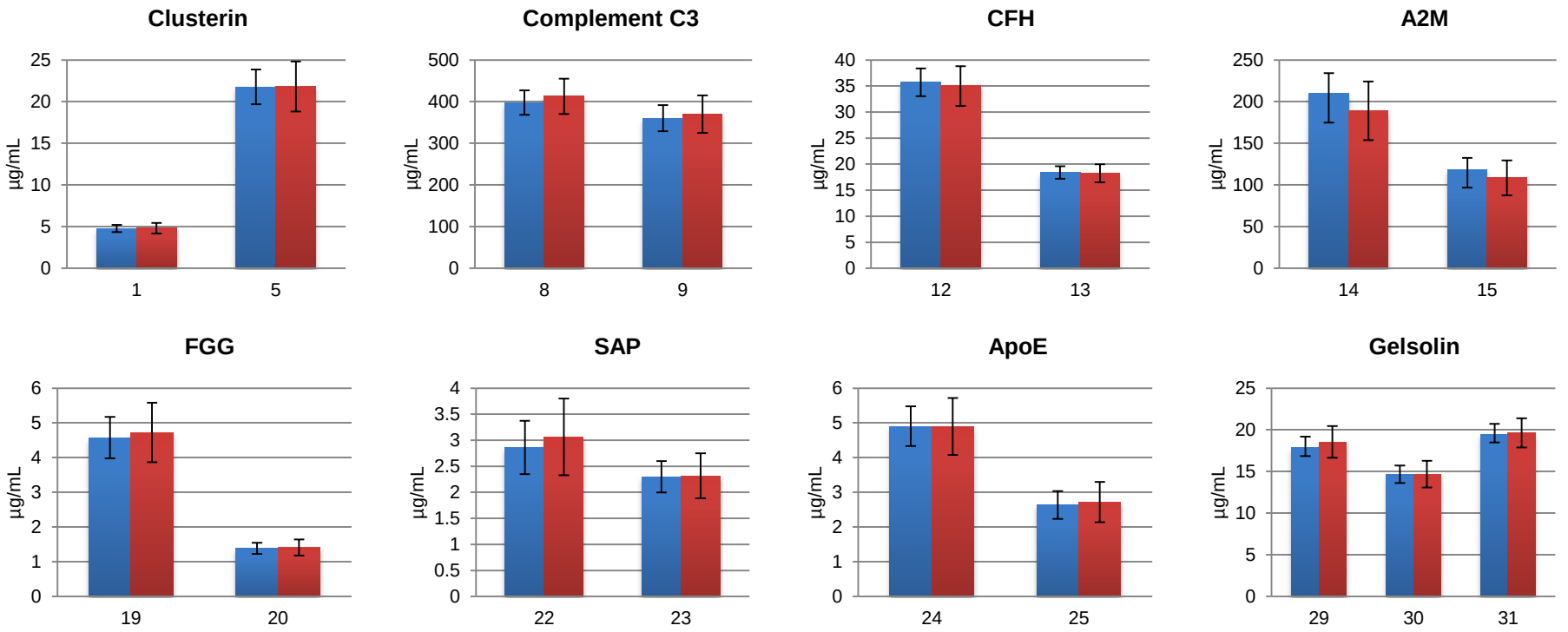

Figure 5.2 Bar charts displaying the difference between AD and NDC for all peptides of each candidate AD biomarker. Peptides of the same protein are plotted on the same graph. Error bars indicate the 95% CI.

Protein	Peptide ID	Mean AD (µg/mL)	Mean NDC (µg/mL)	Fold change AD v NDC	Discovery	Validation TMT-SRM	*p*-value
Clusterin α-chain	1	4.8	4.8	0.99	NSD	NSD	0.9368
Clusterin β-chain	5	21.8	21.8	1.00	NSD	NSD	0.9550
Complement C3	8	397.9	412.6	0.96	↑AD	NSD	0.7623
	9	360.3	369.9	0.97	↑AD	NSD	0.6885
CFH	12	35.7	35.0	1.02	↑AD	NSD	0.8281
	13	18.4	18.2	1.01	↑AD	NSD	0.7757
A2M	14	209.8	189.1	1.11	↑AD	↑AD	0.0069
	15	117.8	108.4	1.09	↑AD	↑AD	0.0434
FGG	19	4.6	4.7	0.97	↑AD	NSD	0.6342
	20	1.4	1.4	0.99	↑AD	NSD	0.6641
SAP	22	2.9	3.1	0.93	↑AD	NSD	0.7720
	23	2.3	2.3	0.99	↑AD	NSD	0.9658
ApoE	24	4.9	4.9	1.00	NSD	NSD	0.9781
	25	2.6	2.7	0.97	NSD	NSD	0.6416
Gelsolin	29	17.9	18.6	0.96	↓AD	NSD	0.5401
	30	14.6	14.7	1.00	↓AD	NSD	0.9388
	31	19.5	19.6	0.99	↓AD	NSD	0.8715

Table 5.3 Plasma amounts (µg/mL) of each peptide in AD and NDC samples as determined by the multiplexed TMT-SRM assay on the QTRAP. It can be seen that peptides of A2M showed a statistically significant ($p < 0.05$) difference between AD and NDC groups, which was expected based on the previous results. For the remainder of the peptides, no significant difference (NSD) was observed. Results are in agreement with the RCD, SCD and NDC comparison.

Protein	Peptide ID	Mean RCD (µg/mL)	Mean SCD (µg/mL)	Mean NDC (µg/mL)	Fold change			*p*-value
					RCD v SCD	RCD v NDC	SCD v NDC	
Clusterin α-chain	1	3.7	3.5	3.7	1.06	1.00	0.95	0.997
Clusterin β-chain	5	21.5	21	21.6	1.02	1.00	0.97	0.781
Complement C3	8	377	365	401.7	1.03	0.94	0.91	0.878
	9	220.6	214.6	219.2	1.03	1.01	0.98	0.996
CFH	12	31.7	31	30.7	1.02	1.03	1.01	0.836
	13	19.1	18.8	18.9	1.02	1.01	0.99	0.881
A2M	14	224.2	211.6	194.2	1.06	1.15	1.09	0.006
	15	142	130.4	124.1	1.09	1.14	1.05	0.031
FGG	19	4.1	3.6	4.0	1.14	1.03	0.90	0.044
	20	1.3	1.2	1.2	1.08	1.08	1.00	0.451
SAP	22	3.1	2.8	3.0	1.11	1.03	0.93	0.243
	23	2.1	1.9	2.2	1.11	0.95	0.86	0.152
ApoE	24	3.1	2.9	3.1	1.07	1.00	0.94	0.988
	25	4.8	4.3	4.6	1.12	1.04	0.93	0.416
Gelsolin	29	17.4	16.8	17.0	1.04	1.02	0.99	0.538
	30	16.2	16.4	16.1	0.99	1.01	1.02	0.955
	31	20.6	20.1	20.2	1.02	1.02	1.00	0.863

Table 5.4 Absolute amounts for each candidate biomarker peptide in RCD, SCD and NDC groups by TMT-SRM on the TSQ Vantage. For each peptide, the protein from which it is derived is indicated along with biomarker discovery results. It can be seen that peptides of A2M showed a statistically significant ($p < 0.05$) difference between RCD, SCD and NDC groups.

and reduced SRM sensitivities for this peptide on the TSQ Vantage may account for this. However, the performance of peptides 24 and 25 was comparable across LC-SRM platforms, despite differences in absolute amounts.

When comparing RCD, SCD and NDC groups for A2M on the TSQ Vantage, a statistically significant increase was observed for peptides 14 and 15 across the three groups and this difference tracked with disease progression (Table 5.4). This was in agreement with the finding on the QTRAP (Figure 5.3, Table 5.5). A statistically significant difference (p = 0.0440) was observed between RCD, SCD and NDC groups for FGG peptide 19. However, as for FGG peptide 20 on the QTRAP, a consistent increase or decrease for the peptide was not observed across the three groups (Table 5.2). Further, the statistical result was not in-line with the second FGG peptide, in this case, peptide 20 and thus, confirmation of its validity was not possible. For the remaining peptides in the assay, no significant differences were observed between RCD, SCD and NDC groups, which is in-line with the previous finding on the QTRAP.

When comparing TMT-SRM quantitation of a single AD group against NDC on the TSQ Vantage, excellent agreement was observed with the results on the QTRAP (Table 5.3; Table 5.6). Both A2M peptides demonstrated a statistically significant increase in AD, confirming the protein as a diagnostic biomarker of AD in plasma. Gelsolin peptide 29 had a statistically significant decrease in AD (p = 0.0200). However, this was not in-line with the other gelsolin peptides in the assay or the TMT-SRM results from the QTRAP. Thus, confirmation of the validity of this result was not possible. The remaining peptides in the TMT-SRM assay had no statistically significant differences between AD and NDC groups.

Equivalent TMT-SRM measurements between instruments were visualised and the agreement between all measurements on the two instruments assessed (Bland and Altman, 1986). The difference between the equivalent samples on each instrument was plotted against the mean of both. This is displayed in Figure 5.4 where different peptides are coloured separately and individual samples represented by a single dot.

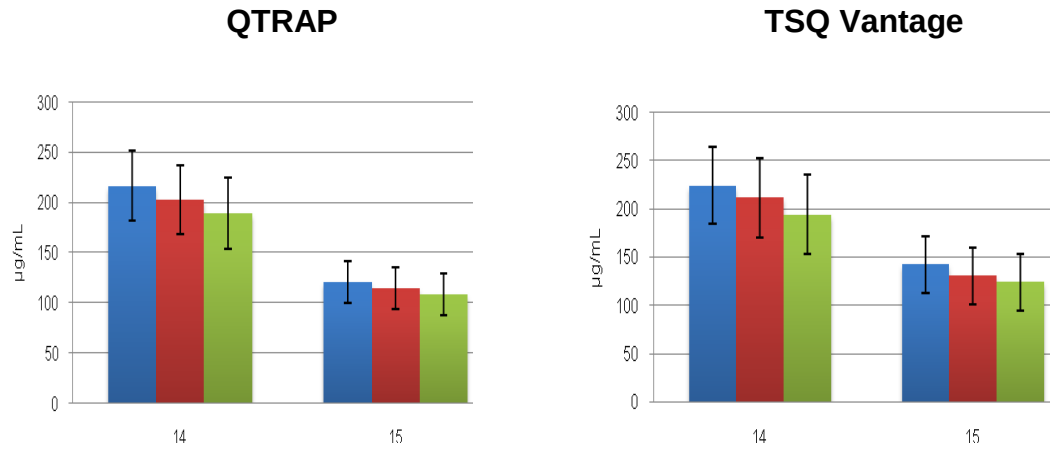

Figure 5.3 Expression of A2M between RCD, SCD and NDC on the QTRAP and TSQ Vantage. Equivalent patterns of expression were observed for both A2M peptides (14 and 15) between RCD (blue), SCD (red) and NDC (green) groups across MS platforms. Data extracted from Tables 5.2 and 5.4.

Instrument	Peptide ID	Mean RCD (µg/mL)	Mean SCD (µg/mL)	Mean NDC (µg/mL)	Fold change			*p*-value
					RCD v SCD	RCD v NDC	SCD v NDC	
QTRAP	14	216.7	203.0	189.1	1.07	1.15	1.07	0.0146
TSQ		224.2	211.6	194.2	1.06	1.15	1.09	0.0060
QTRAP	15	120.8	114.8	108.4	1.05	1.11	1.06	0.0293
TSQ		142.0	130.4	124.1	1.09	1.14	1.05	0.0316

Table 5.5 Absolute amounts of A2M on the QTRAP and TSQ Vantage. A statistically significant ($p < 0.05$) difference was observed between RCD, SCD and NDC groups for peptides 14 and 15 on the QTRAP and TSQ Vantage.

Excellent agreement was observed between corresponding TMT-SRM measurements on both instruments as the majority of measurements cluster around the mean and are within 2 SD of the mean. An example of this agreement is demonstrated by the CFH peptide 12 and A2M peptide 14 (blue and purple in the centre of the plot), which are clustered tightly around the mean. Several peptides show greater variation across the two instruments (*e.g.,* peptide 1, coloured pink). However, as this was the only signature peptide remaining for clusterin α-chain, its continued inclusion in the assay was essential.

Protein	Peptide ID	Mean AD (µg/mL)	Mean NDC (µg/mL)	Fold change AD v NDC	Discovery	Validation TMT-SRM	*p*-value
Clusterin α-chain	1	3.6	3.7	0.98	NSD	NSD	0.9810
Clusterin β-chain	5	21.3	21.6	0.98	NSD	NSD	0.6920
Complement C3	8	371.1	401.7	0.92	↑AD	NSD	0.6920
	9	217.7	219.2	0.99	↑AD	NSD	0.9840
CFH	12	31.3	30.7	1.02	↑AD	NSD	0.7300
	13	19.0	18.9	1.00	↑AD	NSD	0.9910
A2M	14	218.0	194.2	1.12	↑AD	↑AD	0.0001
	15	136.3	124.1	1.10	↑AD	↑AD	0.0327
FGG	19	3.8	4.0	0.95	↑AD	NSD	0.3570
	20	1.3	1.2	1.01	↑AD	NSD	0.9070
SAP	22	3.0	3.1	0.95	↑AD	NSD	0.4510
	23	2.0	2.2	0.90	↑AD	NSD	0.0680
ApoE	24	3.1	3.2	0.99	NSD	NSD	0.9250
	25	4.6	4.6	0.99	NSD	NSD	0.9250
Gelsolin	29	17.1	17.9	0.96	↓AD	↓AD	0.0200
	30	16.2	17.0	0.95	↓AD	NSD	0.1210
	31	20.4	20.2	1.01	↓AD	NSD	0.8560

Table 5.6 Absolute amounts for each candidate biomarker peptide in AD and NDC groups by TMT-SRM on the TSQ Vantage. It can be seen that peptides of A2M showed a statistically significant ($p < 0.05$) difference between AD and NDC groups.

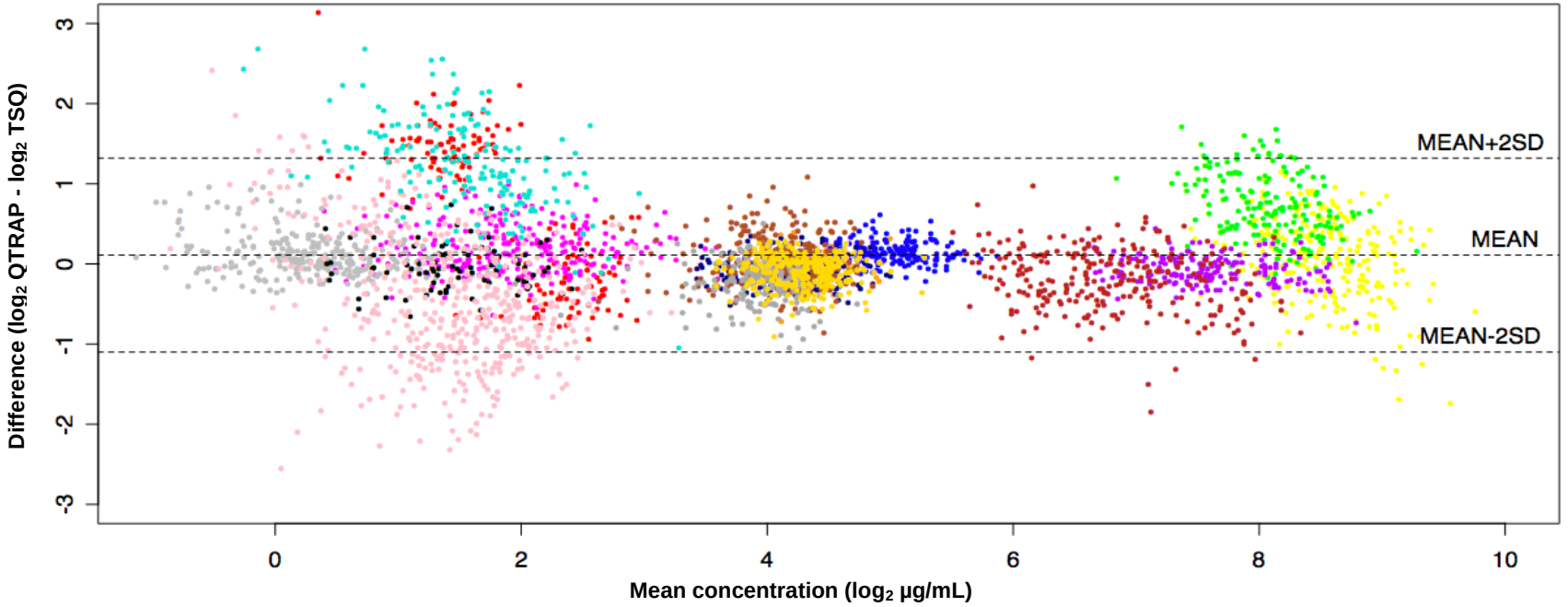

Figure 5.4 Comparison of all TMT-SRM measurements on the QTRAP and TSQ Vantage. The difference between the equivalent samples on each instrument was plotted against the mean of both. All data was log_2 transformed. The mean and mean +/- 2 SD are plotted with dashed lines. Each point represents an individual sample. Points are coloured according to the peptides they represent. A2M peptides are coloured purple (peptide 14) and brown (peptide 15) and are plotted in the centre of the figure, indicating excellent agreement across MS platforms.

Peptide 1 = dark cyan
Peptide 5 = black
Peptide 8 = light yellow
Peptide 9 = green
Peptide 12 = dark yellow
Peptide 13 = dark grey
Peptide 14 = purple
Peptide 15 = brown
Peptide 19 = light cyan
Ppetide 20 = dark red
Peptide 22 = light grey
Peptide 23 = light pink
Peptide 24 = magenta
Peptide 25 = light red
Peptide 29 = dark blue
Peptide 30 = dark brown
Peptide 31 = light blue

5.2.2 Validation of TMT-SRM results

5.2.2.1 Western blotting of A2M and gelsolin

To confirm the findings of the mass spectrometry-based TMT-SRM assay, quantitation of A2M and gelsolin levels was performed on the sample cohort using the standard immuno-based technique of WB. A2M was selected as it was the only protein found to be significantly changing between AD and NDC groups by TMT-SRM. Gelsolin was selected as a decrease was observed for the protein across RCD, SCD and NDC groups in discovery studies which predicted the rate of cognitive decline (Güntert *et al.,* 2010). Further, it was hypothesised that if no significant differences were observed for gelsolin by WB, this would confirm the findings for all target analytes which showed no differential expression by TMT-SRM. SDS-PAGE separation and immuno-based detection of A2M and gelsolin is displayed in Figure 5.5 A. For both A2M and gelsolin, no statistically significant difference was observed between RCD, SCD and NDC groups (Figure 5.5 B and C). The gelsolin result confirms the validity of the TMT-SRM result for each peptide where no significant differential expression was observed between the three groups in the cohort utilised here. This is not in-line with discovery studies for the protein, where a statistically significant decrease was observed across RCD, SCD and NDC groups by WB. Also, when looking at AD and NDC groups only, no statistically significant differences were determined between groups. It was perhaps surprising to find no significant increase in A2M levels between RCD, SCD and NDC or AD and NDC groups by WB. However, the result demonstrated the superior performance of the mass spectrometry-based TMT-SRM assay over the immuno-based approach, *i.e.,* the absolute quantitation provided by the TMT-SRM assay was more sensitive to expression changes between groups than the relative quantitation provided by the WB. This is further demonstrated by ROC analyses in Figure 5.6 where the AUC for A2M peptides/transitions in distinguishing AD from NDC is higher than that by WB.

A

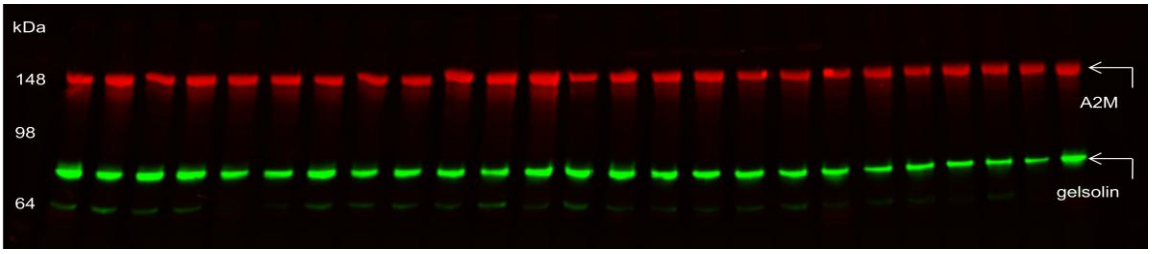

B

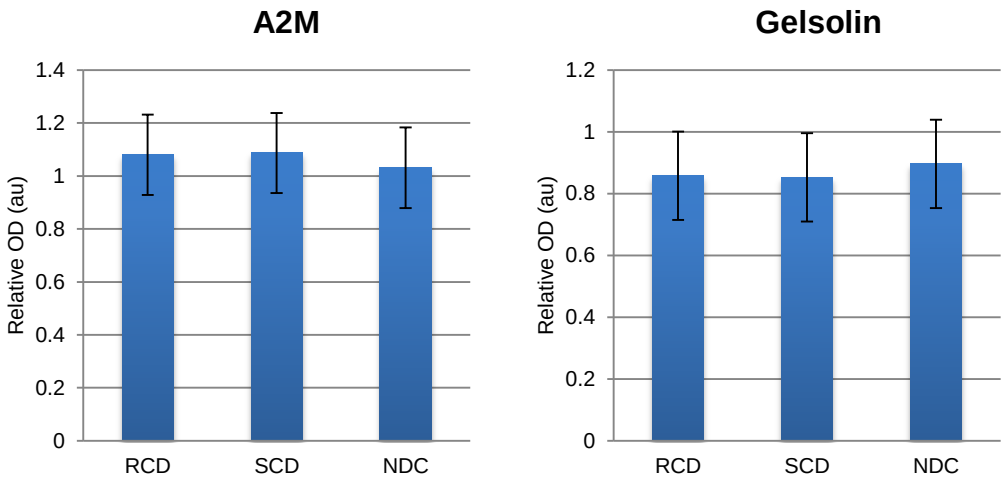

C

Protein	RCD	SCD	NDC	Fold change RCD v SCD	Fold change RCD v NDC	Fold change SCD v NDC	*p*-value
A2M	1.08	1.09	1.03	0.99	1.05	0.95	0.534
Gelsolin	0.86	0.85	0.9	1.01	0.96	1.05	0.658

Figure 5.5 Western blot results for A2M and gelsolin across the sample cohort. **A** A representative blot showing the detection of A2M and gelsolin in the plasma of AD and NDC subjects. Denatured plasma samples were separated by SDS-PAGE and transferred to nitrocellulose membranes. Blots were probed with antibodies against A2M and gelsolin. The *Mr* (kDa) of the marker is displayed on the left. **B** Expression of A2M and gelsolin between RCD, SCD and NDC by WB. Similar expression of each protein was observed between groups. Error bars indicate the 95% CI.**C** Relative ratios of A2M and gelsolin between RCD, SCD and NDC groups. The fold change between each group is indicated. No statistical significant change was observed between groups.

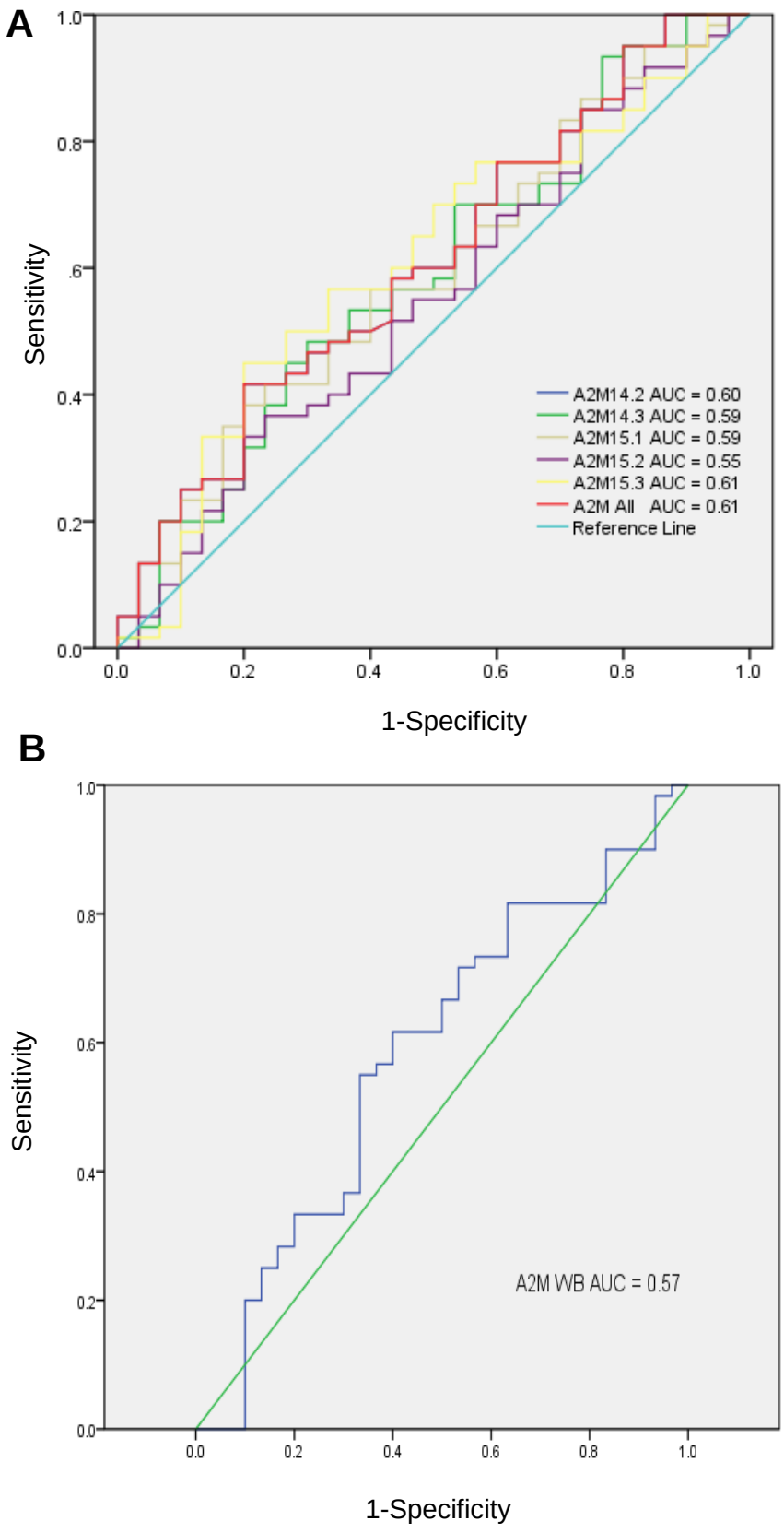

Figure 5.6 ROC analyses for A2M by TMT-SRM and WB. **A** For the TMT-SRM results, a ROC curve is plotted for each transition of each peptide as well as the mean over all transitions/peptides **B** ROC analysis of the A2M WB. For each curve, the AUC is also displayed. A higher AUC is observed for the TMT-SRM results than WB, demonstrating its superior performance.

5.2.2.2 Correlation of QTRAP, TSQ Vantage and WB results

A comparison was made between the MS- and immuno-based platforms for all A2M and gelsolin measurements. More precisely, agreement between values of the same sample obtained by TMT-SRM and WB was assessed. Several analyses were performed, *i.e.,* QTRAP *versus* WB, TSQ Vantage *versus* WB, QTRAP *versus* TSQ Vantage and WB *versus* WB (replicates 1 and 2). For the MS measurements, all 13 transitions of A2M and gelsolin included in the final data analysis were compared to the WB measurement for that protein. The Pearson correlation coefficient was calculated for each comparison. When comparing either QTRAP or TSQ Vantage against WB, a strong correlation was observed for A2M and gelsolin values across MS and WB platforms, with Pearson correlation coefficients ranging from 0.51 – 0.70. Figure 5.7 A and B displays data for the transitions which gave the highest and lowest correlation coefficients on either the QTRAP or TSQ Vantage as compared to WB. The results demonstrate the high agreement between both MS and immuno-based approaches. Very strong correlation was observed when comparing the measurements on the QTRAP to the TSQ Vantage (Pearson correlation coefficients ranged from 0.75 – 0.95, Figure 5.7 C and D), further demonstrating the excellent agreement between TMT-SRM quantitation across both instruments. In general, a weaker correlation was observed between the two WB replicates (Pearson correlation coefficients of 0.43 – 0.70, Figure 5.7 E and F).

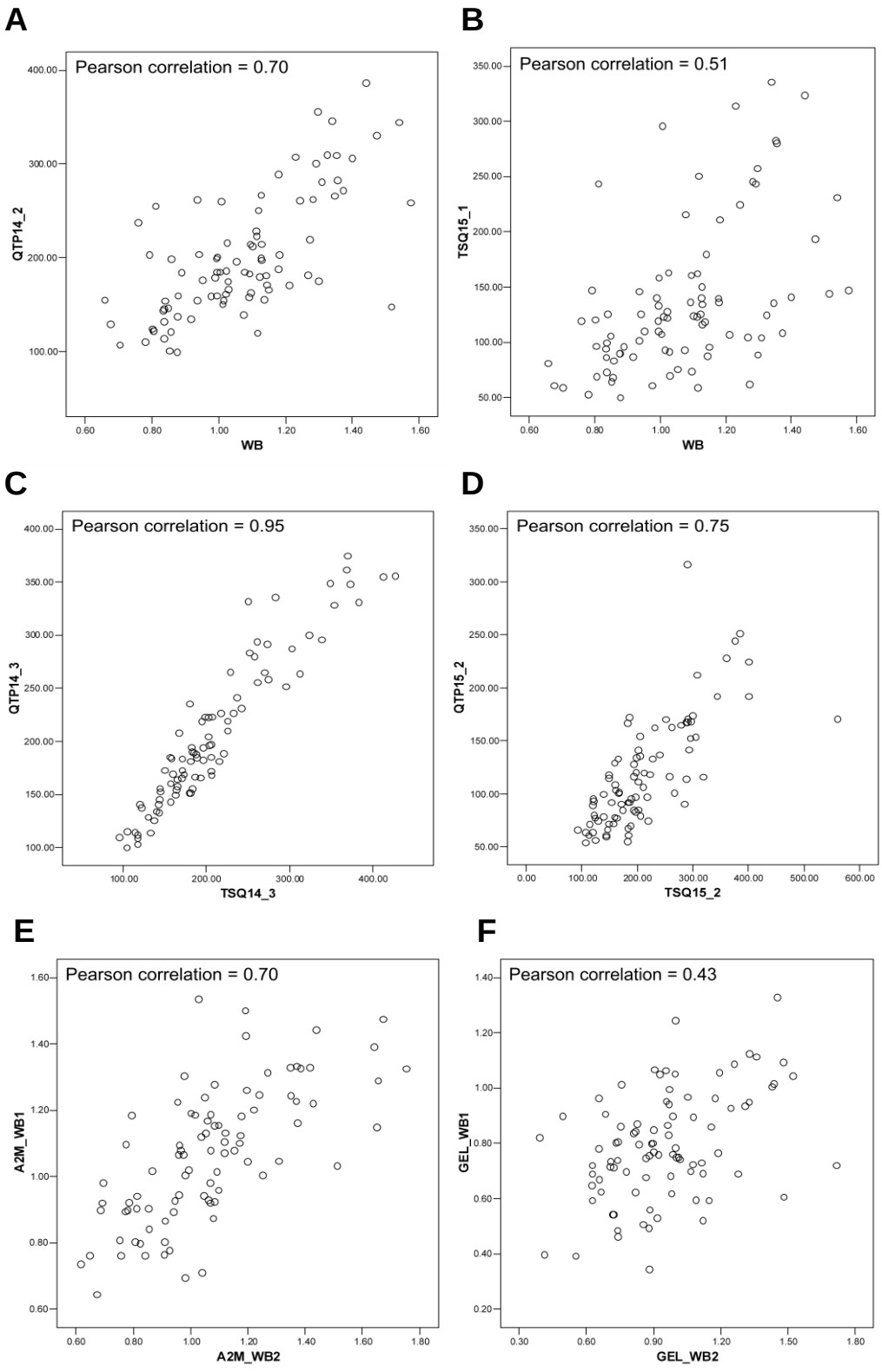

Figure 5.7 Correlation of QTRAP, TSQ Vantage and WB measurements for A2M and gelsolin. **A** Highest correlation (A2M peptide 14, transition 2) of MS (QTRAP) v WB **B** Lowest correlation (A2M peptide 15, transition 1) of MS (TSQ Vantage) v WB **C** Highest correlation (A2M peptide 14, transition 3) of QTRAP v TSQ Vantage **D** Lowest correlation (A2M peptide 15, transition 2) of QTRAP v TSQ Vantage **E** WB1 v WB2 of A2M **F** WB1 v WB2 of gelsolin.

5.3 Summary

- The utility of a TMT-SRM assay was demonstrated for the rapid, selective and multiplexed quantitation of a panel of candidate biomarkers of AD across a clinical cohort.
- In-line with discovery, plasma A2M was found to increase in AD and correlated with the rate of cognitive decline in the disease, thus confirming the protein as a diagnostic and prognostic biomarker of AD.
- The prognostic utility of plasma clusterin as demonstrated in discovery was not confirmed by TMT-SRM. In the same context, the result confirmed discovery studies which showed that the protein did not have use as a diagnostic biomarker of the disease. Further, several groups have demonstrated that plasma ApoE is unchanged in AD and this is in agreement with the TMT-SRM results described here-in.
- The remaining proteins in the panel were not confirmed as prognostic or diagnostic biomarkers of AD in this instance.
- Equivalent absolute amounts were observed for each plasma peptide to those described in the assay validation experiments in Chapter 4, demonstrating the robustness of the TMT-SRM workflow for peptide quantitation across independent sample cohorts.
- TMT-SRM results were equivalent on analogous MS instruments and quantitation provided by the novel MS-based assay was in strong agreement with that provided by a traditional approach using antibodies.

Chapter 6

General Discussion

6.0 The pressing need for sensitive and specific biomarkers of AD

AD is the most prevalent type of dementia. The availability of new treatments for common illnesses and an all-round improvement in healthcare is reflected in a continually aging population, resulting in a recent explosion in the number of people diagnosed with the disease. In addition to the obvious personal strain on both the sufferer and their families, this has major implications in terms of financial burden and effort on healthcare institutions. The current annual cost to the UK economy for treatment of AD is estimated to be £17 billion. Consequently, there is an urgent need for new technologies which can aid in an earlier diagnosis, slow the progression or indeed, improve the symptomatic treatment of AD. Several drug candidates are currently in Phase II and Phase III trials including secretase inhibitors and tau aggregation inhibitors (Pogacic and Herrling, 2009). The beneficial action of such species would have the greatest impact at the very earliest stages of the disease course, before the manifestation of AD pathology and progressive decline in cognitive function become insurmountable.

Currently, AD can only be definitively diagnosed by brain biopsy or upon autopsy after the death of a patient (Davinelli *et al*., 2011). However, in the clinical setting, brain biopsy is rarely performed and diagnosis of MCI and AD states in living subjects is dependant on clinical evaluation using a battery of neuropsychological tests. Such measures may have inherent inaccuracies as they are subject to individual interpretation in the clinic. Changes in peptide and protein levels in human body fluids such as urine, CSF and plasma may reflect the physiological state of healthy or diseased individuals and thus have been proposed as providing a more definitive source of diagnostic and prognostic biomarkers of AD (Blennow *et al.,* 2010). As detailed in the 1998 Consensus Report of the Working Group on Molecular and Biochemical Markers of Alzheimer's Disease, the perfect biological markers of AD would be able to distinguish those people at risk of the disease and would identify AD at its very earliest stages. Further, biomarkers which could reflect changes at the molecular level could enable the stratification between MCI subjects who convert to AD

and those who do not, the characterisation of disease progression and assignment of patients for targeted treatments and the monitoring of treatment response. Further, biomarkers should be specific enough to distinguish AD from other dementias, non-invasive, inexpensive, reliable and simple to perform (The Ronald And Nancy Reagen Research Institute Of The Alzheimer's Association And The National Institute On Aging Working Group, 1998).

Due to its proximity and solubility with the brain *via* the BBB, CSF is an obvious source of sample matrix when looking at biomarkers of neurodegenerative diseases such as AD. Indeed, many studies utilising antibody-based approaches have been published comparing CSF levels of Aβ and tau peptides at different stages of the disease course (Sunderland *et al.,* 2003; Craig-Shapiro *et al.,* 2009; Tapiola *et al.,* 2009; Mattson *et al.,* 2009; Visser *et al.,* 2009). It has been consistently reported that a marked decrease in $A\beta_{1-42}$ and increase in both t-tau and p-tau is observed in the CSF of AD subjects. However, it is very difficult to obtain ethical approval for lumbar puncture extraction of CSF in many countries, including the United Kingdom. Although techniques are improving, CSF sample extraction remains somewhat invasive and difficulty in obtaining large volumes of the fluid makes it unsuitable for routine application. Attention has recently shifted to blood as molecular changes in the AD brain may be reflected in the periphery or indeed, physiological responses to AD may be occurring in the blood itself. The repeatability of venepuncture for blood extraction is relatively easy, quick and inexpensive compared to CSF and thus, blood plasma or serum represent an ideal sample matrix for clinical proteomic studies of the disease. In a similar context, blood tests measuring cholesterol and APOE genotype are currently available for assessment of AD risk (Mayeux *et al.,* 1998). Such 'susceptibility' or 'risk factor' testing indicates whether there is a likelihood of developing late onset AD, but unfortunately, does not provide a diagnostic or prognostic measure of the disease.

Proteomic investigations in plasma by several independent groups have revealed an extensive list of candidate biomarkers of AD (Corder *et al.,* 1994; Chen *et al.,* 1995; Farlow *et al.,* 2004; Ferri *et al.,* 2005; Hye *et al.,* 2006; German *et al.,* 2007;

Cutler *et al.,* 2008; Thambisetty *et al.,* 2010; Güntert *et al.,* 2010). In this thesis, a subset of these proteins was selected for assay development as they showed the most promise from discovery and had confirmed associations with disease pathology. Using 2DE and TMT peptide-labeling technologies, complement C3/C3a, CFH, A2M, FGG, SAP and gelsolin were previously described as differentially expressed in AD patients and may prove to be valuable indicators of AD diagnosis (Hye *et al.,* 2006; Lee *et al.,* 2007; Maier *et al.,* 2008; Thambisetty *et al.,* 2010; Güntert *et al.,* 2010). Further, clusterin and gelsolin may have utility in predicting the progression of the disease. ApoE is of interest as the ApoE ε4 allele has been shown to cause increased susceptibility to AD and this genetic trait may translate at the protein level (Scacchi *et al.,* 1999).

The next stage requires the verification of such species as true biomarkers, sensitive and specific for the disease. The majority of the selected candidate proteins are already associated with other degenerative diseases, *e.g.,* CFH with AMD and clusterin with Huntington's disease (Thakkinstian *et al.,* 2006; Dalrymple *et al.,* 2007). It is therefore expected that a combined panel of proteins may be used and result in enhanced diagnostic and prognostic sensitivity and specificity, than either alone (Mor *et al.,* 2005). Biomarker verification requires the development of rapid, high quality, fit-for-purpose, multiplexed assays to measure target analytes in a sufficient throughput of samples necessary for such analyses. This process ensures only the best candidates are taken through to biomarker validation and qualification stages and to determine if the changes in protein abundance observed in discovery are real (Jaffe *et al.,* 2008). Traditional assay development schemes for peptide and protein quantitation have utilised the highly selective and specific response of antibodies, *e.g.,* ELISA assays (Engvall and Perlman, 1971; Brennan *et al.,* 2010). There are several advantages associated with this technique including the highly specific nature of the antibody-antigen interaction and the high sensitivity of the approach, permitting the quantitation of proteins in plasma down to < ng/mL levels. However, quantitation may be subject to interference from other species within the matrix and the absolute amounts of target

analytes cannot be ascertained (Preissner *et al.,* 2003). ELISA assays in plasma currently remain limited as only one antigen can be robustly and accurately detected at any one time (Leng *et al.,* 2008). This is changing and recently, multiplexed immuno-assays have become available (Ray *et al.,* 2007). However, such techniques are very much in their infancy and their full potential as accurate and specific quantitation strategies has yet to be comprehensively described. The cost associated with immuno-assay development is generally very high, with usually a very long lead time, *i.e.,* usually over one year (Hüttenhain *et al.,* 2009). Ultimately, the success of such assays is exclusively dependent on the availability of high quality antibodies for antigen detection. Unfortunately, the production of requisite antibodies frequently fails. There is thus an urgent need for novel, highly reproducible, high throughput peptide and protein quantitation strategies to improve the success rate of approved biomarkers (Anderson, 2005). Unfortunately, the limited availability of such techniques, capable of testing panels of biomarkers in even moderate sample numbers has created a significant bottleneck in the biomarker pipeline (Rifai *et al.,* 2006; Paulovich *et al.,* 2008).

6.1 Moving from the protein antibody to the peptide autograph

The major difficulty in the analysis of blood-based biomarkers is the huge complexity and vast dynamic range of protein concentrations in human plasma (Anderson and Anderson, 2002). Despite the effort and vast investment to generate lists of candidate biomarkers in discovery studies, there is currently no plasma biomarker of AD routinely used in a clinical setting and this is in part due to the immense technical requirements for their verification and validation. A possible resolution to this problem is the recruitment of more targeted, candidate-based proteomic strategies such as SRM for biomarker assay development. The technique relies on the detection and quantitation of selected surrogate peptides, unique to the candidate biomarker protein of interest (Mallick *et al.,* 2007). In this context, SRM-based assays for biomarker measurement can be directed towards specific protein

isoforms and PTMs, an additional shortfall of immuno-based means. SRM is sensitive (down to low attomolar amounts) and its dynamic range covers over five orders of magnitude (Anderson and Hunter, 2006; Domon and Aebersold, 2006; Stahl-Zeng, 2007). Moreover, the technique is suitable in providing highly precise measurements across independent laboratories, a requisite feature of any robust quantitative assay (Addona *et al.,* 2009). SRM in combination with stable isotope dilution has become increasingly popular where targeted, multiplexed, absolute quantitative amounts of peptides are being pursued (Gerber *et al.,* 2003; Kirkpatrick *et al.,* 2006; Pratt *et al.,* 2006). In an effort to reduce the inherent cost associated with production of heavy isotope-labeled peptides for internal standardisation in such studies, methods utilising isotopic versions of iTRAQ and ICPL in combination with SRM have been recently developed, namely mTRAQ (Lange *et al.,* 2008; DeSouza *et al.,* 2008; DeSouza *et al.,* 2009; DeSouza *et al.,* 2010). In a similar vain, SRM in combination with TMT has been proposed as a comparable strategy for the targeted, multiplexed quantitation of peptides in complex background matrices such as plasma.

There is compelling evidence that medium to high abundant proteins in plasma have value as clinical biomarkers of AD (Hye *et al.,* 2006; Akkufo *et al.,* 2008; Song *et al.,* 2009; Thambisetty and Lovestone, 2010). The feasibility of SRM for the measurement of such medium to high abundant species was first demonstrated by Anderson and Hunter in 2006. As the candidate proteins discussed in this thesis represent plasma species in the same range of abundance as described by the aforementioned study (present down to low µg/mL levels), it was hypothesised that the target analytes could be detected and quantitated in unfractionated plasma by SRM, without the need for prior enrichment such as that using SISCAPA or high abundant protein (*e.g.,* albumin or immunoglobulin G) depletion strategies. This has obvious benefits as the overall workflow is less complex and less prone to errors and minimal sample manipulation will increase throughput and limit sample to sample variability, thereby improving the accuracy of the quantitative measurement. Additionally, immunoaffinity-SRM approaches are dependent on the availability of requisite

antibodies, which additionally has time and cost considerations. To date, no study has been published utilising targeted MS-based methods to validate panels of candidate biomarkers of AD in plasma.

6.2 Developing novel strategies for candidate biomarker verification in plasma

In the first instance, it was important to assess the quantitative performance of utilising isotopic versions of TMT tags as a means of introducing an internal standard into an SRM experiment. In Chapter 2, the TMT-SRM approach was successfully demonstrated as an accurate quantitative strategy for the targeted and parallel measurement of multiple peptides endogenous to plasma at medium to high abundance. Here, a sample preparation workflow was optimised for the production of suitable target peptides of plasma proteins, including the choice of enzyme for digestion, TMT-labeling of proteolytic peptides and sample clean-up using RP and SCX chromatography. All experiments were performed once. Trypsin was selected as an appropriate enzyme for peptide production due to its well-recognised high specificity, *i.e.,* trypsin cleaves protein peptide bonds specifically on the carboxylic side of basic lysine and arginine residues. This cleavage specificity results in protein digestion products of the appropriate size range and charge for MS analysis in positive ionisation mode. In addition to the high efficiency of the TMT-labeling reaction, the data suggested that RP and SCX chromatography were competent for eliminating MS interfering compounds.

The mass difference of 5 Da between light TMT and heavy TMT tags allowed distinguishing between differentially labeled versions of the same peptide. This was true for peptides of multiple charge states and which had varying numbers of TMT attached. This compares to 4 Da per tag and 6 Da per tag in the mTRAQ and ICPL strategies, respectively (Julka and Regnier, 2005; Schmidt *et al.,* 2005; DeSouza *et al.,* 2008). Such differences are important for crosstalk between transitions, *i.e.,* the greater the mass difference introduced, the less chance of crosstalk. This needed to be

assessed in that transitions were selective even when the ion measured in Q3 was of the same *m/z* and the precursor was triply charged. Further, by applying an isotopic TMT-labeling strategy, a mass difference could be introduced between experimental sample peptides and internal standards, allowing for the differential detection of both by SRM. Additionally, light and heavy TMT-labeled versions of the same peptide were shown to perfectly co-elute by LC-SRM. This was crucial, as it allowed for the direct comparison and relative quantitation between different TMT-labeled versions of the same peptide, both here, and in subsequent TMT-SRM experiments. The accuracy achieved was encouraging and comparable to %CV's required for assays (Anderson and Hunter, 2006). Therefore, based on these initial proof-of-principle experiments, an assay was developed for a panel of candidate plasma biomarkers of AD.

By using isotopic versions of TMT, both purified biological sample proteins as well as synthetic peptides can be utilised as internal standards. As described in Chapter 2, tryptic peptides of biological and synthetic proteins provide relatively quick and inexpensive references for TMT-SRM quantitation. During the course of this thesis, TMT-SRM was successfully implemented for the verification of candidate biomarkers of iron regulation in *N. meningitidis* (Byers *et al.,* 2009). Here, a biological pool was utilised for TMT-SRM internal standardisation. This was highly beneficial as it provided an internal standard for all target peptides under consideration and allowed for the determination of the most robust SRM transitions for quantitation. However, the strategy was somewhat limited by the fact that matrix interference on SRM transitions could not truly be deciphered and assay performance characteristics could not be determined. Thus, synthetic peptides were prepared for use as internal standards in the assay under development in this thesis. This resulted in an overall reduction in sample complexity and in so doing, improved the chance of detection and quantitation of the target proteins in undepleted plasma. An added benefit of using synthetic peptides is the ability to fine-tune compound-dependent parameters for individual SRM transitions during the method development process, thus enhancing the final detection of the all target analytes in plasma (Keshishian *et al.,* 2007). Furthermore, on condition

that accurate concentrations are determined by AAA, synthetic peptides enable absolute quantitative amounts to be determined, allowing the comparison of target peptide abundance across experiments and independent sample cohorts. The provision of absolute amounts assumes the efficiency of the trypsin digestion reaction is 100% and the internal standard remains at a constant (known) amount throughout the workflow. Further, it was assumed (and confirmed here-in) that light TMT- and heavy TMT-labeling of the same peptide gives equal SRM sensitivies.

Important determinants in achieving sensitive, specific and accurate quantitative measurements included the selection of peptides which were proteotypic and of an appropriate length (6 - 25 amino acids), fully hydrolysed by trypsin and absent of known PTMs such as phosphorylation and glycosylation (Kitteringham *et al.,* 2007; Picotti *et al.,* 2010). The most important consideration for peptide selection was peptide proteotypicity within the human plasma proteome (Craig *et al.,* 2005). However, due to the overlap between different isoforms of a protein, this was not always possible, *e.g.,* two isoforms of clusterin exist in blood (isoform 1 and 2) as a result of alternative splicing. None of the selected peptides were present in this sequence and thus, the peptides measured either isoform. However, all selected peptides were specific to the respective protein of interest. The reasoning behind such stringent peptide length was that longer peptides are generally more hydrophobic and have a higher overall charge (Steen and Mann, 2004). In the same context, peptides with internal RP/KP and histidine residues were avoided, where possible. As demonstrated within this thesis, more hydrophobic peptides can introduce uncertainty and less accuracy in the quantitative measurement. In the same context, a preference for peptides of 2^+ (more favourable) and 3^+ (less favourable, due to charge splitting and reduction in sensitivity) charge states was taken during the development of the TMT-SRM assay. Furthermore, longer peptides are more expensive to synthesise, whilst shorter peptides (< 6 amino acids) do not provide the required specificity as they are less likely to be proteotypic. Peptides were required to be free of amino acids which may undergo *in vitro* modifications, *e.g.,* cysteine, tryptophan or methionine, although peptides containing

such species may be considered for TMT-SRM only if the choice of suitable peptides is low, as often, such modifications are complete.

As different peptides are subject to differential ionisation efficiencies and fragmentation properties by CID, this can dramatically affect the quality of the TMT-SRM measurement. An approach was taken to select multiple peptides, as opposed to a single peptide, per protein candidate. There are advantages and disadvantages to both strategies. Using a single signature peptide as representative of a target protein has been successfully demonstrated for the quantitation of candidate biomarkers in first trimester Trisomy 21 maternal serum (Lopez *et al.,* 2011). The rationale for this was that multiple peptides might quantify different isoforms of the same protein, thereby producing conflicting results. Further, lower numbers of peptides results in a lower overall complexity of the analytical system. Production of single peptides per protein would additionally minimise costs. However, caution must be taken when limiting oneslf in such a manner as the optimal peptide (in terms of detection, robustness and accuracy) may not be selected at an early enough stage during the analysis. The selection of multiple signature peptides per candidate biomarker protein was therefore chosen for this multi-protein assay to compensate for the fact that different peptides of a protein may give different quantitative amounts depending on the region of the protein from which each species arises, *e.g.,* due to the presence of splice variants or truncations and such biological variances need to be considered (Duncan *et al.,* 2009). In total, 32 peptides were selected for TMT-SRM quantitation, with at least three peptides per protein. From the selected peptides, 16 were observed in biomarker discovery plasma datasets, establishing a link between biomarker discovery using isobaric TMT-labeling and subsequent validation by TMT-SRM (Byers *et al.,* 2009). Multiple measurements for each candidate protein increased the confidence in the TMT-SRM quantitation and enabled the determination of those peptides which provide the most robust quantitative measurements in terms of SRM sensitivity and specificity (Yocum and Chinnaiyan, 2009). As a result, poorly performing peptides were removed at several stages during assay development and validation, with only the most robust

signature peptides of a protein remaining for quantitation in the final TMT-SRM assay. Peptides were removed due to significantly decreased sensitivities upon TMT-labeling or purification, due to poor endogenous detection in plasma or those peptides which had poor accuracy during assay validation. In future studies, experiments could be undertaken in an effort to address the variability in peptide recovery at the various different stages of the TMT-labeling workflow. To assess the effects of TMT-labeling on peptide amounts, a TMT-SRM method may be prepared to measure a plasma sample which has remains unlabeled, to that which has been TMT-labeled. If both samples are combined in a 1:1 ratio, then the % differences in SRM sensitivities, *i.e*., deviation from the expected ratio, could give an estimation of any peptide losses which are due to the TMT-labeling reaction. To quantitate the peptide losses occurring over the complete workflow (and primarily at the RP and SCX purification stage), a known amount amount of peptide standard could be spiked in at the beginning of the process and quantitated by SRM at each stage of the process. To study the effects of storage of plasma proteins over long periods of time, a plasma sample could be stored at - 80ºC for, *e.g*., t = 0, 1, 2, 4, 8, 12, 16, 32, 64 weeks and assessed by comparing endogenous plasma peptides to synthetic peptide internal standards spiked-in immediately before analysis by the developed TMT-SRM method. This analysis could be extended to storage of the plasma sample in several different types of sample vial, *e.g*., glass vials, standard eppendorfs and low adsorption eppendorfs to assess the effects of storage in each (Kraut *et al*., 2009).

A total of 17 peptides demonstrated good endogenous detection in plasma and accurate and robust TMT-SRM measurements and thus were included in the final quantitative assay. Importantly, at least two peptides per protein remained, which enabled continued comparison for peptides within a protein.

The complexity and huge dynamic range of proteins in plasma increases the likelihood of analyte-on-analyte suppression and background matrix effects which can detrimentally influence SRM detection and specificity (Keshishian *et al.,* 2007; Sherman *et al.,* 2009; Abbatiello *et al.,* 2010). As is often the case, many tryptic plasma

peptides share similar *m/z* and t_R properties, which cannot be fully discriminated using current low resolving triple quadrupole instruments. In an effort to combat these deleterious effects, multiple transitions of a peptide were targeted for quantitation. This resulted in a more specific TMT-SRM assay as aberrant transitions affected by non-specific plasma background could be highlighted and removed from the data analysis, or indeed, the method as a whole. The strategy developed in this thesis to determine less specific transitions was based on the overlap of calibration curves for different transitions of the same peptide. Aberrant transitions were highlighted as less specific. Due to this robust way to identify spurious transitions, it was therefore decided not to remove such transitions from the method completely here, as it was demonstrated that different plasma types are subject to varying levels of background interference, *i.e.,* what is true for one plasma species is not necessarily true for all and thus, valuable proteomic information may be lost if such analytes are completely ignored. Further, selection of multiple SRM transitions per peptide added further confidence to the quantitative measurement. In agreement with the literature, the importance of selecting Q3 ions greater than the *m/z* of the precursor ion where possible was highlighted as they provide better selectivity between light TMT and heavy TMT transitions (Kirkpatrick *et al.,* 2005; Lange *et al.,* 2008; Kuzyk *et al*, 2009). A common feature of all TMT-labeled peptides is the presence of high *m/z* pseudo-y ions. Such ions are TMT fragment ions whose *m/z* is always the intact mass of the labeled peptide minus the reporter ion and CO. It was hypothesised that pseudo-y ions may serve as appropriate Q3 SRM transitions ions where no other fragmentation is available. However, as demonstrated here, pseudo y-ions are generated from all TMT-labeled peptides, resulting in less specific SRM transitions and less robust TMT-SRM quantitation.

The TMT-SRM assay for the quantitation of the selected AD candidate biomarkers in human plasma required that target analytes could be quantitated accurately, in parallel, and in a time scale which was viable for the analysis of a large number of samples, on a stable and reproducible analytical platform. The combination of nanoflow LC and nanospray MS was not a robust enough platform for the assay

described here-in, with imprecise TMT-SRM quantitation observed for all target peptides in the AD candidate biomarker panel. An added disadvantage of nanoflow LC flow rates is the requirement of longer analysis times for peptide separation, resulting in a lower throughput of samples. To resolve this, the configuration of the upfront LC was changed to enable microflow rates in combination with ESI. The new analytical platform was confirmed for suitability using a simple target analyte not endogenous to human plasma, namely VATVSLPR peptide. An initial assay design was developed such that the accuracy, linearity, LOD and LOQ were derived for the assay of each analyte in an efficient and workable manner. Upscaled digestion, TMT-labeling and RP and SCX purification protocols allowed for the preparation of the larger protein amounts consumed by microflow LC rates with no compromise to MS sensitivity. As well as significantly reducing individual sample analysis times (from 100 min to 15 min per sample), thus increasing sample throughput, the new system had a more robust LC and mass spectrometer source. Further, sample throughput was additionally increased with the incorporation of a microtitre plate format (as all samples could be lyophilised in parallel prior to SRM analysis) and made for easier sample handling. High accuracy in TMT-SRM quantitation was observed at the higher flow rates and the introduction of glucagon as a peptide scavenger significantly enhanced SRM sensitivities. The new system was deemed a substantial improvement in the overall TMT-SRM quantitation strategy.

6.3 Validation and performance characterisation defines if an assay is fit-for-purpose

The novel, multiplexed assay was successfully validated by comparison of TMT-SRM measurements of plasma gelsolin to those using a traditional biomarker quantitation strategy using antibodies, *i.e.,* WB. The TMT-SRM quantitation of the remaining peptides in the panel provided an initial insight into their performance in terms of robustness in clinical sample cohorts and agreement between peptides within a protein. Absolute quantitation of all target analytes in plasma was acheived by TMT-

SRM, with all measurements within the linear range of quantitation for all peptides. Overall, transitions of the same peptide and peptides of the same protein demonstrated equivalent TMT-SRM performance and patterns of expression between AD and NDC groups. Deviations in the amounts recovered were observed between peptides of the same protein however. This was speculated to be due to the different susceptibilities of each peptide to trypsin cleavage. Further, peptide losses during TMT-labeling or purification stages may have contributed to the observed differences.

It was demonstrated here-in that accurate and equivalent TMT-SRM quantitation could be achieved using SRP as compared to interpolation from the reverse calibration curve strategy. SRP was considered the more favourable approach due to its simplicity and potential for a higher throughput of samples, provided linearity in quantitation was confirmed (Campbell *et al.,* 2011). In another significant advantage to the developed workflow, it was established that technical and analytical repeats had minimal contribution to any observed quantitative variance and thus, only one technical and one analytical repeat could be performed. This has major benefits as doing multiple technical repeats severely impacts on sample throughput.

The performance of each individual target analyte in a quantitative proteomic assay should be comprehensively validated before routine application (Lee *et al.,* 2006). Assay performance was defined for each signature peptide in terms of the dynamic range and linearity of quantitation, LOD, LOQ and accuracy for confirmation of robust quantitative performance. This is quite a challenging but essential undertaking, as a failure to properly define the limits of an assay can result in misguided quantitative interpretation. Moreover, such parameters permit the comparison to established assay technologies such as ELISA and make clear the relevance and clinical applicability of TMT-SRM assays. Peptides of the same protein performed similarly, once again demonstrating the robustness of the TMT-SRM workflow for the preparation of signature tryptic plasma peptides of each candidate AD biomarker. Peptide quantitation was observed at pg/mL levels, which was equivalent to ng/mL protein levels, well within the physiologically relevant range of each target analyte in plasma. Taking clusterin as

an example, a commercial available ELISA kit (as used in the discovery of the candidate marker) is capable of quantitating over two orders of magnitude with a precision of 7.8% (Thambisetty *et al.,* 2010). The developed TMT-SRM assay measured over three orders of magnitude with a precision of 2.7%, thus confirming the superior performance of the MS-based assay compared to the immuno-based approach.

The assessment of assay portability was considered an essential process, giving an indication of the overall robustness of the TMT-SRM assay across MS platforms. A robust, fit-for-purpose assay is particularly crucial if it is to be implemented in independent laboratories. Excellent accordance of fragmentation patterns and thus, transitions, was observed across QTRAP and TSQ Vantage platforms. All transitions of the same peptide plotted equivalent curves and corresponding curves on both triple quadrupole instruments were comparable. Further, equivalent accuracy, LODs, LOQs, linearity and dynamic range was observed for all target analytes and in considered acceptable for a robust, fit-for-purpose assay.

6.4 Plasma A2M is increased and correlates with the rate of decline in AD

A biomarker can be any characteristic that is objectively measured and evaluated as an indicator of normal biologic processes, pathogenic processes, or pharmacologic responses to a therapeutic intervention (Biomarkers Definitions Working Group, 2001). Here, signature peptides of A2M confirmed the protein as both a diagnostic and prognostic biomarker of AD. A statistically significant increase was observed in plasma levels of the protein in AD and this confirmed the original discovery findings (Hye *et al.,* 2006). Further, the ability of A2M in predicting the rate of cognitive decline and ultimately progression of the disease as shown by the multiplexed TMT-SRM assay was in agreement with a separate study where an association of plasma A2M and hippocampal N-acetylaspartate/myo-inositol ratio had utility in predicting disease progression in early AD (Thambisetty *et al.,* 2008). The role of A2M in AD is of

particular interest as the protein has been shown to have very strong affinity for Aβ peptides, with increased A2M immunoreactivity in the amyloid plaques of the hippocampus in the AD brain (Bauer *et al.,* 1991; Strauss *et al.,* 1992; Du *et al.,* 1997). Further, A2M levels were found to be elevated by ELISA in temporal cortices of AD compared to NDCs (Wood *et al.,* 1993).The principle receptor for A2M in the brain is LRP. Activated A2M facilitates Aβ internalisation in the brain *via* the binding to LRP (Narita *et al.,* 1997). Thus, overexpression of A2M in human tissue such as plasma may result in increased amyloid load resulting in plaque pathology associated with AD. Interestingly, the LRP itself has been associated with late onset familial AD (Hollenbach *et al.,* 1998). *In vitro* studies in cultured neurons have shown A2M to be both neuroprotective and neurotoxic. The neurotoxic effect of aggregated Aβ was prevented upon binding of A2M (Du *et al.,* 1997; Hughes *et al.,* 1998). Conversely, activated A2M increased $A\beta_{25-35}$-mediated neurotoxicity in neuroblastoma cells (Fabrizi *et al.,* 1999). The absence of LRP in these cell types resulted in an interference of A2M with TGF-β neuroprotection. Two common polymorphisms within the A2M gene lead to increased risk of AD (Matthijs and Marynen, 1991; Blacker *et al.,* 1998; Saunders *et al.,* 2003). Both polymorphisms are associated with an increase in Aβ deposition in the brain (Myllykangas *et al.,* 1999). However, several other case-control and family-based studies indicate no significant association of the gene polymorphisms with AD (Rogaeva *et al.,* 1999; Gibson *et al.,* 2000, Poduslo *et al.,* 2002; Bertram *et al.,* 2004).

The remaining proteins in the TMT-SRM assay did not show any significant differences between RCD, SCD and NDC groups. Further, AD and NDC groups were compared and no significant differences were observed. The simplest explanation for these results was that there were no expression differences for these proteins between case and control in the cohort utilised. Here, case and control subjects at baseline were matched for age and sex, with MMSE decline described over five timepoints within the space of a year. In the cohort used for the discovery of A2M and CFH for example, AD subjects were on average 6.8 years older than NDCs (Hye *et al.,* 2006). Such differences in selected cohorts may have compounded the diagnostic potential initially

observed in discovery and explain why such differences could not be replicated in the verification phase. In contrast and the more likely, was that the complexity of sample collection across different European centres may have adversely affected the cohort. All of the discovery exercises were performed using the ART cohort, a single centre collection of samples based in the UK. While multi-centre studies are subject to strict sample collection and processing guidelines, potential variations may introduce sample heterogeneity. For biofluids such as plasma, significant attention must be given to potential sources of variation, including the length of sample storage and the number of freeze-thaw cycles. Neglect for such factors may have detrimental effects on the quality of the proteomic data generated (Rogers *et al.,* 2003). The determinent criteria for the selection of the cohort under investigation here was age, sex and the clinical measure of MMSE. This resulted in a cohort which was unbalanced in sample numbers for centre. This may have resulted in a 'cancelling out' effect between the six collection centres when looking at the combined expression differences across centres. This was hinted at when looking at gelsolin peptides 29, 30 and 31 in individual centres (Figure 6.1 A, B and C). When taking peptide 29 for example, no significant differences were observed between groups within the Kuopio (*n* = 17 AD and 5 NDCs) and Perugia (*n* = 17 AD and 6 NDCs) sample collection centres, repectively. However, a statistically significant decrease was observed for the peptide between groups in the London collection centre (*n* = 6 AD and 11 NDCs) and this was in-line with discovery (Güntert *et al.,* 2010). This result was replicated for gelsolin peptide 30. When looking at peptide 31 (the most robust signature peptide of the protein in terms of TMT-SRM assay performance), a statistically significant decrease was observed between groups within Kuopio and London sample collection centres, with no significant differences observed between groups within the Perugia collection centre. Nevertheless, when taking the gelsolin protein as a whole, no statistically significant differences were observed between groups. Despite such conflicting results for at least gelsolin, the increased expression observed for A2M between RCD, SCD and NDC and AD and NDC groups remained in each centre.

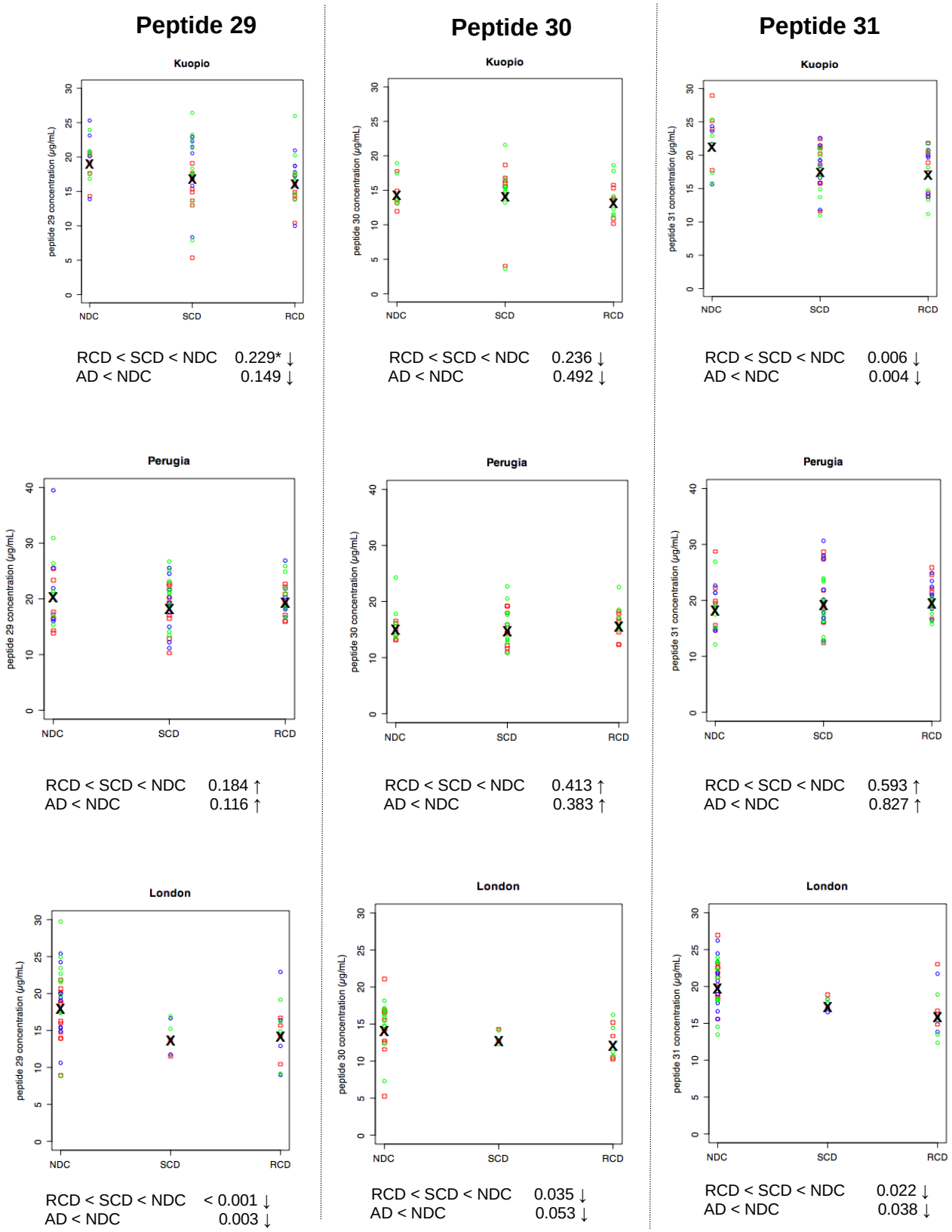

Figure 6.1 Gelsolin peptide measurements within Kuopio, Perugia and London sample collection centres. For each sample collection centre, differential expression across RCD, SCD and NDC or AD and NDC groups (data not plotted) was observed. Statistically significant (p < 0.05) decreases were observed for certain gelsolin peptides, *e.g.,* peptide 31 in Kuopio, but this result was not replicated across all sampling centres.

* indicates the p-value

6.5 Improving the TMT-SRM assay pipeline

A well characterised ELISA can be configured to run approximately 1000 samples over a period of two days (Whiteaker *et al.,* 2010). The current TMT-SRM protocol requires upfront sample preparation including overnight digestion, TMT-labeling and purification. The rate-limiting factor in the workflow was the purification of TMT-labeled peptides, primarily due to the in-house preparation of SCX columns and the low flow-rate used in the chromatographic separation (approximately 1 drop of RP/SCX buffer per second). Purification of approximately 50 samples per day was achievable. In this context, an alternative strategy adopting pre-made SCX cartridges was investigated (data not shown). However, significantly reduced SRM sensitivities were observed for several target peptides (primarily those of a hydrophobic nature) meant such columns were unsatisfactory for the TMT-SRM workflow described here-in. A further way to expediate this process would be to automate sample handling processes to enhance the sample throughput (Kronkvist *et al.,* 1998) and preserve or perhaps improve TMT-SRM assay precision. An added suggestion to maximise the throughput of the TMT-SRM assay would be to use several LC-SRM platforms. Additionally, advances in plasma digestion strategies have been recently published which may significant reduces proteolysis times (Slysz and Schreimer, 2005; Freije *et al.,* 2005; Lopez-Ferrer *et al.,* 2008).

It was observed here-in that there were losses in peptide amounts at several stages of the TMT-SRM workflow, which ultimately affects the quality and accuracy of TMT-SRM data. The main point at which the most significant losses were observed was during the SCX clean-up of TMT-labeled peptides. An SCX LC step was necessary here to remove the SDS that was initially required to fully solubilise the protein content of the sample of interest (Timperman and Aebersold, 2000). Thus, it is essential that alternative approaches be considered to avoid such detrimental losses to the workflow. These could include avoiding the use of SDS completely or implementing a different SDS-removal strategy. As an substitute to SDS, several MS-compatible coumpounds have been developed and are being introduced commercially, including

RapiGest from Waters, Invitrosol from Invitrogen and 3-[3-(1,1-bisalkyloxyethyl)pyridine-1-yl]propane-1-sulfonate from Protein Discovery (Imre *et al*., 2005, Wu *et al*., 2011). Traditionally, urea and guanidine hydrochloride have been used for protein denaturation, although both have distinct disadvantages (Chen *et al*., 2007). Alternatives to SCX for SDS removal include dialysis and ultrafiltration devices such as filter-aided sample preparation or 'FASP' (Hixson *et al*., 2002; Manza *et al*., 2005; Wisniewski *et al.*, 2009; Bereman *et al*., 2011).

The addition of synthetic peptide internal standards can be added either pre- or post-digestion and there is still much debate as to which approach is best. Typically, it is best to add internal standards as early on as possible in the workflow to account for any variation which may be introduced during sample preparation. In spite of this, it has been demonstrated that when internal standard peptides are added prior to digestion, this can lead to elevated and unpredictable results, compared to those added post-digestion (Kuzyk *et al*., 2009). Such variation was also peptide dependent. Possible reasons for this include degradation or chemical modification of the internal standard peptides during the digestion reaction. Further, peptides are liberated from their parent protein upon trypsin cleavage at different rates and spiked internal standard synthetic peptides may be subject to degradation effects which the endogenous peptides are not exposed to. This would therefore lead to inaccuracies in TMT-SRM quantitation. To avoid this, in is more common practice (and performed here-in) to add internal standard peptides post-digestion so that any losses experienced during sample preparation procedures would affect both synthetic and endogenous peptides equally (Ong and Mann, 2005). An added advantage of such a strategy is that much less synthetic peptides are required as only the amount of sample that is necessary for LC-TMT-SRM needs to be prepared. However, the possibility of adding internal standard peptides pre-digestion should not be excluded and an informative future experiment could compare both pre and post-digestion strategies in relation to the TMT-SRM workflow.

To fully realise absolute TMT-SRM quantitation, it is essential to determine the efficiency of the trypsin enzyme reaction, *i.e*., has the reaction gone to completion and

is it equal for all peptides? Failure to achieve full proteolyic activity for the production of tryptic peptides may lead to substantial variatiability in the TMT-SRM quantitation of peptides of the same protein and an underestimation of endogenous protein amounts (Brun *et al.*, 2007). This could partially explain the underestimation of protein amounts as observed in this study. An experiment to resolve such questions would be a useful inclusion in future work. This may be achieved by adding a known amount of recombinant protein not endogenous to human plasma, at the beginning of the TMT-SRM workflow and determining the amount of tryptic peptides of the protein remaining post-digestion by SRM (Zhen *et al*., 2007; Mirzaei *et al.*, 2008).

A significant, but crucial, amount of time was dedicated to the selection of suitable target peptides for SRM measurement. This incorporated the manual searching of MS/MS discovery datasets for the determination of those peptides that were routinely observed during data dependent acquisition and to provide an initial insight into the hydrophobicity of each candidate peptide. Further, shortlisted candidates were manually inspected for the presence of unfavourable amino acids and PTMs which may ultimately affect the accuracy of TMT-SRM quantitation. During the course of this thesis, several new software packages have become available which can streamline such analysis and may significantly reduce the time required for SRM assay development. Assay libraries such as MRMAtlas provide a repository of candidate SRM transitions that have been previously identified (Picotti *et al.,* 2008; Anderson, 2010). Further, the software packages are capable of designing SRM transitions based solely on archived data from previous research efforts, through integration of database information from gpmdb or PeptideAtlas (Walsh *et al*., 2009). This allows for a significiantly larger amount of experimental data to be accessible for the design of SRM transitions.

To enhance the detection of SRM transitions, compound-dependent parameters were optimised using synthetic peptides manually infused into the instrument. In an effort to streamline such processes, LC-SRM experiments ran over a range of compound-dependent instrument voltages within a single analysis have been

demonstrated (Sherwood *et al.,* 2009). Thus, optimal DP, CE and CXP values may be more rapidly ascertained than the approach used here-in. Similarly, computational algorithms can be applied to predict such parameters although thus far, optimisation using empirical means remains the best method for such goals (Maclean *et al.,* 2010). Skyline is a recently developed software package for targeted proteomics method creation and quantitative SRM data analysis (Maclean *et al.,* 2010). It is open source and available without cost for academic and commercial use. The software uses MS/MS spectral libraries to optimise SRM parameters and verify results based on data previously observed on triple quadrupole instrumentation, including both QTRAP and TSQ Vantage mass spectrometers. Pinpoint software (Thermo Scientific) aids in the *in silico* selection of target proteins for SRM assay development and the determination of suitable proteotypic peptides to act as surrogates for SRM quantitation. Further, the software predicts which SRM transitions may provide the most robust quantitation and provide numerical and graphical tools for verification at each stage of the development process. However, it must be considered that *in silico* software packages may be subject to errors and although can be generally in good agreement, cannot surpass the power of selecting target peptides and transitions for SRM quantitation based on experimentally-derived data.

As previously described, three pieces of information are essential for the generation of SRM assays; 1) a list of candidate biomarker target proteins, 2) signature proteotypic peptides need to be defined and 3) selective and specific SRM transitions and their compound-dependent parameters need to be determined (Lange *et al.,* 2008). Selection of peptides and SRM transitions is traditionally derived using empirical data from data dependent acquisition experiments. However, the approach is unsuitable for assay generation of peptides that have not been previously detected or have poor MS sensitivities. Two recent strategies could be incorporated into the TMT-SRM assay development workflow which may ultimately provide a more sensitive and cost-effective assay, including the use of crudely synthesised peptides, *e.g.,* SPOT-synthesis technology and ‘intelligent’ SRM (iSRM). A method has been recently

described for the rapid generation of SRM assays where crude synthetic peptides are used for internal standardisation (Frank, 2002; Picotti *et al.,* 2010). The cost of generating crude peptides using the SPOT-synthesis technology has been estimated to be £3-8 per target analyte. This compares favourably to the on average £300 price tag associated with the synthesis of a pure synthetic peptide. Such technologies would be of benefit for the TMT-SRM assay development process described here, where several peptides were removed at various stages of the development process. Using crude, low-cost synthetic peptide libraries, the most suitable peptides and transitions could be defined in terms of ionisation efficiency, LC-MS properties, instrument parameters and endogenous plasma detection in a rapid and multiplexed manner, at the very earliest stages of the development process. Such prior knowledge would have avoided the cost and effort associated with the synthesis of purer, higher quality peptides (as in the case of this thesis) which ultimately did not provide a robust quantitative measurement. Furthermore, following determination of the best target peptides from the crude peptide set, such peptides could be subsequently synthesised to a high quality for more accurate and absolute quantitation.

The measurement of multiple fragment ions of a peptide has been proven to afford sufficient information for confirmation of target peptide identity (Kiyonami *et al.,* 2011). This intelligent SRM or ‘’iSRM’’ approach utilises a small subset of SRM transitions to trigger a full list of transitions of a peptide, enabling the simultaneous qualitative and quantitative measurement of a species. This could be beneficial to the TMT-SRM strategy described here-in as the best SRM transitions could be more quickly and readily deciphered. Further, iSRM has the potential to measure over 10,000 individual transitions, representing up to 1,000 target peptides in a single experiment. Such a method would have major benefits to the TMT-SRM workflow as the time associated with SRM transition selection would be reduced. Further, prior knowledge of the most sensitive, selective and specific transitions of a target analyte would give confidence to future measurements.

6.6 Conclusions and Future Work

Here, a novel assay has been developed for the targeted, multiplexed quantitation of candidate plasma biomarkers of AD. The TMT-SRM approach takes advantage of the selectivity and sensitivity of SRM MS in combination with the quantitative capabilities of isotopic versions of TMT. Utilising surrogate peptides as representative of candidate proteins, the TMT-SRM assay was fully validated as fit-for-purpose to measure each target analyte in undepleted plasma. Further, the assay was fully characterised in terms of performance, with highly favourable statistics. A2M was confirmed as both a diagnostic and prognostic biomarker of AD and this was in agreement with discovery studies. In comparison to standard immuno-based assays for biomarker quantitation, TMT-SRM assays have relatively short lead times for development, with significantly reduced costs and low patient sample consumption. The approach enables absolute quantitative amounts to be described in a rapid and accurate manner, with the necessary throughput required for biomarker verification. TMT-SRM provides a link between biomarker discovery (using isobaric TMT tagging) and biomarker verification. The definitive nature of the assay means it is universally applicable to other researchers in independent laboratories. TMT-SRM has potential to substitute or at the very least, compliment, antibody-based quantitation of biomarkers in AD and other human disorders in an array of biological fluids not counting plasma, including CSF, urine and saliva.

Even though these initial findings are encouraging for at least A2M, a cohort of 90 samples is relatively small. The study should now be extended and replicated in significantly larger (hundreds to thousands) cohorts of AD samples, as well as those from other dementia types, to determine the full clinical validity of each protein as sensitive and specific biomarkers of AD. The TMT-SRM assay is currently being implemented in a significantly larger cohort (n = 1000 from the AddNeuroMed cohort) of AD, MCI and NDC plasma samples to determine the full clinical validity of the panel of biomarkers in AD diagnosis and prognosis. This is being performed in parallel with a newly established multiplexed antibody-based approach, namely the Luminex xMAP®

system and the agreement between the two platforms will be assessed. This is the first time such a study is being undertaken in such extensive sample numbers and has vast potential and reward for the AD community. Further, the novel TMT-SRM technology is viable for the targeted measurement of potentially any protein in the human proteome, provided sufficient detection by SRM. On condition that SRMs do not cluster significantly around the same elution time, the assay could be expanded, or indeed new assays developed, to allow significantly more SRMs to be measured in a single LC-SRM analysis. The developed TMT-SRM assay measures eight candidate plasma biomarkers of AD. Using the TMT-SRM strategy developed here, it is both theoretically and practically possible to construct further assays for the multiplexed measurement of protein markers in AD and other diseases, in an accurate, sensitive, rapid and cost-friendly manner.

Bibliography

(1946) Proceedings of the American Physical Society. *Physical Review* **69,** 674.

(1998) Consensus report of the Working Group on: "Molecular and Biochemical Markers of Alzheimer's Disease". The Ronald and Nancy Reagan Research Institute of the Alzheimer's Association and the National Institute on Aging Working Group. *Neurobiol.Aging* **19,** 109-116.

Abbatiello SE, Mani DR, Keshishian H, Carr SA (2010) Automated detection of inaccurate and imprecise transitions in peptide quantification by multiple reaction monitoring mass spectrometry. *Clin.Chem.* **56,** 291-305.

Abdi F, Quinn JF, Jankovic J, McIntosh M, Leverenz JB, Peskind E, Nixon R, Nutt J, Chung K, Zabetian C, Samii A, Lin M, Hattan S, Pan C, Wang Y, Jin J, Zhu D, Li GJ, Liu Y, Waichunas D, Montine TJ, Zhang J (2006) Detection of biomarkers with a multiplex quantitative proteomic platform in cerebrospinal fluid of patients with neurodegenerative disorders. *J.Alzheimers.Dis.* **9,** 293-348.

Addona TA, Abbatiello SE, Schilling B, Skates SJ, Mani DR, Bunk DM, Spiegelman CH, Zimmerman LJ, Ham AJ, Keshishian H, Hall SC, Allen S, Blackman RK, Borchers CH, Buck C, Cardasis HL, Cusack MP, Dodder NG, Gibson BW, Held JM, Hiltke T, Jackson A, Johansen EB, Kinsinger CR, Li J, Mesri M, Neubert TA, Niles RK, Pulsipher TC, Ransohoff D, Rodriguez H, Rudnick PA, Smith D, Tabb DL, Tegeler TJ, Variyath AM, Vega-Montoto LJ, Wahlander A, Waldemarson S, Wang M, Whiteaker JR, Zhao L, Anderson NL, Fisher SJ, Liebler DC, Paulovich AG, Regnier FE, Tempst P, Carr SA (2009) Multi-site assessment of the precision and reproducibility of multiple reaction monitoring-based measurements of proteins in plasma. *Nat.Biotechnol.* **27,** 633-641.

Aebersold R, Anderson L, Caprioli R, Druker B, Hartwell L, Smith R (2005) Perspective: a program to improve protein biomarker discovery for cancer. *J.Proteome.Res.* **4,** 1104-1109.

Ahmed N, Barker G, Oliva KT, Hoffmann P, Riley C, Reeve S, Smith AI, Kemp BE, Quinn MA, Rice GE (2004) Proteomic-based identification of haptoglobin-1 precursor as a novel circulating biomarker of ovarian cancer. *Br.J.Cancer* **91,** 129-140.

Ahn YH, Lee JY, Lee JY, Kim YS, Ko JH, Yoo JS (2009) Quantitative analysis of an aberrant glycoform of TIMP1 from colon cancer serum by L-PHA-enrichment and SISCAPA with MRM mass spectrometry. *J.Proteome.Res.* **8,** 4216-4224.

Aisen PS (2002) Anti-inflammatory agents in Alzheimer's disease. *Curr.Neurol. Neurosci.Rep.* **2,** 405-409.

Akiyama H, Yamada T, Kawamata T, McGeer PL (1991) Association of amyloid P component with complement proteins in neurologically diseased brain tissue. *Brain Res.* **548,** 349-352.

Akuffo EL, Davis JB, Fox SM, Gloger IS, Hosford D, Kinsey EE, Jones NA, Nock CM, Roses AD, Saunders AM, Skehel JM, Smith MA, Cutler P (2008) The discovery and early validation of novel plasma biomarkers in mild-to-moderate Alzheimer's disease patients responding to treatment with rosiglitazone. *Biomarkers* **13,** 618-636.

Algotsson A, Winblad B (2007) The integrity of the blood-brain barrier in Alzheimer's disease. *Acta Neurol.Scand.* **115,** 403-408.

Altman DG, Bland JM (1994) Diagnostic tests 2: Predictive values. *BMJ.* **309(6947),** 102.

Alzheimer A, Stelzmann RA, Schnitzlein HN, Murtagh FR (1995) An English translation of Alzheimer's 1907 paper, "Uber eine eigenartige Erkankung der Hirnrinde". *Clin.Anat.* **8,** 429-431.

America AH, Cordewener JH (2008) Comparative LC-MS: a landscape of peaks and valleys. *Proteomics.* **8(4),** 731-749.

Andersen GR, Koch TJ, Dolmer K, Sottrup-Jensen L, Nyborg J (1995) Low resolution X-ray structure of human methylamine-treated alpha 2-macroglobulin. *J.Biol.Chem.* **270,** 25133-25141.

Anderson L, Anderson NG (1977) High resolution two-dimensional electrophoresis of human plasma proteins. *Proc.Natl.Acad.Sci.U.S.A* **74,** 5421-5425.

Anderson L, Hunter CL (2006) Quantitative mass spectrometric multiple reaction monitoring assays for major plasma proteins. *Mol.Cell Proteomics* **5,** 573-588.

Anderson NL, Anderson NG (1991) A two-dimensional gel database of human plasma proteins. *Electrophoresis* **12,** 883-906.

Anderson NL, Anderson NG (2002) The human plasma proteome: history, character, and diagnostic prospects. *Mol.Cell Proteomics.* **1,** 845-867.

Anderson NL, Anderson NG, Haines LR, Hardie DB, Olafson RW, Pearson TW (2004) Mass spectrometric quantitation of peptides and proteins using Stable Isotope Standards and Capture by Anti-Peptide Antibodies (SISCAPA). *J.Proteome.Res.* **3,** 235-244.

Anderson NL, Jackson A, Smith D, Hardie D, Borchers C, Pearson TW (2009) SISCAPA peptide enrichment on magnetic beads using an in-line bead trap device. *Mol.Cell Proteomics.* **8,** 995-1005.

Anderton BH, Betts J, Blackstock WP, Brion JP, Chapman S, Connell J, Dayanandan R, Gallo JM, Gibb G, Hanger DP, Hutton M, Kardalinou E, Leroy K, Lovestone S, Mack T, Reynolds CH, Van SM (2001) Sites of phosphorylation in tau and factors affecting their regulation. *Biochem.Soc.Symp.* 73-80.

Andreasen N, Hesse C, Davidsson P, Minthon L, Wallin A, Winblad B, Vanderstichele H, Vanmechelen E, Blennow K (1999) Cerebrospinal fluid beta-amyloid(1-42) in Alzheimer disease: differences between early- and late-onset Alzheimer disease and stability during the course of disease. *Arch.Neurol.* **56,** 673-680.

Andreasen N, Minthon L, Davidsson P, Vanmechelen E, Vanderstichele H, Winblad B, Blennow K (2001) Evaluation of CSF-tau and CSF-Abeta42 as diagnostic markers for Alzheimer disease in clinical practice. *Arch.Neurol.* **58,** 373-379.

Andreasen N, Minthon L, Davidsson P, Vanmechelen E, Vanderstichele H, Winblad B, Blennow K (2001) Evaluation of CSF-tau and CSF-Abeta42 as diagnostic markers for Alzheimer disease in clinical practice. *Arch.Neurol.* **58,** 373-379.

Annesley TM (2003) Ion suppression in mass spectrometry. *Clin.Chem.* **49(7),** 1041-1044.

Apostol G, Abi-Saab W, Kratochvil CJ, Adler LA, Robieson WZ, Gault LM, Pritchett YL, Feifel D, Collins MA, Saltarelli MD (2011) Efficacy and safety of the novel alpha(4)beta (2) neuronal nicotinic receptor partial agonist ABT-089 in adults with attention-deficit/hyperactivity disorder: a randomized, double-blind, placebo-controlled crossover study. *Psychopharmacology (Berl).*

Arnaiz E, Almkvist O (2003) Neuropsychological features of mild cognitive impairment and preclinical Alzheimer's disease. *Acta Neurol.Scand.Suppl* **179,** 34-41.

Atkinson AJ, Colburn WA, DeGruttola VG, DeMets DL, Downing GJ, Hoth DF, Oates JA, Peck CC, Schooley RT, Spilker BA, Woodcock J, Zeger SL (2001) Biomarkers and surrogate endpoints: Preferred definitions and conceptual framework*. *Clin Pharmacol Ther* **69,** 89-95.

Atkinson JP, Goodship TH (2007) Complement factor H and the hemolytic uremic syndrome. *J.Exp.Med.* **204,** 1245-1248.

Auer J, Camoin L, Guillonneau F, Rigourd V, Chelbi ST, Leduc M, Laparre J, Mignot TM, Vaiman D (2010) Serum profile in preeclampsia and intra-uterine growth restriction revealed by iTRAQ technology. *J.Proteomics.* **73,** 1004-1017.

Baczek T, Wiczling P, Marszall M, Heyden YV, Kaliszan R (2005) Prediction of peptide retention at different HPLC conditions from multiple linear regression models. *J.Proteome.Res.* **4(2),** 555-563.

Baczek T, Kaliszan R (2009) Predictions of peptides' retention times in reversed-phase liquid chromatography as a new supportive tool to improve protein identification in proteomics. *Proteomics.* **9(4),** 835-847.

Bailey RW, Dunker AK, Brown CJ, Garner EC, Griswold MD (2001) Clusterin, a binding protein with a molten globule-like region. *Biochemistry* **40,** 11828-11840.

Barnes J, Lewis EB, Scahill RI, Bartlett JW, Frost C, Schott JM, Rossor MN, Fox NC (2007) Automated measurement of hippocampal atrophy using fluid-registered serial MRI in AD and controls. *J.Comput.Assist.Tomogr.* **31,** 581-587.

Barnidge DR, Goodmanson MK, Klee GG, Muddiman DC (2004) Absolute quantification of the model biomarker prostate-specific antigen in serum by LC-Ms/MS using protein cleavage and isotope dilution mass spectrometry. *J.Proteome.Res.* **3,** 644-652.

Barr JR, Maggio VL, Patterson DG, Jr., Cooper GR, Henderson LO, Turner WE, Smith SJ, Hannon WH, Needham LL, Sampson EJ (1996) Isotope dilution--mass spectrometric quantification of specific proteins: model application with apolipoprotein A-I. *Clin.Chem.* **42,** 1676-1682.

Barrett AJ (1981) Alpha 2-macroglobulin. *Methods Enzymol.* **80 Pt C,** 737-754.

Baty JD, Robinson PR (1977) Single and multiple ion recording techniques for the analysis of diphenylhydantoin and its major metabolite in plasma. *Biomed.Mass Spectrom.* **4(1),** 36-41.

Bauer J, Strauss S, Schreiter-Gasser U, Ganter U, Schlegel P, Witt I, Yolk B, Berger M (1991) Interleukin-6 and alpha-2-macroglobulin indicate an acute-phase state in Alzheimer's disease cortices. *FEBS Lett.* **285,** 111-114.

Bell RD, Sagare AP, Friedman AE, Bedi GS, Holtzman DM, Deane R, Zlokovic BV (2007) Transport pathways for clearance of human Alzheimer's amyloid beta-peptide and apolipoproteins E and J in the mouse central nervous system. *J.Cereb.Blood Flow Metab* **27,** 909-918.

Bereman MS, Egertson JD, Maccoss MJ (2011) Comparison between procedures using SDS for shotgun proteomic analyses of complex samples. *Proteomics.* **11(14),** 2931-2935.

Bermejo P, Martin-Aragon S, Benedi J, Susin C, Felici E, Gil P, Ribera JM, Villar AM (2008) Differences of peripheral inflammatory markers between mild cognitive impairment and Alzheimer's disease. *Immunol.Lett.* **117,** 198-202.

Berna M, Schmalz C, Duffin K, Mitchell P, Chambers M, Ackermann B (2006) Online immunoaffinity liquid chromatography/tandem mass spectrometry determination of a type II collagen peptide biomarker in rat urine: Investigation of the impact of collision-induced dissociation fluctuation on peptide quantitation. *Anal.Biochem.* **356,** 235-243.

Berna M, Ackermann B (2009) Increased throughput for low-abundance protein biomarker verification by liquid chromatography/tandem mass spectrometry. *Anal.Chem.* **81,** 3950-3956.

Bertram L, Parkinson M, Mullin K, Menon R, Blacker D, Tanzi RE (2004) No association between a previously reported OLR1 3' UTR polymorphism and Alzheimer's disease in a large family sample. *J.Med.Genet.* **41,** 286-288.

Bishop KM, Hofer EK, Mehta A, Ramirez A, Sun L, Tuszynski M, Bartus RT (2008) Therapeutic potential of CERE-110 (AAV2-NGF): targeted, stable, and sustained NGF delivery and trophic activity on rodent basal forebrain cholinergic neurons. *Exp.Neurol.* **211(2),** 574-584.

Bitsch A, Horn C, Kemmling Y, Seipelt M, Hellenbrand U, Stiefel M, Ciesielczyk B, Cepek L, Bahn E, Ratzka P, Prange H, Otto M (2002) Serum tau protein level as a marker of axonal damage in acute ischemic stroke. *Eur.Neurol.* **47(1),** 45-51.

Black RS, Sperling RA, Safirstein B, Motter RN, Pallay A, Nichols A, Grundman M (2010) A single ascending dose study of bapineuzumab in patients with Alzheimer disease. *Alzheimer Dis.Assoc.Disord.* **24(2),** 198-203.

Blacker D, Wilcox MA, Laird NM, Rodes L, Horvath SM, Go RC, Perry R, Watson B, Jr., Bassett SS, McInnis MG, Albert MS, Hyman BT, Tanzi RE (1998) Alpha-2 macroglobulin is genetically associated with Alzheimer disease. *Nat.Genet.* **19,** 357-360.

Bland JM, Altman DG (1986) Statistical methods for assessing agreement between two methods of clinical measurement. *Lancet* **1,** 307-310.

Blaschuk O, Burdzy K, Fritz IB (1983) Purification and characterization of a cell-aggregating factor (clusterin), the major glycoprotein in ram rete testis fluid. *J.Biol.Chem.* **258,** 7714-7720.

Blasko I, Jungwirth S, Jellinger K, Kemmler G, Krampla W, Weissgram S, Wichart I, Tragl KH, Hinterhuber H, Fischer P (2008) Effects of medications on plasma amyloid beta (Abeta) 42: longitudinal data from the VITA cohort. *J.Psychiatr.Res.* **42,** 946-955.

Blasko I, Jellinger K, Kemmler G, Krampla W, Jungwirth S, Wichart I, Tragl KH, Fischer P (2008) Conversion from cognitive health to mild cognitive impairment and Alzheimer's disease: prediction by plasma amyloid beta 42, medial temporal lobe atrophy and homocysteine. *Neurobiol.Aging* **29,** 1-11.

Blennow K, Wallin A, Fredman P, Karlsson I, Gottfries CG, Svennerholm L (1990) Blood-brain barrier disturbance in patients with Alzheimer's disease is related to vascular factors. *Acta Neurol.Scand.* **81,** 323-326.

Blennow K, Wallin A, Hager O (1993) Low frequency of post-lumbar puncture headache in demented patients. *Acta Neurol.Scand.* **88,** 221-223.

Blennow K, Wallin A, Agren H, Spenger C, Siegfried J, Vanmechelen E (1995) Tau protein in cerebrospinal fluid: a biochemical marker for axonal degeneration in Alzheimer disease? *Mol.Chem.Neuropathol.* **26,** 231-245.

Blennow K, Vanmechelen E (2003) CSF markers for pathogenic processes in Alzheimer's disease: diagnostic implications and use in clinical neurochemistry. *Brain Res.Bull.* **61,** 235-242.

Blennow K, Nellgard B (2004) Amyloid beta 1-42 and tau in cerebrospinal fluid after severe traumatic brain injury. *Neurology* **62,** 159-160.

Blennow K, Zetterberg H (2010) Is it time for biomarker-based diagnostic criteria for prodromal Alzheimer's disease? *Alzheimers.Res.Ther.* **2,** 8.

Blennow K, Hampel H, Weiner M, Zetterberg H (2010) Cerebrospinal fluid and plasma biomarkers in Alzheimer disease. *Nat.Rev.Neurol.* **6,** 131-144.

Blom ES, Giedraitis V, Zetterberg H, Fukumoto H, Blennow K, Hyman BT, Irizarry MC, Wahlund LO, Lannfelt L, Ingelsson M (2009) Rapid progression from mild cognitive impairment to Alzheimer's disease in subjects with elevated levels of tau in cerebrospinal fluid and the APOE epsilon4/epsilon4 genotype. *Dement.Geriatr.Cogn Disord.* **27,** 458-464.

Bokde AL, Teipel SJ, Drzezga A, Thissen J, Bartenstein P, Dong W, Leinsinger G, Born C, Schwaiger M, Moeller HJ, Hampel H (2005) Association between cognitive performance and cortical glucose metabolism in patients with mild Alzheimer's disease. *Dement.Geriatr.Cogn Disord.* **20,** 352-357.

Bokde AL, Lopez-Bayo P, Meindl T, Pechler S, Born C, Faltraco F, Teipel SJ, Moller HJ, Hampel H (2006) Functional connectivity of the fusiform gyrus during a face-matching task in subjects with mild cognitive impairment. *Brain* **129,** 1113-1124.

Bondar OP, Barnidge DR, Klee EW, Davis BJ, Klee GG (2007) LC-MS/MS quantification of Zn-+¦2 glycoprotein: A potential serum biomarker for prostate cancer. *Clinical Chemistry* **53,** 673-678.

Bondarenko PV, Chelius D, Shaler TA (2002) Identification and relative quantitation of protein mixtures by enzymatic digestion followed by capillary reversed-phase liquid chromatography-tandem mass spectrometry. *Anal.Chem.* **74,** 4741-4749.

Borth W (1992) Alpha 2-macroglobulin, a multifunctional binding protein with targeting characteristics. *FASEB J.* **6,** 3345-3353.

Bowman GL, Kaye JA, Moore M, Waichunas D, Carlson NE, Quinn JF (2007) Blood-brain barrier impairment in Alzheimer disease: stability and functional significance. *Neurology* **68,** 1809-1814.

Braak H, Braak E (1991) Neuropathological stageing of Alzheimer-related changes. *Acta Neuropathol.* **82,** 239-259.

Brennan DJ, O'Connor DP, Rexhepaj E, Ponten F, Gallagher WM (2010) Antibody-based proteomics: fast-tracking molecular diagnostics in oncology. *Nat.Rev.Cancer* **10,** 605-617.

Brioni JD, Esbenshade TA, Garrison TR, Bitner SR, Cowart MD (2011) Discovery of histamine H3 antagonists for the treatment of cognitive disorders and Alzheimer's disease. *J.Pharmacol.Exp.Ther.* **336(1),** 38-46.

Brittain SM, Ficarro SB, Brock A, Peters EC (2005) Enrichment and analysis of peptide subsets using fluorous affinity tags and mass spectrometry. *Nat.Biotechnol.* **23(4),** 463-468.

Brouwers N, Sleegers K, Van BC (2008) Molecular genetics of Alzheimer's disease: an update. *Ann.Med.* **40(8),** 562-583.

Brun V, Dupuis A, Adrait A, Marcellin M, Thomas D, Court M, Vandenesch F, Garin J (2007) Isotope-labeled protein standards: toward absolute quantitative proteomics. *Mol.Cell Proteomics* **6,** 2139-2149.

Brun V, Masselon C, Garin J, Dupuis A (2009) Isotope dilution strategies for absolute quantitative proteomics. *J.Proteomics* **72,** 740-749.

Brunden KR, Trojanowski JQ, Lee VM (2009) Advances in tau-focused drug discovery for Alzheimer's disease and related tauopathies. *Nat.Rev.Drug Discov.* **8,** 783-793.

Buerger K, Zinkowski R, Teipel SJ, Tapiola T, Arai H, Blennow K, Andreasen N, Hofmann-Kiefer K, DeBernardis J, Kerkman D, McCulloch C, Kohnken R, Padberg F, Pirttila T, Schapiro MB, Rapoport SI, Moller HJ, Davies P, Hampel H (2002) Differential diagnosis of Alzheimer disease with cerebrospinal fluid levels of tau protein phosphorylated at threonine 231. *Arch.Neurol.* **59,** 1267-1272.

Buerger K, Teipel SJ, Zinkowski R, Blennow K, Arai H, Engel R, Hofmann-Kiefer K, McCulloch C, Ptok U, Heun R, Andreasen N, DeBernardis J, Kerkman D, Moeller H, Davies P, Hampel H (2002) CSF tau protein phosphorylated at threonine 231 correlates with cognitive decline in MCI subjects. *Neurology* **59,** 627-629.

Buerger K, Ewers M, Pirttila T, Zinkowski R, Alafuzoff I, Teipel SJ, DeBernardis J, Kerkman D, McCulloch C, Soininen H, Hampel H (2006) CSF phosphorylated tau protein correlates with neocortical neurofibrillary pathology in Alzheimer's disease. *Brain* **129,** 3035-3041.

Bullock R (2005) SGS-742 Novartis. *Curr.Opin.Investig.Drugs.* **6(1),** 108-113.

Burggren AC, Bookheimer SY (2002) Structural and functional neuroimaging in Alzheimer's disease: an update. *Curr.Top.Med.Chem.* **2,** 385-393.

Byers HL, Campbell J, van UP, Tommassen J, Ward MA, Schulz-Knappe P, Prinz T, Kuhn K (2009) Candidate verification of iron-regulated Neisseria meningitidis proteins using isotopic versions of tandem mass tags (TMT) and single reaction monitoring. *J.Proteomics.* **73,** 231-239.

Calero M, Rostagno A, Matsubara E, Zlokovic B, Frangione B, Ghiso J (2000) Apolipoprotein J (clusterin) and Alzheimer's disease. *Microsc.Res.Tech.* **50,** 305-315.

Calero M, Rostagno A, Frangione B, Ghiso J (2005) Clusterin and Alzheimer's disease. *Subcell.Biochem.* **38,** 273-298.

Campbell J, Rezai T, Prakash A, Krastins B, Dayon L, Ward M, Robinson S, Lopez M (2011) Evaluation of absolute peptide quantitation strategies using selected reaction monitoring. *Proteomics.* **11,** 1148-1152.

Carden CP, Sarker D, Postel-Vinay S, Yap TA, Attard G, Banerji U, Garrett MD, Thomas GV, Workman P, Kaye SB, de Bono JS (2010) Can molecular biomarker-based patient selection in Phase I trials accelerate anticancer drug development? *Drug Discov.Today* **15,** 88-97.

Carlesimo GA, Oscar-Berman M (1992) Memory deficits in Alzheimer's patients: a comprehensive review. *Neuropsychol.Rev.* **3,** 119-169.

Carr SA, Anderson L (2008) Protein quantitation through targeted mass spectrometry: the way out of biomarker purgatory? *Clin.Chem.* **54,** 1749-1752.

Carrasquillo MM, Belbin O, Hunter TA, Ma L, Bisceglio GD, Zou F, Crook JE, Pankratz VS, Dickson DW, Graff-Radford NR, Petersen RC, Morgan K, Younkin SG (2010) Replication of CLU, CR1, and PICALM associations with alzheimer disease. *Arch.Neurol.* **67,** 961-964.

Carson JA, Turner AJ (2002) Beta-amyloid catabolism: roles for neprilysin (NEP) and other metallopeptidases? *J.Neurochem.* **81,** 1-8.

Cathcart ES, Wollheim FA, Cohen AS (1967) Immunoassay of P-component in amyloidotic sera. *Proc.Soc.Exp.Biol.Med.* **125,** 1123-1125.

Cedazo-Minguez A, Cowburn RF (2001) Apolipoprotein E: a major piece in the Alzheimer's disease puzzle. *J.Cell Mol.Med.* **5,** 254-266.

Celone KA, Calhoun VD, Dickerson BC, Atri A, Chua EF, Miller SL, DePeau K, Rentz DM, Selkoe DJ, Blacker D, Albert MS, Sperling RA (2006) Alterations in memory networks in mild cognitive impairment and Alzheimer's disease: an independent component analysis. *J.Neurosci.* **26,** 10222-10231.

Cham JA, Bianco L, Barton C, Bessant C (2010) MRMaid-DB: a repository of published SRM transitions. *J.Proteome.Res.* **9(1),** 620-625.

Chauhan VP, Ray I, Chauhan A, Wisniewski HM (1999) Binding of gelsolin, a secretory protein, to amyloid beta-protein. *Biochem.Biophys.Res.Commun.* **258,** 241-246.

Chen EI, Cociorva D, Norris JL, Yates JR, III (2007) Optimization of mass spectrometry-compatible surfactants for shotgun proteomics. *J.Proteome.Res.* **6(7),** 2529-2538.

Chen M, Inestrosa NC, Ross GS, Fernandez HL (1995) Platelets are the primary source of amyloid beta-peptide in human blood. *Biochem.Biophys.Res.Commun.* **213,** 96-103.

Chen YT, Chen CL, Chen HW, Chung T, Wu CC, Chen CD, Hsu CW, Chen MC, Tsui KH, Chang PL, Chang YS, Yu JS (2010) Discovery of Novel Bladder Cancer Biomarkers by Comparative Urine Proteomics Using iTRAQ Technology. *J.Proteome.Res.* **9,** 5803-5815.

Cheng D, Hoogenraad CC, Rush J, Ramm E, Schlager MA, Duong DM, Xu P, Wijayawardana SR, Hanfelt J, Nakagawa T, Sheng M, Peng J (2006) Relative and absolute quantification of postsynaptic density proteome isolated from rat forebrain and cerebellum. *Molecular and Cellular Proteomics* **5,** 1158-1170.

Christen Y (2004) Ginkgo biloba and neurodegenerative disorders. *Front Biosci.* **9,** 3091-3104.

Cirrito JR, Deane R, Fagan AM, Spinner ML, Parsadanian M, Finn MB, Jiang H, Prior JL, Sagare A, Bales KR, Paul SM, Zlokovic BV, Piwnica-Worms D, Holtzman DM (2005) P-glycoprotein deficiency at the blood-brain barrier increases amyloid-beta deposition in an Alzheimer disease mouse model. *J.Clin.Invest* **115,** 3285-3290.

Citron M, Oltersdorf T, Haass C, McConlogue L, Hung AY, Seubert P, Vigo-Pelfrey C, Lieberburg I, Selkoe DJ (1992) Mutation of the beta-amyloid precursor protein in familial Alzheimer's disease increases beta-protein production. *Nature* **360,** 672-674.

Citron M, Diehl TS, Gordon G, Biere AL, Seubert P, Selkoe DJ (1996) Evidence that the 42- and 40-amino acid forms of amyloid beta protein are generated from the beta-amyloid precursor protein by different protease activities. *Proc.Natl.Acad.Sci.U.S.A* **93,** 13170-13175.

Cochran DA, Evans CA, Blinco D, Burthem J, Stevenson FK, Gaskell SJ, Whetton AD (2003) Proteomic analysis of chronic lymphocytic leukemia subtypes with mutated or unmutated Ig V(H) genes. *Mol.Cell Proteomics.* **2,** 1331-1341.

Cockrell JR, Folstein MF (1988) Mini-Mental State Examination (MMSE). *Psychopharmacol.Bull.* **24,** 689-692.

Cohen A, Hertz HS, Mandel J, Paule RC, Schaffer R, Sniegoski LT, Sun T, Welch MJ, White E (1980) Total serum cholesterol by isotope dilution/mass spectrometry: a candidate definitive method. *Clin.Chem.* **26,** 854-860.

Comisarow MB, Marshall AG (1996) The early development of Fourier transform ion cyclotron resonance (FT-ICR) spectroscopy. *J.Mass Spectrom.* **31,** 581-585.

Conrads TP, Anderson GA, Veenstra TD, Pasa-Tolic L, Smith RD (2000) Utility of accurate mass tags for proteome-wide protein identification. *Anal.Chem.* **72(14),** 3349-3354.

Coon KD, Myers AJ, Craig DW, Webster JA, Pearson JV, Lince DH, Zismann VL, Beach TG, Leung D, Bryden L, Halperin RF, Marlowe L, Kaleem M, Walker DG, Ravid R, Heward CB, Rogers J, Papassotiropoulos A, Reiman EM, Hardy J, Stephan DA (2007) A high-density whole-genome association study reveals that APOE is the major susceptibility gene for sporadic late-onset Alzheimer's disease. *J.Clin.Psychiatry* **68,** 613-618.

Corder EH, Saunders AM, Strittmatter WJ, Schmechel DE, Gaskell PC, Small GW, Roses AD, Haines JL, Pericak-Vance MA (1993) Gene dose of apolipoprotein E type 4 allele and the risk of Alzheimer's disease in late onset families. *Science* **261,** 921-923.

Corder EH, Saunders AM, Risch NJ, Strittmatter WJ, Schmechel DE, Gaskell PC, Jr., Rimmler JB, Locke PA, Conneally PM, Schmader KE, . (1994) Protective effect of apolipoprotein E type 2 allele for late onset Alzheimer disease. *Nat.Genet.* **7,** 180-184.

Corneveaux JJ, Myers AJ, Allen AN, Pruzin JJ, Ramirez M, Engel A, Nalls MA, Chen K, Lee W, Chewning K, Villa SE, Meechoovet HB, Gerber JD, Frost D, Benson HL, O'Reilly S, Chibnik LB, Shulman JM, Singleton AB, Craig DW, Van Keuren-Jensen KR, Dunckley T, Bennett DA, De Jager PL, Heward C, Hardy J, Reiman EM, Huentelman MJ (2010) Association of CR1, CLU and PICALM with Alzheimer's disease in a cohort of clinically characterized and neuropathologically verified individuals. *Hum.Mol.Genet.* **19,** 3295-3301.

Cortes-Canteli M, Strickland S (2009) Fibrinogen, a possible key player in Alzheimer's disease. *J.Thromb.Haemost.* **7(1),** 146-150.

Cortes-Canteli M, Paul J, Norris EH, Bronstein R, Ahn HJ, Zamolodchikov D, Bhuvanendran S, Fenz KM, Strickland S (2010) Fibrinogen and beta-amyloid association alters thrombosis and fibrinolysis: a possible contributing factor to Alzheimer's disease. *Neuron* **66,** 695-709.

Craig R, Cortens JP, Beavis RC (2005) The use of proteotypic peptide libraries for protein identification. *Rapid Commun.Mass Spectrom.* **19,** 1844-1850.

Cruchaga C, Kauwe JS, Mayo K, Spiegel N, Bertelsen S, Nowotny P, Shah AR, Abraham R, Hollingworth P, Harold D, Owen MM, Williams J, Lovestone S, Peskind ER, Li G, Leverenz JB, Galasko D, Morris JC, Fagan AM, Holtzman DM, Goate AM (2010) SNPs associated with cerebrospinal fluid phospho-tau levels influence rate of decline in Alzheimer's disease. *PLoS.Genet.* **6(9),** e1001101.

Cutler P, Akuffo EL, Bodnar WM, Briggs DM, Davis JB, Debouck CM, Fox SM, Gibson RA, Gormley DA, Holbrook JD, Hunter AJ, Kinsey EE, Prinjha R, Richardson JC, Roses AD, Smith MA, Tsokanas N, Wille DR, Wu W, Yates JW, Gloger IS (2008) Proteomic identification and early validation of complement 1 inhibitor and pigment epithelium-derived factor: Two novel biomarkers of Alzheimer's disease in human plasma. *Proteomics.Clin.Appl.* **2,** 467-477.

Dalrymple A, Wild EJ, Joubert R, Sathasivam K, Bjorkqvist M, Petersen A, Jackson GS, Isaacs JD, Kristiansen M, Bates GP, Leavitt BR, Keir G, Ward M, Tabrizi SJ (2007) Proteomic profiling of plasma in Huntington's disease reveals neuroinflammatory activation and biomarker candidates. *J.Proteome.Res.* **6,** 2833-2840.

Davidsson P, Sjögren M (2006) Proteome studies of CSF in AD patients. *Mechanisms of Ageing and Development* **127,** 133-137.

Davinelli S, Intrieri M, Russo C, Di CA, Zella D, Bosco P, Scapagnini G (2011) The "Alzheimer's disease signature": potential perspectives for novel biomarkers. *Immun.Ageing.* **20; 8(1),** 7.

Dayon L, Hainard A, Licker V, Turck N, Kuhn K, Hochstrasser DF, Burkhard PR, Sanchez JC (2008) Relative quantification of proteins in human cerebrospinal fluids by MS/MS using 6-plex isobaric tags. *Anal.Chem.* **80,** 2921-2931.

de Boer JP, Creasey AA, Chang A, Abbink JJ, Roem D, Eerenberg AJ, Hack CE, Taylor FB, Jr. (1993) Alpha-2-macroglobulin functions as an inhibitor of fibrinolytic, clotting, and neutrophilic proteinases in sepsis: studies using a baboon model. *Infect.Immun.* **61,** 5035-5043.

de Silva HV, Stuart WD, Duvic CR, Wetterau JR, Ray MJ, Ferguson DG, Albers HW, Smith WR, Harmony JA (1990) A 70-kDa apolipoprotein designated ApoJ is a marker for subclasses of human plasma high density lipoproteins. *J.Biol.Chem.* **265,** 13240-13247.

De SB, Saftig P, Craessaerts K, Vanderstichele H, Guhde G, Annaert W, Von FK, Van LF (1998) Deficiency of presenilin-1 inhibits the normal cleavage of amyloid precursor protein. *Nature* **391,** 387-390.

Deane R, Sagare A, Zlokovic BV (2008) The role of the cell surface LRP and soluble LRP in blood-brain barrier Abeta clearance in Alzheimer's disease. *Curr.Pharm.Des* **14,** 1601-1605.

Debayle D, Dessalces G, Grenier-Loustalot MF (2008) Multi-residue analysis of traces of pesticides and antibiotics in honey by HPLC-MS-MS. *Anal.Bioanal.Chem.* **391,** 1011-1020.

DeMattos RB, Brendza RP, Heuser JE, Kierson M, Cirrito JR, Fryer J, Sullivan PM, Fagan AM, Han X, Holtzman DM (2001) Purification and characterization of astrocyte-secreted apolipoprotein E and J-containing lipoproteins from wild-type and human apoE transgenic mice. *Neurochem.Int.* **39,** 415-425.

DeMattos RB, Cirrito JR, Parsadanian M, May PC, O'Dell MA, Taylor JW, Harmony JA, Aronow BJ, Bales KR, Paul SM, Holtzman DM (2004) ApoE and clusterin cooperatively suppress Abeta levels and deposition: evidence that ApoE regulates extracellular Abeta metabolism in vivo. *Neuron* **41,** 193-202.

Dentchev T, Milam AH, Lee VM, Trojanowski JQ, Dunaief JL (2003) Amyloid-beta is found in drusen from some age-related macular degeneration retinas, but not in drusen from normal retinas. *Mol.Vis.* **9,** 184-190.

Desiderio DM, Kai M (1983) Preparation of stable isotope-incorporated peptide internal standards for field desorption mass spectrometry quantification of peptides in biologic tissue. *Biomed.Mass Spectrom.* **10,** 471-479.

Desiderio DM (1983) High-performance liquid chromatography and mass spectrometry of biologically important neuropeptides. *Adv.Chromatogr.* **22,** 1-36.

Desiderio DM, Kai M, Tanzer FS, Trimble J, Wakelyn C (1984) Measurement of enkephalin peptides in canine brain regions, teeth, and cerebrospinal fluid with high-performance liquid chromatography and mass spectrometry. *J.Chromatogr.* **297,** 245-260.

DeSouza L, Diehl G, Rodrigues MJ, Guo J, Romaschin AD, Colgan TJ, Siu KW (2005) Search for cancer markers from endometrial tissues using differentially labeled tags iTRAQ and cICAT with multidimensional liquid chromatography and tandem mass spectrometry. *J.Proteome.Res.* **4,** 377-386.

DeSouza LV, Grigull J, Ghanny S, Dube V, Romaschin AD, Colgan TJ, Siu KW (2007) Endometrial carcinoma biomarker discovery and verification using differentially tagged clinical samples with multidimensional liquid chromatography and tandem mass spectrometry. *Mol.Cell Proteomics* **6,** 1170-1182.

DeSouza LV, Taylor AM, Li W, Minkoff MS, Romaschin AD, Colgan TJ, Siu KW (2008) Multiple reaction monitoring of mTRAQ-labeled peptides enables absolute quantification of endogenous levels of a potential cancer marker in cancerous and normal endometrial tissues. *J.Proteome Res.* **7,** 3525-3534.

DeSouza LV, Romaschin AD, Colgan TJ, Siu KW (2009) Absolute quantification of potential cancer markers in clinical tissue homogenates using multiple reaction monitoring on a hybrid triple quadrupole/linear ion trap tandem mass spectrometer. *Anal.Chem.* **81,** 3462-3470.

DeSouza LV, Krakovska O, Darfler MM, Krizman DB, Romaschin AD, Colgan TJ, Siu KW (2010) mTRAQ-based quantification of potential endometrial carcinoma biomarkers from archived formalin-fixed paraffin-embedded tissues. *Proteomics* **10,** 3108-3116.

Deutsch EW, Lam H, Aebersold R (2008) PeptideAtlas: a resource for target selection for emerging targeted proteomics workflows. *EMBO Rep.* **9(5),** 429-434.

Diamandis EP, Hanash S, Lopez M, Carr S, Petricoin EF, III (2009) Protein quantification by mass spectrometry: is it ready for prime time? *Clin.Chem.* **55,** 1427-1430.

Ding JD, Lin J, Mace BE, Herrmann R, Sullivan P, Bowes RC (2008) Targeting age-related macular degeneration with Alzheimer's disease based immunotherapies: anti-amyloid-beta antibody attenuates pathologies in an age-related macular degeneration mouse model. *Vision Res.* **48,** 339-345.

Dole M, Dole M, Mack LL, Mack LL, Hines RL, Hines RL, Mobley RC, Mobley RC, Ferguson LD, Ferguson LD, Alice MB, Alice MB (1968) Molecular Beams of Macroions. *J.Chem.Phys.* **49,** 2240-2249.

Domon B, Aebersold R (2006) Mass spectrometry and protein analysis. *Science* **312,** 212-217.

Donahue JE, Johanson CE (2008) Apolipoprotein E, amyloid-beta, and blood-brain barrier permeability in Alzheimer disease. *J.Neuropathol.Exp.Neurol.* **67,** 261-270.

Donoso LA, Vrabec T, Kuivaniemi H (2010) The role of complement Factor H in age-related macular degeneration: a review. *Surv.Ophthalmol.* **55,** 227-246.

Doody RS, Gavrilova SI, Sano M, Thomas RG, Aisen PS, Bachurin SO, Seely L, Hung D (2008) Effect of dimebon on cognition, activities of daily living, behaviour, and global function in patients with mild-to-moderate Alzheimer's disease: a randomised, double-blind, placebo-controlled study. *Lancet.* **372,** 207-215.

Doolittle RF (1984) Fibrinogen and fibrin. *Annu.Rev.Biochem.* **53,** 195-229.

Douillet P, Orgogozo JM (2009) What we have learned from the Xaliproden Sanofi-aventis trials. *J.Nutr.Health Aging.* **13(4),** 365-366.

Drzezga A, Grimmer T, Henriksen G, Stangier I, Perneczky R, ehl-Schmid J, Mathis CA, Klunk WE, Price J, DeKosky S, Wester HJ, Schwaiger M, Kurz A (2008) Imaging of amyloid plaques and cerebral glucose metabolism in semantic dementia and Alzheimer's disease. *Neuroimage.* **39,** 619-633.

Du Y, Ni B, Glinn M, Dodel RC, Bales KR, Zhang Z, Hyslop PA, Paul SM (1997) alpha2-Macroglobulin as a beta-amyloid peptide-binding plasma protein. *J.Neurochem.* **69,** 299-305.

Dubois B, Feldman HH, Jacova C, DeKosky ST, Barberger-Gateau P, Cummings J, Delacourte A, Galasko D, Gauthier S, Jicha G, Meguro K, O'brien J, Pasquier F, Robert P, Rossor M, Salloway S, Stern Y, Visser PJ, Scheltens P (2007) Research criteria for the diagnosis of Alzheimer's disease: revising the NINCDS-ADRDA criteria. *Lancet Neurol.* **6,** 734-746.

Duncan MW, Yergey AL, Patterson SD (2009) Quantifying proteins by mass spectrometry: the selectivity of SRM is only part of the problem. *Proteomics.* **9,** 1124-1127.

Dupuis A, Hennekinne JA, Garin J, Brun V (2008) Protein Standard Absolute Quantification (PSAQ) for improved investigation of staphylococcal food poisoning outbreaks. *Proteomics* **8,** 4633-4636.

Earley MC, Vogt RF, Jr., Shapiro HM, Mandy FF, Kellar KL, Bellisario R, Pass KA, Marti GE, Stewart CC, Hannon WH (2002) Report from a workshop on multianalyte microsphere assays. *Cytometry* **50,** 239-242.

Ehehalt R, Keller P, Haass C, Thiele C, Simons K (2003) Amyloidogenic processing of the Alzheimer beta-amyloid precursor protein depends on lipid rafts. *J.Cell Biol.* **160,** 113-123.

Elliott MH, Smith DS, Parker CE, Borchers C (2009) Current trends in quantitative proteomics. *J.Mass Spectrom.* **44,** 1637-1660.

Endres M, Fink K, Zhu J, Stagliano NE, Bondada V, Geddes JW, Azuma T, Mattson MP, Kwiatkowski DJ, Moskowitz MA (1999) Neuroprotective effects of gelsolin during murine stroke. *J.Clin.Invest* **103,** 347-354.

Engstrom G, Hedblad B, Berglund G, Janzon L, Lindgarde F (2007) Plasma levels of complement C3 is associated with development of hypertension: a longitudinal cohort study. *J.Hum.Hypertens.* **21,** 276-282.

Engvall E, Perlmann P (1971) Enzyme-linked immunosorbent assay (ELISA). Quantitative assay of immunoglobulin G. *Immunochemistry.* **8,** 871-874.

Enya M, Morishima-Kawashima M, Yoshimura M, Shinkai Y, Kusui K, Khan K, Games D, Schenk D, Sugihara S, Yamaguchi H, Ihara Y (1999) Appearance of sodium dodecyl sulfate-stable amyloid beta-protein (Abeta) dimer in the cortex during aging. *Am.J.Pathol.* **154,** 271-279.

Ervik M, Hoffmann KJ, Kylberg-Hanssen K (1981) Selected ion monitoring of metoprolol and two metabolites in plasma and urine using deuterated internal standards. *Biomed.Mass Spectrom.* **8(7),** 322-326.

Estrela RC, Ribeiro FS, Seixas BV, Suarez-Kurtz G (2008) Determination of lopinavir and ritonavir in blood plasma, seminal plasma, saliva and plasma ultra-filtrate by liquid chromatography/tandem mass spectrometry detection. *Rapid Commun.Mass Spectrom.* **22,** 657-664.

Fabrizi C, Businaro R, Lauro GM, Starace G, Fumagalli L (1999) Activated alpha2macroglobulin increases beta-amyloid (25-35)-induced toxicity in LAN5 human neuroblastoma cells. *Exp.Neurol.* **155,** 252-259.

Fagan AM, Mintun MA, Mach RH, Lee SY, Dence CS, Shah AR, LaRossa GN, Spinner ML, Klunk WE, Mathis CA, DeKosky ST, Morris JC, Holtzman DM (2006) Inverse relation between in vivo amyloid imaging load and cerebrospinal fluid Abeta42 in humans. *Ann.Neurol.* **59,** 512-519.

Fagan AM, Roe CM, Xiong C, Mintun MA, Morris JC, Holtzman DM (2007) Cerebrospinal fluid tau/beta-amyloid(42) ratio as a prediction of cognitive decline in nondemented older adults. *Arch.Neurol.* **64,** 343-349.

Fan J, Upadhye S, Worster A (2006) Understanding receiver operating characteristic (ROC) curves. *CJEM.* **8(1),** 19-20.

Farkas E, Luiten PG (2001) Cerebral microvascular pathology in aging and Alzheimer's disease. *Prog.Neurobiol.* **64,** 575-611.

Farlow MR, He Y, Tekin S, Xu J, Lane R, Charles HC (2004) Impact of APOE in mild cognitive impairment. *Neurology* **63,** 1898-1901.

Farris W, Mansourian S, Chang Y, Lindsley L, Eckman EA, Frosch MP, Eckman CB, Tanzi RE, Selkoe DJ, Guenette S (2003) Insulin-degrading enzyme regulates the levels of insulin, amyloid beta-protein, and the beta-amyloid precursor protein intracellular domain in vivo. *Proc.Natl.Acad.Sci.U.S.A* **100,** 4162-4167.

Feldman HH, Doody RS, Kivipelto M, Sparks DL, Waters DD, Jones RW, Schwam E, Schindler R, Hey-Hadavi J, DeMicco DA, Breazna A (2010) Randomized controlled trial of atorvastatin in mild to moderate Alzheimer disease: LEADe. *Neurology.* **74(12),** 956-964.

Fenn JB, Mann M, Meng CK, Wong SF, Whitehouse CM (1989) Electrospray ionization for mass spectrometry of large biomolecules. *Science* **246,** 64-71.

Ferri CP, Prince M, Brayne C, Brodaty H, Fratiglioni L, Ganguli M, Hall K, Hasegawa K, Hendrie H, Huang Y, Jorm A, Mathers C, Menezes PR, Rimmer E, Scazufca M (2005) Global prevalence of dementia: a Delphi consensus study. *Lancet* **366,** 2112-2117.

Finney GL, Blackler AR, Hoopmann MR, Canterbury JD, Wu CC, Maccoss MJ (2008) Label-free comparative analysis of proteomics mixtures using chromatographic alignment of high-resolution muLC-MS data. *Anal.Chem.* **80(4),** 961-971.

Fischer B, Grossmann J, Roth V, Gruissem W, Baginsky S, Buhmann JM (2006) Semi-supervised LC/MS alignment for differential proteomics. *Bioinformatics.* **22(14),** e132-e140.

Fleisher AS, Raman R, Siemers ER, Becerra L, Clark CM, Dean RA, Farlow MR, Galvin JE, Peskind ER, Quinn JF, Sherzai A, Sowell BB, Aisen PS, Thal LJ (2008) Phase 2 safety trial targeting amyloid beta production with a gamma-secretase inhibitor in Alzheimer disease. *Arch.Neurol.* **65(8),** 1031-1038.

Fleron M, Greffe Y, Musmeci D, Massart AC, Hennequiere V, Mazzucchelli G, Waltregny D, De Pauw-Gillet MC, Castronovo V, De PE, Turtoi A (2010) Novel post-digest isotope coded protein labeling method for phospho- and glycoproteome analysis. *J.Proteomics.* **73,** 1986-2005.

Foy CM, Nicholas H, Hollingworth P, Boothby H, Willams J, Brown RG, Al-Sarraj S, Lovestone S (2007) Diagnosing Alzheimer's disease--non-clinicians and computerised algorithms together are as accurate as the best clinical practice. *Int.J.Geriatr.Psychiatry* **22,** 1154-1163.

Frank R (2002) The SPOT-synthesis technique. Synthetic peptide arrays on membrane supports--principles and applications. *J.Immunol.Methods* **267,** 13-26.

Fratiglioni L, Launer LJ, Andersen K, Breteler MM, Copeland JR, Dartigues JF, Lobo A, Martinez-Lage J, Soininen H, Hofman A (2000) Incidence of dementia and major subtypes in Europe: A collaborative study of population-based cohorts. Neurologic Diseases in the Elderly Research Group. *Neurology* **54,** S10-S15.

Freije JR, Mulder PP, Werkman W, Rieux L, Niederlander HA, Verpoorte E, Bischoff R (2005) Chemically modified, immobilized trypsin reactor with improved digestion efficiency. *J.Proteome.Res.* **4,** 1805-1813.

French LE, Chonn A, Ducrest D, Baumann B, Belin D, Wohlwend A, Kiss JZ, Sappino AP, Tschopp J, Schifferli JA (1993) Murine clusterin: molecular cloning and mRNA localization of a gene associated with epithelial differentiation processes during embryogenesis. *J.Cell Biol.* **122,** 1119-1130.

Friese MA, Hellwage J, Jokiranta TS, Meri S, Muller-Quernheim HJ, Peter HH, Eibel H, Zipfel PF (2000) Different regulation of factor H and FHL-1/reconectin by inflammatory mediators and expression of the two proteins in rheumatoid arthritis (RA). *Clin.Exp.Immunol.* **121,** 406-415.

Frisardi V, Solfrizzi V, Imbimbo PB, Capurso C, D'Introno A, Colacicco AM, Vendemiale G, Seripa D, Pilotto A, Capurso A, Panza F (2010) Towards disease-modifying treatment of Alzheimer's disease: drugs targeting beta-amyloid. *Curr.Alzheimer Res.* **7(1),** 40-55.

Frisoni GB, Delacourte A (2009) Neuroimaging outcomes in clinical trials in Alzheimer's disease. *J.Nutr.Health Aging* **13,** 209-212.

Fritz IB, Burdzy K, Setchell B, Blaschuk O (1983) Ram rete testis fluid contains a protein (clusterin) which influences cell-cell interactions in vitro. *Biol.Reprod.* **28,** 1173-1188.

Frolich L, Ashwood T, Nilsson J, Eckerwall G (2011) Effects of AZD3480 on cognition in patients with mild-to-moderate Alzheimer's disease: a phase IIb dose-finding study. *J.Alzheimers.Dis.* **24(2),** 363-374.

Fukumoto H, Tennis M, Locascio JJ, Hyman BT, Growdon JH, Irizarry MC (2003) Age but not diagnosis is the main predictor of plasma amyloid beta-protein levels. *Arch.Neurol.* **60,** 958-964.

Fukushima T, Nakamura A, Iwakami N, Nakada Y, Hattori H, Hoki S, Yamaguchi H, Nakagawa M, Terashima N, Narita H (2011) T-817MA, a neuroprotective agent, attenuates the motor and cognitive impairments associated with neuronal degeneration in P301L tau transgenic mice. *Biochem.Biophys.Res.Commun.* **407(4),** 730-734.

Fukuyama R, Mizuno T, Mori S, Nakajima K, Fushiki S, Yanagisawa K (2000) Age-dependent change in the levels of Abeta40 and Abeta42 in cerebrospinal fluid from control subjects, and a decrease in the ratio of Abeta42 to Abeta40 level in cerebrospinal fluid from Alzheimer's disease patients. *Eur.Neurol.* **43,** 155-160.

Furukawa K, Fu W, Li Y, Witke W, Kwiatkowski DJ, Mattson MP (1997) The actin-severing protein gelsolin modulates calcium channel and NMDA receptor activities and vulnerability to excitotoxicity in hippocampal neurons. *J.Neurosci.* **17,** 8178-8186.

Galasko D, Hansen LA, Katzman R, Wiederholt W, Masliah E, Terry R, Hill LR, Lessin P, Thal LJ (1994) Clinical-neuropathological correlations in Alzheimer's disease and related dementias. *Arch.Neurol.* **51,** 888-895.

Galasko D, Chang L, Motter R, Clark CM, Kaye J, Knopman D, Thomas R, Kholodenko D, Schenk D, Lieberburg I, Miller B, Green R, Basherad R, Kertiles L, Boss MA, Seubert P (1998) High cerebrospinal fluid tau and low amyloid beta42 levels in the clinical diagnosis of Alzheimer disease and relation to apolipoprotein E genotype. *Arch.Neurol.* **55,** 937-945.

Gallant M, Aspiotis R, Day S, Dias R, Dube D, Dube L, Friesen RW, Girard M, Guay D, Hamel P, Huang Z, Lacombe P, Laliberte S, Levesque JF, Liu S, Macdonald D, Mancini J, Nicholson DW, Styhler A, Townson K, Waters K, Young RN, Girard Y (2010) Discovery of MK-0952, a selective PDE4 inhibitor for the treatment of long-term memory loss and mild cognitive impairment. *Bioorg.Med.Chem.Lett.* **20(22),** 6387-6393.

Gallien S, Duriez E, Domon B (2011) Selected reaction monitoring applied to proteomics. *J.Mass Spectrom.* **46(3),** 298-312.

Ganea E (2001) Chaperone-like activity of alpha-crystallin and other small heat shock proteins. *Curr.Protein Pept.Sci.* **2,** 205-225.

Ganguli M, Dodge HH, Shen C, DeKosky ST (2004) Mild cognitive impairment, amnestic type: an epidemiologic study. *Neurology* **63,** 115-121.

Gauthier S, Aisen PS, Ferris SH, Saumier D, Duong A, Haine D, Garceau D, Suhy J, Oh J, Lau W, Sampalis J (2009) Effect of tramiprosate in patients with mild-to-moderate Alzheimer's disease: exploratory analyses of the MRI sub-group of the Alphase study. *J.Nutr.Health Aging* **13,** 550-557.

Geldmacher DS, Fritsch T, McClendon MJ, Landreth G (2011) A randomized pilot clinical trial of the safety of pioglitazone in treatment of patients with Alzheimer disease. *Arch.Neurol.* **68(1),** 45-50.

Gerber SA, Rush J, Stemman O, Kirschner MW, Gygi SP (2003) Absolute quantification of proteins and phosphoproteins from cell lysates by tandem MS. *Proc.Natl.Acad.Sci.U.S.A* **100,** 6940-6945.

German DC, Gurnani P, Nandi A, Garner HR, Fisher W, az-Arrastia R, O'Suilleabhain P, Rosenblatt KP (2007) Serum biomarkers for Alzheimer's disease: proteomic discovery. *Biomed.Pharmacother.* **61,** 383-389.

Gervais F, Paquette J, Morissette C, Krzywkowski P, Yu M, Azzi M, Lacombe D, Kong X, Aman A, Laurin J, Szarek WA, Tremblay P (2007) Targeting soluble Abeta peptide with Tramiprosate for the treatment of brain amyloidosis. *Neurobiol.Aging.* **28(4),** 537-547.

Geula C, Mesulam MM (1995) Cholinesterases and the pathology of Alzheimer disease. *Alzheimer Dis.Assoc.Disord.* **9(2),** 23-28.

Gharbi S, Gaffney P, Yang A, Zvelebil MJ, Cramer R, Waterfield MD, Timms JF (2002) Evaluation of two-dimensional differential gel electrophoresis for proteomic expression analysis of a model breast cancer cell system. *Mol.Cell Proteomics.* **1,** 91-98.

Ghiso J, Matsubara E, Koudinov A, Choi-Miura NH, Tomita M, Wisniewski T, Frangione B (1993) The cerebrospinal-fluid soluble form of Alzheimer's amyloid beta is complexed to SP-40,40 (apolipoprotein J), an inhibitor of the complement membrane-attack complex. *Biochem.J.* **293 (1),** 27-30.

Gibson AM, Singleton AB, Smith G, Woodward R, McKeith IG, Perry RH, Ince PG, Ballard CG, Edwardson JA, Morris CM (2000) Lack of association of the alpha2-macroglobulin locus on chromosome 12 in AD. *Neurology* **54,** 433-438.

Gibson GE, Huang HM (2005) Oxidative stress in Alzheimer's disease. *Neurobiol.Aging* **26,** 575-578.

Gillmore JD, Tennent GA, Hutchinson WL, Gallimore JR, Lachmann HJ, Goodman HJ, Offer M, Millar DJ, Petrie A, Hawkins PN, Pepys MB (2010) Sustained pharmacological depletion of serum amyloid P component in patients with systemic amyloidosis. *Br.J.Haematol.* **148(5),** 760-767.

Glen A, Evans CA, Gan CS, Cross SS, Hamdy FC, Gibbins J, Lippitt J, Eaton CL, Noirel J, Wright PC, Rehman I (2010) Eight-plex iTRAQ analysis of variant metastatic human prostate cancer cells identifies candidate biomarkers of progression: An exploratory study. *Prostate* **70,** 1313-1332.

Goedert M, Spillantini MG, Jakes R, Rutherford D, Crowther RA (1989) Multiple isoforms of human microtubule-associated protein tau: sequences and localization in neurofibrillary tangles of Alzheimer's disease. *Neuron* **3,** 519-526.

Goedert M (2004) Tau protein and neurodegeneration. *Semin.Cell Dev.Biol.* **15,** 45-49.

Goedert M, Spillantini MG (2006) A century of Alzheimer's disease. *Science* **314,** 777-781.

Gold M, Alderton C, Zvartau-Hind M, Egginton S, Saunders AM, Irizarry M, Craft S, Landreth G, Linnamagi U, Sawchak S (2010) Rosiglitazone monotherapy in mild-to-moderate Alzheimer's disease: results from a randomized, double-blind, placebo-controlled phase III study. *Dement.Geriatr.Cogn Disord.* **30(2),** 131-146.

Gorshkov AV, Tarasova IA, Evreinov VV, Savitski MM, Nielsen ML, Zubarev RA, Gorshkov MV (2006) Liquid chromatography at critical conditions: comprehensive approach to sequence-dependent retention time prediction. *Anal.Chem.* **78(22),** 7770-7777.

Gotz J, Chen F, van DJ, Nitsch RM (2001) Formation of neurofibrillary tangles in P301l tau transgenic mice induced by Abeta 42 fibrils. *Science* **293,** 1491-1495.

Graff-Radford NR, Crook JE, Lucas J, Boeve BF, Knopman DS, Ivnik RJ, Smith GE, Younkin LH, Petersen RC, Younkin SG (2007) Association of low plasma Abeta42/Abeta40 ratios with increased imminent risk for mild cognitive impairment and Alzheimer disease. *Arch.Neurol.* **64,** 354-362.

Green KN, Steffan JS, Martinez-Coria H, Sun X, Schreiber SS, Thompson LM, LaFerla FM (2008) Nicotinamide restores cognition in Alzheimer's disease transgenic mice via a mechanism involving sirtuin inhibition and selective reduction of Thr231-phosphotau. *J.Neurosci.* **28(45),** 11500-11510.

Green RC, Schneider LS, Amato DA, Beelen AP, Wilcock G, Swabb EA, Zavitz KH (2009) Effect of tarenflurbil on cognitive decline and activities of daily living in patients with mild Alzheimer disease: a randomized controlled trial. *JAMA.* **302(23),** 2557-2564.

Greene JD, Patterson K, Xuereb J, Hodges JR (1996) Alzheimer disease and nonfluent progressive aphasia. *Arch.Neurol.* **53,** 1072-1078.

Grehan S, Tse E, Taylor JM (2001) Two distal downstream enhancers direct expression of the human apolipoprotein E gene to astrocytes in the brain. *J.Neurosci.* **21,** 812-822.

Grimmer T, Riemenschneider M, Forstl H, Henriksen G, Klunk WE, Mathis CA, Shiga T, Wester HJ, Kurz A, Drzezga A (2009) Beta amyloid in Alzheimer's disease: increased deposition in brain is reflected in reduced concentration in cerebrospinal fluid. *Biol.Psychiatry* **65,** 927-934.

Grundman M, Petersen RC, Ferris SH, Thomas RG, Aisen PS, Bennett DA, Foster NL, Jack CR, Jr., Galasko DR, Doody R, Kaye J, Sano M, Mohs R, Gauthier S, Kim HT, Jin S, Schultz AN, Schafer K, Mulnard R, van Dyck CH, Mintzer J, Zamrini EY, Cahn-Weiner D, Thal LJ (2004) Mild cognitive impairment can be distinguished from Alzheimer disease and normal aging for clinical trials. *Arch.Neurol.* **61,** 59-66.

guilar-Mahecha A, Cantin C, O'Connor-McCourt M, Nantel A, Basik M (2009) Development of reverse phase protein microarrays for the validation of clusterin, a mid-abundant blood biomarker. *Proteome.Sci.* **7,** 15.

Guntert A, Campbell J, Saleem M, O'Brien DP, Thompson AJ, Byers HL, Ward MA, Lovestone S (2010) Plasma gelsolin is decreased and correlates with rate of decline in Alzheimer's disease. *J.Alzheimers.Dis.* **21,** 585-596.

Gygi SP, Rist B, Gerber SA, Turecek F, Gelb MH, Aebersold R (1999) Quantitative analysis of complex protein mixtures using isotope-coded affinity tags. *Nat.Biotechnol.* **17,** 994-999.

Haass C, Schlossmacher MG, Hung AY, Vigo-Pelfrey C, Mellon A, Ostaszewski BL, Lieberburg I, Koo EH, Schenk D, Teplow DB, . (1992) Amyloid beta-peptide is produced by cultured cells during normal metabolism. *Nature* **359,** 322-325.

Hageman GS, Anderson DH, Johnson LV, Hancox LS, Taiber AJ, Hardisty LI, Hageman JL, Stockman HA, Borchardt JD, Gehrs KM, Smith RJ, Silvestri G, Russell SR, Klaver CC, Barbazetto I, Chang S, Yannuzzi LA, Barile GR, Merriam JC, Smith RT, Olsh AK, Bergeron J, Zernant J, Merriam JE, Gold B, Dean M, Allikmets R (2005) A common haplotype in the complement regulatory gene factor H (HF1/CFH) predisposes individuals to age-related macular degeneration. *Proc.Natl.Acad.Sci.U.S.A* **102,** 7227-7232.

Hager JW, Yves Le Blanc JC (2003) Product ion scanning using a Q-q-Q linear ion trap (Q TRAP) mass spectrometer. *Rapid Commun.Mass Spectrom.* **17,** 1056-1064.

Hakobyan S, Tortajada A, Harris CL, de C, Sr., Morgan BP (2010) Variant-specific quantification of factor H in plasma identifies null alleles associated with atypical hemolytic uremic syndrome. *Kidney Int.* **78,** 782-788.

Hampel H, Muller-Spahn F, Berger C, Haberl A, Ackenheil M, Hock C (1995) Evidence of blood-cerebrospinal fluid-barrier impairment in a subgroup of patients with dementia of the Alzheimer type and major depression: a possible indicator for immunoactivation. *Dementia* **6,** 348-354.

Hampel H, Mitchell A, Blennow K, Frank RA, Brettschneider S, Weller L, Moller HJ (2004) Core biological marker candidates of Alzheimer's disease - perspectives for diagnosis, prediction of outcome and reflection of biological activity. *J.Neural Transm.* **111,** 247-272.

Han CK, Park YH, Jin DQ, Hwang YK, Oh KB, Han JS (2007) SK-PC-B70M from Pulsatilla koreana improves scopolamine-induced impairments of memory consolidation and spatial working memory. *Brain Res.* **1184,** 254-259.

Hanger DP, Byers HL, Wray S, Leung KY, Saxton MJ, Seereeram A, Reynolds CH, Ward MA, Anderton BH (2007) Novel phosphorylation sites in tau from Alzheimer brain support a role for casein kinase 1 in disease pathogenesis. *J.Biol.Chem.* **282,** 23645-23654.

Hanger DP, Anderton BH, Noble W (2009) Tau phosphorylation: the therapeutic challenge for neurodegenerative disease. *Trends Mol.Med.* **15,** 112-119.

Hanke S, Besir H, Oesterhelt D, Mann M (2008) Absolute SILAC for accurate quantitation of proteins in complex mixtures down to the attomole level. *Journal of Proteome Research* **7,** 1118-1130.

Hanke S, Besir H, Oesterhelt D, Mann M (2008) Absolute SILAC for accurate quantitation of proteins in complex mixtures down to the attomole level. *J.Proteome.Res.* **7(3),** 1118-1130.

Hansen KC, Schmitt-Ulms G, Chalkley RJ, Hirsch J, Baldwin MA, Burlingame AL (2003) Mass spectrometric analysis of protein mixtures at low levels using cleavable 13C-isotope-coded affinity tag and multidimensional chromatography. *Mol.Cell Proteomics.* **2,** 299-314.

Hansson O, Zetterberg H, Buchhave P, Andreasson U, Londos E, Minthon L, Blennow K (2007) Prediction of Alzheimer's disease using the CSF Abeta42/Abeta40 ratio in patients with mild cognitive impairment. *Dement.Geriatr.Cogn Disord.* **23,** 316-320.

Hansson O, Zetterberg H, Vanmechelen E, Vanderstichele H, Andreasson U, Londos E, Wallin A, Minthon L, Blennow K (2010) Evaluation of plasma Abeta(40) and Abeta(42) as predictors of conversion to Alzheimer's disease in patients with mild cognitive impairment. *Neurobiol.Aging* **31,** 357-367.

Haqqani AS, Kelly JF, Stanimirovic DB (2008) Quantitative protein profiling by mass spectrometry using label-free proteomics. *Methods Mol.Biol.* **439,** 241-256.

Hardt M, Witkowska HE, Webb S, Thomas LR, Dixon SE, Hall SC, Fisher SJ (2005) Assessing the effects of diurnal variation on the composition of human parotid saliva: quantitative analysis of native peptides using iTRAQ reagents. *Anal.Chem.* **77,** 4947-4954.

Hardy J, Selkoe DJ (2002) The amyloid hypothesis of Alzheimer's disease: progress and problems on the road to therapeutics. *Science* **297,** 353-356.

Harold D, Abraham R, Hollingworth P, Sims R, Gerrish A, Hamshere ML, Pahwa JS, Moskvina V, Dowzell K, Williams A, Jones N, Thomas C, Stretton A, Morgan AR, Lovestone S, Powell J, Proitsi P, Lupton MK, Brayne C, Rubinsztein DC, Gill M, Lawlor B, Lynch A, Morgan K, Brown KS, Passmore PA, Craig D, McGuinness B, Todd S, Holmes C, Mann D, Smith AD, Love S, Kehoe PG, Hardy J, Mead S, Fox N, Rossor M, Collinge J, Maier W, Jessen F, Schurmann B, van den BH, Heuser I, Kornhuber J, Wiltfang J, Dichgans M, Frolich L, Hampel H, Hull M, Rujescu D, Goate AM, Kauwe JS, Cruchaga C, Nowotny P, Morris JC, Mayo K, Sleegers K, Bettens K, Engelborghs S, De Deyn PP, Van BC, Livingston G, Bass NJ, Gurling H, McQuillin A, Gwilliam R, Deloukas P, Al-Chalabi A, Shaw CE, Tsolaki M, Singleton AB, Guerreiro R, Muhleisen TW, Nothen MM, Moebus S, Jockel KH, Klopp N, Wichmann HE, Carrasquillo MM, Pankratz VS, Younkin SG, Holmans PA, O'Donovan M, Owen MJ, Williams J (2009) Genome-wide association study identifies variants at CLU and PICALM associated with Alzheimer's disease. *Nat.Genet.* **41,** 1088-1093.

Harr SD, Uint L, Hollister R, Hyman BT, Mendez AJ (1996) Brain expression of apolipoproteins E, J, and A-I in Alzheimer's disease. *J.Neurochem.* **66,** 2429-2435.

Hawkins BT, Davis TP (2005) The blood-brain barrier/neurovascular unit in health and disease. *Pharmacol.Rev.* **57,** 173-185.

Hendrix SB, Wilcock GK (2009) What we have learned from the Myriad trials. *J.Nutr.Health Aging.* **13(4),** 362-364.

Henneman WJ, Sluimer JD, Barnes J, van der Flier WM, Sluimer IC, Fox NC, Scheltens P, Vrenken H, Barkhof F (2009) Hippocampal atrophy rates in Alzheimer disease: added value over whole brain volume measures. *Neurology* **72,** 999-1007.

Hermez J, Petrak J, Karkouri M, Riedner G (2010) A review of HIV testing and counseling policies and practices in the Eastern Mediterranean Region. *AIDS* **24 Suppl 2,** S25-S32.

Herrick S, Blanc-Brude O, Gray A, Laurent G (1999) Fibrinogen. *Int.J.Biochem.Cell Biol.* **31,** 741-746.

Heudi O, Barteau S, Zimmer D, Schmidt J, Bill K, Lehmann N, Bauer C, Kretz O (2008) Towards absolute quantification of therapeutic monoclonal antibody in serum by LC-MS/MS using isotope-labeled antibody standard and protein cleavage isotope dilution mass spectrometry. *Analytical Chemistry* **80,** 4200-4207.

Higashi T, Awada D, Shimada K (2001) Simultaneous determination of 25-hydroxyvitamin D2 and 25-hydroxyvitamin D3 in human plasma by liquid chromatography-tandem mass spectrometry employing derivatization with a Cookson-type reagent. *Biol.Pharm.Bull.* **24,** 738-743.

Hirko AC, Meyer EM, King MA, Hughes JA (2007) Peripheral transgene expression of plasma gelsolin reduces amyloid in transgenic mouse models of Alzheimer's disease. *Mol.Ther.* **15,** 1623-1629.

Hixson KK, Rodriguez N, Camp DG, Strittmatter EF, Lipton MS, Smith RD (2002) Evaluation of enzymatic digestion and liquid chromatography-mass spectrometry peptide mapping of the integral membrane protein bacteriorhodopsin. *Electrophoresis.* **23(18),** 3224-3232.

Hollenbach E, Ackermann S, Hyman BT, Rebeck GW (1998) Confirmation of an association between a polymorphism in exon 3 of the low-density lipoprotein receptor-related protein gene and Alzheimer's disease. *Neurology* **50,** 1905-1907.

Hongpaisan J, Sun MK, Alkon DL (2011) PKC epsilon activation prevents synaptic loss, Abeta elevation, and cognitive deficits in Alzheimer's disease transgenic mice. *J.Neurosci.* **31(2),** 630-643.

Hoofnagle AN, Becker JO, Wener MH, Heinecke JW (2008) Quantification of thyroglobulin, a low-abundance serum protein, by immunoaffinity peptide enrichment and tandem mass spectrometry. *Clin.Chem.* **54,** 1796-1804.

Horvatovich P, Hoekman B, Govorukhina N, Bischoff R (2010) Multidimensional chromatography coupled to mass spectrometry in analysing complex proteomics samples. *J.Sep.Sci.* **33,** 1421-1437.

Horwitz B, Warner B, Fitzer J, Tagamets MA, Husain FT, Long TW (2005) Investigating the neural basis for functional and effective connectivity. Application to fMRI. *Philos.Trans.R.Soc.Lond B Biol.Sci.* **360,** 1093-1108.

Hu Q, Noll RJ, Li H, Makarov A, Hardman M, Graham CR (2005) The Orbitrap: a new mass spectrometer. *J.Mass Spectrom.* **40,** 430-443.

Huang JT, McKenna T, Hughes C, Leweke FM, Schwarz E, Bahn S (2007) CSF biomarker discovery using label-free nano-LC-MS based proteomic profiling: technical aspects. *J.Sep.Sci.* **30,** 214-225.

Hughes SR, Khorkova O, Goyal S, Knaeblein J, Heroux J, Riedel NG, Sahasrabudhe S (1998) Alpha2-macroglobulin associates with beta-amyloid peptide and prevents fibril formation. *Proc.Natl.Acad.Sci.U.S.A* **95,** 3275-3280.

Huttenhain R, Malmstrom J, Picotti P, Aebersold R (2009) Perspectives of targeted mass spectrometry for protein biomarker verification. *Curr.Opin.Chem.Biol.* **13,** 518-525.

Hutton M, Lendon CL, Rizzu P, Baker M, Froelich S, Houlden H, Pickering-Brown S, Chakraverty S, Isaacs A, Grover A, Hackett J, Adamson J, Lincoln S, Dickson D, Davies P, Petersen RC, Stevens M, de GE, Wauters E, van BJ, Hillebrand M, Joosse M, Kwon JM, Nowotny P, Che LK, Norton J, Morris JC, Reed LA, Trojanowski J, Basun H, Lannfelt L, Neystat M, Fahn S, Dark F, Tannenberg T, Dodd PR, Hayward N, Kwok JB, Schofield PR, Andreadis A, Snowden J, Craufurd D, Neary D, Owen F, Oostra BA, Hardy J, Goate A, van SJ, Mann D, Lynch T, Heutink P (1998) Association of missense and 5'-splice-site mutations in tau with the inherited dementia FTDP-17. *Nature* **393,** 702-705.

Hye A, Lynham S, Thambisetty M, Causevic M, Campbell J, Byers HL, Hooper C, Rijsdijk F, Tabrizi SJ, Banner S, Shaw CE, Foy C, Poppe M, Archer N, Hamilton G, Powell J, Brown RG, Sham P, Ward M, Lovestone S (2006) Proteome-based plasma biomarkers for Alzheimer's disease. *Brain* **129,** 3042-3050.

Iadecola C (2004) Neurovascular regulation in the normal brain and in Alzheimer's disease. *Nat.Rev.Neurosci.* **5,** 347-360.

Ida N, Hartmann T, Pantel J, Schroder J, Zerfass R, Forstl H, Sandbrink R, Masters CL, Beyreuther K (1996) Analysis of heterogeneous A4 peptides in human cerebrospinal fluid and blood by a newly developed sensitive Western blot assay. *J.Biol.Chem.* **271,** 22908-22914.

Imre T, Schlosser G, Pocsfalvi G, Siciliano R, Molnar-Szollosi E, Kremmer T, Malorni A, Vekey K (2005) Glycosylation site analysis of human alpha-1-acid glycoprotein (AGP) by capillary liquid chromatography-electrospray mass spectrometry. *J.Mass Spectrom.* **40(11),** 1472-1483.

Inestrosa NC, Alarcon R, Arriagada J, Donoso A, Alvarez J, Campos EO (1994) Blood markers in Alzheimer disease: subnormal acetylcholinesterase and butyrylcholinesterase in lymphocytes and erythrocytes. *J.Neurol.Sci.* **122,** 1-5.

Ishiguro K, Ohno H, Arai H, Yamaguchi H, Urakami K, Park JM, Sato K, Kohno H, Imahori K (1999) Phosphorylated tau in human cerebrospinal fluid is a diagnostic marker for Alzheimer's disease. *Neurosci.Lett.* **270,** 91-94.

Ishihama Y, Oda Y, Tabata T, Sato T, Nagasu T, Rappsilber J, Mann M (2005) Exponentially modified protein abundance index (emPAI) for estimation of absolute protein amount in proteomics by the number of sequenced peptides per protein. *Mol.Cell Proteomics* **4,** 1265-1272.

Iwata N, Tsubuki S, Takaki Y, Shirotani K, Lu B, Gerard NP, Gerard C, Hama E, Lee HJ, Saido TC (2001) Metabolic regulation of brain Abeta by neprilysin. *Science* **292,** 1550-1552.

Jack CR, Jr., Petersen RC, Xu YC, O'Brien PC, Smith GE, Ivnik RJ, Boeve BF, Waring SC, Tangalos EG, Kokmen E (1999) Prediction of AD with MRI-based hippocampal volume in mild cognitive impairment. *Neurology* **52,** 1397-1403.

Jack CR, Jr., Slomkowski M, Gracon S, Hoover TM, Felmlee JP, Stewart K, Xu Y, Shiung M, O'Brien PC, Cha R, Knopman D, Petersen RC (2003) MRI as a biomarker of disease progression in a therapeutic trial of milameline for AD. *Neurology* **60,** 253-260.

Jacobsen JS, Comery TA, Martone RL, Elokdah H, Crandall DL, Oganesian A, Aschmies S, Kirksey Y, Gonzales C, Xu J, Zhou H, Atchison K, Wagner E, Zaleska MM, Das I, Arias RL, Bard J, Riddell D, Gardell SJ, Abou-Gharbia M, Robichaud A, Magolda R, Vlasuk GP, Bjornsson T, Reinhart PH, Pangalos MN (2008) Enhanced clearance of Abeta in brain by sustaining the plasmin proteolysis cascade. *Proc.Natl.Acad.Sci.U.S.A.* **105(25),** 8754-8759.

Jaffe JD, Keshishian H, Chang B, Addona TA, Gillette MA, Carr SA (2008) Accurate inclusion mass screening: a bridge from unbiased discovery to targeted assay development for biomarker verification. *Mol.Cell Proteomics.* **7,** 1952-1962.

Jann MW (2000) Rivastigmine, a new-generation cholinesterase inhibitor for the treatment of Alzheimer's disease. *Pharmacotherapy* **20,** 1-12.

Jenne DE, Tschopp J (1989) Molecular structure and functional characterization of a human complement cytolysis inhibitor found in blood and seminal plasma: identity to sulfated glycoprotein 2, a constituent of rat testis fluid. *Proc.Natl.Acad.Sci.U.S.A* **86,** 7123-7127.

Jenne DE, Lowin B, Peitsch MC, Bottcher A, Schmitz G, Tschopp J (1991) Clusterin (complement lysis inhibitor) forms a high density lipoprotein complex with apolipoprotein A-I in human plasma. *J.Biol.Chem.* **266,** 11030-11036.

Jensen M, Hartmann T, Engvall B, Wang R, Uljon SN, Sennvik K, Naslund J, Muehlhauser F, Nordstedt C, Beyreuther K, Lannfelt L (2000) Quantification of Alzheimer amyloid beta peptides ending at residues 40 and 42 by novel ELISA systems. *Mol.Med.* **6,** 291-302.

Ji L, Chauhan A, Chauhan V (2010) Upregulation of cytoplasmic gelsolin, an amyloid-beta-binding protein, under oxidative stress conditions: involvement of protein kinase C. *J.Alzheimers.Dis.* **19,** 829-838.

Jiang Q, Lee CY, Mandrekar S, Wilkinson B, Cramer P, Zelcer N, Mann K, Lamb B, Willson TM, Collins JL, Richardson JC, Smith JD, Comery TA, Riddell D, Holtzman DM, Tontonoz P, Landreth GE (2008) ApoE promotes the proteolytic degradation of Abeta. *Neuron* **58,** 681-693.

Johansson C, Samskog J, Sundstrom L, Wadensten H, Bjorkesten L, Flensburg J (2006) Differential expression analysis of Escherichia coli proteins using a novel software for relative quantitation of LC-MS/MS data. *Proteomics.* **6(16),** 4475-4485.

Johnson GV, Stoothoff WH (2004) Tau phosphorylation in neuronal cell function and dysfunction. *J.Cell Sci.* **117,** 5721-5729.

Johnson LV, Leitner WP, Rivest AJ, Staples MK, Radeke MJ, Anderson DH (2002) The Alzheimer's A beta -peptide is deposited at sites of complement activation in pathologic deposits associated with aging and age-related macular degeneration. *Proc.Natl.Acad.Sci.U.S.A* **99,** 11830-11835.

Jones L, Harold D, Williams J (2010) Genetic evidence for the involvement of lipid metabolism in Alzheimer's disease. *Biochim.Biophys.Acta* **1801,** 754-761.

Jones SE, Jomary C (2002) Clusterin. *Int.J.Biochem.Cell Biol.* **34,** 427-431.

Julka S, Regnier FE (2005) Recent advancements in differential proteomics based on stable isotope coding. *Brief.Funct.Genomic.Proteomic.* **4(2),** 158-177.

Kalaria RN, Grahovac I (1990) Serum amyloid P immunoreactivity in hippocampal tangles, plaques and vessels: implications for leakage across the blood-brain barrier in Alzheimer's disease. *Brain Res.* **516,** 349-353.

Kalaria RN, Galloway PG, Perry G (1991) Widespread serum amyloid P immunoreactivity in cortical amyloid deposits and the neurofibrillary pathology of Alzheimer's disease and other degenerative disorders. *Neuropathol.Appl.Neurobiol.* **17,** 189-201.

Kaliszan R, Baczek T, Cimochowska A, Juszczyk P, Wisniewska K, Grzonka Z (2005) Prediction of high-performance liquid chromatography retention of peptides with the use of quantitative structure-retention relationships. *Proteomics.* **5(2),** 409-415.

Kanai M, Matsubara E, Isoe K, Urakami K, Nakashima K, Arai H, Sasaki H, Abe K, Iwatsubo T, Kosaka T, Watanabe M, Tomidokoro Y, Shizuka M, Mizushima K, Nakamura T, Igeta Y, Ikeda Y, Amari M, Kawarabayashi T, Ishiguro K, Harigaya Y, Wakabayashi K, Okamoto K, Hirai S, Shoji M (1998) Longitudinal study of cerebrospinal fluid levels of tau, A beta1-40, and A beta1-42(43) in Alzheimer's disease: a study in Japan. *Ann.Neurol.* **44,** 17-26.

Kang J, Lemaire HG, Unterbeck A, Salbaum JM, Masters CL, Grzeschik KH, Multhaup G, Beyreuther K, Muller-Hill B (1987) The precursor of Alzheimer's disease amyloid A4 protein resembles a cell-surface receptor. *Nature* **325,** 733-736.

Kang UB, Ahn Y, Lee JW, Kim YH, Kim J, Yu MH, Noh DY, Lee C (2010) Differential profiling of breast cancer plasma proteome by isotope-coded affinity tagging method reveals biotinidase as a breast cancer biomarker. *BMC.Cancer* **10,** 114.

Kang X, Sun L, Guo K, Shu H, Yao J, Qin X, Liu Y (2010) Serum protein biomarkers screening in HCC patients with liver cirrhosis by ICAT-LC-MS/MS. *J.Cancer Res.Clin.Oncol.* **136,** 1151-1159.

Karas M, Hillenkamp F (1988) Laser desorption ionization of proteins with molecular masses exceeding 10,000 daltons. *Anal.Chem.* **60,** 2299-2301.

Karlawish JH, Clark CM (2003) Diagnostic evaluation of elderly patients with mild memory problems. *Ann.Intern.Med.* **138,** 411-419.

Karp NA, Huber W, Sadowski PG, Charles PD, Hester SV, Lilley KS (2010) Addressing accuracy and precision issues in iTRAQ quantitation. *Mol.Cell Proteomics.* **9(9),** 1885-1897.

Katz R (2004) Biomarkers and surrogate markers: an FDA perspective. *NeuroRx.* **1,** 189-195.

Kauwe JS, Cruchaga C, Mayo K, Fenoglio C, Bertelsen S, Nowotny P, Galimberti D, Scarpini E, Morris JC, Fagan AM, Holtzman DM, Goate AM (2008) Variation in MAPT is associated with cerebrospinal fluid tau levels in the presence of amyloid-beta deposition. *Proc.Natl.Acad.Sci.U.S.A.* **105(23),** 8050-8054.

Kawarabayashi T, Shoji M (2008) Plasma biomarkers of Alzheimer's disease. *Curr.Opin.Psychiatry* **21,** 260-267.

Kay RG, Creaser CS (2010) Application of mass spectrometry-based proteomics techniques for the detection of protein doping in sports. *Expert.Rev.Proteomics.* **7,** 185-188.

Kaye JA, Moore MM, Dame A, Quinn J, Camicioli R, Howieson D, Corbridge E, Care B, Nesbit G, Sexton G (2005) Asynchronous regional brain volume losses in presymptomatic to moderate AD. *J.Alzheimers.Dis.* **8,** 51-56.

Kennedy JH, Aurand C, Shirey R, Laughlin BC, Wiseman JM (2010) Coupling desorption electrospray ionization with solid-phase microextraction for screening and quantitative analysis of drugs in urine. *Anal.Chem.* **82,** 7502-7508.

Keshishian H, Addona T, Burgess M, Kuhn E, Carr SA (2007) Quantitative, multiplexed assays for low abundance proteins in plasma by targeted mass spectrometry and stable isotope dilution. *Mol.Cell Proteomics.* **6,** 2212-2229.

Kida E, Pluta R, Lossinsky AS, Golabek AA, Choi-Miura NH, Wisniewski HM, Mossakowski MJ (1995) Complete cerebral ischemia with short-term survival in rat induced by cardiac arrest. II. Extracellular and intracellular accumulation of apolipoproteins E and J in the brain. *Brain Res.* **674,** 341-346.

KIDD M (1963) Paired helical filaments in electron microscopy of Alzheimer's disease. *Nature* **197,** 192-193.

Kim J, Basak JM, Holtzman DM (2009) The role of apolipoprotein E in Alzheimer's disease. *Neuron* **63,** 287-303.

Kirk A, Kertesz A (1991) On drawing impairment in Alzheimer's disease. *Arch.Neurol.* **48,** 73-77.

Kirkpatrick DS, Gerber SA, Gygi SP (2005) The absolute quantification strategy: a general procedure for the quantification of proteins and post-translational modifications. *Methods* **35,** 265-273.

Kirszbaum L, Bozas SE, Walker ID (1992) SP-40,40, a protein involved in the control of the complement pathway, possesses a unique array of disulphide bridges. *FEBS Lett.* **297,** 70-76.

Kito K, Ota K, Fujita T, Ito T (2007) A synthetic protein approach toward accurate mass spectrometric quantification of component stoichiometry of multiprotein complexes. *J.Proteome Res.* **6,** 792-800.

Kiyonami R, Schoen A, Prakash A, Peterman S, Zabrouskov V, Picotti P, Aebersold R, Huhmer A, Domon B (2011) Increased selectivity, analytical precision, and throughput in targeted proteomics. *Mol.Cell Proteomics.* **10,** M110.

Klose J, Spielmann H (1975) Gel isoelectric focusing of mouse lactate dehydrogenase: heterogeneity of the isoenzymes A4 and X4. *Biochem.Genet.* **13,** 707-720.

Klunk WE, Engler H, Nordberg A, Wang Y, Blomqvist G, Holt DP, Bergstrom M, Savitcheva I, Huang GF, Estrada S, Ausen B, Debnath ML, Barletta J, Price JC, Sandell J, Lopresti BJ, Wall A, Koivisto P, Antoni G, Mathis CA, Langstrom B (2004) Imaging brain amyloid in Alzheimer's disease with Pittsburgh Compound-B. *Ann.Neurol.* **55,** 306-319.

Koal T, Burhenne H, Romling R, Svoboda M, Resch K, Kaever V (2005) Quantification of antiretroviral drugs in dried blood spot samples by means of liquid chromatography/tandem mass spectrometry. *Rapid Commun.Mass Spectrom.* **19,** 2995-3001.

Koehler CJ, Strozynski M, Kozielski F, Treumann A, Thiede B (2009) Isobaric peptide termini labeling for MS/MS-based quantitative proteomics. *J.Proteome.Res.* **8(9),** 4333-4341.

Koehler CJ, Arntzen MO, Strozynski M, Treumann A, Thiede B (2011) Isobaric peptide termini labeling utilizing site-specific N-terminal succinylation. *Anal.Chem.* **83(12),** 4775-4781.

Kohnken R, Buerger K, Zinkowski R, Miller C, Kerkman D, DeBernardis J, Shen J, Moller HJ, Davies P, Hampel H (2000) Detection of tau phosphorylated at threonine 231 in cerebrospinal fluid of Alzheimer's disease patients. *Neurosci.Lett.* **287,** 187-190.

Kolla V, Jeno P, Moes S, Tercanli S, Lapaire O, Choolani M, Hahn S (2010) Quantitative proteomics analysis of maternal plasma in Down syndrome pregnancies using isobaric tagging reagent (iTRAQ). *J.Biomed.Biotechnol.* **2010,** e952047.

Kolstoe SE, Ridha BH, Bellotti V, Wang N, Robinson CV, Crutch SJ, Keir G, Kukkastenvehmas R, Gallimore JR, Hutchinson WL, Hawkins PN, Wood SP, Rossor MN, Pepys MB (2009) Molecular dissection of Alzheimer's disease neuropathology by depletion of serum amyloid P component. *Proc.Natl.Acad.Sci.U.S.A* **106,** 7619-7623.

Kondo T, Hirohashi S (2009) Application of 2D-DIGE in cancer proteomics toward personalized medicine. *Methods Mol.Biol.* **577,** 135-154.

Koopman K, Le BN, Martin JJ, Nagels G, De Deyn PP, Engelborghs S (2009) Improved discrimination of autopsy-confirmed Alzheimer's disease (AD) from non-AD dementias using CSF P-tau(181P). *Neurochem.Int.* **55,** 214-218.

Korolainen MA, Goldsteins G, Nyman TA, Alafuzoff I, Koistinaho J, Pirttila T (2006) Oxidative modification of proteins in the frontal cortex of Alzheimer's disease brain. *Neurobiol.Aging* **27,** 42-53.

Kosik KS, Joachim CL, Selkoe DJ (1986) Microtubule-associated protein tau (tau) is a major antigenic component of paired helical filaments in Alzheimer disease. *Proc.Natl.Acad.Sci.U.S.A* **83,** 4044-4048.

Kothakota S, Azuma T, Reinhard C, Klippel A, Tang J, Chu K, McGarry TJ, Kirschner MW, Koths K, Kwiatkowski DJ, Williams LT (1997) Caspase-3-generated fragment of gelsolin: effector of morphological change in apoptosis. *Science* **278,** 294-298.

Kovacs DM (2000) alpha2-macroglobulin in late-onset Alzheimer's disease. *Exp.Gerontol.* **35,** 473-479.

Koya RC, Fujita H, Shimizu S, Ohtsu M, Takimoto M, Tsujimoto Y, Kuzumaki N (2000) Gelsolin inhibits apoptosis by blocking mitochondrial membrane potential loss and cytochrome c release. *J.Biol.Chem.* **275,** 15343-15349.

Krokhin OV (2006) Sequence-specific retention calculator. Algorithm for peptide retention prediction in ion-pair RP-HPLC: application to 300- and 100-A pore size C18 sorbents. *Anal.Chem.* **78(22),** 7785-7795.

Kronkvist K, Gustavsson M, Wendel AK, Jaegfeldt H (1998) Automated sample preparation for the determination of budesonide in plasma samples by liquid chromatography and tandem mass spectrometry. *J.Chromatogr.A* **823,** 401-409.

Kuhn E, Wu J, Karl J, Liao H, Zolg W, Guild B (2004) Quantification of C-reactive protein in the serum of patients with rheumatoid arthritis using multiple reaction monitoring mass spectrometry and 13C-labeled peptide standards. *Proteomics.* **4,** 1175-1186.

Kuhn E, Addona T, Keshishian H, Burgess M, Mani DR, Lee RT, Sabatine MS, Gerszten RE, Carr SA (2009) Developing multiplexed assays for troponin I and interleukin-33 in plasma by peptide immunoaffinity enrichment and targeted mass spectrometry. *Clin.Chem.* **55,** 1108-1117.

Kuo YM, Emmerling MR, Lampert HC, Hempelman SR, Kokjohn TA, Woods AS, Cotter RJ, Roher AE (1999) High levels of circulating Abeta42 are sequestered by plasma proteins in Alzheimer's disease. *Biochem.Biophys.Res.Commun.* **257,** 787-791.

Kuzumaki N, Tanaka M, Sakai N, Fujita H (1997) [Tumor suppressive function of gelsolin]. *Gan To Kagaku Ryoho* **24,** 1436-1441.

Kuzyk MA, Ohlund LB, Elliott MH, Smith D, Qian H, Delaney A, Hunter CL, Borchers CH (2009) A comparison of MS/MS-based, stable-isotope-labeled, quantitation performance on ESI-quadrupole TOF and MALDI-TOF/TOF mass spectrometers. *Proteomics.* **9,** 3328-3340.

Kwiatkowski DJ, Mehl R, Yin HL (1988) Genomic organization and biosynthesis of secreted and cytoplasmic forms of gelsolin. *J.Cell Biol.* **106,** 375-384.

Labie C, Canolle B, Chatelin S, Lafon C, Fournier J (2006) Effects of paliroden (SR57667B) and xaliproden on adult brain neurogenesis. *Curr.Alzheimer Res.* **3(1),** 35-36.

LaDu MJ, Shah JA, Reardon CA, Getz GS, Bu G, Hu J, Guo L, Van Eldik LJ (2001) Apolipoprotein E and apolipoprotein E receptors modulate A beta-induced glial neuroinflammatory responses. *Neurochem.Int.* **39,** 427-434.

LaFerla FM, Green KN, Oddo S (2007) Intracellular amyloid-beta in Alzheimer's disease. *Nat.Rev.Neurosci.* **8(7),** 499-509.

Lalvani A (2007) Diagnosing tuberculosis infection in the 21st century: new tools to tackle an old enemy. *Chest* **131,** 1898-1906.

Lalvani A, Pareek M (2010) Interferon gamma release assays: principles and practice. *Enferm.Infecc.Microbiol.Clin.* **28,** 245-252.

Lambert JC, Heath S, Even G, Campion D, Sleegers K, Hiltunen M, Combarros O, Zelenika D, Bullido MJ, Tavernier B, Letenneur L, Bettens K, Berr C, Pasquier F, Fievet N, Barberger-Gateau P, Engelborghs S, De DP, Mateo I, Franck A, Helisalmi S, Porcellini E, Hanon O, de Pancorbo MM, Lendon C, Dufouil C, Jaillard C, Leveillard T, Alvarez V, Bosco P, Mancuso M, Panza F, Nacmias B, Bossu P, Piccardi P, Annoni G, Seripa D, Galimberti D, Hannequin D, Licastro F, Soininen H, Ritchie K, Blanche H, Dartigues JF, Tzourio C, Gut I, Van BC, Alperovitch A, Lathrop M, Amouyel P (2009) Genome-wide association study identifies variants at CLU and CR1 associated with Alzheimer's disease. *Nat.Genet.* **41,** 1094-1099.

Lange V, Picotti P, Domon B, Aebersold R (2008) Selected reaction monitoring for quantitative proteomics: a tutorial. *Mol.Syst.Biol.* **4,** 222.

Le F, I, Laumet G, Richard F, Fievet N, Berr C, Rouaud O, Delcourt C, Amouyel P, Lambert JC (2010) Association study of the CFH Y402H polymorphism with Alzheimer's disease. *Neurobiol.Aging* **31,** 165-166.

Ledesma MD, Da Silva JS, Crassaerts K, Delacourte A, De SB, Dotti CG (2000) Brain plasmin enhances APP alpha-cleavage and Abeta degradation and is reduced in Alzheimer's disease brains. *EMBO Rep.* **1,** 530-535.

Lee H, Swanwick GR, Coen RF, Lawlor BA (1996) Use of the clock drawing task in the diagnosis of mild and very mild Alzheimer's disease. *Int.Psychogeriatr.* **8,** 469-476.

Lee JW, Devanarayan V, Barrett YC, Weiner R, Allinson J, Fountain S, Keller S, Weinryb I, Green M, Duan L, Rogers JA, Millham R, O'Brien PJ, Sailstad J, Khan M, Ray C, Wagner JA (2006) Fit-for-purpose method development and validation for successful biomarker measurement. *Pharm.Res.* **23,** 312-328.

Lee JW, Namkoong H, Kim HK, Kim S, Hwang DW, Na HR, Ha SA, Kim JR, Kim JW (2007) Fibrinogen gamma-A chain precursor in CSF: a candidate biomarker for Alzheimer's disease. *BMC.Neurol.* **7,** 14.

Lee JW, Namkoong H, Kim HK, Kim S, Hwang DW, Na HR, Ha SA, Kim JR, Kim JW (2007) Fibrinogen gamma-A chain precursor in CSF: a candidate biomarker for Alzheimer's disease. *BMC.Neurol.* **7,** 14.

Lee VM, Goedert M, Trojanowski JQ (2001) Neurodegenerative tauopathies. *Annu.Rev.Neurosci.* **24,** 1121-1159.

Lefranc D, Vermersch P, Dallongeville J, ems-Monpeurt C, Petit H, Delacourte A (1996) Relevance of the quantification of apolipoprotein E in the cerebrospinal fluid in Alzheimer's disease. *Neurosci.Lett.* **212,** 91-94.

Lehr T, Staab A, Tillmann C, Trommeshauser D, Raschig A, Schaefer HG, Kloft C (2007) Population pharmacokinetic modelling of NS2330 (tesofensine) and its major metabolite in patients with Alzheimer's disease. *Br.J.Clin.Pharmacol.* **64(1),** 36-48.

Leissring MA, Farris W, Chang AY, Walsh DM, Wu X, Sun X, Frosch MP, Selkoe DJ (2003) Enhanced proteolysis of beta-amyloid in APP transgenic mice prevents plaque formation, secondary pathology, and premature death. *Neuron* **40,** 1087-1093.

Leng SX, McElhaney JE, Walston JD, Xie D, Fedarko NS, Kuchel GA (2008) ELISA and multiplex technologies for cytokine measurement in inflammation and aging research. *J.Gerontol.A Biol.Sci.Med.Sci.* **63,** 879-884.

Lengqvist J, Andrade J, Yang Y, Alvelius G, Lewensohn R, Lehtio J (2009) Robustness and accuracy of high speed LC-MS separations for global peptide quantitation and biomarker discovery. *J.Chromatogr.B Analyt.Technol.Biomed.Life Sci.* **877,** 1306-1316.

Leroy B, Rosier C, Erculisse V, Leys N, Mergeay M, Wattiez R (2010) Differential proteomic analysis using isotope-coded protein-labeling strategies: comparison, improvements and application to simulated microgravity effect on Cupriavidus metallidurans CH34. *Proteomics.* **10,** 2281-2291.

Levin Y, Schwarz E, Wang L, Leweke FM, Bahn S (2007) Label-free LC-MS/MS quantitative proteomics for large-scale biomarker discovery in complex samples. *J.Sep.Sci.* **30,** 2198-2203.

Lewczuk P, Esselmann H, Otto M, Maler JM, Henkel AW, Henkel MK, Eikenberg O, Antz C, Krause WR, Reulbach U, Kornhuber J, Wiltfang J (2004) Neurochemical diagnosis of Alzheimer's dementia by CSF Abeta42, Abeta42/Abeta40 ratio and total tau. *Neurobiol.Aging* **25,** 273-281.

Lewczuk P, Hornegger J, Zimmermann R, Otto M, Wiltfang J, Kornhuber J (2008) Neurochemical dementia diagnostics: assays in CSF and blood. *Eur.Arch.Psychiatry Clin.Neurosci.* **258(5),** 44-49.

Liu F, Grundke-Iqbal I, Iqbal K, Gong CX (2005) Contributions of protein phosphatases PP1, PP2A, PP2B and PP5 to the regulation of tau phosphorylation. *Eur.J.Neurosci.* **22,** 1942-1950.

Liu F, Grundke-Iqbal I, Iqbal K, Gong CX (2005) Contributions of protein phosphatases PP1, PP2A, PP2B and PP5 to the regulation of tau phosphorylation. *Eur.J.Neurosci.* **22(8),** 1942-1950.

Liu H, Sadygov RG, Yates JR, III (2004) A model for random sampling and estimation of relative protein abundance in shotgun proteomics. *Anal.Chem.* **76,** 4193-4201.

Liu T, Qian WJ, Strittmatter EF, Camp DG, Anderson GA, Thrall BD, Smith RD (2004) High-throughput comparative proteome analysis using a quantitative cysteinyl-peptide enrichment technology. *Anal.Chem.* **76(18),** 5345-5353.

Locascio JJ, Fukumoto H, Yap L, Bottiglieri T, Growdon JH, Hyman BT, Irizarry MC (2008) Plasma amyloid beta-protein and C-reactive protein in relation to the rate of progression of Alzheimer disease. *Arch.Neurol.* **65,** 776-785.

Lopez-Ferrer D, Petritis K, Lourette NM, Clowers B, Hixson KK, Heibeck T, Prior DC, Pasa-Tolic L, Camp DG, Belov ME, Smith RD (2008) On-line digestion system for protein characterization and proteome analysis. *Anal.Chem.* **80,** 8930-8936.

Lopez MF, Kuppusamy R, Sarracino DA, Prakash A, Athanas M, Krastins B, Rezai T, Sutton JN, Peterman S, Nicolaides K (2011) Mass spectrometric discovery and selective reaction monitoring (SRM) of putative protein biomarker candidates in first trimester Trisomy 21 maternal serum. *J.Proteome.Res.* **10,** 133-142.

Lopez OL, Kuller LH, Mehta PD, Becker JT, Gach HM, Sweet RA, Chang YF, Tracy R, DeKosky ST (2008) Plasma amyloid levels and the risk of AD in normal subjects in the Cardiovascular Health Study. *Neurology* **70,** 1664-1671.

Lovely RS, Kazmierczak SC, Massaro JM, D'Agostino RB, Sr., O'Donnell CJ, Farrell DH (2010) Gamma' fibrinogen: evaluation of a new assay for study of associations with cardiovascular disease. *Clin.Chem.* **56,** 781-788.

Lovestone S, Francis P, Kloszewska I, Mecocci P, Simmons A, Soininen H, Spenger C, Tsolaki M, Vellas B, Wahlund LO, Ward M (2009) AddNeuroMed--the European collaboration for the discovery of novel biomarkers for Alzheimer's disease. *Ann.N.Y.Acad.Sci.* **1180,** 36-46.

Lue LF, Kuo YM, Roher AE, Brachova L, Shen Y, Sue L, Beach T, Kurth JH, Rydel RE, Rogers J (1999) Soluble amyloid beta peptide concentration as a predictor of synaptic change in Alzheimer's disease. *Am.J.Pathol.* **155,** 853-862.

Maarouf CL, Andacht TM, Kokjohn TA, Castano EM, Sue LI, Beach TG, Roher AE (2009) Proteomic analysis of Alzheimer's disease cerebrospinal fluid from neuropathologically diagnosed subjects. *Curr.Alzheimer Res.* **6,** 399-406.

Maclean B, Tomazela DM, Abbatiello SE, Zhang S, Whiteaker JR, Paulovich AG, Carr SA, Maccoss MJ (2010) Effect of collision energy optimization on the measurement of peptides by selected reaction monitoring (SRM) mass spectrometry. *Anal.Chem.* **82,** 10116-10124.

Maeda S, Sahara N, Saito Y, Murayama M, Yoshiike Y, Kim H, Miyasaka T, Murayama S, Ikai A, Takashima A (2007) Granular tau oligomers as intermediates of tau filaments. *Biochemistry* **46,** 3856-3861.

Maher-Edwards G, Zvartau-Hind M, Hunter AJ, Gold M, Hopton G, Jacobs G, Davy M, Williams P (2010) Double-blind, controlled phase II study of a 5-HT6 receptor antagonist, SB-742457, in Alzheimer's disease. *Curr.Alzheimer Res.* **7(5),** 374-385.

Mahley RW, Weisgraber KH, Huang Y (2006) Apolipoprotein E4: a causative factor and therapeutic target in neuropathology, including Alzheimer's disease. *Proc.Natl.Acad.Sci.U.S.A* **103,** 5644-5651.

Maier M, Peng Y, Jiang L, Seabrook TJ, Carroll MC, Lemere CA (2008) Complement C3 deficiency leads to accelerated amyloid beta plaque deposition and neurodegeneration and modulation of the microglia/macrophage phenotype in amyloid precursor protein transgenic mice. *J.Neurosci.* **28,** 6333-6341.

Makarov A (2000) Electrostatic axially harmonic orbital trapping: a high-performance technique of mass analysis. *Anal.Chem.* **72,** 1156-1162.

Mallick P, Schirle M, Chen SS, Flory MR, Lee H, Martin D, Ranish J, Raught B, Schmitt R, Werner T, Kuster B, Aebersold R (2007) Computational prediction of proteotypic peptides for quantitative proteomics. *Nat.Biotechnol.* **25,** 125-131.

Manza LL, Stamer SL, Ham AJ, Codreanu SG, Liebler DC (2005) Sample preparation and digestion for proteomic analyses using spin filters. *Proteomics.* **5(7),** 1742-1745.

Marksteiner J, Kemmler G, Weiss EM, Knaus G, Ullrich C, Mechtcheriakov S, Oberbauer H, Auffinger S, Hinterholzl J, Hinterhuber H, Humpel C (2009) Five out of 16 plasma signaling proteins are enhanced in plasma of patients with mild cognitive impairment and Alzheimer's disease. *Neurobiol.Aging*. Epub ahead of print.

Marlar RA, Kressin DC (1989) Activated protein C is not regulated by alpha-2-macroglobulin in plasma. *Thromb.Res.* **54,** 177-185.

Martin B, Brenneman R, Becker KG, Gucek M, Cole RN, Maudsley S (2008) iTRAQ analysis of complex proteome alterations in 3xTgAD Alzheimer's mice: understanding the interface between physiology and disease. *PLoS.One.* **3,** e2750.

Martin DB, Holzman T, May D, Peterson A, Eastham A, Eng J, McIntosh M (2008) MRMer, an interactive open source and cross-platform system for data extraction and visualization of multiple reaction monitoring experiments. *Mol.Cell Proteomics.* **7(11),** 2270-2278.

Masters CL, Multhaup G, Simms G, Pottgiesser J, Martins RN, Beyreuther K (1985) Neuronal origin of a cerebral amyloid: neurofibrillary tangles of Alzheimer's disease contain the same protein as the amyloid of plaque cores and blood vessels. *EMBO J.* **4,** 2757-2763.

Matsubara E, Soto C, Governale S, Frangione B, Ghiso J (1996) Apolipoprotein J and Alzheimer's amyloid beta solubility. *Biochem.J.* **316 (2),** 671-679.

Matsuoka Y, Saito M, LaFrancois J, Saito M, Gaynor K, Olm V, Wang L, Casey E, Lu Y, Shiratori C, Lemere C, Duff K (2003) Novel therapeutic approach for the treatment of Alzheimer's disease by peripheral administration of agents with an affinity to beta-amyloid. *J.Neurosci.* **23,** 29-33.

Matthijs G, Marynen P (1991) A deletion polymorphism in the human alpha-2-macroglobulin (A2M) gene. *Nucleic Acids Res.* **19,** 5102.

Mattsson N, Zetterberg H, Hansson O, Andreasen N, Parnetti L, Jonsson M, Herukka SK, van der Flier WM, Blankenstein MA, Ewers M, Rich K, Kaiser E, Verbeek M, Tsolaki M, Mulugeta E, Rosen E, Aarsland D, Visser PJ, Schroder J, Marcusson J, de LM, Hampel H, Scheltens P, Pirttila T, Wallin A, Jonhagen ME, Minthon L, Winblad B, Blennow K (2009) CSF biomarkers and incipient Alzheimer disease in patients with mild cognitive impairment. *JAMA* **302,** 385-393.

Maury CP, Sletten K, Totty N, Kangas H, Liljestrom M (1997) Identification of the circulating amyloid precursor and other gelsolin metabolites in patients with G654A mutation in the gelsolin gene (Finnish familial amyloidosis): pathogenetic and diagnostic implications. *Lab Invest* **77,** 299-304.

Maurya P, Meleady P, Dowling P, Clynes M (2007) Proteomic approaches for serum biomarker discovery in cancer. *Anticancer Res.* **27,** 1247-1255.

May PC, Lampert-Etchells M, Johnson SA, Poirier J, Masters JN, Finch CE (1990) Dynamics of gene expression for a hippocampal glycoprotein elevated in Alzheimer's disease and in response to experimental lesions in rat. *Neuron* **5,** 831-839.

Mayeux R, Saunders AM, Shea S, Mirra S, Evans D, Roses AD, Hyman BT, Crain B, Tang MX, Phelps CH (1998) Utility of the apolipoprotein E genotype in the diagnosis of Alzheimer's disease. Alzheimer's Disease Centers Consortium on Apolipoprotein E and Alzheimer's Disease. *N.Engl.J.Med.* **338,** 506-511.

Mayeux R (2003) Epidemiology of neurodegeneration. *Annu.Rev.Neurosci.* **26,** 81-104.

Mayeux R, Honig LS, Tang MX, Manly J, Stern Y, Schupf N, Mehta PD (2003) Plasma A[beta]40 and A[beta]42 and Alzheimer's disease: relation to age, mortality, and risk. *Neurology* **61,** 1185-1190.

Mazurov A, Hauser T, Miller CH (2006) Selective alpha7 nicotinic acetylcholine receptor ligands. *Curr.Med.Chem.* **13(13),** 1567-1584.

Mc Donald JM, Savva GM, Brayne C, Welzel AT, Forster G, Shankar GM, Selkoe DJ, Ince PG, Walsh DM (2010) The presence of sodium dodecyl sulphate-stable Abeta dimers is strongly associated with Alzheimer-type dementia. *Brain* **133,** 1328-1341.

McCarten JR (1997) Recognizing dementia in the clinic: whom to suspect, whom to test. *Geriatrics* **52(2),** S17-S21.

McKhann G, Drachman D, Folstein M, Katzman R, Price D, Stadlan EM (1984) Clinical diagnosis of Alzheimer's disease: report of the NINCDS-ADRDA Work Group under the auspices of Department of Health and Human Services Task Force on Alzheimer's Disease. *Neurology* **34,** 939-944.

McLuckey SA, Van Berkel GJ, Goeringer DE, Glish GL (1994) Ion trap mass spectrometry. Using high-pressure ionization. *Anal.Chem.* **66,** 737A-743A.

Mead JA, Bianco L, Ottone V, Barton C, Kay RG, Lilley KS, Bond NJ, Bessant C (2009) MRMaid, the web-based tool for designing multiple reaction monitoring (MRM) transitions. *Mol.Cell Proteomics.* **8(4),** 696-705.

Mecocci P, Cherubini A, Bregnocchi M, Chionne F, Cecchetti R, Lowenthal DT, Senin U (1998) Tau protein in cerebrospinal fluid: a new diagnostic and prognostic marker in Alzheimer disease? *Alzheimer Dis.Assoc.Disord.* **12,** 211-214.

Mehta PD, Pirttila T, Mehta SP, Sersen EA, Aisen PS, Wisniewski HM (2000) Plasma and cerebrospinal fluid levels of amyloid beta proteins 1-40 and 1-42 in Alzheimer disease. *Arch.Neurol.* **57,** 100-105.

Mirzaei H, McBee JK, Watts J, Aebersold R (2008) Comparative evaluation of current peptide production platforms used in absolute quantification in proteomics. *Molecular and Cellular Proteomics* **7,** 813-823.

Mise M, Yadera S, Matsuda M, Hashizume T, Matsumoto S, Terauchi Y, Fujii T (2004) Polymorphic expression of CYP1A2 leading to interindividual variability in metabolism of a novel benzodiazepine receptor partial inverse agonist in dogs. *Drug Metab Dispos.* **32(2),** 240-245.

Modrego PJ (2006) Predictors of conversion to dementia of probable Alzheimer type in patients with mild cognitive impairment. *Curr.Alzheimer Res.* **3,** 161-170.

Molina L, Touchon J, Herpe M, Lefranc D, Duplan L, Cristol JP, Sabatier R, Vermersch P, Pau B, Mourton-Gilles C (1999) Tau and apo E in CSF: potential aid for discriminating Alzheimer's disease from other dementias. *Neuroreport* **10,** 3491-3495.

Moore LJ, Machlan LA (1972) High accuracy determination of calcium in blood serum by isotope dilution mass spectrometry. *Anal.Chem.* **44,** 2291-2296.

Moore SM, Hanlon CA (2010) Rabies-specific antibodies: measuring surrogates of protection against a fatal disease. *PLoS.Negl.Trop.Dis.* **4,** e595.

Mor G, Visintin I, Lai Y, Zhao H, Schwartz P, Rutherford T, Yue L, Bray-Ward P, Ward DC (2005) Serum protein markers for early detection of ovarian cancer. *Proc.Natl.Acad.Sci.U.S.A* **102,** 7677-7682.

Morgan E, Varro R, Sepulveda H, Ember JA, Apgar J, Wilson J, Lowe L, Chen R, Shivraj L, Agadir A, Campos R, Ernst D, Gaur A (2004) Cytometric bead array: a multiplexed assay platform with applications in various areas of biology. *Clin.Immunol.* **110,** 252-266.

Mori T, Town T, Tan J, Yada N, Horikoshi Y, Yamamoto J, Shimoda T, Kamanaka Y, Tateishi N, Asano T (2006) Arundic Acid ameliorates cerebral amyloidosis and gliosis in Alzheimer transgenic mice. *J.Pharmacol.Exp.Ther.* **318(2),** 571-578.

Mosesson MW (2003) Fibrinogen gamma chain functions. *J.Thromb.Haemost.* **1,** 231-238.

Motter R, Vigo-Pelfrey C, Kholodenko D, Barbour R, Johnson-Wood K, Galasko D, Chang L, Miller B, Clark C, Green R, . (1995) Reduction of beta-amyloid peptide42 in the cerebrospinal fluid of patients with Alzheimer's disease. *Ann.Neurol.* **38,** 643-648.

Mulder M, Ravid R, Swaab DF, de Kloet ER, Haasdijk ED, Julk J, van der Boom JJ, Havekes LM (1998) Reduced levels of cholesterol, phospholipids, and fatty acids in cerebrospinal fluid of Alzheimer disease patients are not related to apolipoprotein E4. *Alzheimer Dis.Assoc.Disord.* **12,** 198-203.

Muller-Eberhard HJ, Nilsson U (1960) Relation of Abeta(1)-glycoprotein of human serum to the complement system. *J.Exp.Med.* **111,** 217-234.

Mulot SF, Hughes K, Woodgett JR, Anderton BH, Hanger DP (1994) PHF-tau from Alzheimer's brain comprises four species on SDS-PAGE which can be mimicked by in vitro phosphorylation of human brain tau by glycogen synthase kinase-3 beta. *FEBS Lett.* **349,** 359-364.

Muncer S, Taylor S, Craigie M (2002) Power dressing and meta-analysis: incorporating power analysis into meta-analysis. *J.Adv.Nurs.* **38(3),** 274-280.

Munchbach M, Quadroni M, Miotto G, James P (2000) Quantitation and facilitated de novo sequencing of proteins by isotopic N-terminal labeling of peptides with a fragmentation-directing moiety. *Anal.Chem.* **72,** 4047-4057.

Murphy BF, Kirszbaum L, Walker ID, d'Apice AJ (1988) SP-40,40, a newly identified normal human serum protein found in the SC5b-9 complex of complement and in the immune deposits in glomerulonephritis. *J.Clin.Invest* **81,** 1858-1864.

Myllykangas L, Polvikoski T, Sulkava R, Verkkoniemi A, Crook R, Tienari PJ, Pusa AK, Niinisto L, O'Brien P, Kontula K, Hardy J, Haltia M, Perez-Tur J (1999) Genetic association of alpha2-macroglobulin with Alzheimer's disease in a Finnish elderly population. *Ann.Neurol.* **46,** 382-390.

Myrick JE, Caudill SP, Hubert IL, Robinson MK, Adams MJ, Jr., Pueschel SM (1990) Identification of haptoglobin alpha-2FF variants in mid-trimester maternal serum as potential markers for Down syndrome. *Appl.Theor.Electrophor.* **1,** 233-241.

Nalivaeva NN, Fisk LR, Belyaev ND, Turner AJ (2008) Amyloid-degrading enzymes as therapeutic targets in Alzheimer's disease. *Curr.Alzheimer Res.* **5,** 212-224.

Narita M, Holtzman DM, Schwartz AL, Bu G (1997) Alpha2-macroglobulin complexes with and mediates the endocytosis of beta-amyloid peptide via cell surface low-density lipoprotein receptor-related protein. *J.Neurochem.* **69,** 1904-1911.

Naslund J, Thyberg J, Tjernberg LO, Wernstedt C, Karlstrom AR, Bogdanovic N, Gandy SE, Lannfelt L, Terenius L, Nordstedt C (1995) Characterization of stable complexes involving apolipoprotein E and the amyloid beta peptide in Alzheimer's disease brain. *Neuron* **15,** 219-228.

Nicol GR, Han M, Kim J, Birse CE, Brand E, Nguyen A, Mesri M, FitzHugh W, Kaminker P, Moore PA, Ruben SM, He T (2008) Use of an immunoaffinity-mass spectrometry-based approach for the quantification of protein biomarkers from serum samples of lung cancer patients. *Mol.Cell Proteomics.* **7,** 1974-1982.

Norden AG, Sharratt P, Cutillas PR, Cramer R, Gardner SC, Unwin RJ (2004) Quantitative amino acid and proteomic analysis: very low excretion of polypeptides >750 Da in normal urine. *Kidney Int.* **66(5),** 1994-2003.

Nybo M, Olsen H, Jeune B, ndersen-Ranberg K, Holm NE, Svehag SE (1998) Increased plasma concentration of serum amyloid P component in centenarians with impaired cognitive performance. *Dement.Geriatr.Cogn Disord.* **9,** 126-129.

O'Farrell PH (1975) High resolution two-dimensional electrophoresis of proteins. *J.Biol.Chem.* **250,** 4007-4021.

Oda T, Wals P, Osterburg HH, Johnson SA, Pasinetti GM, Morgan TE, Rozovsky I, Stine WB, Snyder SW, Holzman TF, . (1995) Clusterin (apoJ) alters the aggregation of amyloid beta-peptide (A beta 1-42) and forms slowly sedimenting A beta complexes that cause oxidative stress. *Exp.Neurol.* **136,** 22-31.

Ogata Y, Charlesworth MC, Higgins L, Keegan BM, Vernino S, Muddiman DC (2007) Differential protein expression in male and female human lumbar cerebrospinal fluid using iTRAQ reagents after abundant protein depletion. *Proteomics.* **7,** 3726-3734.

Ohya K, Sano M (1977) Analysis of drugs by pyrolysis. I. Selected ion monitoring combined with a pyrolysis method for the determination of carpronium chloride in biological samples. *Biomed.Mass Spectrom.* **4(4),** 241-247.

Old WM, Meyer-Arendt K, veline-Wolf L, Pierce KG, Mendoza A, Sevinsky JR, Resing KA, Ahn NG (2005) Comparison of label-free methods for quantifying human proteins by shotgun proteomics. *Mol.Cell Proteomics* **4,** 1487-1502.

Olsen JV, Andersen JR, Nielsen PA, Nielsen ML, Figeys D, Mann M, Wisniewski JR (2004) HysTag--a novel proteomic quantification tool applied to differential display analysis of membrane proteins from distinct areas of mouse brain. *Mol.Cell Proteomics.* **3(1),** 82-92.

Ong SE, Mann M (2005) Mass spectrometry-based proteomics turns quantitative. *Nat.Chem.Biol.* **1(5),** 252-262.

Onisko B, Dynin I, Requena JR, Silva CJ, Erickson M, Carter JM (2007) Mass spectrometric detection of attomole amounts of the prion protein by nanoLC/MS/MS. *J.Am.Soc.Mass Spectrom.* **18,** 1070-1079.

Osborn TM, Verdrengh M, Stossel TP, Tarkowski A, Bokarewa M (2008) Decreased levels of the gelsolin plasma isoform in patients with rheumatoid arthritis. *Arthritis Res.Ther.* **10,** 117.

Otto M, Wiltfang J, Tumani H, Zerr I, Lantsch M, Kornhuber J, Weber T, Kretzschmar HA, Poser S (1997) Elevated levels of tau-protein in cerebrospinal fluid of patients with Creutzfeldt-Jakob disease. *Neurosci.Lett.* **225,** 210-212.

Otto M, Esselmann H, Schulz-Shaeffer W, Neumann M, Schroter A, Ratzka P, Cepek L, Zerr I, Steinacker P, Windl O, Kornhuber J, Kretzschmar HA, Poser S, Wiltfang J (2000) Decreased beta-amyloid1-42 in cerebrospinal fluid of patients with Creutzfeldt-Jakob disease. *Neurology* **54,** 1099-1102.

Ow SY, Salim M, Noirel J, Evans C, Wright PC (2011) Minimising iTRAQ ratio compression through understanding LC-MS elution dependence and high-resolution HILIC fractionation. *Proteomics.* **11(11),** 2341-2346.

Pan S, Aebersold R, Chen R, Rush J, Goodlett DR, McIntosh MW, Zhang J, Brentnall TA (2009) Mass spectrometry based targeted protein quantification: methods and applications. *J.Proteome.Res.* **8,** 787-797.

Pangburn MK, Schreiber RD, Muller-Eberhard HJ (1977) Human complement C3b inactivator: isolation, characterization, and demonstration of an absolute requirement for the serum protein beta1H for cleavage of C3b and C4b in solution. *J.Exp.Med.* **146,** 257-270.

Patel VJ, Thalassinos K, Slade SE, Connolly JB, Crombie A, Murrell JC, Scrivens JH (2009) A comparison of labeling and label-free mass spectrometry-based proteomics approaches. *J.Proteome Res.* **8,** 3752-3759.

Paul J, Strickland S, Melchor JP (2007) Fibrin deposition accelerates neurovascular damage and neuroinflammation in mouse models of Alzheimer's disease. *J.Exp.Med.* **204,** 1999-2008.

Paulovich AG, Whiteaker JR, Hoofnagle AN, Wang P (2008) The interface between biomarker discovery and clinical validation: The tar pit of the protein biomarker pipeline. *Proteomics.Clin.Appl.* **2,** 1386-1402.

Pepe MS, Etzioni R, Feng Z, Potter JD, Thompson ML, Thornquist M, Winget M, Yasui Y (2001) Phases of biomarker development for early detection of cancer. *J.Natl.Cancer Inst.* **93,** 1054-1061.

Pepys MB, Dyck RF, de Beer FC, Skinner M, Cohen AS (1979) Binding of serum amyloid P-component (SAP) by amyloid fibrils. *Clin.Exp.Immunol.* **38,** 284-293.

Pepys MB, Tennent GA, Booth DR, Bellotti V, Lovat LB, Tan SY, Persey MR, Hutchinson WL, Booth SE, Madhoo S, Soutar AK, Hawkins PN, Van Zyl-Smit R, Campistol JM, Fraser PE, Radford SE, Robinson CV, Sunde M, Serpell LC, Blake CC (1996) Molecular mechanisms of fibrillogenesis and the protective role of amyloid P component: two possible avenues for therapy. *Ciba Found.Symp.* **199,** 73-81.

Pepys MB, Herbert J, Hutchinson WL, Tennent GA, Lachmann HJ, Gallimore JR, Lovat LB, Bartfai T, Alanine A, Hertel C, Hoffmann T, Jakob-Roetne R, Norcross RD, Kemp JA, Yamamura K, Suzuki M, Taylor GW, Murray S, Thompson D, Purvis A, Kolstoe S, Wood SP, Hawkins PN (2002) Targeted pharmacological depletion of serum amyloid P component for treatment of human amyloidosis. *Nature* **417,** 254-259.

Peskind ER, Riekse R, Quinn JF, Kaye J, Clark CM, Farlow MR, Decarli C, Chabal C, Vavrek D, Raskind MA, Galasko D (2005) Safety and acceptability of the research lumbar puncture. *Alzheimer Dis.Assoc.Disord.* **19,** 220-225.

Petersen RC, Smith GE, Waring SC, Ivnik RJ, Tangalos EG, Kokmen E (1999) Mild cognitive impairment: clinical characterization and outcome. *Arch.Neurol.* **56,** 303-308.

Petersen RC, Parisi JE, Dickson DW, Johnson KA, Knopman DS, Boeve BF, Jicha GA, Ivnik RJ, Smith GE, Tangalos EG, Braak H, Kokmen E (2006) Neuropathologic features of amnestic mild cognitive impairment. *Arch.Neurol.* **63,** 665-672.

Petricoin EF, Liotta LA (2004) SELDI-TOF-based serum proteomic pattern diagnostics for early detection of cancer. *Curr.Opin.Biotechnol.* **15,** 24-30.

Petritis K, Kangas LJ, Ferguson PL, Anderson GA, Pasa-Tolic L, Lipton MS, Auberry KJ, Strittmatter EF, Shen Y, Zhao R, Smith RD (2003) Use of artificial neural networks for the accurate prediction of peptide liquid chromatography elution times in proteome analyses. *Anal.Chem.* **75(5),** 1039-1048.

Piau A, Nourhashemi F, Hein C, Caillaud C, Vellas B (2011) Progress in the development of new drugs in Alzheimer's disease. *J.Nutr.Health Aging.* **15(1),** 45-57.

Picotti P, Rinner O, Stallmach R, Dautel F, Farrah T, Domon B, Wenschuh H, Aebersold R (2010) High-throughput generation of selected reaction-monitoring assays for proteins and proteomes. *Nat.Methods* **7,** 43-46.

Pierce A, Unwin RD, Evans CA, Griffiths S, Carney L, Zhang L, Jaworska E, Lee CF, Blinco D, Okoniewski MJ, Miller CJ, Bitton DA, Spooncer E, Whetton AD (2008) Eight-channel iTRAQ enables comparison of the activity of six leukemogenic tyrosine kinases. *Mol.Cell Proteomics.* **7,** 853-863.

Pitas RE, Boyles JK, Lee SH, Foss D, Mahley RW (1987) Astrocytes synthesize apolipoprotein E and metabolize apolipoprotein E-containing lipoproteins. *Biochim.Biophys.Acta* **917,** 148-161.

Pluta R, Ulamek M, Januszewski S (2006) Micro-blood-brain barrier openings and cytotoxic fragments of amyloid precursor protein accumulation in white matter after ischemic brain injury in long-lived rats. *Acta Neurochir.Suppl* **96,** 267-271.

Poduslo JF, Ramakrishnan M, Holasek SS, Ramirez-Alvarado M, Kandimalla KK, Gilles EJ, Curran GL, Wengenack TM (2007) In vivo targeting of antibody fragments to the nervous system for Alzheimer's disease immunotherapy and molecular imaging of amyloid plaques. *J.Neurochem.* **102(2),** 420-433.

Poduslo SE, Shook B, Drigalenko E, Yin X (2002) Lack of association of the two polymorphisms in alpha-2 macroglobulin with Alzheimer disease. *Am.J.Med.Genet.* **110,** 30-35.

Pogacic V, Herrling P (2009) List of drugs in development for neurodegenerative diseases. Update June 2008. *Neurodegener.Dis.* **6,** 37-86.

Pomara N, Willoughby LM, Sidtis JJ, Mehta PD (2005) Selective reductions in plasma Abeta 1-42 in healthy elderly subjects during longitudinal follow-up: a preliminary report. *Am.J.Geriatr.Psychiatry* **13,** 914-917.

Prakash A, Tomazela DM, Frewen B, Maclean B, Merrihew G, Peterman S, Maccoss MJ (2009) Expediting the development of targeted SRM assays: using data from shotgun proteomics to automate method development. *J.Proteome.Res.* **8(6),** 2733-2739.

Pratt JM, Simpson DM, Doherty MK, Rivers J, Gaskell SJ, Beynon RJ (2006) Multiplexed absolute quantification for proteomics using concatenated signature peptides encoded by QconCAT genes. *Nat.Protoc.* **1,** 1029-1043.

Preissner CM, O'Kane DJ, Singh RJ, Morris JC, Grebe SK (2003) Phantoms in the assay tube: heterophile antibody interferences in serum thyroglobulin assays. *J.Clin.Endocrinol.Metab* **88,** 3069-3074.

Price BH, Gurvit H, Weintraub S, Geula C, Leimkuhler E, Mesulam M (1993) Neuropsychological patterns and language deficits in 20 consecutive cases of autopsy-confirmed Alzheimer's disease. *Arch.Neurol.* **50,** 931-937.

Pride M, Seubert P, Grundman M, Hagen M, Eldridge J, Black RS (2008) Progress in the active immunotherapeutic approach to Alzheimer's disease: clinical investigations into AN1792-associated meningoencephalitis. *Neurodegener.Dis.* **5(3-4),** 194-196.

Qiao H, Koya RC, Nakagawa K, Tanaka H, Fujita H, Takimoto M, Kuzumaki N (2005) Inhibition of Alzheimer's amyloid-beta peptide-induced reduction of mitochondrial membrane potential and neurotoxicity by gelsolin. *Neurobiol.Aging* **26,** 849-855.

Querfurth HW, LaFerla FM (2010) Alzheimer's disease. *N.Engl.J.Med.* **362,** 329-344.

Quinn JF, Raman R, Thomas RG, Yurko-Mauro K, Nelson EB, Van DC, Galvin JE, Emond J, Jack CR, Jr., Weiner M, Shinto L, Aisen PS (2010) Docosahexaenoic acid supplementation and cognitive decline in Alzheimer disease: a randomized trial. *JAMA.* **304(17),** 1903-1911.

Rabinovici GD, Furst AJ, O'Neil JP, Racine CA, Mormino EC, Baker SL, Chetty S, Patel P, Pagliaro TA, Klunk WE, Mathis CA, Rosen HJ, Miller BL, Jagust WJ (2007) 11C-PIB PET imaging in Alzheimer disease and frontotemporal lobar degeneration. *Neurology* **68,** 1205-1212.

Raje S, Patat AA, Parks V, Schechter L, Plotka A, Paul J, Langstrom B (2008) A positron emission tomography study to assess binding of lecozotan, a novel 5-hydroxytryptamine-1A silent antagonist, to brain 5-HT1A receptors in healthy young and elderly subjects, and in patients with Alzheimer's disease. *Clin.Pharmacol.Ther.* **83(1),** 86-96.

Rapoport M, Dawson HN, Binder LI, Vitek MP, Ferreira A (2002) Tau is essential to beta -amyloid-induced neurotoxicity. *Proc.Natl.Acad.Sci.U.S.A* **99,** 6364-6369.

Rappsilber J, Ryder U, Lamond AI, Mann M (2002) Large-scale proteomic analysis of the human spliceosome. *Genome Res.* **12,** 1231-1245.

Ray I, Chauhan A, Wegiel J, Chauhan VP (2000) Gelsolin inhibits the fibrillization of amyloid beta-protein, and also defibrillizes its preformed fibrils. *Brain Res.* **853,** 344-351.

Ray P, Le MY, Riou B, Houle TT (2010) Statistical evaluation of a biomarker. *Anesthesiology.* **112(4),** 1023-1040.

Ray S, Britschgi M, Herbert C, Takeda-Uchimura Y, Boxer A, Blennow K, Friedman LF, Galasko DR, Jutel M, Karydas A, Kaye JA, Leszek J, Miller BL, Minthon L, Quinn JF, Rabinovici GD, Robinson WH, Sabbagh MN, So YT, Sparks DL, Tabaton M, Tinklenberg J, Yesavage JA, Tibshirani R, Wyss-Coray T (2007) Classification and prediction of clinical Alzheimer's diagnosis based on plasma signaling proteins. *Nat.Med.* **13,** 1359-1362.

Reddy PH, Beal MF (2005) Are mitochondria critical in the pathogenesis of Alzheimer's disease? *Brain Res.Brain Res.Rev.* **49,** 618-632.

Ren D, Julka S, Inerowicz HD, Regnier FE (2004) Enrichment of cysteine-containing peptides from tryptic digests using a quaternary amine tag. *Anal.Chem.* **76(15),** 4522-4530.

Rhein V, Song X, Wiesner A, Ittner LM, Baysang G, Meier F, Ozmen L, Bluethmann H, Drose S, Brandt U, Savaskan E, Czech C, Gotz J, Eckert A (2009) Amyloid-beta and tau synergistically impair the oxidative phosphorylation system in triple transgenic Alzheimer's disease mice. *Proc.Natl.Acad.Sci.U.S.A* **106,** 20057-20062.

Rifai K, Ernst T, Kretschmer U, Haller H, Manns MP, Fliser D (2006) Removal selectivity of Prometheus: a new extracorporeal liver support device. *World J.Gastroenterol.* **12,** 940-944.

Rifai N, Gillette MA, Carr SA (2006) Protein biomarker discovery and validation: the long and uncertain path to clinical utility. *Nat.Biotechnol.* **24,** 971-983.

Ripoche J, Day AJ, Harris TJ, Sim RB (1988) The complete amino acid sequence of human complement factor H. *Biochem.J.* **249,** 593-602.

Rivers J, Simpson DM, Robertson DH, Gaskell SJ, Beynon RJ (2007) Absolute multiplexed quantitative analysis of protein expression during muscle development using QconCAT. *Mol.Cell Proteomics* **6,** 1416-1427.

Roberson ED, Scearce-Levie K, Palop JJ, Yan F, Cheng IH, Wu T, Gerstein H, Yu GQ, Mucke L (2007) Reducing endogenous tau ameliorates amyloid beta-induced deficits in an Alzheimer's disease mouse model. *Science* **316,** 750-754.

Rodriguez de CS, Esparza-Gordillo J, Goicoechea de JE, Lopez-Trascasa M, Sanchez-Corral P (2004) The human complement factor H: functional roles, genetic variations and disease associations. *Mol.Immunol.* **41,** 355-367.

Roepstorff P, Fohlman J (1984) Proposal for a common nomenclature for sequence ions in mass spectra of peptides. *Biomed.Mass Spectrom.* **11,** 601.

Rogaeva EA, Premkumar S, Grubber J, Serneels L, Scott WK, Kawarai T, Song Y, Hill DL, bou-Donia SM, Martin ER, Vance JJ, Yu G, Orlacchio A, Pei Y, Nishimura M, Supala A, Roberge B, Saunders AM, Roses AD, Schmechel D, Crane-Gatherum A, Sorbi S, Bruni A, Small GW, Conneally PM, Haines JL, Van LF, St George-Hyslop PH, Farrer LA, Pericak-Vance MA (1999) An alpha-2-macroglobulin insertion-deletion polymorphism in Alzheimer disease. *Nat.Genet.* **22,** 19-22.

Rogers MA, Clarke P, Noble J, Munro NP, Paul A, Selby PJ, Banks RE (2003) Proteomic profiling of urinary proteins in renal cancer by surface enhanced laser desorption ionization and neural-network analysis: identification of key issues affecting potential clinical utility. *Cancer Res.* **63,** 6971-6983.

Roher AE, Esh CL, Kokjohn TA, Castano EM, Van Vickle GD, Kalback WM, Patton RL, Luehrs DC, Daugs ID, Kuo YM, Emmerling MR, Soares H, Quinn JF, Kaye J, Connor DJ, Silverberg NB, Adler CH, Seward JD, Beach TG, Sabbagh MN (2009) Amyloid beta peptides in human plasma and tissues and their significance for Alzheimer's disease. *Alzheimers.Dement.* **5,** 18-29.

Roher AE, Maarouf CL, Sue LI, Hu Y, Wilson J, Beach TG (2009) Proteomics-derived cerebrospinal fluid markers of autopsy-confirmed Alzheimer's disease. *Biomarkers* **14,** 493-501.

Romas SN, Tang MX, Berglund L, Mayeux R (1999) APOE genotype, plasma lipids, lipoproteins, and AD in community elderly. *Neurology* **53,** 517-521.

Rombouts SA, Goekoop R, Stam CJ, Barkhof F, Scheltens P (2005) Delayed rather than decreased BOLD response as a marker for early Alzheimer's disease. *Neuroimage.* **26,** 1078-1085.

Rose GM, Ong VS, Woodruff-Pak DS (2007) Efficacy of MEM 1003, a novel calcium channel blocker, in delay and trace eyeblink conditioning in older rabbits. *Neurobiol.Aging.* **28(5),** 766-773.

Rosen WG, Mohs RC, Davis KL (1984) A new rating scale for Alzheimer's disease. *Am.J.Psychiatry* **141,** 1356-1364.

Ross PL, Huang YN, Marchese JN, Williamson B, Parker K, Hattan S, Khainovski N, Pillai S, Dey S, Daniels S, Purkayastha S, Juhasz P, Martin S, Bartlet-Jones M, He F, Jacobson A, Pappin DJ (2004) Multiplexed protein quantitation in Saccharomyces cerevisiae using amine-reactive isobaric tagging reagents. *Mol.Cell Proteomics.* **3,** 1154-1169.

Sahu A, Lambris JD (2001) Structure and biology of complement protein C3, a connecting link between innate and acquired immunity. *Immunol.Rev.* **180,** 35-48.

Salzman C, Jeste DV, Meyer RE, Cohen-Mansfield J, Cummings J, Grossberg GT, Jarvik L, Kraemer HC, Lebowitz BD, Maslow K, Pollock BG, Raskind M, Schultz SK, Wang P, Zito JM, Zubenko GS (2008) Elderly patients with dementia-related symptoms of severe agitation and aggression: consensus statement on treatment options, clinical trials methodology, and policy. *J.Clin.Psychiatry* **69,** 889-898.

Samgard K, Zetterberg H, Blennow K, Hansson O, Minthon L, Londos E (2010) Cerebrospinal fluid total tau as a marker of Alzheimer's disease intensity. *Int.J.Geriatr.Psychiatry* **25,** 403-410.

Samson K (2010) NerveCenter: Phase III Alzheimer trial halted: Search for therapeutic biomarkers continues. *Ann.Neurol.* **68,** A9-A12.

Sasse J, Gallagher SR (2004) Staining proteins in gels. *Curr.Protoc.Immunol.* **Chapter 8,** Unit.

Saunders AJ, Bertram L, Mullin K, Sampson AJ, Latifzai K, Basu S, Jones J, Kinney D, Kenzie-Ingano L, Yu S, Albert MS, Moscarillo TJ, Go RC, Bassett SS, Daly MJ, Laird NM, Wang X, Velicelebi G, Wagner SL, Becker DK, Tanzi RE, Blacker D (2003) Genetic association of Alzheimer's disease with multiple polymorphisms in alpha-2-macroglobulin. *Hum.Mol.Genet.* **12,** 2765-2776.

Scacchi R, Gambina G, Ruggeri M, Martini MC, Ferrari G, Silvestri M, Schiavon R, Corbo RM (1999) Plasma levels of apolipoprotein E and genetic markers in elderly patients with Alzheimer's disease. *Neurosci.Lett.* **259,** 33-36.

Scheuner D, Eckman C, Jensen M, Song X, Citron M, Suzuki N, Bird TD, Hardy J, Hutton M, Kukull W, Larson E, Levy-Lahad E, Viitanen M, Peskind E, Poorkaj P, Schellenberg G, Tanzi R, Wasco W, Lannfelt L, Selkoe D, Younkin S (1996) Secreted amyloid beta-protein similar to that in the senile plaques of Alzheimer's disease is

increased in vivo by the presenilin 1 and 2 and APP mutations linked to familial Alzheimer's disease. *Nat.Med.* **2,** 864-870.

Schmidt A, Kellermann J, Lottspeich F (2005) A novel strategy for quantitative proteomics using isotope-coded protein labels. *Proteomics.* **5,** 4-15.

Schoenherr RM, Zhao L, Whiteaker JR, Feng LC, Li L, Liu L, Liu X, Paulovich AG (2010) Automated screening of monoclonal antibodies for SISCAPA assays using a magnetic bead processor and liquid chromatography-selected reaction monitoring-mass spectrometry. *J.Immunol.Methods* **353,** 49-61.

Schupf N, Tang MX, Fukuyama H, Manly J, Andrews H, Mehta P, Ravetch J, Mayeux R (2008) Peripheral Abeta subspecies as risk biomarkers of Alzheimer's disease. *Proc.Natl.Acad.Sci.U.S.A* **105,** 14052-14057.

Schwaeble W, Zwirner J, Schulz TF, Linke RP, Dierich MP, Weiss EH (1987) Human complement factor H: expression of an additional truncated gene product of 43 kDa in human liver. *Eur.J.Immunol.* **17,** 1485-1489.

Scott LJ, Goa KL (2000) Galantamine: a review of its use in Alzheimer's disease. *Drugs* **60,** 1095-1122.

Selkoe DJ (2001) Alzheimer's disease: genes, proteins, and therapy. *Physiol Rev.* **81,** 741-766.

Seshadri S, Fitzpatrick AL, Ikram MA, DeStefano AL, Gudnason V, Boada M, Bis JC, Smith AV, Carassquillo MM, Lambert JC, Harold D, Schrijvers EM, Ramirez-Lorca R, Debette S, Longstreth WT, Jr., Janssens AC, Pankratz VS, Dartigues JF, Hollingworth P, Aspelund T, Hernandez I, Beiser A, Kuller LH, Koudstaal PJ, Dickson DW, Tzourio C, Abraham R, Antunez C, Du Y, Rotter JI, Aulchenko YS, Harris TB, Petersen RC, Berr C, Owen MJ, Lopez-Arrieta J, Varadarajan BN, Becker JT, Rivadeneira F, Nalls MA, Graff-Radford NR, Campion D, Auerbach S, Rice K, Hofman A, Jonsson PV, Schmidt H, Lathrop M, Mosley TH, Au R, Psaty BM, Uitterlinden AG, Farrer LA, Lumley T, Ruiz A, Williams J, Amouyel P, Younkin SG, Wolf PA, Launer LJ, Lopez OL, van Duijn CM, Breteler MM (2010) Genome-wide analysis of genetic loci associated with Alzheimer disease. *JAMA* **303,** 1832-1840.

Seubert P, Vigo-Pelfrey C, Esch F, Lee M, Dovey H, Davis D, Sinha S, Schlossmacher M, Whaley J, Swindlehurst C, . (1992) Isolation and quantification of soluble Alzheimer's beta-peptide from biological fluids. *Nature* **359,** 325-327.

Shaw LM, Vanderstichele H, Knapik-Czajka M, Figurski M, Coart E, Blennow K, Soares H, Simon AJ, Lewczuk P, Dean RA, Siemers E, Potter W, Lee VM, Trojanowski JQ (2011) Qualification of the analytical and clinical performance of CSF biomarker analyses in ADNI. *Acta Neuropathol.*

Shen F, Smith JA, Chang R, Bourdet DL, Tsuruda PR, Obedencio GP, Beattie DT (2011) 5-HT(4) receptor agonist mediated enhancement of cognitive function in vivo and amyloid precursor protein processing in vitro: A pharmacodynamic and pharmacokinetic assessment. *Neuropharmacology.* **61(1-2),** 69-79.

Sherman J, McKay MJ, Ashman K, Molloy MP (2009) How specific is my SRM?: The issue of precursor and product ion redundancy. *Proteomics.* **9,** 1120-1123.

Sherwood CA, Eastham A, Lee LW, Risler J, Mirzaei H, Falkner JA, Martin DB (2009) Rapid optimization of MRM-MS instrument parameters by subtle alteration of precursor and product m/z targets. *J.Proteome.Res.* **8,** 3746-3751.

Sherwood CA, Eastham A, Lee LW, Peterson A, Eng JK, Shteynberg D, Mendoza L, Deutsch EW, Risler J, Tasman N, Aebersold R, Lam H, Martin DB (2009) MaRiMba: a software application for spectral library-based MRM transition list assembly. *J.Proteome.Res.* **8(10),** 4396-4405.

Shi J, Perry G, Aliev G, Smith MA, Ashe KH, Friedland RP (1999) Serum amyloid P is not present in amyloid beta deposits of a transgenic animal model. *Neuroreport* **10,** 3229-3232.

Shibata M, Yamada S, Kumar SR, Calero M, Bading J, Frangione B, Holtzman DM, Miller CA, Strickland DK, Ghiso J, Zlokovic BV (2000) Clearance of Alzheimer's amyloid-ss(1-40) peptide from brain by LDL receptor-related protein-1 at the blood-brain barrier. *J.Clin.Invest* **106,** 1489-1499.

Silacci P, Mazzolai L, Gauci C, Stergiopulos N, Yin HL, Hayoz D (2004) Gelsolin superfamily proteins: key regulators of cellular functions. *Cell Mol.Life Sci.* **61,** 2614-2623.

Silkensen JR, Skubitz KM, Skubitz AP, Chmielewski DH, Manivel JC, Dvergsten JA, Rosenberg ME (1995) Clusterin promotes the aggregation and adhesion of renal porcine epithelial cells. *J.Clin.Invest* **96,** 2646-2653.

Silva JC, Denny R, Dorschel CA, Gorenstein M, Kass IJ, Li GZ, McKenna T, Nold MJ, Richardson K, Young P, Geromanos S (2005) Quantitative proteomic analysis by accurate mass retention time pairs. *Anal.Chem.* **77,** 2187-2200.

Singh RJ, Taylor RL, Reddy GS, Grebe SK (2006) C-3 epimers can account for a significant proportion of total circulating 25-hydroxyvitamin D in infants, complicating accurate measurement and interpretation of vitamin D status. *J.Clin.Endocrinol.Metab* **91,** 3055-3061.

Slysz GW, Schriemer DC (2009) Integrating accelerated tryptic digestion into proteomics workflows. *Methods Mol.Biol.* **492,** 241-254.

Snow AD, Wight TN (1989) Proteoglycans in the pathogenesis of Alzheimer's disease and other amyloidoses. *Neurobiol.Aging* **10,** 481-497.

Somiari RI, Somiari S, Russell S, Shriver CD (2005) Proteomics of breast carcinoma. *J.Chromatogr.B Analyt.Technol.Biomed.Life Sci.* **815,** 215-225.

Song F, Poljak A, Smythe GA, Sachdev P (2009) Plasma biomarkers for mild cognitive impairment and Alzheimer's disease. *Brain Res.Rev.* **61,** 69-80.

Sottrup-Jensen L (1989) Alpha-macroglobulins: structure, shape, and mechanism of proteinase complex formation. *J.Biol.Chem.* **264,** 11539-11542.

Srinivasan N, White HE, Emsley J, Wood SP, Pepys MB, Blundell TL (1994) Comparative analyses of pentraxins: implications for protomer assembly and ligand binding. *Structure.* **2,** 1017-1027.

Stocklin R, Vu L, Vadas L, Cerini F, Kippen AD, Offord RE, Rose K (1997) A stable isotope dilution assay for the in vivo determination of insulin levels in humans by mass spectrometry. *Diabetes* **46,** 44-50.

Stadtman ER, Levine RL (2003) Free radical-mediated oxidation of free amino acids and amino acid residues in proteins. *Amino.Acids* **25,** 207-218.

Stahl-Zeng J, Lange V, Ossola R, Eckhardt K, Krek W, Aebersold R, Domon B (2007) High sensitivity detection of plasma proteins by multiple reaction monitoring of N-glycosites. *Mol.Cell Proteomics* **6,** 1809-1817.

Stahl SM (2000) The new cholinesterase inhibitors for Alzheimer's disease, Part 2: illustrating their mechanisms of action. *J.Clin.Psychiatry* **61,** 813-814.

Steele LS, Glazier RH (1999) Is donepezil effective for treating Alzheimer's disease? *Can.Fam.Physician* **45,** 917-919.

Steen H, Mann M (2004) The ABC's (and XYZ's) of peptide sequencing. *Nat.Rev.Mol.Cell Biol.* **5,** 699-711.

Stenstad T, Magnus JH, Syse K, Husby G (1993) On the association between amyloid fibrils and glycosaminoglycans; possible interactive role of Ca2+ and amyloid P-component. *Clin.Exp.Immunol.* **94,** 189-195.

Strauss S, Bauer J, Ganter U, Jonas U, Berger M, Volk B (1992) Detection of interleukin-6 and alpha 2-macroglobulin immunoreactivity in cortex and hippocampus of Alzheimer's disease patients. *Lab Invest* **66,** 223-230.

Strittmatter EF, Ferguson PL, Tang K, Smith RD (2003) Proteome analyses using accurate mass and elution time peptide tags with capillary LC time-of-flight mass spectrometry. *J.Am.Soc.Mass Spectrom.* **14(9),** 980-991.

Strittmatter WJ, Weisgraber KH, Huang DY, Dong LM, Salvesen GS, Pericak-Vance M, Schmechel D, Saunders AM, Goldgaber D, Roses AD (1993) Binding of human apolipoprotein E to synthetic amyloid beta peptide: isoform-specific effects and implications for late-onset Alzheimer disease. *Proc.Natl.Acad.Sci.U.S.A* **90,** 8098-8102.

Strohmeyer R, Ramirez M, Cole GJ, Mueller K, Rogers J (2002) Association of factor H of the alternative pathway of complement with agrin and complement receptor 3 in the Alzheimer's disease brain. *J.Neuroimmunol.* **131,** 135-146.

Strozyk D, Blennow K, White LR, Launer LJ (2003) CSF Abeta 42 levels correlate with amyloid-neuropathology in a population-based autopsy study. *Neurology* **60,** 652-656.

Suh TT, Holmback K, Jensen NJ, Daugherty CC, Small K, Simon DI, Potter S, Degen JL (1995) Resolution of spontaneous bleeding events but failure of pregnancy in fibrinogen-deficient mice. *Genes Dev.* **9,** 2020-2033.

Sun HQ, Yamamoto M, Mejillano M, Yin HL (1999) Gelsolin, a multifunctional actin regulatory protein. *J.Biol.Chem.* **274,** 33179-33182.

Sundelof J, Giedraitis V, Irizarry MC, Sundstrom J, Ingelsson E, Ronnemaa E, Arnlov J, Gunnarsson MD, Hyman BT, Basun H, Ingelsson M, Lannfelt L, Kilander L (2008) Plasma beta amyloid and the risk of Alzheimer disease and dementia in elderly men: a prospective, population-based cohort study. *Arch.Neurol.* **65,** 256-263.

Sunderland T, Linker G, Mirza N, Putnam KT, Friedman DL, Kimmel LH, Bergeson J, Manetti GJ, Zimmermann M, Tang B, Bartko JJ, Cohen RM (2003) Decreased beta-amyloid1-42 and increased tau levels in cerebrospinal fluid of patients with Alzheimer disease. *JAMA* **289,** 2094-2103.

Sutherland FC, de Jager AD, Badenhorst D, Scanes T, Hundt HK, Swart KJ, Hundt AF (2001) Sensitive liquid chromatography-tandem mass spectrometry method for the determination of loratadine and its major active metabolite descarboethoxyloratadine in human plasma. *J.Chromatogr.A* **914,** 37-43.

Tamaoka A, Fukushima T, Sawamura N, Ishikawa K, Oguni E, Komatsuzaki Y, Shoji S (1996) Amyloid beta protein in plasma from patients with sporadic Alzheimer's disease. *J.Neurol.Sci.* **141,** 65-68.

Tamaoka A, Sawamura N, Fukushima T, Shoji S, Matsubara E, Shoji M, Hirai S, Furiya Y, Endoh R, Mori H (1997) Amyloid beta protein 42(43) in cerebrospinal fluid of patients with Alzheimer's disease. *J.Neurol.Sci.* **148,** 41-45.

Tanaka J, Sobue K (1994) Localization and characterization of gelsolin in nervous tissues: gelsolin is specifically enriched in myelin-forming cells. *J.Neurosci.* **14,** 1038-1052.

Tapiola T, Alafuzoff I, Herukka SK, Parkkinen L, Hartikainen P, Soininen H, Pirttila T (2009) Cerebrospinal fluid {beta}-amyloid 42 and tau proteins as biomarkers of Alzheimer-type pathologic changes in the brain. *Arch.Neurol.* **66,** 382-389.

Taylor G (1964) Disintegration of Water Drops in an Electric Field. *Proceedings of the Royal Society of London.Series A, Mathematical and Physical Sciences* **280,** 383-397.

Tennent GA, Lovat LB, Pepys MB (1995) Serum amyloid P component prevents proteolysis of the amyloid fibrils of Alzheimer disease and systemic amyloidosis. *Proc.Natl.Acad.Sci.U.S.A* **92,** 4299-4303.

Thakkinstian A, Bowe S, McEvoy M, Smith W, Attia J (2006) Association between apolipoprotein E polymorphisms and age-related macular degeneration: A HuGE review and meta-analysis. *Am.J.Epidemiol.* **164,** 813-822.

Thambisetty M, Hye A, Foy C, Daly E, Glover A, Cooper A, Simmons A, Murphy D, Lovestone S (2008) Proteome-based identification of plasma proteins associated with hippocampal metabolism in early Alzheimer's disease. *J.Neurol.* **255,** 1712-1720.

Thambisetty M, Lovestone S (2010) Blood-based biomarkers of Alzheimer's disease: challenging but feasible. *Biomark.Med.* **4,** 65-79.

Thambisetty M, Simmons A, Velayudhan L, Hye A, Campbell J, Zhang Y, Wahlund LO, Westman E, Kinsey A, Guntert A, Proitsi P, Powell J, Causevic M, Killick R, Lunnon K, Lynham S, Broadstock M, Choudhry F, Howlett DR, Williams RJ, Sharp SI, Mitchelmore C, Tunnard C, Leung R, Foy C, O'Brien D, Breen G, Furney SJ, Ward M, Kloszewska I, Mecocci P, Soininen H, Tsolaki M, Vellas B, Hodges A, Murphy DG, Parkins S, Richardson JC, Resnick SM, Ferrucci L, Wong DF, Zhou Y, Muehlboeck S, Evans A, Francis PT, Spenger C, Lovestone S (2010) Association of plasma clusterin concentration with severity, pathology, and progression in Alzheimer disease. *Arch.Gen.Psychiatry* **67,** 739-748.

Thompson A, Schafer J, Kuhn K, Kienle S, Schwarz J, Schmidt G, Neumann T, Johnstone R, Mohammed AK, Hamon C (2003) Tandem mass tags: a novel quantification strategy for comparative analysis of complex protein mixtures by MS/MS. *Anal.Chem.* **75,** 1895-1904.

Thorsell A, Bjerke M, Gobom J, Brunhage E, Vanmechelen E, Andreasen N, Hansson O, Minthon L, Zetterberg H, Blennow K (2010) Neurogranin in cerebrospinal fluid as a marker of synaptic degeneration in Alzheimer's disease. *Brain Res.* **1362,** 13-22.

Tiberti N, Hainard A, Lejon V, Robin X, Mumba ND, Turck N, Matovu E, Enyaru J, Mathu Ndung UJ, Scherl A, Dayon L, Sanchez JC (2010) Discovery and verification of osteopontin and beta-2-microglobulin as promising markers for staging human African trypanosomiasis. *Mol.Cell Proteomics.*

Timperman AT, Aebersold R (2000) Peptide electroextraction for direct coupling of in-gel digests with capillary LC-MS/MS for protein identification and sequencing. *Anal.Chem.* **72(17),** 4115-4121.

Togashi S, Lim SK, Kawano H, Ito S, Ishihara T, Okada Y, Nakano S, Kinoshita T, Horie K, Episkopou V, Gottesman ME, Costantini F, Shimada K, Maeda S (1997) Serum amyloid P component enhances induction of murine amyloidosis. *Lab Invest* **77,** 525-531.

Trougakos IP, Gonos ES (2002) Clusterin/apolipoprotein J in human aging and cancer. *Int.J.Biochem.Cell Biol.* **34,** 1430-1448.

Tsugawa N, Suhara Y, Kamao M, Okano T (2005) Determination of 25-hydroxyvitamin D in human plasma using high-performance liquid chromatography--tandem mass spectrometry. *Anal.Chem.* **77,** 3001-3007.

Tumani H, Lehmensiek V, Lehnert S, Otto M, Brettschneider J (2010) 2D DIGE of the cerebrospinal fluid proteome in neurological diseases. *Expert.Rev.Proteomics.* **7,** 29-38.

Turtoi A, Mazzucchelli GD, De PE (2010) Isotope coded protein label quantification of serum proteins--comparison with the label-free LC-MS and validation using the MRM approach. *Talanta* **80,** 1487-1495.

Ujiie M, Dickstein DL, Carlow DA, Jefferies WA (2003) Blood-brain barrier permeability precedes senile plaque formation in an Alzheimer disease model. *Microcirculation.* **10,** 463-470.

Unlu M, Morgan ME, Minden JS (1997) Difference gel electrophoresis: a single gel method for detecting changes in protein extracts. *Electrophoresis* **18,** 2071-2077.

Urakami K, Mori M, Wada K, Kowa H, Takeshima T, Arai H, Sasaki H, Kanai M, Shoji M, Ikemoto K, Morimatsu M, Hikasa C, Nakashima K (1999) A comparison of tau protein in cerebrospinal fluid between corticobasal degeneration and progressive supranuclear palsy. *Neurosci.Lett.* **259,** 127-129.

Urbanyi Z, Sass M, Laszy J, Takacs V, Gyertyan I, Pazmany T (2007) Serum amyloid P component induces TUNEL-positive nuclei in rat brain after intrahippocampal administration. *Brain Res.* **1145,** 221-226.

Utermann G (1988) Apolipoprotein polymorphism and multifactorial hyperlipidaemia. *J.Inherit.Metab Dis.* **11 Suppl 1,** 74-86.

van Marum RJ (2008) Current and future therapy in Alzheimer's disease. *Fundam.Clin.Pharmacol.* **22,** 265-274.

Van Weemen BK, Schuurs AH (1971) Immunoassay using antigen-enzyme conjugates. *FEBS Lett.* **15,** 232-236.

van OM, Hofman A, Soares HD, Koudstaal PJ, Breteler MM (2006) Plasma Abeta(1-40) and Abeta(1-42) and the risk of dementia: a prospective case-cohort study. *Lancet Neurol.* **5,** 655-660.

van UP, Kuhn K, Prinz T, Legner H, Schmid P, Baumann C, Tommassen J (2009) Identification of proteins of Neisseria meningitidis induced under iron-limiting conditions using the isobaric tandem mass tag (TMT) labeling approach. *Proteomics.* **9,** 1771-1781.

Vandenbogaert M, Li-Thiao-Te S, Kaltenbach HM, Zhang R, Aittokallio T, Schwikowski B (2008) Alignment of LC-MS images, with applications to biomarker discovery and protein identification. *Proteomics.* **8(4),** 650-672.

Vanderstichele H, Van KE, Hesse C, Davidsson P, Buyse MA, Andreasen N, Minthon L, Wallin A, Blennow K, Vanmechelen E (2000) Standardization of measurement of beta-amyloid(1-42) in cerebrospinal fluid and plasma. *Amyloid.* **7,** 245-258.

Vanmechelen E, Vanderstichele H, Davidsson P, Van KE, Van Der PB, Sjogren M, Andreasen N, Blennow K (2000) Quantification of tau phosphorylated at threonine 181 in human cerebrospinal fluid: a sandwich ELISA with a synthetic phosphopeptide for standardization. *Neurosci.Lett.* **285,** 49-52.

Vaughn CP, Crockett DK, Lim MS, Elenitoba-Johnson KS (2006) Analytical characteristics of cleavable isotope-coded affinity tag-LC-tandem mass spectrometry for quantitative proteomic studies. *J.Mol.Diagn.* **8,** 513-520.

Veerhuis R, Van Breemen MJ, Hoozemans JM, Morbin M, Ouladhadj J, Tagliavini F, Eikelenboom P (2003) Amyloid beta plaque-associated proteins C1q and SAP enhance the Abeta1-42 peptide-induced cytokine secretion by adult human microglia in vitro. *Acta Neuropathol.* **105,** 135-144.

Vetrivel KS, Cheng H, Lin W, Sakurai T, Li T, Nukina N, Wong PC, Xu H, Thinakaran G (2004) Association of gamma-secretase with lipid rafts in post-Golgi and endosome membranes. *J.Biol.Chem.* **279,** 44945-44954.

Visser PJ, Verhey F, Knol DL, Scheltens P, Wahlund LO, Freund-Levi Y, Tsolaki M, Minthon L, Wallin AK, Hampel H, Burger K, Pirttila T, Soininen H, Rikkert MO, Verbeek MM, Spiru L, Blennow K (2009) Prevalence and prognostic value of CSF markers of Alzheimer's disease pathology in patients with subjective cognitive impairment or mild cognitive impairment in the DESCRIPA study: a prospective cohort study. *Lancet Neurol.* **8,** 619-627.

Vissers JP, Langridge JI, Aerts JM (2007) Analysis and quantification of diagnostic serum markers and protein signatures for Gaucher disease. *Mol.Cell Proteomics* **6,** 755-766.

Vogeser M, Kyriatsoulis A, Huber E, Kobold U (2004) Candidate reference method for the quantification of circulating 25-hydroxyvitamin D3 by liquid chromatography-tandem mass spectrometry. *Clin.Chem.* **50,** 1415-1417.

Vogeser M (2010) Quantification of circulating 25-hydroxyvitamin D by liquid chromatography-tandem mass spectrometry. *J.Steroid Biochem.Mol.Biol.* **121,** 565-573.

Wahrle SE, Shah AR, Fagan AM, Smemo S, Kauwe JS, Grupe A, Hinrichs A, Mayo K, Jiang H, Thal LJ, Goate AM, Holtzman DM (2007) Apolipoprotein E levels in cerebrospinal fluid and the effects of ABCA1 polymorphisms. *Mol.Neurodegener.* **2,** 7.

Wallin AK, Hansson O, Blennow K, Londos E, Minthon L (2009) Can CSF biomarkers or pre-treatment progression rate predict response to cholinesterase inhibitor treatment in Alzheimer's disease? *Int.J.Geriatr.Psychiatry* **24,** 638-647.

Walsh DM, Selkoe DJ (2007) A beta oligomers - a decade of discovery. *J.Neurochem.* **101,** 1172-1184.

Walsh GM, Lin S, Evans DM, Khosrovi-Eghbal A, Beavis RC, Kast J (2009) Implementation of a data repository-driven approach for targeted proteomics experiments by multiple reaction monitoring. *J.Proteomics.* **72(5),** 838-852.

Wang PN, Lirng JF, Lin KN, Chang FC, Liu HC (2006) Prediction of Alzheimer's disease in mild cognitive impairment: a prospective study in Taiwan. *Neurobiol.Aging* **27,** 1797-1806.

Wang S, Wang R, Chen L, Bennett DA, Dickson DW, Wang DS (2010) Expression and functional profiling of neprilysin, insulin-degrading enzyme, and endothelin-converting enzyme in prospectively studied elderly and Alzheimer's brain. *J.Neurochem.* **115,** 47-57.

Washburn MP, Wolters D, Yates JR, III (2001) Large-scale analysis of the yeast proteome by multidimensional protein identification technology. *Nat.Biotechnol.* **19,** 242-247.

Wasinger VC, Cordwell SJ, Cerpa-Poljak A, Yan JX, Gooley AA, Wilkins MR, Duncan MW, Harris R, Williams KL, Humphery-Smith I (1995) Progress with gene-product mapping of the Mollicutes: Mycoplasma genitalium. *Electrophoresis* **16,** 1090-1094.

Webber KM, Smith MA, Lee HG, Harris PL, Moreira P, Perry G, Zhu X (2005) Mitogen- and stress-activated protein kinase 1: convergence of the ERK and p38 pathways in Alzheimer's disease. *J.Neurosci.Res.* **79,** 554-560.

Weiler JM, Daha MR, Austen KF, Fearon DT (1976) Control of the amplification convertase of complement by the plasma protein beta1H. *Proc.Natl.Acad.Sci.U.S.A* **73,** 3268-3272.

Weingarten MD, Lockwood AH, Hwo SY, Kirschner MW (1975) A protein factor essential for microtubule assembly. *Proc.Natl.Acad.Sci.U.S.A* **72,** 1858-1862.

Weisel JW (2005) Fibrinogen and fibrin. *Adv.Protein Chem.* **70,** 247-299.

Welge V, Fiege O, Lewczuk P, Mollenhauer B, Esselmann H, Klafki HW, Wolf S, Trenkwalder C, Otto M, Kornhuber J, Wiltfang J, Bibl M (2009) Combined CSF tau, p-tau181 and amyloid-beta 38/40/42 for diagnosing Alzheimer's disease. *J.Neural Transm.* **116,** 203-212.

Welge V, Fiege O, Lewczuk P, Mollenhauer B, Esselmann H, Klafki HW, Wolf S, Trenkwalder C, Otto M, Kornhuber J, Wiltfang J, Bibl M (2009) Combined CSF tau, p-tau181 and amyloid-beta 38/40/42 for diagnosing Alzheimer's disease. *J.Neural Transm.* **116(2),** 203-212.

Wells JM, McLuckey SA (2005) Collision-induced dissociation (CID) of peptides and proteins. *Methods Enzymol.* **402,** 148-185.

Wen D, Corina K, Chow EP, Miller S, Janmey PA, Pepinsky RB (1996) The plasma and cytoplasmic forms of human gelsolin differ in disulfide structure. *Biochemistry* **35,** 9700-9709.

White E, Welch VM, Sun T, Sniegoski LT, Schaffer R, Hertz HS, Cohen A (1982) The accurate determination of serum glucose by isotope dilution mass spectrometry--two methods. *Biomed.Mass Spectrom.* **9,** 395-405.

Whiteaker JR, Zhao L, Zhang HY, Feng LC, Piening BD, Anderson L, Paulovich AG (2007) Antibody-based enrichment of peptides on magnetic beads for mass-spectrometry-based quantification of serum biomarkers. *Anal.Biochem.* **362,** 44-54.

Whiteaker JR, Zhao L, Anderson L, Paulovich AG (2010) An automated and multiplexed method for high throughput peptide immunoaffinity enrichment and multiple reaction monitoring mass spectrometry-based quantification of protein biomarkers. *Mol.Cell Proteomics.* **9,** 184-196.

Whiteaker JR, Zhao L, Abbatiello SE, Burgess M, Kuhn E, Lin C, Pope ME, Razavi M, Anderson NL, Pearson TW, Carr SA, Paulovich AG (2011) Evaluation of large scale quantitative proteomic assay development using peptide affinity-based mass spectrometry. *Mol.Cell Proteomics.*

Whitwell JL, Przybelski SA, Weigand SD, Knopman DS, Boeve BF, Petersen RC, Jack CR, Jr. (2007) 3D maps from multiple MRI illustrate changing atrophy patterns as subjects progress from mild cognitive impairment to Alzheimer's disease. *Brain* **130,** 1777-1786.

Wiessner C, Wiederhold KH, Tissot AC, Frey P, Danner S, Jacobson LH, Jennings GT, Luond R, Ortmann R, Reichwald J, Zurini M, Mir A, Bachmann MF, Staufenbiel M (2011) The second-generation active Abeta immunotherapy CAD106 reduces amyloid accumulation in APP transgenic mice while minimizing potential side effects. *J.Neurosci.* **31(25),** 9323-9331.

Wiley WC, Wiley WC, McLaren IH, McLaren IH (1955) Time-of-Flight Mass Spectrometer with Improved Resolution. *Rev.Sci.Instrum.* **26,** 1150-1157.

Wilkins MR, Sanchez JC, Williams KL, Hochstrasser DF (1996) Current challenges and future applications for protein maps and post-translational vector maps in proteome projects. *Electrophoresis* **17,** 830-838.

Wilm M, Mann M (1996) Analytical properties of the nanoelectrospray ion source. *Anal.Chem.* **68,** 1-8.

Wilson MR, Yerbury JJ, Poon S (2008) Potential roles of abundant extracellular chaperones in the control of amyloid formation and toxicity. *Mol.Biosyst.* **4,** 42-52.

Wisniewski HM, Narang HK, Terry RD (1976) Neurofibrillary tangles of paired helical filaments. *J.Neurol.Sci.* **27,** 173-181.

Wisniewski JR, Zougman A, Nagaraj N, Mann M (2009) Universal sample preparation method for proteome analysis. *Nat.Methods.* **6(5),** 359-362.

Wisniewski T, Frangione B (1992) Apolipoprotein E: a pathological chaperone protein in patients with cerebral and systemic amyloid. *Neurosci.Lett.* **135,** 235-238.

Witke W, Sharpe AH, Hartwig JH, Azuma T, Stossel TP, Kwiatkowski DJ (1995) Hemostatic, inflammatory, and fibroblast responses are blunted in mice lacking gelsolin. *Cell* **81,** 41-51.

Wollnik H (1993) Time-of-flight mass analyzers. *Mass Spectrometry Reviews* **12,** 89-114.

Wood JA, Wood PL, Ryan R, Graff-Radford NR, Pilapil C, Robitaille Y, Quirion R (1993) Cytokine indices in Alzheimer's temporal cortex: no changes in mature IL-1 beta or IL-1RA but increases in the associated acute phase proteins IL-6, alpha 2-macroglobulin and C-reactive protein. *Brain Res.* **629,** 245-252.

Wu F, Sun D, Wang N, Gong Y, Li L (2011) Comparison of surfactant-assisted shotgun methods using acid-labile surfactants and sodium dodecyl sulfate for membrane proteome analysis. *Anal.Chim.Acta.* **698(1-2),** 36-43.

Xue H, Lu B, Zhang J, Wu M, Huang Q, Wu Q, Sheng H, Wu D, Hu J, Lai M (2010) Identification of serum biomarkers for colorectal cancer metastasis using a differential secretome approach. *J.Proteome Res.* **9,** 545-555.

Yalow RS, Berson SA (1960) Immunoassay of endogenous plasma insulin in man. *J.Clin.Invest* **39,** 1157-1175.

Yao M, Ma L, Humphreys WG, Zhu M (2008) Rapid screening and characterization of drug metabolites using a multiple ion monitoring-dependent MS/MS acquisition method on a hybrid triple quadrupole-linear ion trap mass spectrometer. *J.Mass Spectrom.* **43,** 1364-1375.

Ye H, Sun L, Huang X, Zhang P, Zhao X (2010) A proteomic approach for plasma biomarker discovery with 8-plex iTRAQ labeling and SCX-LC-MS/MS. *Mol.Cell Biochem.* **343,** 91-99.

Yocum AK, Chinnaiyan AM (2009) Current affairs in quantitative targeted proteomics: multiple reaction monitoring-mass spectrometry. *Brief.Funct.Genomic.Proteomic.* **8,** 145-157.

Yocum AK, Khan AP, Zhao R, Chinnaiyan AM (2010) Development of selected reaction monitoring-MS methodology to measure peptide biomarkers in prostate cancer. *Proteomics.* **10,** 3506-3514.

Zetterberg H, Tullhog K, Hansson O, Minthon L, Londos E, Blennow K (2010) Low incidence of post-lumbar puncture headache in 1,089 consecutive memory clinic patients. *Eur.Neurol.* **63,** 326-330.

Zetterberg M, Landgren S, Andersson ME, Palmer MS, Gustafson DR, Skoog I, Minthon L, Thelle DS, Wallin A, Bogdanovic N, Andreasen N, Blennow K, Zetterberg H (2008) Association of complement factor H Y402H gene polymorphism with Alzheimer's disease. *Am.J.Med.Genet.B Neuropsychiatr.Genet.* **147B,** 720-726.

Zhang J, Goodlett DR, Quinn JF, Peskind E, Kaye JA, Zhou Y, Pan C, Yi E, Eng J, Wang Q, Aebersold RH, Montine TJ (2005) Quantitative proteomics of cerebrospinal fluid from patients with Alzheimer disease. *J.Alzheimers.Dis.* **7,** 125-133.

Zhang R, Sioma CS, Thompson RA, Xiong L, Regnier FE (2002) Controlling deuterium isotope effects in comparative proteomics. *Anal.Chem.* **74,** 3662-3669.

Zhen EY, Berna MJ, Jin Z, Pritt ML, Watson DE, Ackermann BL, Hale JE (2007) Quantification of heart fatty acid binding protein as a biomarker for drug-induced cardiac and musculoskeletal necroses. *Proteomics.Clin.Appl.* **1(7),** 661-671.

Zipser BD, Johanson CE, Gonzalez L, Berzin TM, Tavares R, Hulette CM, Vitek MP, Hovanesian V, Stopa EG (2007) Microvascular injury and blood-brain barrier leakage in Alzheimer's disease. *Neurobiol.Aging* **28,** 977-986.

Zlokovic BV (2004) Clearing amyloid through the blood-brain barrier. *J.Neurochem.* **89,** 807-811.

Appendix

Intervention	Study phase	Company	Reference
Anti-amyloid agents			
Active immunisation with CAD106	II	Novartis	Weissner *et al*., 2011
Active immunisation with ACC-001	II	Wyeth	Pride *et al.*, 2008
Passive immunisation with PF-04360365	II	Pfizer	Poduslo *et al.*, 2007
Passive immunisation with AAB-001 (Bapineuzumab)	III	Elan Pharmaceuticals	Black *et al.*, 2010
Gamma secretase inhibitor MPC-7869 (Flurizan)	III	Myriad Pharmaceuticals	Hendrix and Wilcock, 2009
Gamma secretase inhibitor LY450139	III	Eli Lilly and Company	Fleisher *et al.*, 2008
Protein Kinase C stimulator: Bryostatin-1	II	Rockefeller Neurosciences Institute	Hongpaisan *et al.*, 2011
Beta amyloid synthesis inhibitor : Tarenflurbil (Flurbiprofen)	III	Myriad Pharmaceuticals	Green *et al.*, 2009
Plasminogen activator inhibitor: PAZ 417	III	Wyeth	Jacobsen *et al.*, 2008
Anti-aggregation agent: tramiprosate (3APS)	III	Neurochem/Bellus Health Inc	Gervais *et al.*, 2007
Chelating agent: PBT-2	II	Prana Biotechnology Ltd	Frisardi *et al*., 2010
Anti-aggregation/fibrillisation agents ELND005 (AZD-103)	II	Elan Pharmaceuticals	Piau *et al*., 2011
Cholesterol lowering agent: simvastatin (CLASP study)	III	National Institute on Aging	Piau *et al*., 2011
Cholesterol lowering agent: atorvastatin (LEADe study)	III	Pfizer	Feldman *et al.*, 2010
RAGE inhibitor: TTP488 (PF 04494700)	II	Pfizer	Piau *et al*., 2011
Tau aggregation inhibitor			
TRx0014	II	TauRx Therapeutics Ltd	Piau *et al*., 2011
Neuroprotective agents			
Vitamin E and Memantine (TEAM-AD)	III	Department of Veterans Affairs	Geldmacher *et al.*, 2011
Docosahexaenoic acid (DHA)	III	National Institute on Aging	Quinn *et al.*, 2010
Fish oil vs Fish oil and Alpha lipoic acid	II	National Institute on Aging	Piau *et al*., 2011
EGB 761 (Ginkgo Biloba extract)	II	Ipsen	Christen, 2004
Isoflavones (Novasoy)	II	University of Wisconsin	Piau *et al*., 2011
T-817MA (Benzothiophene derivative)	II	Toyama chemical Co Ltd	Fukushima *et al*., 2011
DCB-AD1 (Herbal Medicine)	II	Development Center dor biotechnology	Piau *et al*., 2011
Anti-inflammatory agent: IFN-alpha2A (in addition to donepezil)	II	National Center for Research Resources	Piau *et al*., 2011
Resveratrol supplement	III	Medical College of Wisconsin	Piau *et al*., 2011
Curcumin	II	John Douglas French Foundation	Piau *et al*., 2011
Protection of dopaminergic neurons: Arundic acid (ONO-25-06)	II	Ono Pharmaceutical	Mori *et al*., 2006
Neuroprotectant agent derived from herbal medicine: DCB-AD1	II	National Taiwan University Hospital	Piau *et al*., 2011
Neramexane	III	Forest laboratories	Piau *et al*., 2011

Appendix Table 1.1 List of drugs currently in development for the treatment of Alzheimer's disease.

Intervention	Study phase	Company	Reference
Neurorestorative factors			
Neurotrophic growth factor : SR57667B (Paliroden)	II	Sanofi-Aventis	Labie *et al.*, 2006
Neurotrophic growth factor: CERE-110	II	Ceregene	Bishop *et al.*, 2008
Neurotrophic growth factor : SR57746A (Xaliproden)	III	Sanofi-Aventis	Douillet and Orgogozo, 2009
Cholinergic agents			
Acetyl cholinesterase inhibitor: Huperzine A	II	National Institute on Aging	Piau *et al*., 2011
Acetyl cholinesterase inhibitor: ZT-1	II	Debiopharm S.A.	Piau *et al*., 2011
Salvia officinalis	III	National Center for Comp. and Alt. Med.	Piau *et al*., 2011
Nicotinic partial agonist: ABT-089	II	Abbott	Apostol *et al*., 2011
Nicotinic agonist: GTS-21 (DMXA)	II	CoMentis	Piau *et al*., 2011
Nicotinic modulator: MEM-3454	II	Memory Pharmaceuticals	Mazurov *et al.*, 2007
Nicotinic partial agonist : SSR-180711C	II	Sanofi-Aventis	Piau *et al*., 2011
Nicotinic partial agonist : Varenicicline	II	Pfizer	Piau *et al*., 2011
Nicotinic agonist: AZD3480	II	AstraZeneca	Frölich *et al.*, 2011
Thiazolidinediones and insulin			
SNIFF 120 study: insulin administered as a "nasal spray"	II	National Institute on Aging	Piau *et al*., 2011
NIC5-15 (natural product with mild insuline sensitizing effects)	II	Department of Veterans Affairs	Piau *et al*., 2011
Thiazolidinedione: Rosiglitazone	III	GlaxoSmithKline	Gold *et al.*, 2010
Ketone bodies: AC-1202 (Ketasyn™)	III	Accera Inc	Piau *et al*., 2011
Hormonal therapy			
SERMs: Raloxifene	II	National Institute on Aging	Piau *et al*., 2011
Testosterone (Androgel 1%)	II	Solvay Pharmaceuticals	Piau *et al*., 2011
Glucocorticoid receptor antagonist: Mifepristone	II	Institute for the Study of Aging /Corcept	Piau *et al*., 2011
7-hydroxysteroid pathway modulator: HF0220	II	Hunter-Fleming Ltd	Piau *et al*., 2011

Appendix Table 1.1 (continued)

Intervention	Study phase	Company	Reference
Other treatments			
5-HT 1a antagonist: Lecozotan SR (SRA-333)	III	Wyeth	Raje *et al.*, 2008
5-HT 1a agonist: Xaliprodene	III	Sanofi-Aventis	Piau *et al*., 2011
5-HT 6 receptor antagonist: SB-742457	II	GlaxoSmithKline	Maher-Edwards *et al.*, 2010
5-HT 6 receptor antagonist: SAM-531	II	Wyeth	Pogacic and Herrling, 2007
5-HT 4 agonist: PRX-03140	II	Epix Pharmaceuticals, Inc	Shen *et al*., 2011
Anti Histamine Agent: Dimebon	III	Medivation	Doody *et al.*, 2008
Mono amine oxydase inhibitor: Rasagiline	II	Eisai Medical Research Inc	Piau *et al*., 2011
Monoamine uptake inhibitor: Tesofensine	II	Boehringer Ingelheim Pharmaceuticals	Piau *et al*., 2011
Enantiomer of a dihydro pyridine: MEM 1003	II	Memory Pharmaceuticals	Rose *et al.*, 2007
GABA receptor antagonist: SGS742	II	Saegis Pharmaceuticals	Bullock, 2005
Benzodiazepin inverse agonist: AC-3933	II	Danippon Sumitomo Pharma America	Mise *et al.*, 2004
Cannabinoid CB1 antagonist: AVE-1625	II	Sanofi-Aventis	Piau *et al*., 2011
Dopamine modulator/ neuronal growth factor agonist: PYM50028	II	Phytopharm	Piau *et al*., 2011
Neurotransmitter modulator: Tesofensine (NS2330)	II	Boehringer Ingelheim Pharmaceuticals	Lehr *et al*., 2007
Oleonic glycosides saponins: SK-PC-B70M	II	SK Chemicals Co., Ltd	Han *et al.*, 2007
Nicotinamide	II	University of California	Green *et al.*, 2008
CNS modulator: MK-0249	II	Merck	Brioni *et al.*, 2011
CNS modulator: MK-0952	II	Merck	Gallant *et al.*, 2010

Appendix Table 1.1 (continued)

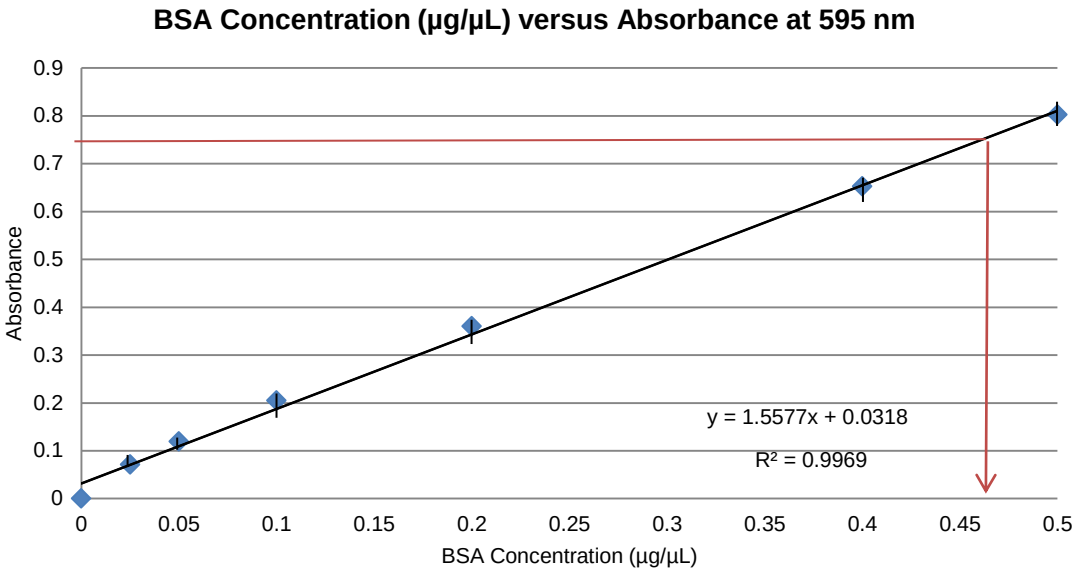

Appendix Figure 2.1 Standard Bradford protein assay to estimate the protein amount in a standard plasma sample. Each point on the curve is the mean of three replicates. The concentration of the plasma sample, as interpolated from the curve, is indicated by the arrow.

Peptide 2			T 1			T 1, 2, 3	T 1, 2, 3
L/H	A 1	A 2	A 3	Mean L/H	%CV	Mean L/H	%CV
0.33:1	0.41	0.45	0.34	0.4	13.5	0.43	4.34
1:1	1.1	1.25	1.35	1.24	10.4	1.2	7.68
3:1	3	3.44	3.41	3.28	7.51	3.46	4.44
9:1	9.75	9.23	11.2	10.4	9.95	11.1	8.78
27:1	32	31.5	35.3	32.9	6.32	34.3	9.34

Peptide 4			T 1			T 1, 2, 3	T 1, 2, 3
L/H	A 1	A 2	A 3	Mean L/H	%CV	Mean L/H	%CV
0.33:1	0.43	0.45	0.48	0.46	6.02	0.42	11.14
1:1	1.04	1.24	1.33	1.2	12.1	1.14	7.7
3:1	2.46	2.7	2.98	2.71	9.5	3.42	20.6
9:1	8.34	10.5	9.53	9.45	11.3	11.5	15.58
27:1	30.6	37.3	38.5	35.5	12	36	3.11

Peptide 6			T 1			T 1, 2, 3	T 1, 2, 3
L/H	A 1	A 2	A 3	Mean L/H	%CV	Mean L/H	%CV
0.33:1	0.41	0.4	0.36	0.39	8	0.37	6.69
1:1	1.17	1.05	9.12	1.04	12.3	1.06	11.39
3:1	3.3	3.06	2.68	3.01	10.4	3.17	7.45
9:1	9.08	7.96	8.49	8.51	6.58	8.73	7.12
27:1	31	25.2	27.4	27.9	10.5	29.1	9.71

Peptide 9			T 1			T 1, 2, 3	T 1, 2, 3
L/H	A 1	A 2	A 3	Mean L/H	%CV	Mean L/H	%CV
0.33:1	0.37	0.42	0.41	0.4	5.71	0.44	9.78
1:1	1.11	1.19	1.26	1.19	6.36	1.32	8.96
3:1	3.33	3.61	3.29	3.41	6.04	3.59	4.82
9:1	11.7	10.7	11.2	11.2	4.37	11.9	7.23
27:1	36.2	33.3	37.5	35.6	5.9	35.7	3.54

Appendix Table 2.1 Accuracy of TMT-SRM for BSA peptides quantitated in the presence of buffer-only. As an example of the accuracy of analytical repeats, the individual trueness (L/H ratio) for all analytical repeats (A 1, A 2 and A 3) of technical replicate 1 (T 1) is displayed. Furthermore, mean trueness and precision values across all technical replicates (T1, T2 and T3) are displayed.

Protein	SwissProt	Peptide sequence	Frequency
Clusterin	**P10909**	IDSLLENDR	2
		DQTVSDNELQEMSNQGSK	2
Not proteotypic		EPQDTYHYLPFSLPHR	2
Containing C, M or W		ALQEYR	2
≠ 6 - 25 amino acids		SLMPFSPYEPLNFHAMFQPFLEMIHEAQQAMDIHFHSPAFQHPPTEFIR	2
Internal R, K or H		EILSVDCSTNNPSQAK	2
N-terminal E or Q		ELDESLQVAER	2
Shortlisted for TMT-SRM		ELPGVCNETMMALWEECKPCLK	2
		FMETVAEK	2
		RPHFFFPK	2
		TNEER	2
		EDALNETR	2
		DQCDK	2
		YNELLK	2
		SGSGLVGR	2
		EIQNAVNGVK	2
		VTTVASHTSDSDVPSGVTEVVVK	2
		EGDDDR	2
		MLNTSSLLEQLNEQFNWVSR	2
		QQTHMLDVMQDHFSR	2
		LFDSDPITVTVPVEVSR[a]	2
		QLEEFLNQSSPFYFWMNGDR	2
		ASSIIDELFQDR	2
		LANLTQGEDQYYLR	2
		HNSTGCLR	2
		QTCMK	2
		TLLSNLEEAK	2
		SYQWK	2
		ESETK	3
		TLIEK	5
		FYAR	5
		TVCR	6
		FFTR	7
		YVNK	10
		EE	14
		VCR	88
		IVR	136
		QIK	160
		NPK	166
		EIR	263
		LTR	272
		CR	1190
		HR	1777
		MK	2058
		SR	3579
		LK	4679
		LR	4729
		K	15378
		R	15485

Appendix Table 3.1 Clusterin *in silico* peptide selection for TMT-SRM.
[a] previously synthesised and known to be poor.

Protein	SwissProt	Peptide sequence	Frequency
Complement C3	P01024	AELQCPQPAAR	1
		TMQALPYSTVGNSNNYLHLSVLR	2
Not proteotypic		GLEVTITAR[a]	2
Containing C, M or W		QDSLSSQNQLGVLPLSWDIPELVNMGQWK	2
≠ 6 - 25 amino acids		LESEETMVLEAHDAQGDVPVTVTVHDFPGK	2
Internal R, K or H		LLPVGR	2
N-terminal E or Q		ADIGCTPGSGK	2
Shortlisted for TMT-SRM		EVVADSVWVDVK	2
		TVMVNIENPEGIPVK	2
		AYYENSPQQVFSTEFEVK	2
		FLYGK	2
		IEGDHGAR	2
		VVLVSLQSGYLFIQTDK	2
		SPMYSIITPNILR	2
		IFTVNHK	2
		VLLDGVQNPR	2
		VPVAVQGEDTVQSLTQGDGVAK	2
		YYTYLIMNK	2
		QPVPGQQMTLK	2
		TIYTPGSTVLYR	2
		SGQSEDR	2
		ISLPESLK	2
		EYVLPSFEVIVEPTEK	2
		VEGTAFVIFGIQDGEQR	2
		GVFVLNK	2
		IPIEDGSGEVVLSR	2
		DSCVGSLVVK	2
		QELSEAEQATR	2
		YFKPGMPFDLMVFVTNPDGSPAYR	2
		IWDVVEK	2
		VVLVAVDK	2
		TELRPGETLNVNFLLR	2
		SLYVSATVILHSGSDMVQAER	2
		EPGQDLVVLPLSITTDFIPSFR	2
		FYYIYNEK	2
		TVLTPATNHMGNVTFTIPANR	2
		SGIPIVTSPYQIHFTK	2
		DYAGVFSDAGLTFTSSSGQQTAQR	2
		FVTVQATFGTQVVEK	2
		AEDLVGK	2
		LVAYYTLIGASGQR	2
		LSINTHPSQKPLSITVR	2
		FSCQR	3
		CCEDGMR	3
		VFLDCCNYITELR	3
		FISLGEACK	3
		ASHLGLAR	3
		IHWESASLLR	3
		AHEAK	3
		SVQLTEK	3
		LVLSSEK	3
		*	4

Appendix Table 3.2 Complement C3 *in silico* peptide selection for TMT-SRM. * 113 peptide sequences with a frequency > 4.

[a] those peptides which are not highlighted were not shortlisted for quantitation in this instance. However, they did satisfy the criteria for TMT-SRM target analyte selection, *i.e.,* proteotypicity, suitable length and absence of charged or modifiable residues. Thus, such peptides may have potential in future studies.

Protein	SwissProt	Peptide sequence	Frequency
Complement C3a	**P01024**	ASHLGLA	1
		FSCQR	3
Not proteotypic		SVQLTEK	3
Containing C, M or W		VFLDCCNYITELR	3
≠ 6 - 25 amino acids		FISLGEACK	3
Internal R, K or H		CCEDGMR	3
N-terminal E or Q		ENPMR	4
Shortlisted for TMT-SRM		QHAR	11
		YPK	74
		MDK	107
		VGK	170
		ELR	591
		TR	2394
		K	15378
		R	15485

Appendix Table 3.3 Complement C3a *in silico* peptide selection for TMT-SRM.

Protein	SwissProt	Peptide sequence	Frequency
CFH	**P08603**	VSVLCQENYLIQEGEEITCK	1
		WSSPPQCEGLPCK	1
Not proteotypic		CVEISCK	1
Containing C, M or W		EGWIHTVCINGR	1
≠ 6 - 25 amino acids		NGFYPATR[a]	1
Internal R, K or H		HGGLYHENMR	1
N-terminal E or Q		TGESVEFVCK	1
Shortlisted for TMT-SRM		GEWVALNPLR	1
		LGYVTADGETSGSITCGK	1
		VGEVLK	1
		AVYTCNEGYQLLGEINYR	1
		EQVQSCGPPPELLNGNVK	1
		LNDTLDYECHDGYESNTGSTTGSIVCGYNGWSDLPICYER	1
		SIDVACHPGYALPK	1
		EEYGHSEVVEYYCNPR	1
		FVCNSGYK	1
		CLGEK	1
		NTEILTGSWSDQTYPEGTQAIYK	1
		ECELPK	1
		SSNLIILEEHLK	1
		CRPGYR	1
		ISEENETTCYMGK	1
		WDPEVNCSMAQIQLCPPPPQIPNSHNMTTTLNYR	1
		RPCGHPGDTPFGTFTLTGGNVFEYGVK	1

Appendix Table 3.4 CFH *in silico* peptide selection for TMT-SRM. * 40 peptide sequences with a frequency > 3.

[a] those peptides which are not highlighted were not shortlisted for quantitation in this instance. However, they did satisfy the criteria for TMT-SRM target analyte selection, *i.e.,* proteotypicity, suitable length and absence of charged or modifiable residues. Thus, such peptides may have potential in future studies.

Protein	SwissProt	Peptide sequence	Frequency
CFH	**P08603**	GDAVCTESGWRPLPSCEEK	1
		CLPVTAPENGK	1
Not proteotypic		CTSTGWIPAPR	1
Containing C, M or W		NDFTWFK	1
≠ 6 - 25 amino acids		SPDVINGSPISQK	1
Internal R, K or H		IEGDEEMHCSDDGFWSK	1
N-terminal E or Q		ECDTDGWTNDIPICEVVK	1
Shortlisted for TMT-SRM		AQTTVTCMENGWSPTPR	1
		WSHPPSCIK	1
		DTSCVNPPTVQNAYIVSR	1
		WQSIPLCVEK	1
		TDCLSLPSFENAIPMGEK	1
		IDVHLVPDR	1
		SCDNPYIPNGDYSPLR	1
		CFEGFGIDGPAIAK	1
		EFDHNSNIR	1
		WTGRPTCR	1
		EYHFGQAVR	1
		DGWSAQPTCIK	1
		AGEQVTYTCATYYK	1
		SITCIHGVWTQLPQCVAIDK	1
		YYSYYCDEHFETPSGSYWDHIHCTQDGWSPAVPCLR	1
		TGDEITYQCR	1
		SCDIPVFMNAR	1
		MDGASNVTCINSR	1
		FSCKPGFTIVGPNSVQCYHFGLSPDLPICK	1
		CTLKPCDYPDIK	1
		IPCSQPPQIEHGTINSSR	1
		SSIDIENGFISESQYTYALK	1
		SSQESYAHGTK	1
		IQCVDGEWTTLPVCIVEESTCGDIPELEHGWAQLSSPPYYYGDSVEFNCSESFTMIGHR	1
		SLGNVIMVCR	1
		EDCNELPPR	1
		SPPEISHGVVAHMSDSYQYGEEVTYK	1
		CNMGYEYSER	1
		IVSSAMEPDR	1
		LSYTCEGGFR	1
		GNTAK	2
		CYFPYLENGYNQNYGR	2
		TTCWDGK	2
		CLHPCVISR	2
		LEYPTCAK	2
		CGPPPPIDNGDITSFPLSVYAPASSVEYQCQNLYQLEGNK	2
		RPYFPVAVGK	2
		EIMENYNIALR	2
		SHTLR	2
		SPYEMFGDEEVMCLNGNWTEPPQCK	2
		YPSGER	2
		*	3

Appendix Table 3.4 (continued)

Protein	SwissProt	Peptide sequence	Frequency
A2M	P01023	TEVSSNHVLIYLDK	1
		GCVLLSYLNETVTVSASLESVR	1
Not proteotypic		FEVQVTVPK	1
Containing C, M or W		VGFYESDVMGR	1
≠ 6 - 25 amino acids		DLKPAIVK	1
Internal R, K or H		VIFIR	1
N-terminal E or Q		MCPQLQQYEMHGPEGLR	1
Shortlisted for TMT-SRM		YFPETWIWDLVVVNSAGVAEVGVTVPDTITEWK	1
		GGVEDEVTLSAYITIALLEIPLTVTHPVVR	1
		TGTHGLLVK	1
		EQAPHCICANGR	1
		SIYKPGQTVK	1
		FQVDNNNR[a]	1
		FSGQLNSHGCFYQQVK	1
		QEDMK	1
		GEAFTLK	1
		DLGNA	1
		QQNAQGGFSSTQDTVVALHALSK	1
		EEFPFALGVQTLPQTCDEPK	1
		AIGYLNTGYQR	1
		SSSNEEVMFLTVQVK	1
		TEHPFTVEEFVLPK	1
		DTVIKPLLVEPEGLEK	1
		YSDASDCHGEDSQAFCEK	1
		QSSEITR	1
		LVHVEEPHTETVR	1
		AHTSFQISLSVSYTGSR	1
		AVDQSVLLMKPDAELSASSVYNLLPEK	1
		GNEANYYSNATTDEHGLVQFSINTTNVMGTSLTVR	1
		VFQLK	1
		DLTGFPGPLNDQDDEDCINR	1
		AAQVTIQSSGTFSSK	1
		QGIPFFGQVR	1
		LVDGK	1
		LHTEAQIQEEGTVVELTGR	1
		VSVQLEASPAFLAVPVEK	1
		LPPNVVEESAR	1
		SASNMAIVDVK	1
		QFSFPLSSEPFQGSYK	1
		IITILEEEMNVSVCGLYTYGKPVPGHVTVSICR	1
		NALFCLESAWK	1
		NEDSLVFVQTDK	1
		SLFTDLEAENDVLHCVAFAVPK	1
		GPTQEFK	1
		VDLSFSPSQSLPASHAHLR	1
		SLNEEAVK	1
		LSFYYLIMAK	1
		SNHVSR	1
		SFVHLEPMSHELPCGHTQTVQAHYILNGGTLLGLK	1

Appendix Table 3.5 A2M *in silico* peptide selection for TMT-SRM. * 20 peptide sequences with a frequency > 3.

[a] those peptides which are not highlighted were not shortlisted for quantitation in this instance. However, they did satisfy the criteria for TMT-SRM target analyte selection, *i.e.,* proteotypicity, suitable length and absence of charged or modifiable residues. Thus, such peptides may have potential in future studies.

Protein	SwissProt	Peptide sequence	Frequency
A2M	**P01023**	LSFVK	1
		GGIVR	1
Not proteotypic		IAQWQSFQLEGGLK	1
Containing C, M or W		SVSGKPQYMVLVPSLLHTETTEK	1
≠ 6 - 25 amino acids		VSNQTLSLFFTVLQDVPVR	1
Internal R, K or H		VTGEGCVYLQTSLK	1
N-terminal E or Q		ALLAYAFALAGNQDK	1
Shortlisted for TMT-SRM		GHFSISIPVK	1
		ASVSVLGDILGSAMQNTQNLLQMPYGCGEQNMVLFAPNIYVLDYLNETQQLTPEVK	1
		ETTFNSLLCPSGGEVSEELSLK	1
		LLLQQVSLPELPGEYSMK	1
		VYDYYETDEFAIAEYNAPCSK	1
		DNSVHWERPK	1
		SDIAPVAR	1
		TAQEGDHGSHVYTK	1
		HYDGSYSTFGER	1
		HNVYINGITYTPVSSTNEK	1
		VVSMDENFHPLNELIPLVYIQDPK	1
		LLIYAVLPTGDVIGDSAK	1
		SLGNVNFTVSAEALESQELCGTEVPSVPEHGR	1
		QTVSWAVTPK	1
		VTAAPQSVCALR	1
		YDVENCLANK	1
		TTVMVK	1
		SPCYGYQWVSEEHEEAHHTAYLVFSPSK	1
		APVGHFYEPQAPSAEVEMTSYVLLAYLTAQPAPTSEDLTSATNIVK	1
		AYIFIDEAHITQALIWLSQR	1
		DMYSFLEDMGLK	1
		QLNYK	2
		AFTNSK	2
		AFQPFFVELTMPYSVIR	2
		NQGNTWLTAFVLK	2
		VDSHFR	2
		SSGSLLNNAIK	2
		MVSGFIPLKPTVK	2
		YGAATFTR	2
		VVVQK	2
		TFAQAR	2
		YNILPEK	2
		EYEMK	2
		DNGCFR	2
		GVPIPNK	2
		AGAFCLSEDAGLGISSTASLR	2
		ATVLNYLPK	2
		*	3

Appendix Table 3.5 (continued)

Protein	SwissProt	Peptide sequence	Frequency
FGG	**P02679**	LTIGEGQQHHLGGAK	1
		YLQEIYNSNNQK[a]	1
Not proteotypic		FEGNCAEQDGSGWWMNK	1
Containing C, M or W		FGSYCPTTCGIADFLSTYQTK	1
≠ 6 - 25 amino acids		NWIQYK	1
Internal R, K or H		TSEVK	1
N-terminal E or Q		DNCCILDER	1
Shortlisted for TMT-SRM		ANQQFLVYCEIDGSGNGWTVFQK	1
		VAQLEAQCQEPCK	1
		VELEDWNGR	1
		IVNLK	1
		LDGSVDFK	1
		WYSMK	1
		K.I]HLISTQSAIPYALR.V	1
		ASTPNGYDNGIIWATWK	1
		DLQSLEDILHQVENK	1
		LTYAYFAGGDAGDAFDGFDFGDDPSDK	1
		YVATR	1
		DCQDIANK	1
		VGPEADK	1
		QVRPEHPAETEYDSLYPEDDL	1
		CHAGHLNGVYYQGGTYSK	1
		TSTADYAMFK	1
		EGFGHLSPTGTTEFWLGNEK	1
		MLEEIMK	1
		AIQLTYNPDESSKPNMIDAATLK	1
		FFTSHNGMQFSTWDNDNDK	1
		QSGLYFIKPLK	1
		IIPFNR	1
		YEASILTHDSSIR	1
		IHLISTQSAIPYALR	1
		DTVQIHDITGK	1
		TTMK	3
		QLIK	14
		VDK	156
		GAK	217
		YR	1540
		TR	2394
		SR	3579
		EK	4547
		K	15378
		R	15485

Appendix Table 3.6 FGG *in silico* peptide selection for TMT-SRM.

[a] those peptides which are not highlighted were not shortlisted for quantitation in this instance. However, they did satisfy the criteria for TMT-SRM target analyte selection, *i.e.,* proteotypicity, suitable length and absence of charged or modifiable residues. Thus, such peptides may have potential in future studies.

Protein	SwissProt	Peptide sequence	Frequency
SAP	**P02743**	GYVIIKPLVWV	1
		DNELLVYK	2
Not proteotypic		VGEYSLYIGR	2
Containing C, M or W		IVLGQEQDSYGGK	2
≠ 6 - 25 amino acids		FPAPVHICVSWESSSGIAEFWINGTPLVK	2
Internal R, K or H		SQSFVGEIGDLYMWDSVLPPENILSAYQGTPLPANILDWQALNYEIR	2
N-terminal E or Q		ESVTDHVNLITPLEKPLQNFTLCFR	2
Shortlisted for TMT-SRM		AYSDLSR	2
		AYSLFSYNTQGR	2
		HTDLSGK	2
		VFVFPR	2
		QGYFVEAQPK	2
		VTSK	12
		VIEK	19
		FDR	70
		GLR	362
		HK	1558
		ER	3797
		K	15378

Appendix Table 3.7 SAP *in silico* peptide selection for TMT-SRM.

Protein	SwissProt	Peptide sequence	Frequency
ApoE	**P02649**	SWFEPLVEDMQR	1
		WVQTLSEQVQEELLSSQVTQELR	1
Not proteotypic		QWAGLVEK	1
Containing C, M or W		VQAAVGTSAAPVPSDNH	1
≠ 6 - 25 amino acids		LDEVK	1
Internal R, K or H		LQAEAFQAR	1
N-terminal E or Q		WELALGR	1
Shortlisted for TMT-SRM		VEQAVETEPEPELR	1
		LGADMEDVCGR	1
		QQTEWQSGQR	1
		SELEEQLTPVAEETR	1
		GEVQAMLGQSTEELR	1
		LAVYQAGAR	1
		EQVAEVR	1
		AQAWGER	1
		LGPLVEQGR	1
		GLSAIR	1
		FWDYLR	1
		DADDLQK	1
		ELQAAQAR	1
		ALMDETMK	1
		AATVGSLAGQPLQER	1
		LASHLR	1
		MEEMGSR	1
		LEEQAQQIR	1
		EGAER	2
		LVQYR	2
		*	90

Appendix Table 3.8 ApoE *in silico* peptide selection for TMT-SRM. * 14 peptide sequences with a frequency > 90.

Protein	SwissProt	Peptide	Frequency
Gelsolin	**P06396**	AATASR	1
		MAPHRPAPALLCALSLALCALSLPVR	1
Not proteotypic		VPEARPNSMVVEHPEFLK	1
Containing C, M or W		GASQAGAPQGR[a]	1
≠ 6 - 25 amino acids		MVVEHPEFLK	1
Internal R, K or H		VVQGK	2
N-terminal E or Q		EDAANR	2
Shortlisted for TMT-SRM		EPAHLMSLFGGKPMIIYK	2
		EPAHLMSLFGGKPMIIYK	2
		TASDFITK	2
		FVIEEVPGELMQEDLATDDVMLLDTWDQVFVWVGK	2
		YIETDPANR	2
		EPGLQIWR	2
		MDAHPPR	2
		AGALNSNDAFVLK	2
		QANTEER	2
		QTQVSVLPEGGETPLFK	2
		LFACSNK	2
		VSNGAGTMSVSLVADENPFAQGALK	2
		ATQVSK	2
		VPVDPATYGQFYGGDSYIILYNYR	2
		ANSAGATR	2
		GGVASGFK	2
		DSQEEEK	2
		ATQVSK	2
		TPITVVK	2
		FDLVPVPTNLYGDFFTGDAYVILK	2
		DSQEEEK	2
		QANTEER	2
		SEDCFILDHGK	2
		QGFEPPSFVGWFLGWDDDYWSVDPLDR	2
		GGVASGFK	2
		VHVSEEGTEPEAMLQVLGPKPALPAGTEDTAK	2
		VPFDAATLHTSTAMAAQHGMDDDGTGQK	2
		TPITVVK	2
		LFACSNK	2
		FDLVPVPTNLYGDFFTGDAYVILK	2
		IFVWK	2
		AMAELAA	2
		AQPVQVAEGSEPDGFWEALGGK	2
		AVEVLPK	2
		TEALTSAK	2
		VHVSEEGTEPEAMLQVLGPKPALPAGTEDTAK	2
		DPDQTDGLGLSYLSSHIANVER	2
		HVVPNEVVVQR	2
		AGALNSNDAFVLK	2
		LFQVK	2
		QIWR	2
		VPVDPATYGQFYGGDSYIILYNYR	2

Appendix Table 3.9 Gelsolin *in silico* peptide selection for TMT-SRM. * 78 peptide sequences with a frequency > 4.

[a] those peptides which are not highlighted were not shortlisted for quantitation in this instance. However, they did satisfy the criteria for TMT-SRM target analyte selection, *i.e.,* proteotypicity, suitable length and absence of charged or modifiable residues. Thus, such peptides may have potential in future studies.

Protein	SwissPort	Peptide	Frequency
Gelsolin	**P06396**	EVQGFESATFLGYFK	2
		VSNGAGTMSVSLVADENPFAQGALK	2
Not proteotypic		SEDCFILDHGK	2
Containing C, M or W		TPSAAYLWVGTGASEAEK	2
≠ 6 - 25 amino acids		ATEVPVSWESFNNGDCFILDLGNNIHQWCGSNSNR	2
Internal R, K or H		QGQIIYNWQGAQSTQDEVAASAILTAQLDEELGGTPVQSR	2
N-terminal E or Q		AMAELAA	2
Shortlisted for TMT-SRM		DPDQTDGLGLSYLSSHIANVER	2
		TGAQELLR	2
		FVIEEVPGELMQEDLATDDVMLLDTWDQVFVWVGK	2
		VVQGK	2
		LFQVK	2
		QGFEPPSFVGWFLGWDDDYWSVDPLDR	2
		AQPVQVAEGSEPDGFWEALGGK	2
		QIWR	2
		IFVWK	2
		IEGSNK	2
		YIETDPANR	2
		QTQVSVLPEGGETPLFK	2
		EVQGFESATFLGYFK	2
		QGQIIYNWQGAQSTQDEVAASAILTAQLDEELGGTPVQSR	2
		TEALTSAK	2
		EDAANR	2
		NGNLQYDLHYWLGNECSQDESGAAAIFTVQLDDYLNGR	2
		ATEVPVSWESFNNGDCFILDLGNNIHQWCGSNSNR	2
		MDAHPPR	2
		EPGLQIWR	2
		EGGQTAPASTR	2
		ANSAGATR	2
		NGNLQYDLHYWLGNECSQDESGAAAIFTVQLDDYLNGR	2
		EGGQTAPASTR	2
		TPSAAYLWVGTGASEAEK	2
		VPFDAATLHTSTAMAAQHGMDDDGTGQK	2
		*	4

Appendix Table 3.9 (continued)

Peptide ID	mean t_R (min)	DP (V)			CE (V)			CXP (V)		
		Q3 (1)	Q3 (2)	Q3 (3)	Q3 (1)	Q3 (2)	Q3 (3)	Q3 (1)	Q3 (2)	Q3 (3)
1	47.5	120	120	120	48.4	48.1	48.3	16.2	18.3	16.5
2	64.5	120	120	120	52.8	48.4	42.7	15.6	18.8	25.9
3	41.8	90	90	90	43.2	42.2	37.8	12.1	13.1	18.2
4	37.5	90	90	90	52.8	45	44.2	19.9	20.4	22.2
5	20	90	90	90	36.3	30.1	31.8	7.2	9.7	13.9
6	36	100	100	100	44.8	41.9	41.5	11.3	13.5	14
7	39	80	80	80	22	29.8	24.2	11	12.8	14.8
8	46.5	100	100	100	47.9	46.9	45.7	13	15.1	21.7
9	55	130	130	130	53.4	52.1	52.2	22.8	22.8	24.3
10	23.2	80	80	80	37.8	30	23.9	6.8	6.9	9.7
11	31.3	110	110	110	54.5	53.3	50	18.6	20.3	21.1
12	34.2	80	80	80	28.2	25.6	26.6	7.8	8.4	11.2
13	31.5	100	100	100	42.6	36.3	36.8	8.9	10.9	12.1
14	33.5	100	100	100	44.9	45	44.2	17.9	18.7	19.5
15	26	120	120	120	47.6	45.3	42.7	11.3	14.4	18.1
16	72.7	80	80	80	33.3	31.9	30.1	13.5	17.5	21.6
17	36	90	90	90	41.4	40	40	11.3	12.8	13.2
18	39.3	130	130	130	55.1	55	54.4	22.9	21.9	21.5
19	38.5	120	120	120	42.8	39.1	39	12.9	15	17.3
20	19.8	90	90	90	41.2	39.9	37.1	12.5	13	13.9
21	35.8	120	120	120	54.9	52	51	18.1	21	27.1
22	41.9	120	120	120	46	42.8	42.1	14.7	17.3	18
23	43.5	110	110	110	48.8	48.5	48.9	16.1	20.1	22.6
24	34	100	100	100	40.7	38	39.2	10.3	12.3	13.4
25	29.3	110	110	110	43.9	41.9	42	11.6	15	18.4
26	71	140	140	140	59.9	59	58.1	18.8	20.2	24
27	50.3	80	80	80	35.6	31	26.9	13.5	16	21.7
28	44	140	140	140	59.8	57.1	50	21.9	21	22.4
29	33.7	100	100	100	44.6	44.5	44	11.1	14.5	17.2
30	33.1	110	110	110	41.5	38.8	37.9	12	12.4	16.9
31	22.5	70	70	70	23.9	28.5	29.1	7.8	8.7	11.5
32	75.5	100	100	100	41.8	37.1	37.3	11.3	14.6	14

Appendix Table 3.10 Optimisation of the TMT-SRM method for the enhanced detection of each candidate AD peptide in plasma. For each transition of peptides 1 - 32, the optimised DP, CE and CXP are given. Also displayed is the t_R for SRM scheduling, applied to maximise SRM dwell time.

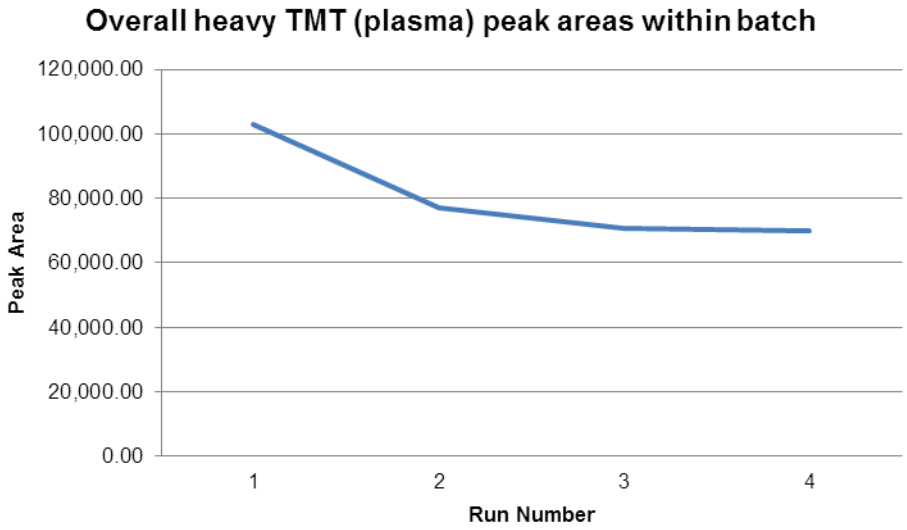

Appendix Figure 3.1 Stability of plasma peak areas during TMT-SRM reproducibility experiments. The mean heavy TMT (plasma) peak area for all transitions of all peptides is plotted over the course of four runs, *i.e.*, a batch, within the TMT-SRM reproducibility experiments on the nano-LC platform. No increase in area was observed over the course of the runs, demonstrating that plasma carryover o/c was not observed.

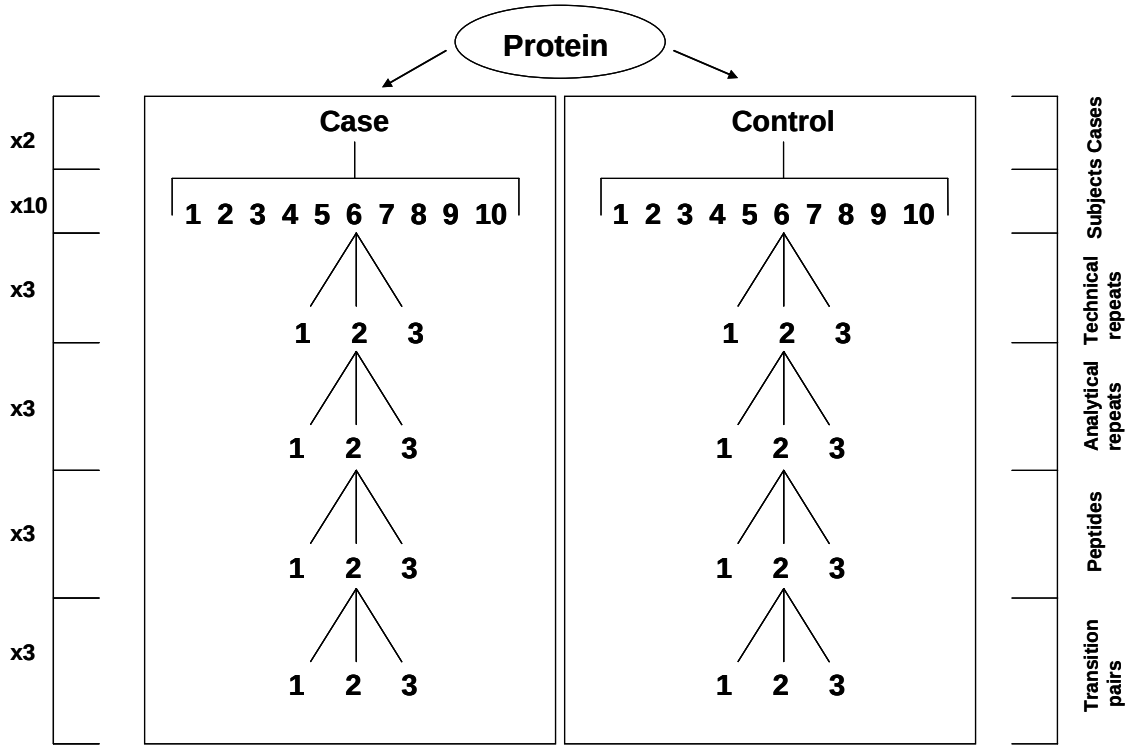

Appendix Figure 4.1 Overview of the TMT-SRM assay validation experiment. Ten disease and ten control samples were selected for each protein. Three digests were performed on each sample (technical digests) followed by three analytical measurements of each digest. Each protein had approximately three peptides for quantitation, which was determined from three transition pairs per peptide.

```
UNIANOV
peak.area.ratio BY case digest analysis transition
/RANDOM = digest analysis transition
/METHOD = SSTYPE(3)
/INTERCEPT = INCLUDE
/EMMEANS = TABLES(OVERALL)
/EMMEANS = TABLES(case)
/EMMEANS = TABLES(digest)
/EMMEANS = TABLES(analysis)
/EMMEANS = TABLES(transition)
/CRITERIA = ALPHA (0.05)
/DESIGN = case case(digest) case(digest(analysis)) case(digest(analysis(transition)))
.
```

Appendix Figure 4.2 Syntax script used in SPSS for TMT-SRM assay validation experiments.

Protein	Peptide ID	t_R (min)	S-Lens (V)	CE (V)			
				Transition 1	Transition 2	Transition 3	Transition4
Clusterin α-chain	1	13.42	189	34	33	29	NA
Clusterin β-chain	5	5.34	155	24	21	19	NA
Complement C3	8	12.85	192	32	30	30	NA
	9	14.55	188	36	36	36	NA
CFH	12	11.16	127	19	16	17	NA
	13	10.57	170	27	26	24	NA
A2M	14	10.38	178	30	30	30	31
	15	9.74	193	30	31	25	32
FGG	19	11.54	174	27	28	28	NA
	20	6.31	177	26	25	26	NA
SAP	22	11.90	193	30	30	30	31
	23	11.97	198	33	33	34	NA
ApoE	24	9.63	190	26	25	26	NA
	25	10.64	190	30	32	27	26
Gelsolin	29	10.53	188	25	28	27	33
	30	11.09	198	25	25	25	28
	31	8.51	122	16	19	19	NA

Appendix Table 4.1 Determination of t_R and TSQ Vantage instrument voltages for TMT-SRM method development. Mean t_R values used to apply SRM scheduling and the optimal S-Lens for each peptide ion and CE for each transition of each target analyte are displayed. NA = not applicable.

	SEG1	SEG2	SEG3	SEG4	SEG5	SEG6	SEG7
Time (min)	0.00-9.07	9.07-10.07	10.07-10.24	10.24-10.88	10.88-11.14	11.14-12.92	12.92-22.00
Δ Time (min)	9.07	1.00	0.17	0.64	0.26	1.78	9.08
Peptide ID	5	25	25	14	29	30	8
	20	15	15	29	13	12	9
	31	14	14	13	24	19	1
		29	29	24	30	22	
			13	30	12	23	
			24	12	19	8	
No. of Transitions	18	24	36	36	36	36	18
Cycle time (sec)	0.36	0.48	0.72	0.72	0.72	0.72	0.36

Appendix Table 4.2 SRM scheduling scheme for TMT-SRM analysis of candidate AD peptides on a TSQ Vantage. Peptides were separated into a segmented scheduling scheme to increase the number of data points for each transition. A minimal 1 min SRM scheduling window was applied to all transitions, with a maximal cycle time of 0.72 sec per segment.

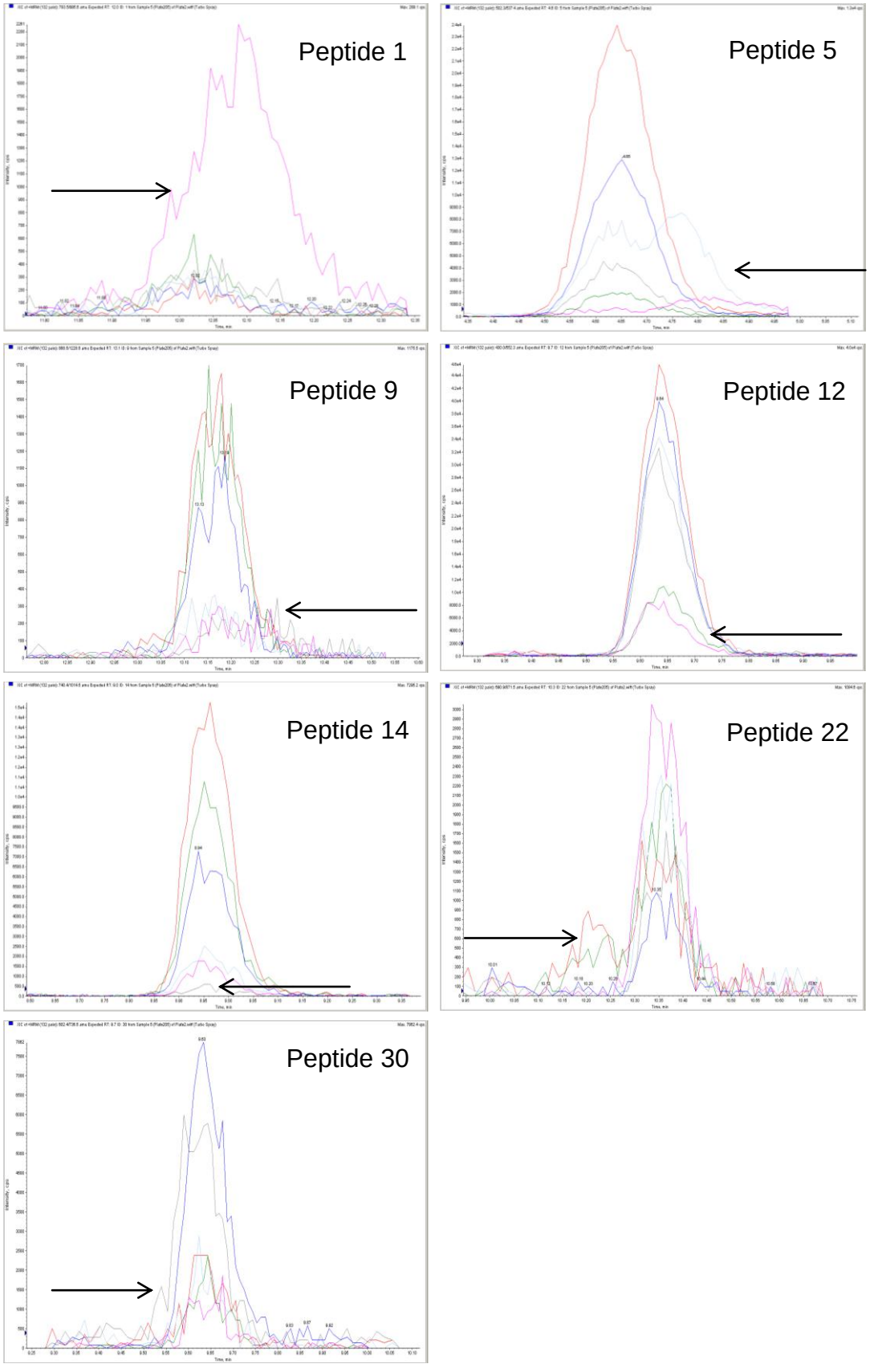

Appendix Figure 4.3 TMT-SRM transitions affected by plasma background interference. The transitions which were detrimentally affected by plasma background and thus, removed from the analysis are indicated by an arrow.

Protein	Peptide	95% CI	80% CI
Clusterin α-chain	1	23*	15
Clusterin β-chain	5	19	12
Complement C3	8	4	3
	9	5	4
CFH	12	5	4
	13	4	3
A2M	14	638	386
	15	17	11
FGG	19	20	13
	20	198	120
SAP	22	8	6
	23	7	5
ApoE	24	35607	21507
	25	16	10

Appendix Table 5.1 *A priori* power analysis to determine minimum number of samples required for biomarker validation experiments. Based on the fold changes observed between AD and NDC samples in Section 4.2.1, low sample numbers were projected to have sufficient power in achieving equivalent fold changes for the majority of peptides.
***** sample number

```
UNIANOV
peak.area.ratio BY case transition
/RANDOM = transition
/METHOD = SSTYPE(3)
/INTERCEPT = INCLUDE
/EMMEANS = TABLES(OVERALL)
/EMMEANS = TABLES(case)
/EMMEANS = TABLES(transition)
/CRITERIA = ALPHA (0.05)
/DESIGN = case case(transition)
.
```

Appendix Figure 5.1 Synthax script used in SPSS for biomarker evaluation by TMT-SRM.

No.	Description	Diagnosis	Gender	ApoE	Age Of Onset (yrs)	Disease duration (yrs)	MMSE V1	MMSE V2	MMSE V3	MMSE V4	MMSE V5	MMSE decline regression
1	KPOADC004	RCD	F	34	62	4.7	26	25	24	25	22	-3.20
2	KPOADC002	SCD	F	44	66	2.3	26	25	25	24	25	-1.20
3	KPOCTL008	NDC	F	34	NA	NA	30	NA	NA	NA	30	0.00
4	KPOADC005	RCD	F	33	78	5.1	17	13	9	5	1	-16.00
5	KPOADC006	SCD	M	33	69	10.5	27	26	27	25	NA	-2.00
6	KPOCTL011	NDC	F	33	NA	NA	30	NA	NA	NA	30	0.00
7	KPOADC008	RCD	F	33	82	0.8	21	13	19	16	17	-2.00
8	KPOADC007	SCD	F	34	68	3.4	25	24	25	28	24	0.80
9	KPOCTL023	NDC	M	33	NA	NA	30	NA	NA	NA	30	0.00
10	KPOADC009	RCD	F	44	71	5.0	15	10	9	6	5	-9.60
11	KPOADC011	SCD	M	34	79	2.2	24	27	26	27	NA	3.20
12	LNDCTL004	NDC	F	33	NA	NA	30	NA	NA	NA	30	0.00
13	KPOADC010	RCD	M	33	80	7.8	25	24	22	14	6	-19.20
14	KPOADC013	SCD	M	44	71	2.3	28	25	30	28	26	-0.40
15	LNDCTL005	NDC	M	23	NA	NA	30	NA	NA	NA	30	0.00
16	KPOADC012	RCD	F	34	62	4.6	25	20	21	20	19	-4.80
17	KPOADC017	SCD	F	33	75	2.5	26	22	23	24	25	0.00
18	LNDCTL006	NDC	F	34	NA	NA	30	NA	NA	NA	30	0.00
19	KPOADC034	RCD	M	44	72	6.6	12	6	9	NA	6	-6.00
20	KPOADC018	SCD	F	34	68	4.4	24	24	22	25	22	-1.20
21	LNDCTL043	NDC	M	33	NA	NA	30	NA	NA	NA	30	0.00
22	LDZADC008	RCD	F	33	55	3.6	22	19	16	13	10	-12.00
23	KPOADC031	SCD	M	33	81	1.7	26	26	29	28	25	0.00
24	LNDCTL044	NDC	F	33	NA	NA	30	NA	NA	NA	30	0.00
25	LNDADC006	RCD	M	33	83	5.5	20	22	17	21	17	-2.80
26	KPOADC039	SCD	F	34	70	5.8	25	26	25	24	25	-0.80
27	LNDCTL061	NDC	F	34	NA	NA	30	NA	NA	NA	30	0.00
28	THSADC029	RCD	F	33	80	2.2	23	19	18	21	NA	-2.80
29	LDZADC014	SCD	F	34	70	1.1	27	NA	26	NA	27	0.00
30	LNDCTL062	NDC	F	33	NA	NA	30	NA	NA	NA	30	0.00

Appendix Table 5.2 Selection criteria for TMT-SRM biomarker validation. For each sample, the collection centre description, diagnosis, gender, APOE genotype, age and disease duration is indicated. Also displayed are the MMSE scores over five visits (V1 – V5) and a regression index showing decline in MMSE scores over the timepoints. All factors were considered during experimental cohort selection.

No.	Description	Diagnosis	Gender	ApoE	Age Of Onset (yrs)	Disease duration (yrs)	MMSE V1	MMSE V2	MMSE V3	MMSE V4	MMSE V5	MMSE decline regression
31	LNDADC017	1	F	23	78	1.4	26	24	20	24	20	-4.80
32	LNDADC020	1	M	34	78	0.5	26	26	27	26	27	0.80
33	LNDCTL056	0	F	44	NA	NA	27	NA	NA	NA	27	0.00
34	LNDADC029	1	F	34	68	7.3	30	27	27	27	25	-4.00
35	LNDADC030	1	F	33	77	2.4	30	30	30	29	28	-2.00
36	LNDCTL070	0	F	34	NA	NA	30	NA	NA	NA	30	0.00
37	LNDADC031	1	F	44	75	4.8	22	21	21	23	17	-3.20
38	PRGADC003	1	F	33	65	5.4	24	22	22	21	22	-2.00
39	LNDCTL074	0	M	23	NA	NA	30	NA	NA	NA	30	0.00
40	PRGADC005	1	M	33	70	6.8	27	24	22	21	22	-5.20
41	PRGADC017	1	F	33	79	0.2	21	20	17	19	21	-0.40
42	PRGCTL011	0	F	33	NA	NA	30	NA	NA	NA	30	0.00
43	PRGADC025	1	F	33	75	1.9	24	16	20	19	19	-2.80
44	PRGADC018	1	F	44	69	1.2	18	NA	16	19	16	-1.03
45	PRGCTL032	0	M	33	NA	NA	30	NA	NA	NA	30	0.00
46	PRGADC026	1	F	34	68	9.0	16	16	15	16	11	-4.00
47	PRGADC019	1	F	34	73	9.6	21	20	20	19	21	-0.40
48	PRGCTL043	0	F	33	NA	NA	30	NA	NA	NA	30	0.00
49	PRGADC028	1	F	34	68	4.9	22	NA	22	23	17	-3.66
50	PRGADC042	1	F	24	76	3.5	26	25	27	27	26	0.80
51	PRGCTL048	0	F	33	NA	NA	30	NA	NA	NA	30	0.00
52	PRGADC031	1	F	34	72	-0.5	26	NA	27	24	22	-4.00
53	PRGADC047	1	M	33	84	1.8	12	12	10	10	12	-0.80
54	THSCTL016	0	M	23	78	0.2	30	NA	NA	NA	30	0.00
55	PRGADC045	1	F	34	70	2.0	25	24	25	NA	19	-5.83
56	PRGADC049	1	F	44	69	2.1	21	22	20	21	20	-1.20
57	THSCTL019	0	F	34	NA	NA	30	NA	NA	NA	30	0.00
58	PRGADC046	1	F	33	75	7.3	17	16	NA	14	14	-3.20
59	PRGADC053	1	F	33	80	-0.6	16	16	NA	NA	15	-1.08
60	TLSCTL705	0	F	33	65	2.4	30	NA	NA	NA	30	0.00

No.	Description	Diagnosis	Gender	ApoE	Age Of Onset (yrs)	Disease duration (yrs)	MMSE V1	MMSE V2	MMSE V3	MMSE V4	MMSE V5	MMSE decline regression
61	THSADC002	1	F	44	66	2.4	12	12	7	NA	9	-3.66
62	THSADC041	1	F	33	76	4.6	12	18	NA	NA	10	-4.00
63	KPOCTL009	0	F	23	NA	NA	29	NA	NA	NA	29	0.00
64	THSADC007	1	M	33	71	4.5	19	17	16	16	16	-2.80
65	THSADC018	1	F	34	74	0.2	24	26	27	27	25	1.20
66	TLSCTL720	0	F	34	NA	NA	30	NA	NA	NA	30	0.00
67	THSADC014	1	F	33	64	7.3	24	19	21	19	21	-2.40
68	THSADC037	1	F	34	74	2.7	12	12	12	15	12	1.20
69	LDZCTL002	0	F	33	NA	NA	29	NA	NA	NA	29	0.00
70	THSADC025	1	F	34	68	3.0	25	24	25	22	20	-4.80
71	THSADC040	1	F	44	62	5.4	26	NA	26	26	26	0.00
72	LDZCTL011	0	F	34	NA	NA	29	NA	NA	NA	29	0.00
73	THSADC034	1	F	33	69	6.8	22	17	12	7	2	-20.00
74	THSADC049	1	M	33	68	3.6	25	23	22	NA	23	-1.71
75	LNDCTL042	0	F	33	NA	NA	29	NA	NA	NA	29	0.00
76	THSADC042	1	M	34	76	4.6	12	8	7	NA	2	-10.00
77	KPOADC035	1	F	44	66	1.9	21	26	28	29	20	0.40
78	KPOCTL005	0	F	33	NA	NA	29	NA	NA	NA	29	0.00
79	THSADC043	1	F	33	67	5.2	17	NA	NA	15	14	-2.92
80	PRGADC004	1	F	34	67	5.8	22	28	24	17	21	-1.20
81	THSCTL004	0	F	23	NA	NA	29	NA	NA	NA	29	0.00
82	THSADC046	1	F	34	71	2.6	17	8	10	10	3	-2.80
83	TLSADC511	1	F	33	64	6.1	23	20	20	17	22	-2.00
84	TLSCTL716	0	F	33	47	19.4	28	NA	NA	NA	30	2.00
85	THSADC051	1	F	33	73	1.6	19	15	17	18	14	-0.40
86	PRGADC009	1	F	34	73	7.4	18	20	16	14	17	-7.20
87	PRGCTL022	0	F	33	NA	NA	29	NA	NA	NA	30	1.00
88	TLSADC505	1	F	34	60	1.9	19	13	15	11	11	-0.40
89	THSADC035	1	F	33	68	2.4	17	15	11	14	15	-2.00
90	PRGCTL053	0	F	33	NA	NA	29	NA	NA	NA	30	1.00